THE ROLE OF GLUTATHIONE IN ALLERGIC CONTACT DERMATITIS.

This thesis is submitted in accordance with the requirements of the University of Liverpool for the degree of Doctor of Philosophy by

Sandrine Spriggs

November 2017

Declaration

I declare that the work presented in this thesis is all my own work and has not been submitted for any other degree.

……

Sandrine Spriggs (MSc)

Acknowledgements

Firstly, I would like to thank Dr Dean Naisbitt for giving me the opportunity to carry out this piece of research at the University of Liverpool under his supervision. Dr Naisbitt and his team have made sure that I felt very welcome during each of my visits to Liverpool. I am very grateful for all the time they have spent to sort out the technicalities of me carrying out experiments in their lab in the short time allocated. Equally, I would like to thank Dr Neil Kitteringham for his time and advice during the writing of the publications associated with this thesis.

Secondly, all my heartfelt thanks to Unilever Safety and Environmental Assurance Centre (SEAC) for sponsoring this piece of research and especially to Dr Maja Aleksic, my external supervisor. Her guidance has been much appreciated as she has helped me improving my scientific project design skills greatly. I would also like to mention Mr Richard Cubberley and Dr Steve Gutsell, who jointly covered Dr Aleksic's supervising role while she was on maternity leave. I reserve a special thanks to all my Unilever colleagues with experimental toxicology skills, especially Mrs Annette Furniss and Mrs Penny Jones, who kindly shared they invaluable experience of skin cells and skin related 3D models and overviewed my cell culture training.

I also wish to thank my family for all their various degrees of involvement in my student life. First of all to my husband Danny, for his constant support throughout my six years of study. During the past few years, our relationship has blossomed and we have now become a very happy family. My father, for being an inspiration to me and fully endorsing my wishes to become a scientist in a field he knew very little about. To my in-laws in the UK, thank you so much for being there for me when I am in need of comfort and reassurance. And last but not least, I need to thank my newly born son Xavier, for keeping incredibly quiet day and night thus allowing me to get the final touches to this manuscript.

Contents

Abbreviations

2-AAPA	2-acetylamino-3-[4-(2-acetylamino-2-carboxyethylsulfanylthiocarbonylamino) phenylthiocarbamoylsulfanyl] propionic acid
ABC	ATP binding cassette
ACD	Allergic contact dermatitis
AOP	Adverse outcome pathway
ATP	Adenosine triphosphate
BA	Benzaldehyde
BCNU	1,3-Bis(2-chloroethyl)-1-nitrosourea (or carmustine)
BSO	L-buthionine sulfoximine
COMT	Catechol-O-methyl transferase
CYP	Cytochrome P450 mono-oxygenase
DEM	Diethyl maleate
DMEM	Dulbecco's modified Eagle's medium
DNBB	1-bromo-2,4-dinitrobenzene
DNCB	1-chloro-2,4-dinitrobenzene
DNFB	1-fluoro-2,4-dinitrobenzene
DNP-SG	S-(2,4-dinitrophenyl)glutathione
DPCP	Diphenylcyclopropenone
EC_3	Effect concentration 3 (estimated concentration of a chemical required to produce a 3-fold stimulation of draining lymph node cell proliferation compared with concurrent controls, expressed as a %)
EC_{50}	concentration of reagent able to deplete 50% of the reduced GSH available in GSH depletion assay
ESI	Electrospray ionisation
FCS	Foetal calf serum
GCL	Glutamate-cysteine ligase
GPx	Glutathione peroxidase

GSH	Reduced glutathione
GR	Glutathione reductase
GSSG	Glutathione disulphide
GST	Glutathione s-transferase
HaCaT	Human Adult low Calcium high Temperature
HP	Hydrogen peroxide
IAA	Iodoacetamide
LC	Liquid chromatography
LLNA	Local lymph node assay
MIE	Molecular initiating event
MRM	Multiple reaction monitoring
mRNA	Messenger ribonucleic acid
MRP	Multidrug resistance- associated protein
MS	Mass spectrometry
MTT	3-(4,5-dimethyl thiazol-2-yl)-2,5-diphenyltetrazolium bromide (or methyl tetrazolium)
NADPH	Nicotinamide adenine dinucleotide phosphate
NAT	N-acetyltransferase
NHEK	Normal human epidermal keratinocytes
NMR	Nuclear magnetic resonance
Nrf2	Nuclear factor erythroid 2-related factor 2
OECD	Organisation for Economic Co-operation and Development
PA	Phenylacetaldehyde
PAPS	3'-Phosphoadenosine-5'-phosphosulfate
PBS	Phosphate buffer saline
RHE	Reconstructed Human Epidermis
ROS	Reactive oxygen species
RT	Retention time
SAM	S-adenosylmethionine
S_NAr	Aromatic nucleophilic substitution reaction

TMT	Thiol methyltransferase
UDPGA	Uridine diphosphoglucoronic acid
UGT	UDP-glucoronosyl transferase
UPLC	Ultra performance liquid chromatography
UV	Ultra Violet

Publications

Published papers

Sandrine Jacquoilleot, David Sheffield, Adedamola Olayanju, Rowena Sison-Young, Neil R. Kitteringham, Dean J. Naisbitt, Maja Aleksic. Glutathione metabolism in the HaCaT cell line as a model for the detoxification of the model sensitisers 2,4-dinitrohalobenzenes in human skin. Toxicology Letters. **237**(1): p. 11-20. 2015

Sandrine Spriggs, David Sheffield, Adedamola Olayanju, Neil R Kitteringham, Dean J Naisbitt, Maja Aleksic. Effect of repeated daily dosing with 2,4-dinitrochlorobenzene on glutathione biosynthesis and Nrf2 activation in Reconstructed Human Epidermis. Toxicological Sciences. **154** (1): p. 5-15. 2016

Manuscripts in preparation

Sandrine Spriggs, Maja Aleksic, Richard Cubberley, Paul Loadman, Dean J Naisbitt and Antonia Wierzbicki. Glutathione clearance of DEM, DNCB, and DPCP in human skin models, a case study. *This draft publication will use the results from chapter 4 and 5 and include some results obtained during a collaboration with Bradford University*.

Richard Cubberley, Sandrine Spriggs, Paul Loadman, David Sheffield and Antonia Wierzbicki. A study of inter-individual variability in the Phase II metabolism of xenobiotics in human skin. *This draft publication will use the results a collaboration with Bradford University, where significant input and advice was given for GSH metabolism in skin and an active participation to writing of the manuscript was made.*

Abstracts

Sandrine Jacquoilleot, Maja Aleksic, Richard Cubberley, Steve Gutsell, Neil R. Kitteringham, Dean J. Naisbitt. The role of Glutathione as a clearance system in skin. Oral presentation, 2nd Skin Metabolism Meeting- Skin Forum in Nice, France (October, 2013).

Sandrine Jacquoilleot, Maja Aleksic, Dean J. Naisbitt. Understanding the role of skin metabolism in Allergic Contact Dermatitis: Glutathione as a clearance system. Oral

presentation, 25th Meeting of the European Research Group on Experimental Contact Dermatitis (ERGECD 2014) in Paris, France (June, 2014).

Abstract

Allergic Contact Dermatitis is a skin condition that affects up to twenty percent of the North American and Western European population. The molecular initiating event (MIE) of this type IV delayed hypersensitivity is the formation of antigenic species by covalent modification of endogenous proteins. Cysteine residues, though not the most prevalent residues in skin proteins, are prone to react with small electrophilic molecules and thus play a crucial role in protein haptenation. The role of cysteine is also very prominent in removal of electrophiles. Glutathione (GSH) is the most prominent antioxidant in cells and contains a cysteine residue, providing a free reactive thiol for GSH conjugation of electrophiles and their subsequent removal. It is also the co-factor of an important set of enzymes involved in the metabolic clearance system, glutathione S-transferases (GST). However, it remains unclear whether the reactivity of small exogenous electrophiles with intracellular GSH could be a key factor in determining the epidermal bioavailability of sensitising chemicals.

GST activity has been demonstrated both in skin and in most *in vitro* skin equivalents but so far studies have focussed on specific chemical clearance. The GSH cycle (synthesis, conjugation, recycling) has not been comprehensively studied in the HaCaT cell line, which is often used as a surrogate model for human skin. We showed that the model sensitisers 2,4-dinitrohalobenzenes, reacting with thiols via a SNAr mechanism, depleted intracellular GSH within the first hour of exposure in HaCaT cells, in a dose dependent manner. Synthesis of *de novo* GSH was investigated 24 hours after treatment with a single non-toxic dose of 10 µM of three dinitrohalobenzenes. GSH concentration was found similar or slightly higher than the level measured in control cells for 1-chloro-2,4-dinitrobenzene (DNCB) and 1-fluoro-2,4-dinitrobenzene (DNFB) but not for 1-bromo-2,4-dinitrobenzene (DNBB), which appeared to partially prevent GSH repletion. This data inferred that the repletion step was the differentiating factor between chemicals belonging to the same reactivity domain. The toxicity of the halogen released in the cells was most likely the reason for observing these differences and this might have been missed if only the clearance kinetics were investigated. Activation of the nuclear factor E2-related factor 2 (Nrf2) pathway was concomitantly observed for all compounds within two hours, and at concentrations less than 10 µM.

Nrf2 activation is the precursor event for the overproduction of Phase II metabolic enzymes such as GSTs, enzymes involved in the synthesis of GSH such as Glutamyl cysteine ligase (GCL) and Glutathione synthetase (GS) as well as GSH related enzymes acting against oxidative stress such as Glutathione Reductase (GR). HaCaT cells treated with the model aldehydes benzaldehyde and phenylacetaldehyde, which oxidised cysteine residues *in chemico,* did not suffer a significant depletion of GSH levels at sub-toxic concentrations. In addition, these aldehydes have been shown to react with amines via a Schiff base mechanism to form stable protein adducts. Our set of data indicated that the Schiff base mechanism was most probably favoured and that an oxidation of GSH (a reduction of the GSH:GSSG ratio), was effectively and rapidly controlled by GR activity. The volatility of aldehydes was likely to limit the bioavailability of these compounds intracellularly, possibly increasing the probability of haptenation with cell membrane proteins.

Skin sensitisers are often defined by their potency (ranging from extreme to non-sensitising) rather than their chemical reactivity domain. We compared the clearance of two extreme sensitisers by the GSH pathway: DNCB and diphenylcyclopropenone (DPCP). We demonstrated that two chemicals able to react with thiols *in chemico* via different mechanisms (SNAr for DNCB and Michael addition for DPCP) were affecting GSH levels differently in HaCaT cells. DNCB induced GSH depletion at non-toxic concentrations, while exposure to DPCP decreased cell viability at concentrations for which GSH stock was not significantly reduced. DPCP reactivity with thiols has been suggested in cell membranes. Contrary to the results obtained for DPCP, diethyl maleate (DEM), a moderate sensitiser also reacting via Michael addition, was cleared by GSH at a rate similar to the rate of *de novo* GSH synthesis, masking the overall depletion of GSH. Exposure to DEM induced an overproduction of GSH after 24 hours that was more pronounced than the one observed for the more potent sensitiser DNCB, showing that the sensitising potency of chemicals could not be correlated solely to the ability to be conjugated by GSH (i.e. weak sensitisers would be cleared rapidly while potent sensitisers would not).

These experiments demonstrated that the defence mechanisms in the HaCaT cell line were providing a rapid response to chemical stress. To investigate the effects of chemical exposure on GSH lifecycle in reconstructed human epidermis (RHE), we attempted repeated cycles of 2 hour exposure to DNCB over a week long period. For three consecutive treatments, each exposure to DNCB led to GSH depletion. Replenishment to basal level was observed after a 22 hour recovery period. Accumulation of Nrf2 in the cytosol also occurred within the two hours of exposure to DNCB but returned to baseline during each recovery period. The amount of GSH conjugate formed (dinitrophenyl glutathione) increased after each exposure, suggesting that the metabolic capacity of skin may be enhanced in response to exposure to exogenous compounds.

In conclusion, the GSH cycle is fully active in skin and participates in the clearance of some exogenous compounds with electrophilic properties. GSH skin metabolism can also potentially be enhanced after repeated exposures to small quantities of electrophiles. Future risk assessments for skin sensitisation potential of topically applied chemicals could integrate these findings to correlate more realistically to in vivo scenarios.

Chapter 1: General Introduction

Contents

1.1 Introduction.

Cellular defence mechanisms against exogenous or endogenous reactive small molecules rely on the conjugation of these electrophilic species to endogenous nucleophilic molecules such as glutathione (GSH), spontaneously or enzymatically mediated, resulting in readily excretable inert compounds. The irreversible nature of such chemical reactions does not differ significantly from the covalent binding of these same electrophiles to nucleophilic targets in skin proteins, resulting in the formation of antigens that are recognised by the immune system as foreign and in the induction of skin sensitisation. Additionally, some reactive molecules have the capacity to oxidise GSH to its disulfide form (GSSG) without conjugation, thus altering the balance of GSH:GSSG and contributing to danger signalling.

Better understanding the detoxification capacity of skin, particularly the role of GSH, will enable scientists to fully utilise understanding of reactivity in the context of skin allergy. Detoxification processes in the skin, namely GSH conjugation, are a key factor in determining the epidermal bioavailability of potentially sensitising chemicals, which have penetrated into the viable skin tissue. This section presents an overview of the skin sensitisation process, detailing the key mechanisms and where the investigation of GSH, as a skin clearance process, could fit into the determination of the bioavailability of a chemical for antigen formation in skin. Typical *in vitro* skin models available for such investigations are also reviewed.

1.2 The human skin structure.

1.2.1 Definition.

The skin is the first line of defence against various external influences. Human skin is a complex organ, covering an average area of two square meters. It is constituted of several layers *(stratum corneum*, epidermis, dermis and hypodermis), each demonstrating different biological and physical properties (Fig 1.1).

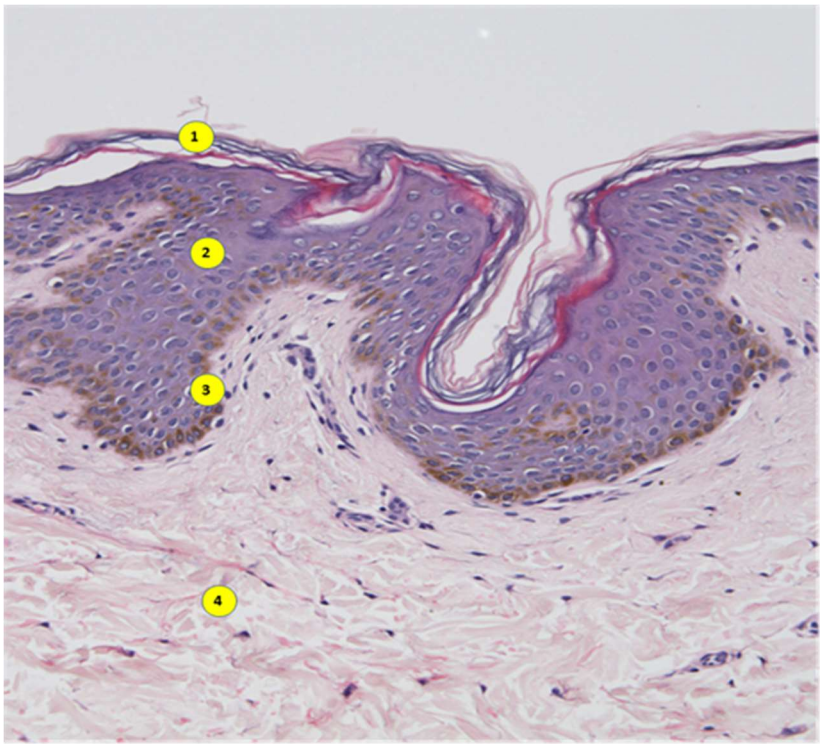

Figure 1.1: Skin structure depicting 1) the *stratum corneum*, 2) the epidermis, 3) the *stratum basale*, in which the dark coloration is due to the high concentration in melanin (skin donor of Caribbean ethnicity), 4) the dermis. (Image provided by H. Minter, SEAC, Unilever).

1.2.2 Stratum corneum.

The *stratum corneum* is not a definite layer of the skin per se, as it is the continuity of the epidermis. However, it is often designated as a separate layer due to its different physical characteristics compared to the lower layers of the epidermis. The cells constituting the *stratum corneum* are dead cells called corneocytes, tightly packed in a multilayer. The number of layers of the *stratum corneum* varies depending on the area

of the body where the skin is located. Relatively well protected areas such as eyelids and the forehead can contain as little as 9 layers, while the *stratum corneum* of hardwearing feet soles can be constituted of up to 50 layers [1]. Corneocytes are the ultimate result of the differentiation of keratinocytes present in the epidermis that have specialised to generate high quantities of keratin and lipids. The cells are packed together, each cell following an approximate hexagonal pattern, being linked to its immediate neighbour cells by glycoprotein structures called desmosomes. The interstitial space between cells is filled with lipids organised in lamellae. The *stratum corneum* is thus a relatively lipophilic environment, acting as a physical barrier against external compounds and regulating water permeation [2]. Its organised structure has been described as “bricks and mortar” by a number of scientists.

1.2.3 Epidermis.

The epidermis is the layer of the skin which contains the highest concentration and diversity of cells, mainly keratinocytes (90%) but also melanocytes (5-10%), Merkel cells and Langerhans cells, all with different nature and roles.

The epidermis is organised in sub-layers of keratinocytes at different stages of differentiation. Considering the state of specialisation the keratinocytes and their shape, distinct layers of the epidermis can be separated [3]: the *stratum basale* (where keratinocytes are still in their primary state and able to divide to keep the level of primary cells constant while some cells migrate to upper layers and differentiate), the *stratum spinosum* (where the keratinocytes start to shrink), the *stratum granulosum* (distinctive by the presence of granules of proteins and lipids in the keratinocytes), the

startum lucidum (where the cells have lost their nucleus and the granules have been expelled into the intercellular space) and the *stratum corneum* already described above.

The deepest level of the epidermis, the *stratum basale*, also contains a number of other cells. The role of melanocytes is to produce melanin, which, once incorporated into the specialised keratinocytes of the upper layers, will give the skin its pigmentation. Merkel cells are also present in this layer of skin. Their role is not clearly defined yet, but they are thought to be involved in the sensory function of skin [4]. These cells have the ability to chemically communicate with neurone endings in the skin and in close proximity, form a "Merkel cell-neurite complex".

Finally, the representation of the immune system in the epidermis is assured by the presence of a type of dendritic cell called Langerhans cells. These cells, in steady state conditions, stay in close contact with keratinocytes and have a lifespan higher than other dendritic cells. However, when the cells process an antigen, they enter a maturation process, which trigger their migration first through the dermis and then to the draining lymph nodes, where they present their antigen to T-cells [5].

1.2.4 Dermis.

The dermis is located directly underneath the epidermis. It exhibits the highest level of elasticity due to its composition, which is rich in fibres. The dermis is mainly constituted of fibroblasts which are fixed, mostly in the upper part of the dermis at the interface with the epidermis (the dermal papillae), into a collagen rich matrix containing elastin and reticular fibres. Due to this high concentration of collagen, the dermis has been seen, in a simplistic way, as a "gel phase" in which hair follicles and sweat glands are rooted, while blood capillaries circulate through it to reach the epidermis above [6].

1.2.5 Hypodermis.

The hypodermis is a few millimetres thick subcutaneous fat layer separating the dermis from muscles and other body tissues [6]. Its primary functions are energy storage and body insulation, helping to maintain body temperature and protecting muscles against external physical shocks. Veins and nerves usually run through the hypodermis to reach the dermis above.

1.3 Allergic Contact Dermatitis.

Dermatologists diagnose patients that have developed an allergy either coming from routinely handling chemicals contained within hair dyes, detergents, paints, concrete, pesticides, etc [7] in the workplace or linked to the use of some of these products at home. This has led to a lot of scientific research to try and understand the mechanisms that caused these allergic reactions [8].

1.3.1 Definition.

The skin condition Allergic Contact Dermatitis (ACD) is a delayed-type hypersensitivity response to external compounds that affect a small but significant percentage of the population [9]. It is characterised by a visible redness or rash on the skin after successive exposures. The only method to deliver a reliable medical diagnosis of ACD is to conduct a patch test on the patient, using the suspected allergen under controlled conditions [10]. Determined allergens should be avoided by patients who have been diagnosed [11].

1.3.2 Mechanistic understanding of ACD.

1.3.2.1 Pathway to skin sensitisation.

Not all chemicals are harmful, but some have the ability to react with proteins within the skin, by permanently modifying the nucleophilic sites available on them. Such compounds are called haptens and the process by which they react with proteins is called haptenation. The protein-hapten adducts resulting from interactions of allergenic chemicals and skin proteins can be recognised as an antigen by the human body (Fig 1.2). The presentation of this antigen by the Langerhans cells to the T cells of the immune system, in the lymph nodes, leads to the recognition of the chemical as foreign and induces an immune response. This first exposure to the chemical is the induction step of ACD. On following re-exposures, even at lower concentrations, clinical symptoms of ACD (redness, rash, oedema…) are likely to be observed on patients that have been previously sensitised (elicitation step).

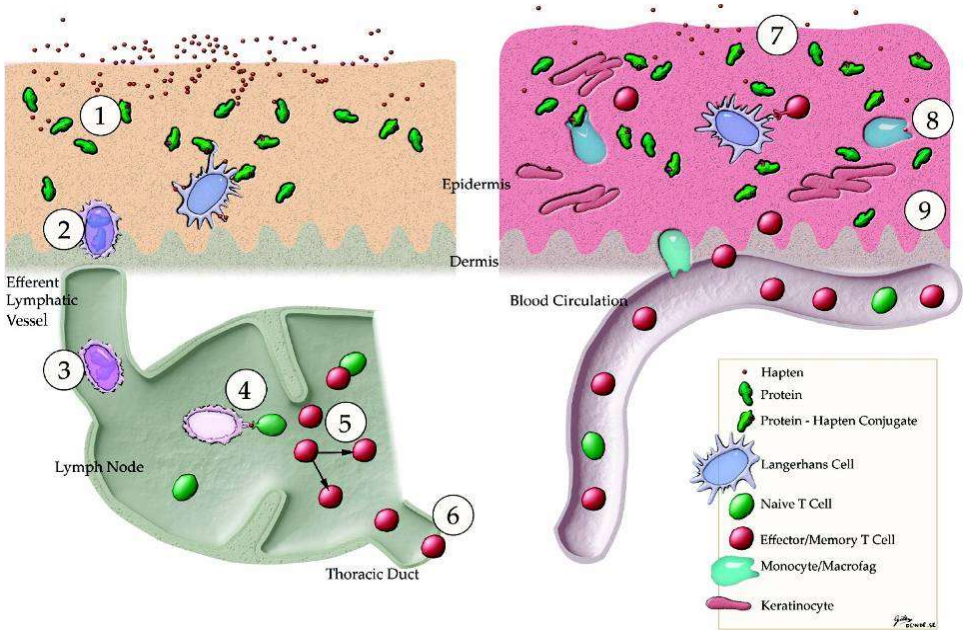

Figure 1.2 : *C*hemical pathway to skin sensitisation where 1) is haptenation (chemical binding to proteins) 2) antigen collection by Langerhans cell and cell activation 3) migration to lymph node 4) presentation to T-cells 5) T-cells specialisation and proliferation 6) migration out of lymph node 7) re-exposure to chemical 8) signalling to T-cells 9) inflammation of skin. Figure reproduced from [12].

The Organisation for Economic Co-operation and Development (OECD) has released a document formalising the Adverse outcome pathway (AOP) for skin sensitisation, i.e the full sequence of mechanistic steps involved in the process from the penetration and reaction of a chemical to the inflammation observed on skin at the organ level [13] (Fig 1.3).

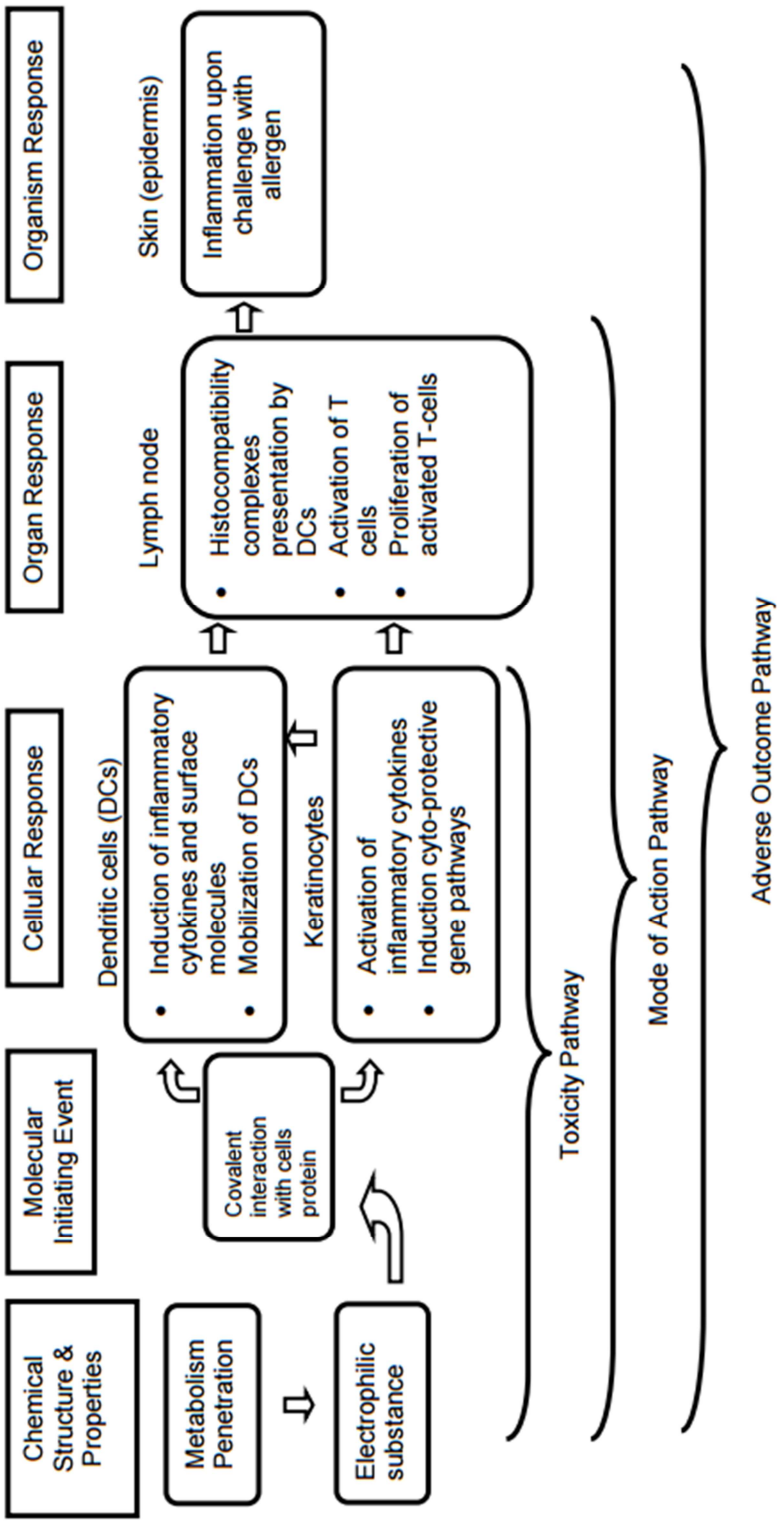

Figure 1.3: Flow diagram of the pathways associated with skin sensitisation. Figure reproduced from [13].

1.3.2.2 Protein haptenation.

Protein haptenation has long been recognised as the key molecular initiating event (MIE) in the skin sensitisation AOP. Many investigations have been focused on understanding the mechanism of reaction involved in the process of haptenation (e.g. [14-16]) and the consequences of covalent modifications on proteins (e.g. [17, 18]). To assess the reactivity of chemicals towards nucleophiles, *in vitro* assays developed throughout the years tend to use model nucleophiles, thus limiting the level of complexity linked to a larger protein.

The reactivity of the nucleophilic residues lysine, cysteine and histidine with a selection of skin sensitizers of various potencies has been reported [19]. Even though trying to predict the level of skin sensitisation induced by a chemical in humans using a single *in vitro* assay would be overly simplistic and prone to errors, this assay demonstrated a correlation between the potential for sensitisation of the sensitizers used and their ability to react with cysteine and lysine.

Later, the use of a single small peptide derived from a native protein called Coronin1 in a peptide reactivity assay has been reported [20]. This peptide, containing two lysine and one cysteine residues (sequence Ac-NKKCDLF), was incubated with over 80 chemicals of various sensitising potential. The major improvement on the previously reported methods came from the introduction of Liquid Chromatography-Mass Spectrometry (LC-MS) as the analytical technique used to measure the level of depletion of the peptide after 24 hours incubation. LC-MS not only enabled the quantification of peptide remaining after incubation but also the characterisation of adduct(s) formed between the test chemical and the peptide (if any) and the potential dimerisation of the peptide due to an oxidative process.

Which nucleophiles would be modified in a given skin protein where a selection of them would be available is still not clearly understood. The investigation of the reactivity of the potent skin sensitiser 1-chloro-2,4-dinitrobenzene (DNCB) with human serum albumin [21, 22] and two other model proteins present in skin, human cytokeratin K14 and cofilin [23] illustrated the complexity of the problem lying ahead for the understanding of skin protein haptenation. Indeed, even though DNCB reacts with nucleophiles following only one chemical mechanism (aromatic substitution of the chlorine) the modification of different residues can be observed (Cys, Tyr, Lys, N-terminus) and varies between proteins. Even the prioritisation of the reactivity of the lysine residues alone, present on the three proteins investigated, is difficult to establish, as the presence of neighbouring amino acids and the pH conditions at which the protein has been stored for commercialisation (presence of urea for cytokeratin K14) influence the reactivity observed.

As a result, the use of small peptides containing only one reactive site for mechanistic understanding of hapten reactivity was extended to a selection of nucleophiles (lysine and cysteine but also histidine, tyrosine, arginine and the NH_2 present on the N-terminal amino acid of the peptide chain)[24]. This publication also presents initial kinetic measurements obtained by slight modification of the assay, allowing the monitoring of the peptide depletion over several hours, from which a pseudo first order kinetic reaction assumption was used to determine the rate constant of the reaction between the peptide and the chemical investigated.

1.4 Human skin *in vitro* models.

Fresh *ex vivo* human skin is very difficult to source and the level of viability of the skin depends largely on the techniques used to preserve it after biopsy or surgery and the timing involved [25, 26]. This can lead to low levels of reproducibility of experimental

results. Alternative models to human skin have been developed for laboratory use. Some skin equivalents available to facilitate the development of *in vitro* experiments are described below. The aim of these models is not to replace the use of *ex vivo* skin, in terms of experimental results. Reviews have highlighted that cell co-cultures in 2D and even 3D structures lack the complexity levels of *in vivo* skin and lead to different response in cell signalling, migration and phenotype, the cells being forced to adjust to the plastic structure of plates [3]. More complex models called organotypic skin cultures, which aim to reconstruct human skin *in vitro*, can even contain hair follicles or immune cells [27]. However, to construct such models it is necessary to have access to *ex vivo* skin to harvest each type of cell and the model development is very time and labour intensive. The models presented below are relatively easy to obtain and can serve as tools enabling mechanistic understanding of skin biology.

1.4.1 Cell cultures.

1.4.1.1 Normal human epidermal keratinocytes.

Normal Human Epidermal Keratinocytes (NHEK) are primary epidermal cells. For laboratory research, they can be bought from a supplier as a cryopreserved stock, cultured in a keratinocyte specific medium and are usually ready for use after the second passage [28, 29]. These cells are particularly useful for scientists investigating the differentiation of keratinocytes at different levels of specification.

1.4.1.2 HaCaT cell line.

The HaCaT cell line is derived from epidermal keratinocytes that have been spontaneously immortalized during culture. At the time, Boukamp and colleagues [30] were investigating culture conditions for human keratinocytes obtained from an adult male donor. Immortalisation was obtained when cells were cultured in a medium containing a low level of calcium under slightly elevated temperature (38.5 °C), hence the denomination of the new cell line: HaCaT (Human Adult, Low Calcium, High Temperature).

This cell line is favoured by scientists as the cells can keep their integrity for many passages, as long as the culture conditions are maintained, and their subculture is relatively straightforward and well documented in the literature [31]. HaCaT cells are easily maintained in a basal state when cultured under low calcium concentrations and commence differentiation when calcium levels are increased. Once excess calcium is removed, HaCaT cells go back to basal level of differentiation.

1.4.1.3 Skin fibroblasts.

As with NHEK, skin fibroblasts are usually isolated from skin samples freshly obtained post-surgery and cultured in medium as primary cells. Fibroblasts are dermis cells that can be used as a 1D culture to complement the information obtained with keratinocytes studies. For example, fibroblasts can be used alongside keratinocytes and whole skin explants to assess skin damage linked to the use of irritants and sensitisers [32].

1.4.1.4 Cell co-culture.

The epidermis is a complex layer of skin, which does not include exclusively keratinocytes, even though these are in excess. In an attempt to produce more relevant

experimental results, comparable to the results obtained *in vivo* during a clinical study, co-cultures of a variety of epidermal cells were developed by various laboratories.

A co-culture of immortalised murine melanocytes and keratinocytes has been used when putting in place a protocol enabling the measurement of pigmentation level of the melanocytes after application of chemicals enhancing or suppressing the production of melanin. It was observed that the trends for each chemical were more pronounced when a co-culture was used compared to melanocytes alone, highlighting the importance of considering the communication between cell types when developing *in vitro* models [33].

A co-culture of HaCaT and THP-1 (monocytic cell line derived from the blood of a patient with acute monocytic leukemia) cells has also been used to check the influence of keratinocytes in the process of skin sensitisation. It was shown that this *in vitro* assay helped to differentiate between haptens and pro-haptens using the expression of CD86, CD54 and CD40 from the THP-1 cells, while information about the metabolites formed from these haptens could be obtained by investigation of the metabolic activity of HaCaT cells [34].

1.4.2 3D skin models.

Comparisons of the skin models commercially available have been carried out, where minor differences have been detailed [35, 36]. Overall, the described models all bear close resemblance to viable epidermis in terms of layers of differentiated keratinocytes, even though the cells can vary in shape compared to natural skin. However, the expression of certain markers can sometimes vary from model to model and the barrier function of the skin, essential when skin absorption studies are carried out, could not be satisfactorily reproduced.

1.4.2.1 Models available from Episkin®.

Reconstructed Human Epidermis™ (RHE) is a skin model derived from the 3D culture of NHEK available from Episkin [37]. It expresses some major differentiation markers and basal membrane markers, similar to the ones expressed in natural epidermis, which are used by the manufacturer to ensure reproducibility of batch production. This skin model can be delivered at different stages of maturation (after 10, 12 or 17 days of culture at the air liquid interface), in different sizes (0.5 cm^2 or 4 cm^2) or in a 24 or 96-well plate format. Its use for corrosion and irritation *in vitro* tests has been validated and is now recommended by the European Union Reference Laboratory for alternatives to animal testing (EURL-ECVAM). Another skin model, Episkin™, is also commercialised by the same company. The model is usually delivered after 13 days of keratinocyte differentiation. For specific skin penetration studies, the model can be cultured for 20 days, to thicken the *stratum corneum*. The uses of the Episkin model are similar to those of RHE.

1.4.2.2 Models available from MatTek Corporation®.

EpiDerm™ is a skin model derived from the 3D culture of NHEK available from MatTek [38]. Each set of skin models is shipped in 24-well plates and can be kept at 4 °C for up to 6 days before starting culture at the air liquid interface. The integrity of the tissue has been evaluated for up to three weeks, when the culture medium is changed every other day. On arrival, the skin culture should contain at a minimum 8 to 12 layers of keratinocytes at different stages of differentiation (*stratum basale, spinosum* and

granulosum) and 10 to 15 layers of corneocytes (*stratum corneum*). More recently, MatTek has developed a model more representative of human skin, Epiderm FT™, composed of an epidermis layer (keratinocytes) grown on a layer of cultured fibroblasts in collagen.

1.4.2.3 Other commercialised models.

The Phenion™ full-thickness model, commercialised by Henkel® [39] is a similar type of model containing an epidermis and a dermis. It is sold as a 1.5 cm^2 model and has been evaluated for use in skin penetration studies [40] but also its potential for use in skin metabolism studies [41].

The Labskin™ model, commercialised by Innovenn UK Ltd [42], is very similar to the other full thickness models available, containing an epidermis and a dermis. The differences offered seem to come from the gel phase into which the fibroblasts are cultured, which is not collagen based. So far this model has primarily been used for microbiological assessment of cosmetics after topical application but has not been used to assess skin metabolism, linked to the GSH pathway or not.

1.4.3 Culture and maintenance of *ex vivo* skin.

Skin explants are usually obtained post-surgery and cultured at the air-liquid interface of a medium based on Dulbecco's Modified Eagle's Medium (DMEM). Explants viability has been maintained for a day for immediate DNA studies [43], seven days for the study of scarring processes [44] and up to two weeks for immunohistochemistry investigations linked to fibrosis [45]. The maintenance and use of such models is subject to stringent

ethics regulations and might require the research laboratory to set up a tissue bank. However, skin explants are now commercially available and can be purchased when working in conjunctions with companies that have been set up as branches from academic research laboratories and comply with all the required ethics regulations for the sourcing of their samples [46].

1.5 Skin metabolism.

1.5.1 Transformation (Phase I).

The general terminology used in metabolism studies to characterise the modification of xenobiotics by enzymes has been artificially separated into three Phases. Phase I metabolism covers all the types of enzymatic reactions which result in a functionalisation of xenobiotics, i.e. either changing their hydrophilicity levels (for example the hydrolysis of an ester to an alcohol would increase water solubility) or increasing their reactivity towards molecules involved in phase II enzymatic reactions to favour their excretion. It has long been observed that some sensitising chemicals are not directly reactive but have a potential to be metabolically activated. This unwanted consequence of metabolism needs to be investigated because of the susceptibility of these new species to react with proteins. Chemicals presenting these properties need to be considered as potential skin sensitisers and have been denominated as prohaptens in the literature [7].

The transformations of xenobiotics in Phase I metabolism cover a wide range of reactions, from oxidative processes to reductions and hydrolysis. An excellent review of enzymes having a gene expression in skin is available [47]. While the expression of a number of cytochrome P450 mono-oxygenases (CYP) enzymes and flavin

monooxygenase enzymes genes was reported in skin biopsies and cell cultures, the detection of the proteins themselves and their activity levels were not usually reported and are poorly understood.

A comparison of Phase I enzymes present in *ex vivo* skin and skin models highlighted the problems linked with the detection of enzymes in skin [48]. While the probes used in the assays have been successfully developed for enzymes in the liver, almost all measurements of CYP enzymes carried out in skin yielded results below the limit of detection. In contrast, cyclooxygenase activity was successfully measured above the limit of detection in all models, albeit with some result variability. While skin and 3D-epidermis models showed activity around 20 pmol/min/mg, activity of immortalised cell lines such as HaCaT was below 1 pmol/min/mg, demonstrating that models were not always absolutely representative of human skin, especially considering metabolic capability. A more systematic comparison of 3D skin models enzymatic activity was carried out and drew similar conclusions [49]. While the CYP activity was in the low pmol/mg protein/6 h range and sometimes close to the limit of detection of the assay for 3D skin models and *ex vivo* skin alike, esterase activity was easily measurable and the clearance values were of the same order of magnitude for all models.

A review of CYP enzymes, carboxylesterases, alcohol dehydrogenases and flavin-dependent monooxygenases, all involved in functionalisation of chemicals that could potentially increase their reactivity, was published [50]. This review covered the main skin models developed for *in vitro* testing including cells and 3D skin models. Another recent review included both Phase I and Phase II enzymes in human skin and skin models [51].

More work needs to be carried out to completely characterise human skin and the newly developed skin equivalents and the relevance of the results that they generate for phase

I metabolism, especially for CYP activity. However, due to the scarcity of viable *ex vivo* skin samples, models can be used whenever convenient, for a first assessment.

1.5.2 Conjugation (Phase II).

The conjugation reactions grouped in Phase II metabolism have as a biological purpose the inactivation of xenobiotics by addition of a small, hydrophilic moiety which will facilitate their evacuation from cells into the blood system, making them available for excretion by the kidneys. It is important to note that xenobiotics do not necessarily have to go through the Phase I reaction process to be metabolised by a Phase II enzyme. Indeed, most skin sensitisers are directly reactive. Phase II reactions are extensively reviewed by Lee and colleagues and include the following [52]:

- Sulfation, reaction using 3'-phosphoadenosine-5'-phosphosulfate (PAPS) as a cofactor, the enzymes involved being members of the sulfotransferases family.
- Acylation, mainly involving N-acetyltransferases (NATs) enzymes that use acetyl coenzyme A as a cofactor.
- Glucuronidation, reaction with cofactor uridine diphosphoglucoronic acid (UDPGA) facilitated by UDP-glucoronosyl transferases (UGTs)
- Methylation, reaction using S-adenosylmethionine (SAM) as a cofactor, the enzymes involved being members of the methyltransferase family. These are mostly enabling the methylation of aliphatic thiols, thiol methyltransferase (TMT) family, aromatic or heteroaromatic thiols, thiorupine methyltransferase family or catechols, catechol-*O*-methyltransferase (COMT) family. A few examples of N-methylation of amine containing drugs, such as nicotine have also been reported.

- Glutathione addition, reaction with glutathione mediated by glutathione S tranferases (GST). Details on GSTs present in skin will be given further below.

As for Phase I metabolism, the activity levels of phase II enzymes in human skin and skin models has been evaluated [53]. Contrary to phase I metabolism enzymes, Phase II enzymes show higher levels of activity (in the nmol/min/mg) range in this study. This facilitated their quantification and at the same time, emphasised the fact that skin is a very active detoxifying organ. The study demonstrated that 3D epidermal models showed slightly lower GSTs activity while UGTs and NATs were comparable. Higher Phase II metabolic activity compared to Phase I in 3D skin equivalents and *ex vivo* skin has also been reported elsewhere [49]. Very recent studies demonstrated that GSH conjugation, methylation, N-acetylation, sulfation and glucuronidation all took place to some extent in freshly excised skin (maintained in medium and used immediately) but the addition of cofactors to the maintenance medium did not increase the clearance rates of the chemical probes tested [54].

Previous studies already determined that the HaCaT cell line is a promising cell line for the investigation of phase II metabolism. The N-acetylated product of 4-amino-2-hydroxytoluene, a common hair dye, has been reported in both *ex vivo* skin and a HaCaT cell line [55]. The activity level of NAT 1 enzyme in this cell line was also measured alongside non immortalised keratinocytes [28]. While CYP activity (Phase I) was again at the very low end of the limit of detection, NAT 1 could be measured and the levels were comparable to the results obtained in a NHEK cell line.

1.5.3 Transportation (Phase III).

Phase III metabolism is the denomination given to the processing of metabolites that have been generated by a conjugation reaction (phase II) and their excretion. It usually

consists of 1) further processing of the metabolite by modifying the molecule that has been conjugated to the original xenobiotic (for example a modification of the glutathione moiety of a glutathione-xenobiotic conjugate) and 2) the transport of the substrate through the cell membrane by transporters, the energy required for this being released by the consumption of adenosine triphosphate (ATP). These proteins are called ATP binding cassette (ABC) transporters and 46 ABCs have been identified in humans to date [56]. A brief review of the mechanisms involved in the transport of glutathione conjugates out of cells is given in Section 1.7.3.

1.6 Glutathione.

1.6.1 Definition.

Glutathione or γ-L-Glutamyl-L-cysteinyl-glycine is a tripeptide which is formed by the conjunction of L-glutamate, L-cysteine and glycine featuring a characteristic γ-glutamyl bond (Fig 1.4). It was first discovered in 1888 by J. De Rey-Pailhade [57] but since then thousands of publications related to this molecule have been released (Table 1.1).

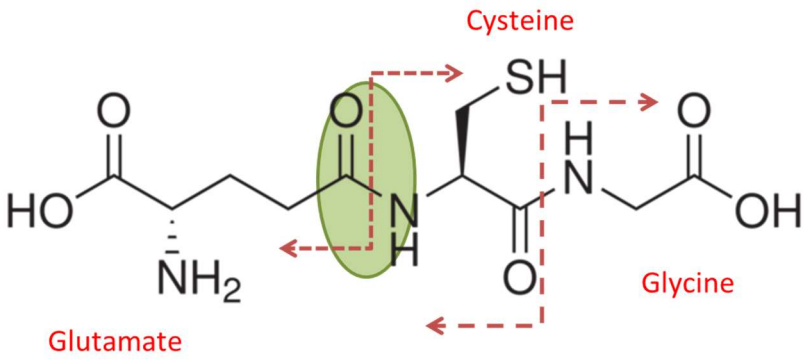

Figure 1.4 : Chemical structure of glutathione, highlighting the characteristic γ-glutamyl bond with the cysteine residue (green), which differs from the conventional α-peptide bond. The specificity of this bond protects GSH from cleavage by general peptidases and requires the presence of γ-glutamyl transpeptidase (GGT) to occur.

glutathione					
year	count	year	count	year	count
2017	2882	1986	1286	1955	45
2016	5829	1985	1138	1954	42
2015	6084	1984	1156	1953	61
2014	6093	1983	941	1952	50
2013	6070	1982	832	1951	50
2012	5768	1981	724	1950	28
2011	5238	1980	694	1949	15
2010	5038	1979	557	1948	11
2009	4776	1978	497	1947	15
2008	4568	1977	432	1946	8
2007	4604	1976	469	1945	6
2006	4503	1975	439	1943	4
2005	4825	1974	370	1941	2
2004	4612	1973	347	1939	4
2003	4371	1972	312	1938	3
2002	4101	1971	332	1937	2
2001	3846	1970	324	1936	5
2000	3770	1969	305	1935	6
1999	3361	1968	280	1934	4
1998	3274	1967	226	1933	7
1997	3247	1966	213	1932	5
1996	3137	1965	226	1931	3
1995	2948	1964	264	1930	7
1994	2666	1963	151	1929	3
1993	2420	1962	90	1928	1
1992	2245	1961	75	1927	4
1991	2011	1960	56	1926	3
1990	1774	1959	62	1925	5
1989	1597	1958	72	1924	2
1988	1537	1957	47	1923	1
1987	1352	1956	54	No publications	

Table 1.1 : Number of references related to glutathione found in Pubmed.

GSH is usually present at millimolar (mM) levels in tissues, throughout the body. In humans, the main generator of glutathione is the liver, while the main glutathione consumers are the kidneys. Unfortunately, GSH is mostly an intracellular peptide, which cannot enter the cell membrane without being turned back into amino acids. However, GSH can be taken out of cells using transporters, a process that has been described for hepatic cells, meaning that some GSH can be delivered throughout the body using the

blood system. Nevertheless, the level of GSH in plasma is usually low (in the µM concentrations level), which means that cells will usually synthesise their own pool of GSH, starting from constitutive amino acids [58].

1.6.2 Synthesis.

The synthesis of glutathione is carried out in two steps, first the formation of the peptide bond between L-glutamate and L-cysteine and then the addition of glycine. A schematic of glutathione synthesis is presented in Fig 1.5.

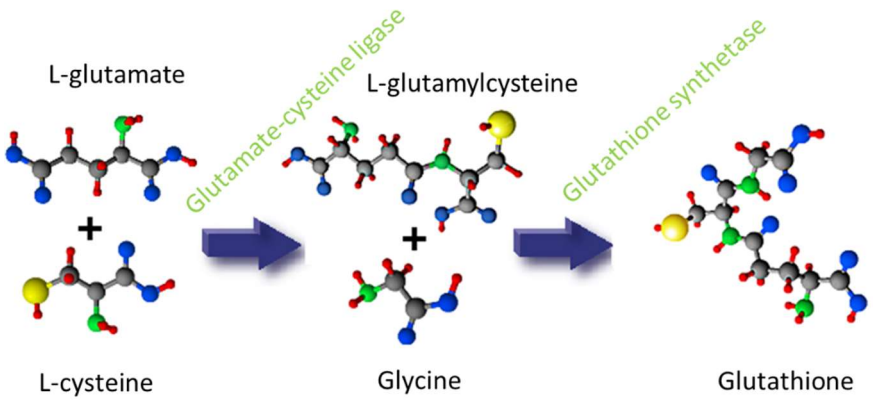

Figure 1.5: Synthesis of glutathione, where atoms colouring key is *grey*: carbon, *blue*: oxygen, *red:* hydrogen, *yellow*: sulphur and *green*: nitrogen.

1.6.2.1 Linking glutamate and cysteine.

The GSH cycle in the human body, from formation to usage has been extensively characterised [59-61]. The first step in the generation of *de novo* GSH is the conjugation of L-glutamate with L-cysteine, mediated by the enzyme glutamate-cysteine ligase (GCL). Some scientific publications use the denomination γ-glutamylcysteine synthetase to (GCS) for this enzyme [62, 63], but nowadays the term GCL is preferred. This reaction is considered to be the rate limiting step of the overall synthesis.

1.6.2.2 Intracellular glutamate.

Similarly to GSH, glutamate is not readily available to cells as it cannot pass through the cell membrane and needs to be "synthesised on demand". The rate of formation of glutamate was measured in erythrocytes using a mixture of ^{1}H-^{13}C Nuclear magnetic resonance (NMR) technique and Mass spectrometry (MS) technique [64]. While levels of *de novo* radiolabelled GSH were below the limit of detection for NMR analysis, MS data were used to prove that it was formed by consumption of radiolabelled glutamate produced by the alanine aminotransferase pathway (enzyme mediating the formation of glutamate and pyruvate from reaction between α-ketoglutarate and alanine), which was not considered to be the major contributor before. Other pathways for the formation of glutamate involve an aspartate aminotransferase pathway, similar to the one described above, and an enzymatic conversion of glutamine to glutamate using glutamine aminohydrolase.

Glutamate can also be made available to the cell by consumption of extracellular GSH [65]. In short, transpeptidases present on the cell membrane can catalyze the tranformation of GSH back into glutamate and cysteinylglycine. The glutamate then forms a new peptide bond with another extracellular amino acid and the resulting "gamma-glutamyl amino acid" can then penetrate into the cell. This intermediate can then be hydrolysed back to the free amino acid and a cyclic version of glutamate, 5-oxoproline, intracellularly. The mechanism of conversion of 5-oxoproline to glutamate has been described in detail [59].

1.6.2.3 Sourcing cysteine.

Cysteine is a semi-essential amino acid that can be synthesized in the body from a variety of precursors such as N-acetylcysteine. It is obtained in the liver by degradation of proteins, L-homocysteine or L-cystine [66]. When cysteine cannot be sourced from a precursor in cells, cells might use extracellular GSH instead. As the liver excretes some GSH to the blood system to maintain a plasma level of GSH of a few µM [67], this extracellular GSH can then be degraded back to cysteinylglycine (as described above for the sourcing of glutamate) which is then degraded further to cysteine by the action of a dipeptidase.

1.6.2.4 Linking glutamyl-cysteine and glycine.

The second step in the synthesis of GSH is the linkage of the glutamyl-cysteine peptide with the final amino acid required, glycine. Glycine is readily available in cells by enzymatic degradation of serine by serine hydroxymethyltransferase. The reaction between glutamyl-cysteine and glycine is enzymatically mediated by glutathione synthetase (GS).

1.7 Glutathione in skin metabolism.

1.7.1 Reactivity.

The detoxification of xenobiotics by GSH can occur either by direct binding of this molecule to the reactive species involved, or by conjugation reactions enzymatically mediated by GSTs.

The ability of GSH to react non-enzymatically with electrophiles has been considered as an advantage to investigate possibilities for the development of *in vitro* tests for skin sensitisation. In this context, GSH has mostly been used as a model peptide for measuring the reactivity level of chemicals with thiols, regardless of the biological relevance of GSH itself in skin detoxification. Strong and extreme sensitisers have been shown to deplete a significant amount of GSH within 15 minutes, when a 100 molar excess of chemical compare to GSH was used, whereas non-sensitisers did not [19].

Direct reaction with GSH has been assessed for 24 skin sensitisers, for which a sensitisation potential had previously been established using the Local Lymph Node Assay (LLNA) [68]. The output of this assay was the concentration of reagent able to deplete 50 % of the reduced glutathione available, called EC_{50}. For practical reasons, toxicologists tend to define a pEC_{50} value, which is the negative logarithm of EC_{50}. Even though the results of this assay cannot be used on their own to discriminate between different potencies of sensitisation, it is noticeable that all skin sensitisers had a pEC_{50} value higher than -0.55. Bearing in mind that a level lower than this threshold is not a guarantee that this chemical cannot be modified metabolically to become reactive, this approach can still be used as part of a first screening assessment, as a part of a selection of assays, to determine the potential of a chemical to be a direct sensitiser.

It is noticeable, that sometimes, the GSH conjugates formed with certain xenobiotics do exhibit comparable or even enhanced levels of toxicity to the cell than the original compound itself. This finding was highlighted in a review publication of the different aspects of GSH cellular involvement, citing the reactivity of the conjugate 2-bromoethylglutathione [69], based on the work carried out by others [70]. The nephrotoxicity of GSH conjugates derived from halogenated alkenes has also been demonstrated [71]. A mechanistic pathway was presented, explaining that toxicity was obtained from the degradation of glutathione S-conjugates, formed in rat liver, which

were transported to the kidneys where they got processed back into cysteine conjugates and finally bioactivated to very reactive thione (R – C = S) or thioketene (R = C = S) derivatives by cysteine conjugate β-lyase.

Increase in reactivity after reaction with GSH has also been reported. The reaction of the strong skin sensitiser 5-chloro-2-methylisothiazol-3-one with histidine residues of human serum albumin, used here as a model protein for haptenation studies, has been enhanced when the compound was first left to react with catalytic amount of GSH, yielding a chlorothioacyl intermediate, which showed a considerably increased reactivity towards protein nucleophiles [72].

1.7.2 Glutathione S transferases (GSTs) in skin.

GSTs are one of the major superfamily of enzymes catalysing conjugation reactions and have been classified into subfamilies. Approximately 90 % of GSTs in humans belong to the α, μ, or π families, while τ, σ, ω, ζ and κ families are represented to a much lower extent [73]. An example of human GSTA1-1 in complex with GSH is presented in Fig 1.6.

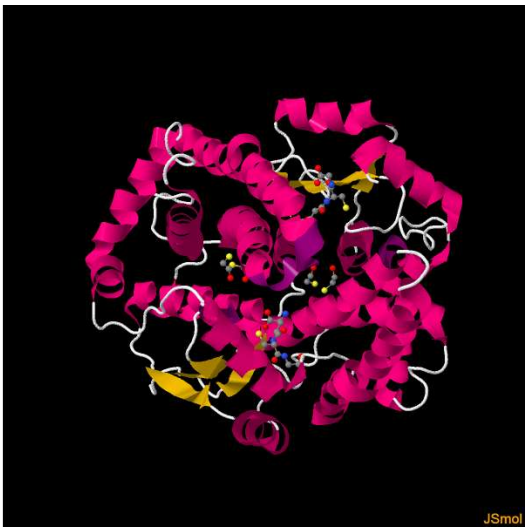

Figure 1.6: Crystal structure of human glutathione transferase (GST) A1-1 in complex with glutathione. Figure reproduced from Protein Data Bank [74].

GSTs are dimeric structures, with each monomer containing two reactive domains [75]. The first domain is called the N-terminal domain and is the preferred location for the activation of GSH (detail of the activation next to a Tyr amino acid is presented in Fig 1.7) to enhance its reactivity by increasing the nucleophilicity of the sulphur (GSH can then be represented by a GS^- species bound to the enzyme).

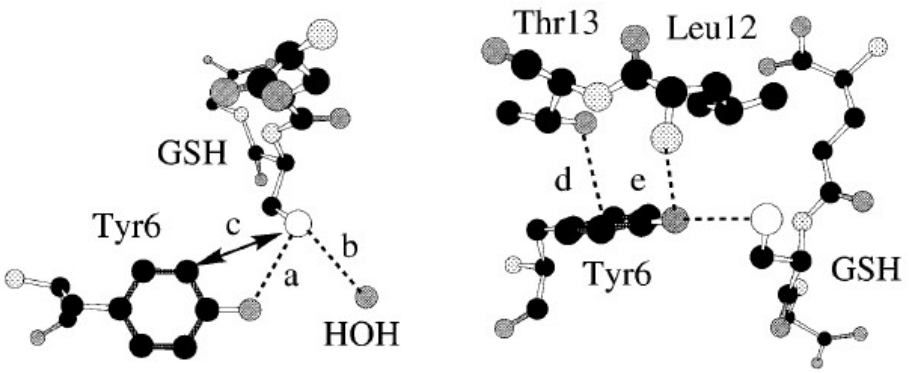

Figure 1.7 : Two views of the first-sphere and second-sphere electrostatic interactions in the active site of the M1-1 GSH transferase from rat. The first-sphere interactions with the sulfur of GSH include: a) the hydrogen bond with the hydroxyl group of Y6, b) a coordinated solvent molecule (or NH_4^+) and c) an interaction with the electropositive edge of the aromatic ring of Tyr6. The second-sphere interactions involve: d) an on-face hydrogen bond between the hydroxyl group of Thr13 and the π-electron cloud of Tyr6 and e) a hydrogen bond between the main –chain amide of Leu12 and the hydroxyl group of Tyr6. Carbon, oxygen, nitrogen and sulfur atoms are illustrated in black, gray, light-gray and white respectively. Figure reproduced from [75].

The second domain contains the xenobiotic binding site and is referred to as the C-terminal domain. This is where the electrophile is located, ready for reaction with the activated GSH.

Intermediates of reaction can be observed inside the active site of the enzyme and after completion, the product glutathione-conjugate tends to face on the outside of the site, ready for release [75]. The catalysed reaction of GSH with 1,3,5-trinitrobenzene yields S-(*p*-bromobenzyl)-glutathione and the chemical intermediate of this reaction is known as the Meisenheimer complex (Fig 1.8). This particular complex was used to illustrate

the transition state happening inside hP1-1 GST during nucleophilic substitution at the aromatic ring of electrophiles [76].

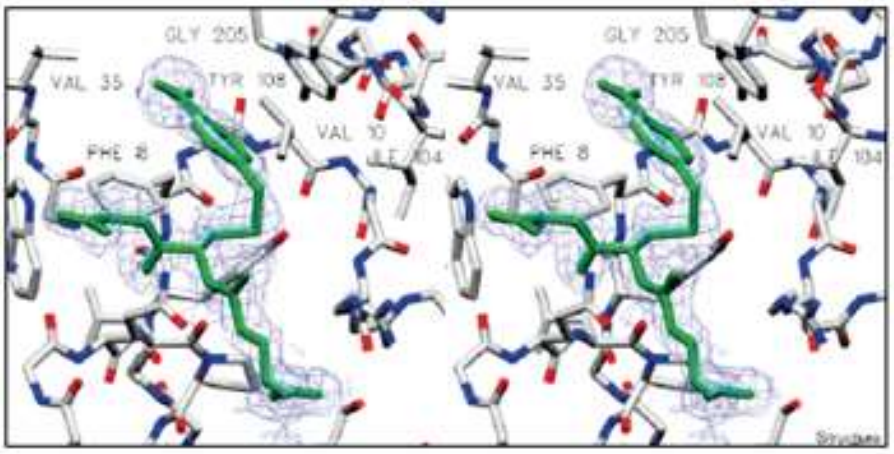

Figure 1.8 : Representation of the Meisenheimer complex in the active site of GST *h*P1-1*:* Stereo representation of the active site of GST *h*P1-1 in complex with S-(p-bromobenzyl)-glutathione (cyan). The [2Fo-Fo] map is derived from this structure and contoured at 1.0σ (shown in blue). All residues from one monomer participating in the active site are shown, but only the residues from the H-site are labelled. The S-(p-nitrobenzyl)-glutathione moiety, from the structure of GST *m*P1-1 in complex with it is superimposed and shown in green. Figure reproduced from [76].

Several studies investigated the presence and enzymatic activity of GSTs in human skin. The three main isozymes of GST that could be found in skin all belonged to either the alpha-family or pi-family of GSTs [77]. Also the 10-15 % of enzyme activity that could not be recovered using their affinity column could be putatively assigned to isozymes of the theta family. Samples were differentiated as per gender (6 females and 8 males) and it was reported that GST activity levels towards DNCB were higher in women than men by a 1.7 fold, the GST activity expressed as mU per g of wet tissue being 1320±180 and 760 ±120 respectively. GST protein levels were also found to be higher in females than males.

To confirm the presence of these isoenzymes, histological studies of skin samples were carried out separating the skin strata. The presence of class pi-GSTs was demonstrated in all skin cells, with the majority of enzymes being located in the *stratum basale*. Class mu-GSTs have also been mainly found in the *stratum basale*. In contrast, most of the

class alpha-GSTs were found in the upper layers of the epidermis. All GST classes were poorly represented in the dermis, where low level of staining could be observed in fibroblasts [78].

Cell cultures have been used to investigate the involvement of GST-P1 1(pi- family) in signalling pathways linked to detoxification, even though the total GST activity measured seemed to vary significantly depending on the type of cell used [79].

1.7.3 Excretion of glutathione conjugates.

Glutathione conjugates and GSSG are toxic for cells and therefore need to be removed from the intercellular space. Glutathione conjugates can be transported as they are or after conversion to mercapturic acid derivatives (this is achieved by a combination of enzymes: glutamyltranspeptidase removes the glutamyl group after which N-acetyltransferase acetylates amine of the cysteine residue) [80]. The transport through the cell membrane is ATP dependent and carried out by transporters called multidrug resistance-associated protein (MRP). There are six isoforms of MRP in human. These proteins have been described as “efflux pump” systems and have been identified in different kind of cells and tissues.

It has been shown that MRP1 and MRP2 are involved in the transport of glutathione conjugates [81] but this role can also be carried out by MRP6 as has been highlighted in a Chinese hamster ovary cell line [82]. The efflux of GSSG from blood cells by MRP1 transport has recently been demonstrated [83]. Few studies have tried to characterise efflux pumps in human skin, but it has been reported that MRP1 played a role in the absorption of drugs. The skin absorption of rhodamine 123, [^{3}H]-vinblastine, and [^{3}H]-LTC4 was significantly decreased when the skin was previously treated with MRP1 inhibitors [84].

1.8 Glutathione antioxidant properties.

1.8.1 Definitions.

1.8.1.1 Oxidative stress

Whatever the nature of the chemical modification occurring during or after absorption, the skin tries to detoxify foreign compounds using a battery of mechanisms, among which antioxidants play a major role. Depending on nature and chemical structure, certain external chemicals can interact with some biomolecules leading to the formation of radical species and/or Reactive Oxygen Species (ROS), able to cause further oxidative damage. Oxidative stress is a broad term used to qualify, on the one hand, the process involved in the formation of ROS and on the other hand, the ending result due to the imbalance induced in the biological system studied.

1.8.1.2 Redox state

Technically, the Redox state of a living cell can be defined as the sum of the variation of all the potentials of the redox couples present in it. Even though the potential of the cell would remain relatively stable, in theory, while the cell is in an undisturbed healthy state usually maintained by the principle of homeostasis, sudden imposed variations lead to an imbalance of these potentials and this is what most scientists defined as oxidative stress. This is why the investigation of redox state has gained importance over the years [85]. However, very few studies describe biological systems in the way they would describe an electrochemical cell [86]. This is probably due to the fact that 1) there are many redox couples involved in the homeostasis of cells and measuring all of them simultaneously is unrealistic, 2) the potentials need to be measured in an isolated

system such as a single cell, while the system is still viable, which is technically challenging.

1.8.2 Role of glutathione in the cell redox state.

The protective role of GSH, both by conjugation with electrophiles and reduction by oxidative species, has been recently reviewed [58]. Indeed, GSH has the ability to act as a radical scavenger by oxidation of its cysteine residue and therefore helps to maintain the level of ROS in cells. The oxidised cysteine can then react with another cysteine residue in a nearby molecule of GSH, resulting in the formation of GSSG. This reaction is enzymatically controlled by Glutathione Peroxidase (GPx). In mammals, four isoenzymes of GPx have been identified: cytosolic GPx, plasma GPx, phospholipid hydroperoxide GPx and gastrointestinal GPx, whose location in the body, abundance and function are tissue specific [87].

GSSG is actually harmful to a cell, therefore to maintain a healthy level, GSSG needs to be excreted or regenerated back to GSH. The reduction of GSSG into two molecules of GSH is an enzymatic reaction involving Glutathione Reductase (GR) and Nicotinamide adenine dinucleotide phosphate (NADPH) as a reducing agent (Fig 1.9). To investigate the role of GR in re-establishing the levels of GSH after chemical exposure, it is possible to inhibit this enzyme using 1,3-bis(2-chloroethyl)-N-nitrosurea (BCNU) or carmustine. A thorough review of the enzymes involved in the redox cycle of GSH is available [88].

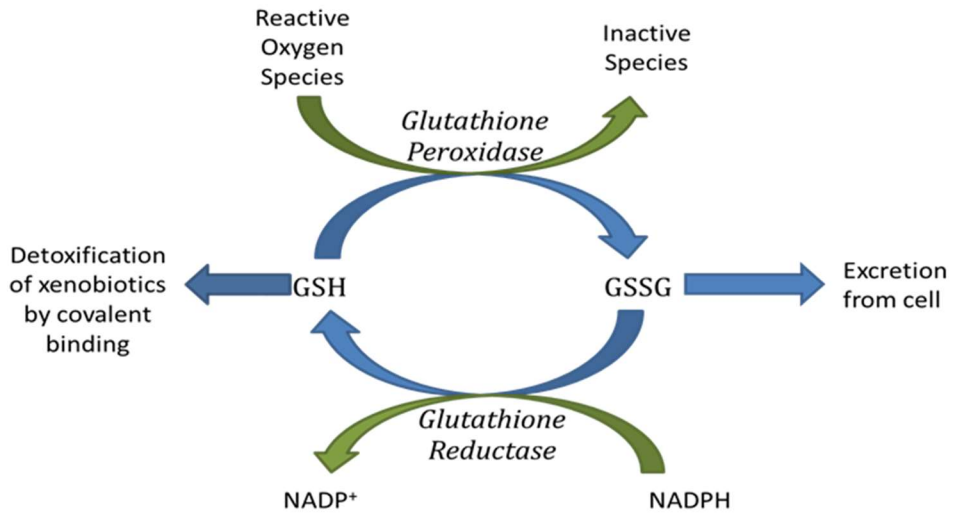

Figure 1.9 : The redox cycle of GSH

The role of GSH as a protective mechanism against ROS has been investigated in the HaCaT cell line [89] using highly reactive quinones. Cells were exposed to various 1,4-naphthoquinones and then analysed for total glutathione, ROS formation and DNA damage. The level of GSH and GSSG were determined and most of the quinones tested highly depleted the pool of GSH, sometimes in conjunction with formation of GSSG, especially when the production of ROS was enhanced in the cells.

The effect of cadmium on the cellular antioxidant systems was similarly studied [90]. HaCaT cells were treated with different concentrations of Cd (3 to 100 µM) with or without previous treatment with a reagent capable of depleting the GSH pool available, L-buthionine sulfoximine (BSO). The level of total glutathione was evaluated and levels of activity for GPx and GR were measured. Both GSH and GSSG levels increased in cells treated with Cd only, but GSSG levels were not linked to modifications of enzyme activities. A decrease in the ratio GSH/GSSG was observed and linked to a modification of intracellular redox status probably due to an increased generation of ROS. Indeed, when cells were pretreated with BSO, a high concentration of Cd induced DNA damage.

Even though GSH is mostly acting as a scavenger of ROS, its reducing capacity towards metal can sometimes be a disadvantage in terms of detoxification. Indeed, GSH can actually increase the production of ROS. When a metal ion is reduced by GSH, it can consequently be regenerated to its ion state by molecular oxygen, which acts in this context as an electron acceptor, yielding a superoxide anion [69].

1.8.3 The GSH:GSSG ratio.

The variation of the ratio GSH:GSSG is accepted as a reliable way of measuring the effect of oxidative stress [67]. This is a direct consequence of the assessment of the variation in potential in the cell (expressed in mV) due to the variation in concentration of the compounds of the redox couple 2GSH:GSSG [86].

The Nersnst equation for this redox couple, at a temperature of 25 °C, is as follows:

$$\Delta E = \Delta E° - 59.1/2 \times \log Q$$

Where: ΔE = voltage of the electrochemical cell studied (in mV, at a fixed pH), $\Delta E°$= voltage at standard conditions (for example at pH 7.4 and 25 °C $\Delta E°$=-240mV for the 2GSH/GSSG redox couple) and $Q = (\text{Concentration of GSH})^2 / (\text{concentration GSSG})$.

Therefore, the measurement of Q is a way to estimate oxidative stress in cell. However, for convenience, most publications report the ratio GSH:GSSG instead of GSH^2:GSSG. Even though the exact ratio GSH:GSSG can vary depending on the type of organelles, cells or tissues investigated, it is estimated that the overall ratio, in healthy cells resting at homeostasis state, should be approximately 100:1 [52, 86].

Difficulties with assessing the levels, and hence, the ratio, of GSH and GSSG in biological samples such as blood, have long been linked to sample preparation. It was suggested that up to 2-3 % of the glutathione present could be turned into GSSG during sample preparation, leading to an erroneous evaluation of the ratio [91]. This issue was

removed when a thiol blocking reagent was used to derivatise the reduced GSH and enzymes were inhibited using acidic conditions.

1.9 Analytical methods to identify and measure glutathione.

A number of studies have reported a variety of analytical techniques used for the measurement of reduced and oxidised glutathione [92-95]. Methods include spectrophotometric detection, fluorescence analysis, electrochemistry measurements, High Pressure Liquid Chromatography (HPLC) and more recently Mass Spectrometric (MS) methods.

1.9.1 Spectrometric assays.

Most spectrometric assays have been developed using at least one enzyme involved in the glutathione cycle. The analytical technique relies on monitoring the formation of adduct formed by reaction of GSH with a selected reagent. A method to measure the amount of GSH available in hepatic homogenates has been developed by Brigelius and colleagues [96], based on the reaction of available glutathione with DNCB after the addition of glutathione S transferase. The formation of the resulting conjugate is monitored spectrophotometrically at 340-400 nm. This methodology forms the basis of many commercially available kits for measuring glutathione S transferase activity levels. Another procedure has been developed to assess both GSH and GSSG using 5,5'-dithiobis(2-nitrobenzoic acid) (DTNB) and glutathione reductase in the presence of NADPH [97].

1.9.2 Fluorescence assays.

Fluorescence assays are based on the detection of glutathione after its derivatisation with a reagent such as monobromobimane, o-phtalaldehyde [98, 99] or a naphthalene derivative containing selenium [100], the latter presenting the advantage of being an effective colorimetric agent as well. The resulting glutathione-reagent conjugate exhibits fluorescent properties and can be measured using a fluorescent spectrophotometer. These assays are especially popular as they only require simple sample preparation and the analytical equipment used is relatively inexpensive compared to mass spectrometers. Their major drawback however, is the range of concentrations covered by these assays, usually optimum for samples containing hundreds of μM to mM levels of GSH.

1.9.3 Liquid Chromatography-Mass Spectrometry.

High Pressure Liquid Chromatography (HPLC) is used to physically separate a selection of analytes by their affinity with the solid phase of a chromatographic column. This piece of equipment is used in conjunction with Ultra Violet (UV) [101], fluorescence (described above) or chemiluminescence [102] detectors as well as mass spectrometers. Due to the high hydrophilicity of GSH, poor retention on conventional reverse-phase columns is observed. To solve this problem, as well as protect the thiol group of GSH from autoxidation into its disulfide, GSH is usually derivatised with a reagent such as N-ethylmaleimide (NEM) [103, 104], Ellman's reagent [105] or iodoacetic acid [101, 106]. More recently HILIC (Hydrophilic Interaction Liquid Chromatography) separation technology has been used for the analysis of GSH and GSSG [107].

Liquid Chromatography-Mass Spectrometry (LC-MS) is routinely carried out using an ESI (Electrospray) source operating in positive ionisation mode. The detection of the parent ion $(M+H)^+$ for both GSH and GSSG can be achieved using most types of mass spectrometers. When GSH has been modified by haptenation and the mass of the final adduct is unknown it is possible to track back its presence by monitoring the neutral loss of m/z 129 (formed by the loss of pyroglutamate moiety, characteristic method for MS glutathione detection) in newly appearing peaks (Fig 1.10).

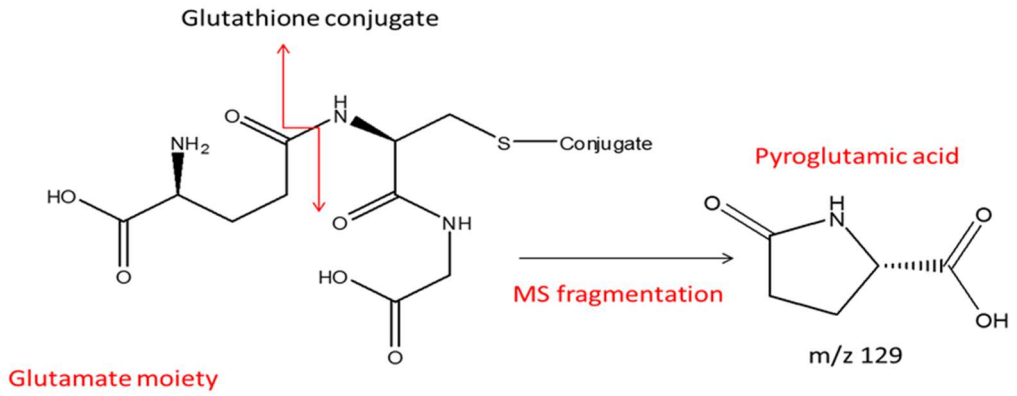

Figure 1.10 : Mass spectrometric fragmentation of GSH conjugate showing the neutral loss m/z 129

1.10 Thesis aims and objectives.

1.10.1 Hypothesis.

Current mechanistic understanding of the role of reactivity in skin sensitisation rests on the premise that a reactive chemical has the potential to sensitise via irreversible conjugation to protein nucleophiles in the skin and thus generate an antigen. The modification of cysteine residues present in proteins has been demonstrated to be an important reaction for a range of skin sensitisers. The aim of this report is to demonstrate that the reactivity of such sensitisers with a small free thiol, GSH, plays an

important role in the clearance mechanism of human skin, thus potentially preventing or at least limiting the amount of reactive compound available to react with proteins. The study also highlights the ability of human skin to generate *de novo* GSH as a defense mechanism against xenobiotics and thus compensate for the consumption of the thiol involved in the clearance process to maintain healthy levels of protective GSH in cells.

1.10.2 Choice of chemicals.

This investigation covered a range of chemicals, with various potential for skin sensitisation.

DNCB (Fig 1.11) is a chemical intermediate with few reported commercial uses on its own and is mostly used for the production of various dyes [108]. It can also be used for synthesising 2,4- dinitrophenylhydrazine, a reagent used for the characterization of carbonyl compounds or dinitrophenylrhodanate, an insecticide.

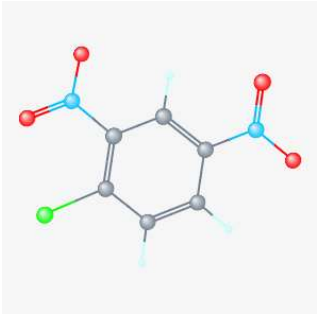

Figure 1.11 : 1-chloro-2,4-dinitrobenzene 3D chemical structure. Reproduced from PubChem [109], where the colouring of atoms is *grey*: carbon, *white*: hydrogen, *blue*: nitrogen , *red*: oxygen and *green*: chlorine.

DNCB is mostly used for laboratory research purposes and a few clinical assessments involving topical application [110, 111]. Contact allergy to DNCB is a cell mediated hypersensitivity that has been used as a tool to detect patients with deficiencies in cell mediated immunity since the 60s. Potent contact sensitisers, such as DNCB, have been used by a few dermatological clinics to treat conditions such as alopecia areata and viral

warts, with various degree of success [112]. DNCB is also a very good substrate for GST [113] and is usually provided as part of commercial kits to measure GST enzymatic activity spectrometrically.

1-bromo-2,4-dinitrobenzene (DNBB) (Fig 1.12a) and 1-fluoro-2,4-dinitrobenzene (DNFB) (Fig 1.12b) are structurally related to DNCB.

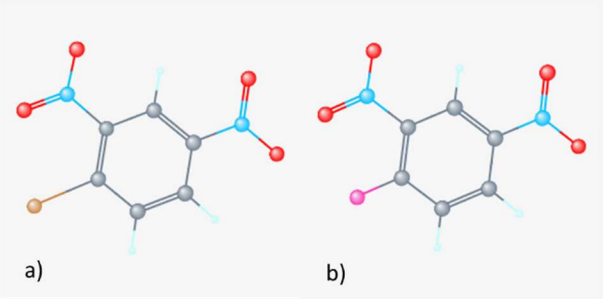

Figure 1.12 : a) 1-bromo-2,4-dinitrobenzene and b) 1-fluoro-2,4-dinitrobenzene 3D chemical structures. Reproduced from PubChem [109] where the colouring of atoms is *grey*: carbon, *white*: hydrogen, *blue*: nitrogen , *red*: oxygen, *orange*: bromine and *pink*: fluorine.

DNBB has little use on its own. However DNFB is used in the sequencing of polypeptides. The analysis of terminal amino acids after reaction with DNFB to sequence the polypeptides is based on the work of Sanger, who used it in his discovery of bovine insulin [114], hence DNFB is often called Sanger's reagent. Both compounds react with GSH *in chemico* [115].

The synthesis of diphenylcyclopropenone (DPCP) (Fig 1.13) was reported for the first time in 1959 [116] and was also obtained by another research group following a different synthesis route in 1960 [117]. This chemical was found to be a potent sensitiser with cases of contact dermatitis reported in the 70s, and started to be used for clinical treatment of alopecia areata [112, 118].

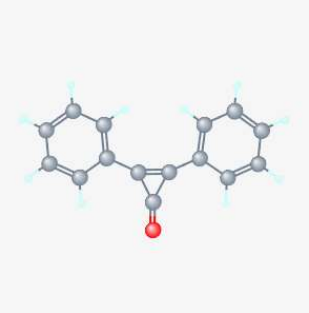

Figure 1.13 : Diphenylcyclopropenone 3D chemical structure. Reproduced from PubChem [109] where the colouring of atoms is *grey*: carbon, *white*: hydrogen and *red*: oxygen.

DPCP and its precursor of synthesis α,α'-dibromobenzylketone have been fully characterised for stability in solution and mechanism of sensitisation [119]. DPCP now tends to replace DNCB in alopecia areata treatment in the UK. It is known to react with GSH [19].

Diethyl maleate (DEM) (Fig 1.14) is a chemical intermediate involved in the synthesis of many industrial products including polymers [120].

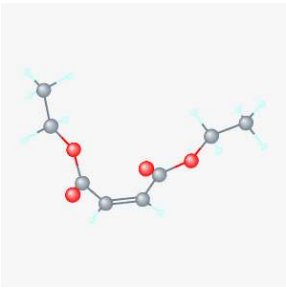

Figure 1.14 : Diethyl maleate 3D chemical structure. Reproduced from PubChem [109] where the colouring of atoms is *grey*: carbon, *white*: hydrogen and *red*: oxygen.

It has a moderate potential to be a skin sensitiser. When, DEM was applied as part of a battery of patch tests for patients with suspected allergy to dimethyl fumarate, 21 out of the 37 patients had a positive reaction [121]. DEM is known to react with GSH [19] and has been used to deplete stocks of GSH in tissues [122]. The level of depletion reported, however, is not complete and residual level of GSH is observed, with total

depletion only observed when both DEM and L-buthionine sulfoximine (BSO) are used simultaneously [123].

Benzaldehyde (BA) (Fig 1.15a) is a colourless liquid, industrially prepared from toluene.

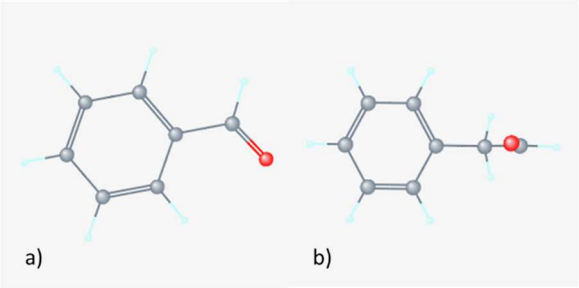

Figure 1.15 : a) Benzaldehyde and b) phenylacetaldehyde 3D chemical structures. Reproduced from PubChem [109] where the colouring of atoms is *grey*: carbon, *white*: hydrogen and *red*: oxygen.

It is widely used in the industry as a chemical intermediate to produce other more complex organic compounds. As BA has a pleasant almond smell it is also used directly as a flavouring or fragrance additive in consumers products. BA is not considered to be a skin sensitiser in the LLNA [124], however there are a few reports of allergy to BA [125]. Its volatility and quick metabolism to benzoic acid in skin make it generally safe to use [126]. Phenylacetaldehyde (PA) (Fig 1.15b) is a common fragrance that is structurally very similar to BA with the addition of one carbon between the benzoic ring and the aldehyde function. It is widely used in perfumed personal care products due to its pleasant hyacinth smell. It is considered a moderate skin sensitiser in the LLNA [124]. It did not react with GSH in the specific experimental conditions used in the *in chemico* assay used by Gerberick et al [19].

1.10.2 Research overview.

As the maintenance of metabolic activity in *ex vivo* skin is still variable and dependent on the techniques used to handle the freshly collected samples before they reach a tissue bank, experimental work investigating the detoxification of sensitisers was carried out using the HaCaT cell line and the RHE model.

First, the study aimed to characterise the GSH cycle in the HaCaT cell line. The GSH basal level was determined in healthy cells. The activity of GSH related enzymes was then altered and the overall effect on GSH levels measured. The inhibition of GCL, essential to the *de novo* synthesis of GSH, was carried out with BSO. To generate an imbalance in the ratio of GSH: GSSG in the cells the model oxidant H_2O_2, as well as aldehydes (BA and PA), were used. The detection of GSSG was attempted by blocking, or at least reducing, the activity of Glutathione Reductase (GR) with inhibitors such as 2-AAPA and carmustine (BCNU).

The HaCaT cell line was then used to demonstrate the detoxification of model sensitisers of different potencies by GSH. GSH dose response to sensitisers as well as 24h time course experiments were carried out with a moderate sensitiser (DEM), an extreme sensitiser (DPCP) and a series of dinitrohalobenzenes, which were also extreme sensitisers (DNCB, DNFB and DNBB).

The metabolic clearance of these sensitisers in the HaCaT cell line, though similar in terms of GSH reactivity to the expected metabolic activity of GSTs in skin, might differ in terms of kinetics, mostly due to the ease of penetration of the compounds in monolayer cultures. To compensate for this phenomenon, the detoxification of DNCB was investigated after topical application on a 3D keratinocyte culture, the Reconstructed Human Epidermis (RHE) model. The first experiments aimed at establishing the suitability of the RHE model for DNCB clearance over 24 hours, by measuring the level of GSH and the formation of the GSH conjugate DNP-SG. However, the main advantage of the RHE model remained the fact that the samples could potentially be maintained in culture for

long periods of time (at least 48 hours when cultured according to the manufacturer's recommendations). This allowed for the development of an *in vitro* strategy to investigate exposure to a chemical (in this case the model sensitiser DNCB) applied on a daily basis. This approach was tested for three cycles of exposure on the RHE model and could provide information on the biological impact (i.e variations of metabolic capacity) of daily exposure to cosmetic products on human skin.

The data generated using this methodology provides information on the chemistry involved in the detoxification of potential sensitisers and, though not an MIE of skin sensitisation in itself, is to be considered along with haptenation to proteins, which could lead to ACD, for future risk assessment. The protective effect of Phase II metabolism, especially GSH clearance, is not currently quantified in skin and information about the bioavailability of potential skin sensitisers mostly rely on skin penetration experiments. It is expected that data generated *in vitro* using 3D skin models exposed daily to new chemicals can be extrapolated into a mechanistic model for assessing their skin sensitisation potential for the general population.

Chapter 2: Materials and Methods.

Contents

2.1 Materials.

2.1.1 Skin models.

The HaCaT cell line was a kind gift from Prof. N. Fusenig (University of Heidelberg, Germany), received at passage 30 and 34 in 1993, cryopreserved in Unilever laboratories.

Reconstructed Human Epidermis (0.5 cm^2 aged for 17 days) was supplied by Episkin (Lyon, France).

2.1.2 Chemicals and reagents.

2-acetylamino-3-[4-(2-acetylamino-2-carboxyethylsulfanylthiocarbonylamino) phenylthiocarbamoylsulfanyl] propionic acid (2-AAPA), ammonium bicarbonate, benzaldehyde (BA), carmustine (BCNU), L-buthionine sulfoximine (BSO), diethyl maleate (DEM), 1-bromo-2,4-dinitrobenzene (DNBB), 1-chloro-2,4-dinitrobenzene (DNCB), 1-fluoro-2,4-dinitrobenzene (DNFB), diphenylcyclopropenone (DPCP), reduced glutathione (GSH), glutathione disulfide (GSSG), glutathione-[glycine $^{13}C_2$,^{15}N], iodoacetic acid (IAA), 3-(4,5-dimethyl thiazol-2-yl)-2,5-diphenyltetrazolium bromide (methyl tetrazolium, MTT), phenylacetaldehyde (PA), radio immunoprecipitation assay (RIPA) buffer, sulfosalicylic acid, and trypsin-ethylenediamine tetraacetic acid (EDTA) solution (containing 0.25 % trypsin) were purchased from Sigma Aldrich (Gillingham, UK) and used without further purification.

Solvents with a minimum HPLC grade purity were purchased from VWR (Lutterworth, UK) or Sigma Aldrich (Gillingham, UK).

Dulbecco's Modified Eagle's Medium (DMEM) high glucose content, sodium bicarbonate, L-glutamine and sodium pyruvate were supplied by Life Technologies Ltd under the brand Gibco© (Paisley, UK). Foetal calf serum (FCS) and penicillin/streptomycin solution were supplied by PAA Laboratories Ltd (Yeovil, UK). Reagents required for Western blotting were supplied by Life Technologies Ltd under the brand NuPage© (Paisley, UK). Anti-Nrf2 and anti-beta actin antibodies were supplied by Abcam (Cambridge, UK). The secondary antibodies anti-rabbit IgG and anti-mouse IgG were supplied by Sigma Aldrich (Gillingham, UK).

RHE maintenance medium and RHE growth medium were supplied by Episkin (Lyon, France).

Dinitrophenyl-glutathione (DNP-SG) was synthesised using a method described elsewhere [127] with a few modifications. Briefly, 0.3 g of GSH were dissolved into 8 mL of ultrapure water and 0.2 g of DNCB were dissolved into 3 mL of acetonitrile. The two solutions were mixed and the pH adjusted to approximately 8 using a few drops of 1 N sodium hydroxide. The mixture was mixed at ambient temperature for 30 minutes after which the supernatant was collected. This solution was dried using a Thermo Savant Explorer vacuum centrifuge and the resulting crystals collected. Purity was assessed by Nuclear Magnetic Resonance (NMR). The crystals contained 39 % DNP-SG and DNP-SG stability in aqueous solution was unaffected for 26 hours at ambient temperature.

2.2 Methods.

2.2.1 Skin models culture and maintenance.

2.2.1.1 HaCaT cell line.

HaCaT cells were cultured as described by Boukamp and colleagues [30]. Briefly, the cells were maintained in cell culture medium consisting of DMEM high glucose content supplemented with final concentrations of 0.37 % sodium bicarbonate, 10 % heat inactivated FCS, 2 mM L-glutamine, 1 mM Sodium pyruvate and 100 U/mL /100 µg/mL penicillin/streptomycin, in an atmosphere of 5 % carbon dioxide in air at 37 °C. Cells were subcultured by trypsinisation at intervals of 3-4 days.

2.2.1.1 RHE samples.

The RHE samples were delivered in agarose-filled plates for model preservation. Upon receipt, the inserts were removed from the agarose bedding and immediately placed in 6-well plates containing 2 mL maintenance or growth medium per well. The plates were then incubated at 37 °C in an atmosphere containing 5 % CO_2 until use. The medium was refreshed daily as recommended by the supplier.

Initial method development was carried out to select an appropriate medium into which the RHE samples could be cultured so that their ability to synthesise GSH was not compromised. Samples were cultured in maintenance medium for up to 48 h (maximum use time of the maintenance medium as recommended by the supplier), in growth medium for up to 7 days and in HaCaT cell medium for up to 7 days for comparison. The GSH level was measured periodically for each experiment using the methods described below. In all following experiments involving RHE samples the medium used was the RHE growth medium unless specified otherwise.

2.2.2 Model compounds cytotoxicity evaluation.

2.2.2.1 MTT assay on HaCaT cells.

HaCaT cells were subcultured by trypsinisation, disaggregated into a single cell suspension and reseeded in a 96-well plate at 2 x10^4 cells/100 µL HaCaT cell culture medium/well. Cells were then incubated overnight in an atmosphere of 5 % carbon dioxide in air at 37 °C.

Stock solutions of DNCB, DNFB, DNBB, DEM, DPCP, BA and PA were prepared in dimethylsulfoxide (DMSO), stock solutions of BSO were prepared in sterile water. All stock solutions were then diluted as required in HaCaT cell culture medium so that the final DMSO content used in assays was 0.5 %. Concentrations are detailed in Table 2.1.

Compound	Concentration range
BSO	0-450 µM
DEM	0-600 µM
DPCP	0-50 µM
DNCB	0-30 µM
DNFB	0-30 µM
DNBB	0-30 µM
BA	0-20 µg/mL and 0-23 µM 0-500 µg/mL (occluded)
PA	0-500 µg/mL (occluded)

Table 2.1 : Model compounds concentrations used in the MTT assay

The MTT assay was carried out as described elsewhere [128] with a few modifications. In brief, each well was exposed to a 100 µL aliquot of reagent or solvent and the plate was incubated for 24 hours. Due to the volatility of BA and PA, the assay was also carried out under occluded conditions (96-well plate sealed with plastic adhesive film) for 2

hours. The plate was subsequently rinsed with PBS and treated with MTT (100 µL, 0.5 mg/mL) for 3 hours. The MTT solution was removed and the resulting formazan crystals were rinsed with PBS and dissolved in isopropanol (150 µL). The absorbance in each well was read at 570 nm using a SpectraMax M2e microplate reader.

Cell viability was calculated by ratio of absorbance read in cells treated with model compounds over absorbance of controls cells treated with HaCaT culture medium containing 0.5 % DMSO. The results were expressed as a percentage. Acceptable viability for in vitro experiments using the HaCaT cell line was fixed at a minimum of 80%.

2.2.2.2 MTT assay on RHE samples.

A stock solution of DNCB was prepared in DMSO and appropriate dilutions of final concentrations 0.05, 0.1, 0.5, 1 and 10 mM prepared in RHE growth medium containing 10 % DMSO.

RHE samples were treated with 50 µL of DNCB solution (range 0.05-10 mM). Positive control RHE models were treated with 50 µL of 10 % DMSO in RHE growth medium. Samples were incubated for 24 hours. RHE samples were incubated in 2 mL RHE growth medium so the DMSO content in final experiments did not exceed 0.25 %. Following treatment, each RHE sample was washed with PBS, transferred to a 24-well plate containing 0.3 mL of 1 mg/mL MTT solution in RHE growth medium per well and incubated for approximately 3 hours in an atmosphere of 5 % carbon dioxide in air at 37 °C. The RHE samples were then carefully washed with PBS and transferred to a 12-well plate containing 2 mL of isopropanol per well. The plate was shaken at approximately 300 rpm for 10 minutes, placed into a sealable plastic bag and stored refrigerated overnight to extract the formazan crystals formed. Aliquots of each isopropanol extract were

transferred to a 96-well plate and the remaining steps of the assay carried out as described previously.

2.2.3 Model sensitisers treatment of the HaCaT cell line: Dose responses.

HaCaT cells were seeded in 6-well plates at 4 x10^5 cells per well and incubated overnight. Dilutions of DEM, DPCP, DNCB, DNFB, DNBB, BA and PA were prepared in HaCaT cell culture medium enriched with 0.5 % DMSO for use within the assay. Concentrations are detailed in Table 2.2.

The cells were treated with 2 mL of the appropriate concentration of model sensitiser solution, the plates covered and incubated (37 °C, 5 % CO_2) for 1 hour or 24 hours. The reagent solution was removed from the 6-well-plates and the cells rinsed twice with PBS. The cells were lysed by addition of 200 µL ultrapure water and one cycle of freeze-thawing at -80 °C.

The assay was modified significantly for volatile compounds BA and PA. The 6-well plates were sealed with plastic adhesive film immediately after treatment and the plates incubated for 10 minutes.

Compound	Concentration range
BSO	0-55 µM
DEM	0-150 µM
DPCP	0-30 µM
DNCB	0-30 µM
DNFB	0-30 µM
DNBB	0-30 µM
BA	0-500 µg/mL (occluded)

PA	0-200 µg/mL (occluded)

Table 2.2 : Model compounds concentrations used in dose response experiments

2.2.4 Model sensitisers treatment of the HaCaT cell line: 24 hour time course.

HaCaT cells were seeded in 6-well plates at 4 x10^5 cells per well and incubated overnight. The cells were treated with 2 mL of 10 µM of DNCB, DNFB or DNBB, 2 µM DPCP or 50 µM DEM. The plates were covered and incubated (37 °C, 5 % CO_2) for up to 24 hours. The time points investigated were 0, 10, 20 and 30 minutes and 1, 2, 4, 6, 7 and 24 hours. The reagent solution was then removed from the 6-well-plates and the cells rinsed twice with PBS. The cells were lysed by addition of 200 µL ultrapure water and one cycle of freeze-thawing at -80 °C.

2.2.5 Determination of Nrf2 release by Western blot.

HaCaT cells were seeded in 12-well plates at 1 x10^5 cells per well and incubated overnight. The cells were then exposed to concentrations of DNCB, DNBB and DNFB ranging 1-15 µM for 2 hours, rinsed twice with culture medium and lysed with 80 µL of RIPA buffer enriched with 0.2 % protease inhibitor per well. Control experiments were carried out with 0.5 % DMSO in culture medium.

Required amounts of lysates (10 µg protein for DNCB and DNFB samples, 8 µg for DNBB, adjusted for protein concentration) were denatured by reaction with 5 µL of NuPage sample reducing reagent (Life Technologies, Paisley, UK) at 85 °C for 10 minutes, loaded on gels (NuPage 4-12 % Bis-Tris gel) and separated by electrophoresis at 90 V for 10 minutes followed by 170 V for 1 hour. The content of each gel was then transferred to a nitrocellulose blotting membrane (230 mA for 65 minutes), which was stained with

Ponceau S and blocked with non-fat dry milk solution (10 % in Tris-Buffered Saline) overnight. Membranes were treated with rabbit anti-Nrf2 primary antibody for 3 hours (or mouse anti-actin primary antibody for 30 minutes) and Nrf2 secondary antibody for 1 hour. Membranes were treated with a Western Lightning plus enhanced chemiluminescence (ECL) reagent kit (Perkin Elmer, Coventry, UK) for film development. Quantification of free Nrf2 was carried out using a GS-800 calibrated densitometer and the Quantity One software version 4.6.1. Data were normalised to actin.

2.2.6 BSO treatment of the HaCaT cell line: GSH synthesis inhibition.

BSO was used an inhibitor of GCL, enzyme necessary for *de novo* GSH synthesis. HaCaT cells were seeded in 6-well plates at 4 x10^5 cells per well and incubated overnight.

In dose response experiments, the cells were treated with 2 mL of BSO solution prepared in HaCaT cell culture medium (nominal range 0-50 µM). The plates were then covered and incubated (37 °C, 5 % CO_2) for 1 hour or 24 hours.

A 24 hour time course experiment was also carried out by treating the cells with a 50 µM BSO solution (2 mL). The time points investigated were 0, 0.5, 1, 2, 4, 6, 7 and 24 hours. A control experiment was carried out with untreated cells for the same period of time. The level of GSH in each set of experiments was compared.

2.2.7 BCNU and 2-AAPA treatment of the HaCaT cell line: GSH reductase inhibition.

Stock solutions of BCNU were prepared in DMSO. Dilutions of BCNU were prepared in HaCaT cell culture medium enriched with 0.5 % DMSO (nominal range 10-200 µM). The cells were dosed with 2 mL of the various solutions and the plates incubated at 37 °C in

an atmosphere containing 5 % CO_2 for 30 minutes and 1 hour respectively. From this experiment, the influence of BCNU on GSH levels in the HaCaT cell line was investigated. The maximum concentration in BCNU that could be applied to HaCaT cells without observing any significant depletion of GSH was the maximum investigated (200 µM, 1 hour). In subsequent experiments, cells were treated with concentration of BCNU for 1 hour then washed with PBS prior to further compound dosing.

Due to the low availability of 2-AAPA, influence on the GSH/GSSG ratio was not investigated as a function of the dose applied. Instead, the concentration of 2-AAPA used to inhibit GR was based on the work published by [129]. A stock solution of 2-AAPA was prepared in a mixture water: DMSO (v/v 50:50) and diluted in HaCaT culture medium to prepare a 50 µM nominal solution. The cells were dosed with 2 mL of 50 µM 2-AAPA and the plates incubated for 2 hours at 37 °C in an atmosphere containing 5 % CO_2. The cells were then washed with PBS prior to further compound dosing.

2.2.8 BA and PA treatment of the HaCaT cell line: GSH oxidation.

HaCaT cells were plated out at 4 x10^5 cells per well in 6-well-plates and incubated at 37 °C, overnight in an atmosphere containing 5 % CO_2. Cells were either directly treated with aldehydes or pre-incubated with 2-AAPA (50 µM, 2 hours) or BCNU (200 µM, 1 hour) to inhibit GR. BA and PA stock solutions were prepared in DMSO. Subsequent dilutions were made with HaCaT cell culture medium containing 0.5 % DMSO.

For use in a 2 hour exposure time course assay, a 0.1 mg/mL BA solution and a 0.025 mg/mL PA solution were prepared. These concentrations were chosen as they do not induce more than 20 % cell death over 2 hours, as determined by the MTT assay. HaCaT cells were treated with 2 mL of each solution, the plates sealed with adhesive plastic foil and the cells left in an incubator (37 °C, atmosphere containing 5 % CO_2) for the period

of time specified (10 minutes to 2 hours).

A dose response experiment, in which cells were treated with BA at 0.1, 0.2 and 0.5 mg/mL concentration or PA at 0.025, 0.05, 0.1 or 0.2 mg/mL concentration, was also carried out. The total exposure time was 10 minutes in occluded conditions. As previously described, the experiment was carried out with cells pre-treated with 2-AAPA and cells where the activity of GR enzymes was not compromised (no pre-treatment).

H_2O_2 (HP) is known to oxidise GSH. For comparison, a dose response experiment was carried out for 4 hours in the HaCaT cell line (HP range 0-2.5 mM) and a 24 hour time course experiment was carried out with 1 mM and 2 mM HP solutions.

2.2.9 GSH incubations with model compounds *in chemico*.

All incubations were carried out in buffered conditions so that the GSH:chemical ratio was 1:10. The pH was either fixed at pH 7.4 to mimic physiological systems or pH 9.5 as the pKa of thiol in GSH is reported between 9.2 and 9.4 [130, 131].

A 50 mM buffer solution of potassium phosphate (monobasic/dibasic) at pH 7.4 was prepared in water. A 10 mM solution of ammonium bicarbonate was prepared in water. The pH was adjusted to pH 9.5 using ammonia.

GSH and GSSG solutions were prepared in buffer solution at pH 7.4 or pH 9.5 for use in the incubations. Chemicals (DEM, DPCP, BA, PA and HP) were dissolved in acetonitrile and appropriately diluted so that the final concentration was approximately 10 mM.

GSH incubations contained 1 mL of 100 µM GSH (pH 7.4 or pH 9.5) and 100 µL of each chemical in acetonitrile. Control incubations contained 1 mL of 100 µM GSH (pH 7.4 or pH 9.5) and 100 µL acetonitrile or 1 mL of 100 µM GSSG (pH 7.4 or pH 9.5) and 100 µL acetonitrile. Stock solutions of GSH and GSSG were analysed by LC-MS after 24 h refrigerated storage.

2.2.10 RHE samples single exposure to DNCB.

2.2.10.1 Initial GSH basal level determination in RHE samples.

In the first experiment, the suitability of the RHE maintenance medium (recommended by the supplier for model maintenance for up to 48 hours) was evaluated. GSH level was measured in duplicate RHE samples on the day of arrival (*t*= 0 h), after brief equilibration in maintenance medium (*t*= 3 h), which is a realistic representation of the time required to prepare solutions to treat the models, *t*= 24 h, which is a usual time at which a read-out of the experiment is carried out (i.e. end of 24 hours MTT assay) and *t*= 48 h, which is the maximum time for which the models can be maintained in the RHE maintenance medium (as recommended by the supplier). The RHE samples were washed with sterile PBS by removing each insert from the 6-well plates and continuously irrigating for 10-15 seconds. Each RHE sample was excised from the insert, placed in a heat-proof glass vial and homogenised in 2 mL of RIPA buffer using a Soniprep 150plus (MSE Ltd, London, UK). The amplitude of sonication of the probe was fixed at 6.5. Five bursts of sonication of 1 minute each were carried out per sample. The lysate produced was stored at -80 °C until analysis. A second experiment was carried out, in which the RHE samples were cultured in HaCaT cell culture medium or RHE growth medium for a period of 7 days. The medium was refreshed daily in all 6-well plates. GSH level was measured in single replicate analysis on RHE samples cultured in each medium, every 24 hours.

2.2.10.2 RHE samples exposure to DNCB: 24 hour experiment.

A stock solution of DNCB was prepared in DMSO. Solutions of 1 mM or 0.1 mM of DNCB were prepared in growth medium containing 1 % DMSO for the dosing of the RHE samples.

Triplicate RHE samples were lysed at the start of the experiment (*t*= 0 h). RHE samples were treated with 50 µL of the 1 mM (0.1 mM) solution of DNCB. After 2 hours of exposure, all RHE samples were washed with PBS. PBS rinses and growth medium aliquots from each well were collected and stored frozen at -80 °C for further analysis.

Triplicate RHE samples were lysed (*t*= 2 h) and the remaining samples placed into 2 mL of fresh growth medium and the plates incubated at 37 °C in an atmosphere containing 5 % CO_2. Triplicate RHE samples were lysed at *t*=4 h, *t*=6 h and t=24 h. For each RHE sample aliquots of growth medium and PBS rinse were collected when the lysing procedure was carried out.

2.2.11 RHE repeated treatment with DNCB.

2.2.11.1 Three cycles of treatment with DNCB: 72 hour experiment.

A stock solution of DNCB was prepared in DMSO. Solutions of 0.1 mM, 0.5 mM or 1 mM of DNCB were prepared daily in growth medium containing 1 % DMSO for the treatment of the RHE samples.

The time points investigated were *t*=0, 2, 24, 26, 48, 50 and 72 h. Triplicate RHE samples were lysed at each time point. RHE samples were treated with 50 µL of the 1 mM (0.1 mM) solution of DNCB at *t*=0, 24 and 48 h. All RHE samples were washed with PBS at *t*=2, 26, 50 and 72 h. PBS rinses and growth medium aliquots from each well were collected and stored frozen at -80 °C for further analysis.

RHE samples were incubated at 37 °C in an atmosphere containing 5 % CO_2. RHE growth medium was refreshed at *t*=2, 26 and 50 h.

The general procedure for the experiment is summarised in Fig 2.1.

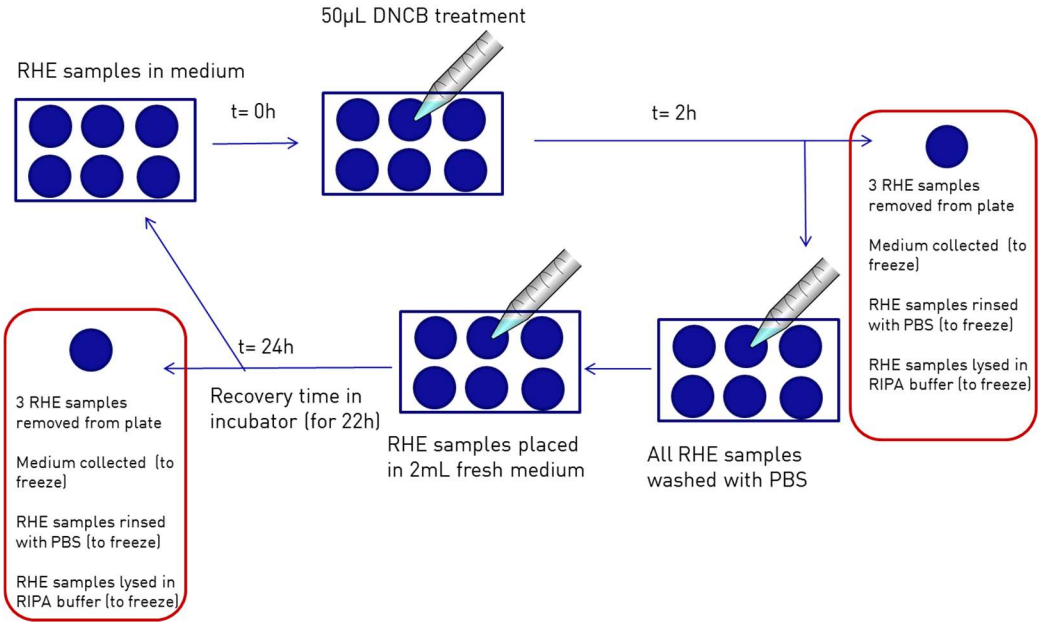

Figure 2.1: Daily exposure of RHE samples to 0.1, 0.5 or 1 mM of DNCB for 2 hours, followed by 22 hours of recovery time in fresh growth medium: experimental set-up and samples collection.

2.2.11.2 Daily 1 mM treatment with DNCB: 7 day experiment.

A stock solution of DNCB was prepared in DMSO. Solutions of 1 mM of DNCB were prepared daily in growth medium containing 1 % DMSO for the treatment of the RHE samples.

RHE samples were treated daily with a 1 mM DNCB solution following the procedure described in section 2.211.1.One RHE sample was lysed at *t*=0, 2, 24, 26, 48, 50, 72, 74, 96, 98, 120, 122, 144, 146 and 168 h. PBS rinses and growth medium samples were collected as previously described.

2.2.12 RHE lysates, PBS rinses and growth medium samples preparation for DNP-SG measurements.

400 µL of each RHE lysate or growth medium sample were mixed with 100 µL of acetonitrile and the mixture filtered through a 0.2 µm nylon centrifuge filter by centrifugation (10000 rpm, 10 min). The resulting samples were analysed. PBS rinses were analysed without any further sample preparation.

2.2.13 Determination of Nrf2 activation by Western blot.

RHE samples were submitted to three cycles of 0.5 mM DNCB treatment (72 hours experiment) as described in section 2.2.11.1. Triplicate samples were lysed at each time point in 1 mL RIPA buffer containing 1 % protease inhibitor. The samples were maintained on ice in the Soniprep 150plus (MSE Ltd, London, UK). The amplitude of sonication of the probe was fixed at 6.5 and the lysing time was 5 times 1 minute.

8 µg of lysates were denatured by reaction with 5 µL of NuPage sample reducing reagent at 85 °C for 10 minutes, loaded on gels (NuPage 4-12 % Bis-Tris gel) and separated by electrophoresis at 90 V for 10 minutes followed by 170 V for 1 hour. The content of each gel was then transferred to a nitrocellulose blotting membrane (230 mA for 65 minutes), which was stained with Ponceau S and blocked with non-fat dry milk solution (10 % in TBS) overnight. Membranes were treated with rabbit anti-Nrf2 primary antibody overnight (or mouse anti-actin primary antibody for 30 minutes) and Nrf2 or actin secondary antibody for 1 hour. Membranes were treated with a Western Lightning plus enhanced chemiluminescence (ECL) reagent kit (Perkin Elmer, Coventry, UK) for film development. Quantification of free Nrf2 was carried out using a GS-800 calibrated densitometer and the Quantity One software version 4.6.1. Data were normalised to actin.

2.2.14 Glutathione assay:Derivatisation with iodoacetamide.

The samples were derivatised using iodoacetamide (IAA) to prevent formation of disulphide bonds, following methods described by [106] [132] . Briefly, 1 mM stock solution of GSH was prepared in ultrapure water and subsequently diluted with ultrapure water to prepare a set of calibration standards covering the range 0.5-200 µM (final concentrations analysed 0.05 to 20 µM). An identical procedure was used to prepare a matching set of calibration standards for GSSG (final concentrations analysed 0.025 to 10 µM).

An aliquot of 100 µL of each GSH standard or cell/RHE sample was mixed with 50 µL of glutathione glycine-$^{13}C_2$,^{15}N (100 µM) and 100 µL of IAA (10 mM, prepared in 10 mM ammonium bicarbonate aqueous solution and adjusted to pH 9.5) in an amber glass vial and left to react for approximately 1.5 h. The structure of the derivatised GSH is presented in Fig 2.2.

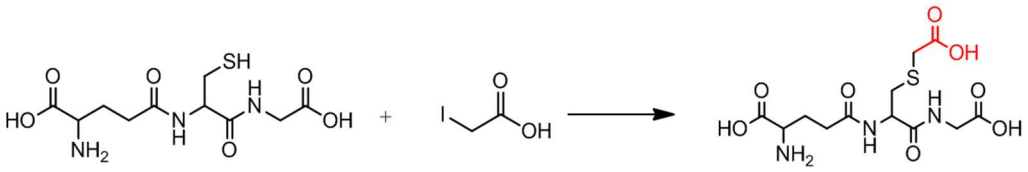

Figure 2.2: Iodoacetic acid reacts with the free thiol on GSH at pH 9.5.

An aliquot of 50 µL of sulfosalicyclic acid (10 % w/w in water) was added to facilitate the precipitation of proteins present in the cell lysates. Cell samples were filtered through 0.2 µm filters by centrifugation (10,000 rpm, 10 minutes). 50 µL of each GSSG solution were added to the matching GSH standards. All standards and samples were then diluted to 1 mL with a solution of 0.1 % formic acid in LC-MS grade water.

2.2.15 Mass spectrometric analyses.

2.2.15.1 GSH assay.

The Acquity Ultra-High Pressure Liquid Chromatography (UPLC) system (Waters, Elstree, UK) was used for the LC separation of the compounds of interest. Chromatographic separation was achieved using an Acquity HSS T3 (150 x 2.1 mm, 1.8 µm particle size) column (Waters, Elstree, UK) set at 4 0°C, following recommendations for the chromatographic separation of GSH in biological matrices reported by [107] - using gradient elution with 0.1 % formic acid in water (mobile phase A) and acetonitrile (mobile phase B) at a flow rate of 0.2 mL/min. Initially, the mobile phase composition was set to 2 % B, held for 2 minutes and then increased to 95 % B over a further 7 minutes. The composition was held for a further 3 minutes, returned to the initial conditions over 1 minute and held at 2 % B for a further 2 minutes.

The Quattro Premier mass spectrometer (Waters, Elstree, UK) was used with an ESI (Electrospray Ionisation) source operating in positive ionisation mode. The mass spectrometer was operated with a capillary voltage of 3.2 kV. The temperature of the source was set at 130 °C and the desolvation temperature was set at 300 °C. Other parameters were set at values according to the manufacturer's recommendations.

All samples were analysed using Multiple Reaction Monitoring (MRM) for the complete length of the UPLC acquisition time (15 min). The MRM transition used for IAA-derivatised glutathione glycine- $^{13}C_2$,^{15}N was m/z 369.10 > 176.80 and for IAA-derivatised glutathione was m/z 366.02 >173.80, with the mass spectrometer operating with a cone energy fixed at 25 V and collision energy fixed at 20 eV for both analyses. The MRM transition used for GSSG was 613.10 > 355.10 with a cone energy fixed at 30 V and collision energy fixed at 20 eV. All data processing was carried out using the

Quanlynx quantification software, part of the Masslynx software (version 4.1) (Waters) controlling both Acquity UPLC and Premier mass spectrometer.

2.2.15.2 GSH incubations with model compounds.

The UPLC method was identical to the one described in the GSH assay section, with the exception of the flow rate, which was fixed at 0.3 mL/min. The mass spectrometer parameters were identical to the ones described in the previous section with the exception that the ESI source was operating in positive mode with a Cone voltage fixed at 20 V.

All samples were analysed in full scan mode over the range m/z 100-1000 for the complete length of the UPLC acquisition time (15 min).

2.2.15.3 Dinitrophenyl-glutathione measurements.

Samples were analysed in MRM for the complete length of the UPLC acquisition time (15 min, method described in GSH assay Section). The MRM transition used for dinitrophenyl-glutathione (DNP-SG) was m/z 474.1 > 242.1 with the mass spectrometer operating with a cone energy fixed at 10 V and collision energy fixed at 25 eV.

2.2.16 Protein quantification by bicinchoninic acid assay.

The protein content of each RHE sample was assessed by the bicinchoninic acid (BCA) assay using methodology described by [133] with a few adaptations specific to the Micro BCA protein assay kit (Thermo Scientific,Rockford, USA). All RHE lysates were diluted 1/10 in ultrapure water before analysis, to minimise the influence of the presence of RIPA buffer.

Calibration standards of Bovine Serum Albumin (BSA) were prepared in ultrapure water to cover the range 0.5-200 µg/mL, with the addition of a standard blank (ultrapure water only). The absorbance was read at 562 nm using a Spectramax M3 microplate reader operated with Softmax Pro software.

2.2.17 Statistical analysis.

- MTT assay in HaCaT cells. Experiments were carried out in a single day. Eight wells of the 96-well plate were treated with the same concentration of test reagent (n=8). The mean absorbance of controls cells treated with HaCaT culture medium containing 0.5 % DMSO was used to define the viability in control cells and fixed at 100%. The viability of each well treated with test reagent was expressed as the ratio of absorbance in treated cells over the mean of absorbance in control cells (mean value) and expressed as a percentage. The percentage viability was reported as Mean ± Standard deviation (n=8) for each concentration tested.
- MTT assay in RHE models. Experiments were carried out in a single day. Three models were cultured in medium + 10 % DMSO for the required time (n=3). Each concentration of test reagent was applied on RHE models in triplicate (n=3). Viability was calculated as described for HaCaT cells experiments. The percentage viability was reported as Mean ± Standard deviation (n=3) for each concentration tested.
- Model sensitisers: Dose response in HaCaT cells. Experiments were carried out in a single day. Each concentration was applied to the wells in triplicate (n=3). To evaluate the difference in GSH levels between treated cells and solvent treated control cells, the Student t-test was applied between the mean at each concentration (n=3) and the mean at 0 µM. Significant statistical difference was obtained when the P value was <0.05.

- Model sensitisers: 24-hour time course in HaCaT cells. Experiments were carried out in quadruplicate (n=2 on two separate occasions) for dinitrohalobenzenes. To evaluate the difference in GSH levels between treated cells at a specific time point and control cells at the start of the experiment (t = 0), a Student t-test was carried out to measure difference between the mean at each time point and the mean at t= 0. Significant statistical difference was obtained when the P value was <0.05.

  Other experiments were carried out in duplicate or triplicate in a single day. Statistical analysis for figure 3.12 used a Student t-test where the P value was fixed at 0.1.

  To evaluate the difference in GSH levels between cells treated with 10 µM of different dinitrohalobenzenes for 24 hours, a ANOVA test was carried out. Statistical difference between the three dinitrohalobenzenes DNCB, DNFB and DNBB was obtained for this concentration with a P value <0.05.

- Determination of Nrf2 activation by Western Blot: HaCaT cells. Experiments were carried out in triplicate measurements on two separate occasions for cell treatments (n= 2 and n= 1). For t=0 h three control samples were pooled to generate a single t=0 sample, with value fixed at ratio 1 (100 % baseline value) and used to calculate the "ratio over controls" for the other samples. Results were normalised to actin and presented as Mean ratio over controls ± Standard deviation.

- RHE repeated treatment with DNCB. Experiments were carried out in triplicate. Statistical difference between the mean value for GSH level in treated RHE samples and the mean value for GSH level in RHE samples lysed before treatment (t= 0 hour) was evaluated using a Student's t-test. Statistical difference was obtained when the P value < 0.05.

- Determination of Nrf2 activation by Western Blot: RHE models. RHE models were treated with DNCB for the appropriate length of time (time course experiment). Lysates

were used to carry out Western Blot analysis showing Nrf2 release (n=3). Data was normalised to actin, NQO1 enzyme measured as positive control of Nrf2 activation. For t=0 h three control samples were pooled to generate a single t=0 sample, with value fixed at ratio 1 (100 % baseline value) and used to calculate the "ratio over controls" for the other samples. A Student t-test was carried out to measure the difference between each time point and t= 0 for NQO1. Statistical difference with a p value < 0.1 was obtained at 72 h. To evaluate the difference between the first, second and third exposure to DNCB on nrf2 levels, a ANOVA test was carried out and statistical difference was obtained with a P value < 0.05.

Chapter 3: Modulation of GSH oxido-reduction mechanism in the HaCaT cell line.

Contents

3.1 Overview.

3.1.1 GSH in skin.

The level of total glutathione in human skin (GSH and its disulfide form GSSG) has rarely been reported and the values available to date are variable (summarised in Table 3.1). Significant differences were found in one study between the epidermis and the dermis levels of GSH, with the epidermis containing more than five times the amount of total GSH present in the dermis (expressed in nmol/g of wet tissue) [134], whilst another study found similar levels in both layers [135]. The location at which the sample was taken also appears to play a role. For example, Kaur and colleagues reported values of total GSH in healthy skin of patients and observed that GSH levels doubled in skin lesions linked to chronic contact dermatitis [136].

Total GSH (nmol/g)	Technique used	Number of donors	Reference
480 (epidermis) 85 (dermis)	Ellman's reagent-GR recycling assay	6 (healthy)	Shindo *et al* (1994)
250-450 (epidermis) 280-530 (dermis)	Ellman's reagent-GR recycling assay	7 (mean 21y.old) 9 (mean 71y.old)	Rhie *et al* (2001)
195 (healthy whole skin) 442 (lesional skin)	Ellman's reagent-GR recycling assay	5 (healthy skin) 6 (ICD or ACD on hands)	Kaur *et al* (2001)

Table 3.1: Total GSH (reduced and oxidised) measured in human skin samples.

3.1.2 GSH formation in the HaCaT cell line.

The synthesis of glutathione has been described in Section 1.6.2 in the Introduction: two enzymes, Glutamate cysteine ligase (GCL) and glutathione synthetase (GS) enable cells to generate *de novo* glutathione from its constitutive amino acids.

The presence of GCL and GS in HaCaT cells has been demonstrated at both mRNA level and protein level [137, 138]. An increase of GCL at the mRNA level after treatment with alpha-tocopherol or arsenic has been linked to an increase in GSH level in the cells [137, 139]. It is generally accepted that the availability of cysteine is the limiting factor in the formation of the *de novo* GSH. This is difficult to demonstrate as reducing the amount of cysteine available without drastically changing the cell's culture medium is challenging *in vitro*. Hence, researchers have investigated ways to modulate GSH synthesis by inhibition of the GCL enzyme. L-buthionine sulfoximine (BSO, structure detailed in Fig 3.1) has been used as an inhibitor of GCL (Fig 3.2) in numerous studies.

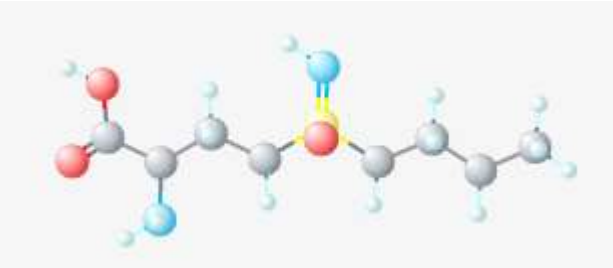

Figure 3.1: L-buthionine sulfoximine 3D chemical structure. Reproduced from PubChem [109] where the colouring of atoms is *grey*: carbon, *white*: hydrogen, *red*: oxygen, *blue*: nitrogen and *yellow*: sulphur.

Most protocols detailed how µM levels of BSO inhibited the synthesis of GSH and following treatment with a specific probe such as Cadmium, enhanced the GSH depletion observed compared to cells that were not treated with BSO [90].

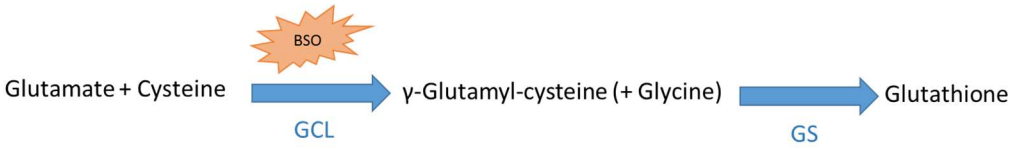

Figure 3.2: L-buthionine sulfoximine inhibits GCL and prevents the formation of *de novo* γ-glutamyl-cysteine

BSO is a mechanism-based enzyme inhibitor that has been purposefully designed to inhibit the GCL enzyme by Griffith and various colleagues in the 1980s [140, 141]. BSO is first phosphorylated on the nitrogen atom of the sulfoximine group and, in contact with GCL, form a complex with ADP, which can very tightly but not covalently bind into the reactive site of GCL. Mechanistic investigations of this "GCL-BSO complex" has been carried out by Biterova *et al* [142] and the complex is reproduced in Fig. 3.3. This complex is stable for a period of time long enough that glutamate and cysteine cannot enter the reactive site and γ-glutamylcysteine cannot be formed for several hours, hence BSO is often called an irreversible inhibitor.

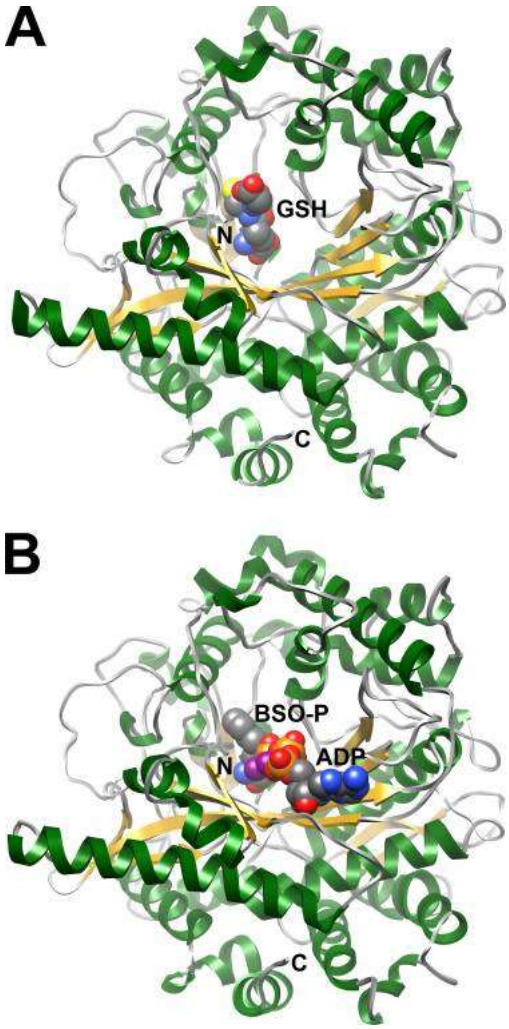

Figure 3.3: Ribbon representations of the crystal structures of ScGCL in complex with inhibitors. An ScGCL monomer is contained in the asymmetric unit, and the N- and C-terminal residues are indicated. β-Strands are colored in *yellow*, and α-helices are depicted in *green. A*, bound GSH is shown in space filling representation with carbon atoms colored in *gray*, oxygen atoms are in *red*, sulfur atoms are in *yellow*, and nitrogen atoms are in *blue*. The glutathione-binding site overlaps the glutamate binding site within the active site funnel. *B*, ADP and the transition state analogue, phosphorylated BSO (*BSO-P*), are shown in space filling representation. Phosphorus and magnesium atoms are colored in *orange* and *purple*, respectively, with the remaining atoms colored as in *A*. Kindly reproduced from Betirova *et al* [142].

3.1.3 GSH in oxido-reduction mechanisms.

GSH, being the most prominent thiol antioxidant in cells, plays a major role in the quenching of radicals and detoxification of ROS. The mechanism by which ROS are inactivated by the GSH pathway relies on GSH being oxidised to $GS^{\cdot}$. Disulphide bond is

then formed between the two oxidised glutathione molecules, yielding GSSG, which is often called oxidised glutathione. The oxidation of GSH into its disulphide GSSG can be a non-enzymatic phenomenon or can be greatly enhanced by Glutathione Peroxidase (GPx). Most cells require GSSG to either be quickly expelled or reduced back to two molecules of GSH, using Glutathione Reductase (GR).

A common technique to prevent the recycling of GSSG back to GSH is to inhibit GR activity chemically. Carmustine (or BCNU, structure detailed in Fig 3.4) has long been used for such purposes [143, 144]. It is part of the nitrosoureas compounds, where the nitroso and the urea group are N-N linked and can be used as a chemotherapeutic agent.

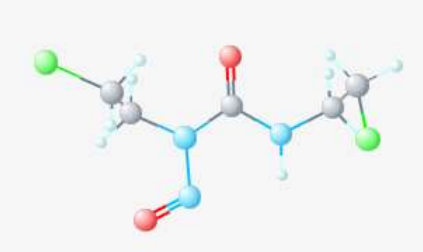

Figure 3.4: carmustine 3D chemical structure. Reproduced from PubChem [109] where the colouring of atoms is *grey*: carbon, *white*: hydrogen, *red*: oxygen, *blue*: nitrogen and *green*: chlorine.

This GR inhibitor is not solely designed to interact with GR and has also been shown to target DNA and RNA [145] and non-related enzymes in red blood cells [146], thus the concentrations required to demonstrate loss of GR activity are quite high. The mechanism by which GR is inhibited is not completely elucidated either: Shinohara *et al* originally thought that the inhibition was somehow linked to a change in redox state in the cells [146]. Later a mouse study where a 50 mg/kg BCNU dose was used showed that GR activity was depleted after only 10-30 min in organs such as liver, lungs and heart and was sustained for up to 48-96 h. However, a lower dose of 25 mg/kg showed almost no effect [147]. An explanation for this inhibition, is that GR is irreversibly

modified by covalent binding with BCNU as Cohen *et al* later demonstrated that GR activity in murine leukemia cells could only recover after exposure to BCNU if the ability to synthesise *de novo* GR protein was maintained. They observed that when protein synthesis was blocked GR activity was permanently lost [148]. Studies have shown that the inhibition of purified human GR had an IC_{50} value of approximately 55 µM and GR activity was reduced to 10 % of its original value after 3 hours of incubation with a 200 µM of BCNU [144]. For future experiments, a concentration approximating this value will be used if no specific adverse effect linked to the HaCaT cell line is seen.

Another inhibitor, developed much more recently by Guan and Seefeldt, is 2-acetylamino-3-[4-(2-acetylamino-2-carboxyethylsulfanylthiocarbonylamino) phenylthiocarbamoylsulfanyl]propionic acid (2-AAPA, structure detailed in Fig 3.5) [129, 149, 150].

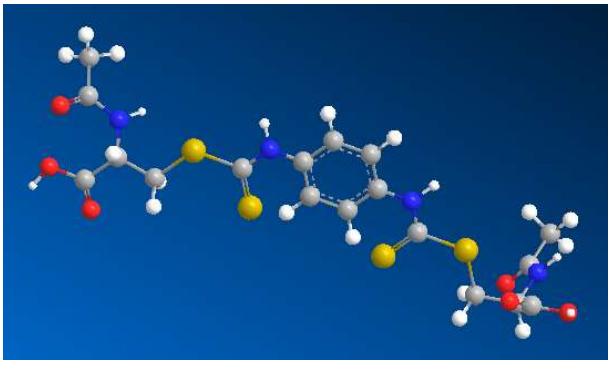

Figure 3.5: 2-AAPA 3D chemical structure (ChemBio3D Ultra version 12.0) where the colouring of atoms is *grey*: carbon, *white*: hydrogen, *red*: oxygen, *blue*: nitrogen and *yellow*: sulphur.

It results from the reaction of one molecule of 1,4-diisothiocyanatobenzene with two molecules of N-acetylcysteine (NAC), both commercially available. This inhibitor is thought to be more specific than BCNU, but can also induce some DNA damage as well as inhibit GR. 2-AAPA is an irreversible inhibitor as it reacts covalently with GR at the GSSG binding site of the enzyme (with departure of one or both molecules of NAC in the

process) [149]. The 2-AAPA inhibited GR enzyme has been isolated and analysed by Q-ToF LC-MS and the structure is presented in Fig 3.6.

Observed and calculated *m/z* values of the monothiocarbamoylated GR monomers (GR monomer + 356 Da) and bisthiocarbamoylated GR monomers (GR monomer + 194 Da)

Yeast GR (1 mg/ml) was treated with 2-AAPA (0.1 mM) for 2 h at room temperature. The observed *m/z* values were obtained from the MS analysis of the sample where 44% of GR activity was inhibited by 2-AAPA. The asterisks indicate that the sulfur atom was from the thiol groups of cysteine in the active site of the enzyme.

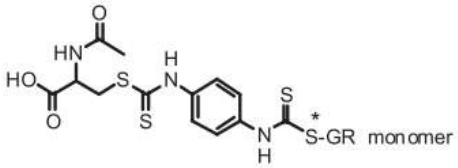

Monothiocarbamoylated GR monomer (M + 356)

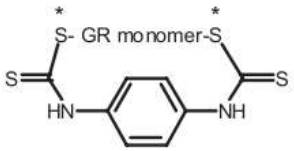

Bisthiocarbamoylated GR monomer (M + 194)

Figure 3.6: Nature of covalent modification of GR monomer by 2-AAPA. Reproduced from Seefeldt *et al [149].*

2-AAPA was evaluated as an inhibitor of GR in different human cancerous cell lines, including skin, breast, lung and ovary and used in conjunction with X-ray radiation to increase the level of GSSG and oxidative stress in these cells. In this study, the cytotoxicity of 2-AAPA was estimated to have an IC_{50} value of 70 μM in all cell lines. The recommended pre-treatment with 2-AAPA is for 2 hours [129].

Both of these inhibitors were considered in this study when inhibition of GR was required to highlight the potential increase in GSSG observed by inducing oxidative stress on HaCaT cells using a model aldehyde with skin sensitising properties, phenylacetaldehyde (PA).

3.1.4 Reactivity of aldehydes.

Benzaldehyde (BA) and phenylacetaldehyde (PA) are fragrant aldehydes that can be used in products that are applied on the skin. Due to its volatility and ability to rapidly

oxidise to benzoic acid, BA is considered relatively safe [126]. It is classified as a non-sensitiser in the LLNA assay [124]. However a patch test study has reported sensitisation to BA in patients who had already been diagnosed with fragrance allergy in 3 out of 747 cases [125]. PA, however close in chemical structure to BA, is considered a moderate sensitiser in the LLNA assay [151]. Historical patch testing of PA, prepared at 0.5 % in alcohol, led to an allergic reaction in 3 out of 275 volunteers [152]. A case of contact allergy to PA was reported after an occupational accident in a fragrance factory [153]. The mechanism of reaction by which PA induces skin sensitization has not been described in detail. *In chemico* studies showed that reactivity of aldehydes or ketones with primary amines, such as the one present on Lysine residues, can happen via a Schiff base mechanism, yielding an imine. The reactivity of aldehydes with primary amines is illustrated in Fig 3.7.

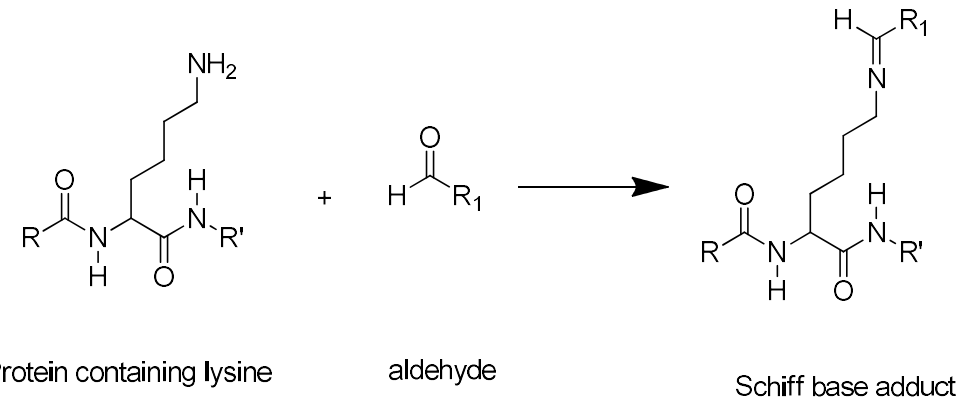

Figure 3.7: Schiff base formation between a protein containing an available lysine residue and an aldehyde.

PA is prone to form Schiff base with lysine containing peptides *in chemico* but assay conditions such as chemical:peptide ratio or temperature have a significant influence on the % peptide depletion reported in assays. While Gerberick *et al* reported a % depletion of their lysine containing peptide of 22.6 % [19], Aleksic *et al* obtained

complete depletion within 24 hours [24]. Both assays highlight the potential of PA for Schiff base formation. It is also worth noting that in the second assay [24], incubations of the lysine peptide with BA led to partial peptide depletion of 26.7 %, while incubations with a peptide containing a terminal NH_2 group (N-term) at pH 7.4 rather than 10, resulted in a 82.1 % depletion of this peptide.

In chemico studies have also demonstrated that PA reacts as an oxidant with Cys peptides. PA incubations with the cor1-C420 peptide (containing a single Cys residue) used in the LC-MS based peptide reactivity assay described by Natsch *et al* [20] showed >95 % peptide depletion solely due to dimerisation of the peptide. These results are similar to the ones obtained with a less complex peptide where only one reactive site is available for modification, AcFAACAA, containing a Cys residue, that was 100 % dimerised after reaction with PA [24]. Results concerning the oxidation of Cys residues by BA are more difficult to interpret. While AcFAACAA was again completely depleted by dimerization in the same conditions [24], cor1-C420 was not significantly depleted by BA (approximately 5 %) and no significant amount of dimer was observed.

It is therefore difficult to predict which mechanism would be prevalent in skin based on *in chemico* assays alone. For instance, the variability of results observed for BA might be due to the assay conditions and choice of peptide or to the volatility of BA itself. How the volatility of BA would influence the results of assays involving *ex vivo* skin, or a cell line, in culture is unknown. The ratio of available cysteine residues in skin/keratinocytes proteins compared to lysine is also not completely defined, even though initial data suggests that lysine would be significantly more prominent than cysteine for reactivity with skin proteins [154]. GSH being a tri-peptide of relatively simple structure that contains a Cys residue, it was anticipated that it could be oxidised into its disulfide form GSSG by reaction with one or both of the model aldehydes BA or PA, to a comparable extent to the oxidation of cysteine residues on proteins. This mechanism was

investigated both *in chemico* and in the HaCaT cell line to explore the fate of GSH in reaction with such aldehydes in skin.

3.2 Aims and objectives.

The GSH pathway complexity has been defined [61, 66] but has not been fully characterised in *in vitro* skin cells. The overall aim of was to understand the GSH pathway in a skin relevant model, the HaCaT cell line, and how this pathway can be modulated in the context of skin defence. The first step to achieve this was to measure the homeostatic level of GSH in HaCaT cells and characterise the synthesis of *de novo* GSH in this cell line. This was followed by investigations of clearance potential of model aldehydes, considered to be oxidants with skin sensitisation relevance.

3.3 Results.

3.3.1 GSH quantification in the HaCaT cell line.

Human epidermis is formed mainly of keratinocytes (95 %), therefore the use of immortalized keratinocytes such as HaCaT cells as an *in vitro* tool for estimation of GSH in healthy skin was investigated. The level of GSH measured in HaCaT cells seeded at $4x10^5$ cells/well after overnight incubation in 6-well plates was 4.2±1.1 µmol/L (n=10) and doubling to 9.8±1.3 µmol/L (n=10) at 48 h, demonstrating that GSH concentration is proportional to the multiplication rate of healthy cells.

3.3.2 GSH depletion by inhibition of GSH synthesis.

Following application of a non-toxic concentration of BSO, the GSH level was depleted to less than 10 % of that of untreated controls at 24 h (Fig 3.8), demonstrating an active GSH cycle in HaCaT cells.

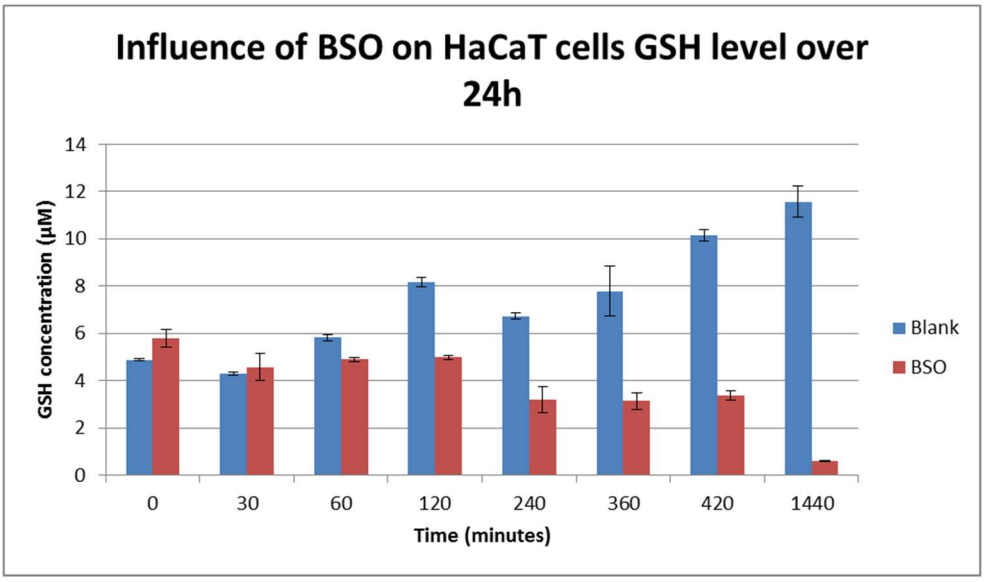

Figure 3.8: 50 µM treatment with BSO for 24 h versus absence of treatment. Each well (400 000 cells/well) was treated with 50 µM BSO or left undisturbed for the length of time required. Each well was rinsed twice with PBS and the cells lysed by adding 200 µL of sterile water and storing at -80 °C. 100 µL of lysate was derivatised with iodoacetamide, GSH quantified in this lysate and concentration reported in µM GSH (n=2). The figure shows that BSO inhibits the synthesis of GSH in HaCaT cells. The level of GSH slowly depleted over time, as part of normal antioxidant cellular defence. Results for each time point are presented as mean ± standard deviation.

BSO does not deplete GSH directly. During the 24 hours of reaction it was likely that the cells used up their stock of GSH, which could not be replenished.

3.3.3 GSH depletion by oxidation with hydrogen peroxide.

3.3.3.1. Enhancing ROS levels with hydrogen peroxide treatment.

Oxidation of GSH to its disulphide GSSG can be achieved by enhancing the level of ROS in cells. In this experiment, cells were treated with hydrogen peroxide (H_2O_2, HP) for 4

hours. The level of GSH decreased in cells treated with 1.5 mM or more, compared to untreated controls (Fig 3.9).

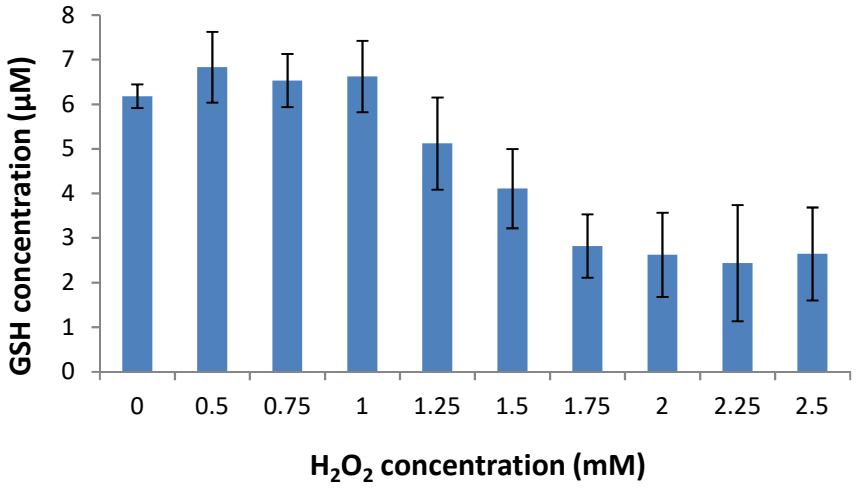

Figure 3.9: GSH level in HaCaT cells treated with hydrogen peroxide. Treatment was carried out in each well (400 000 cells) for 4 h (range 0-2.5 mM) after which cells were rinsed with PBS twice, 200 µL sterile water was added and the cells lysed by storage at -80 °C. Half the lysate (equivalent to 200 000 cells) was derivatised with iodoacetamide and the GSH content measured and reported in µM (n=3). The Figure shows that the level of GSH in HaCaT cells can be depleted with an increased level of ROS. However, cell viability decreased simultaneously as GSH was consumed. Result for each time point is reported as mean ± standard deviation.

The level of GSSG measured in the cells was always below the limit of detection of the assay (0.1 µM). Cytotoxicity of HP was investigated by MTT assay and demonstrated that cell viability quickly decreases for concentrations above 1 mM (data not shown). The low level of GSH measured in this experiment was therefore directly linked to the low level of viable cells in the wells. Discerning whether GSH depletion induced cell death or whether cell death led to the GSH being leached into the medium and discarded (resulting in a low GSH value) was difficult to assess.

3.3.3.2. GSH oxidation by hydrogen peroxide *in chemico.*

Incubations using HP at a concentration 10 times higher than GSH, resulted in chromatograms that only contained a small peak of GSSG, without the presence of any other peaks. This was observed at both pH studied (pH 7.4 and pH 9.5). The nature of the experiment did not allow for quantitation of total glutathione but the GSSG peak observed was unlikely to account for the amount of GSH initially introduced. It is also possible that HP generated some ion suppression in the samples (compared to controls containing exclusively GSH and buffer) in the mass spectrometry experiment.

3.3.4. GSH oxidation by aldehydes.

Due to the volatility of fragrant aldehydes, all experiments involving HaCaT cells were limited to 2 hours maximum and were carried out as much as possible in occluded conditions.

3.3.4.1. Cytotoxicity of Benzaldehyde and phenylacetaldehyde

The results obtained using the MTT assay showed that BA did not induce more than 20 % cell death for concentrations up to 100 µg/mL (Fig 3.10a). For PA, the toxicity seemed to reach a plateau at approximately 80 % viability for the concentration range 25-100 µg/mL (Fig 3.10b). Overall, PA appeared to be more toxic to HaCaT cells than BA.

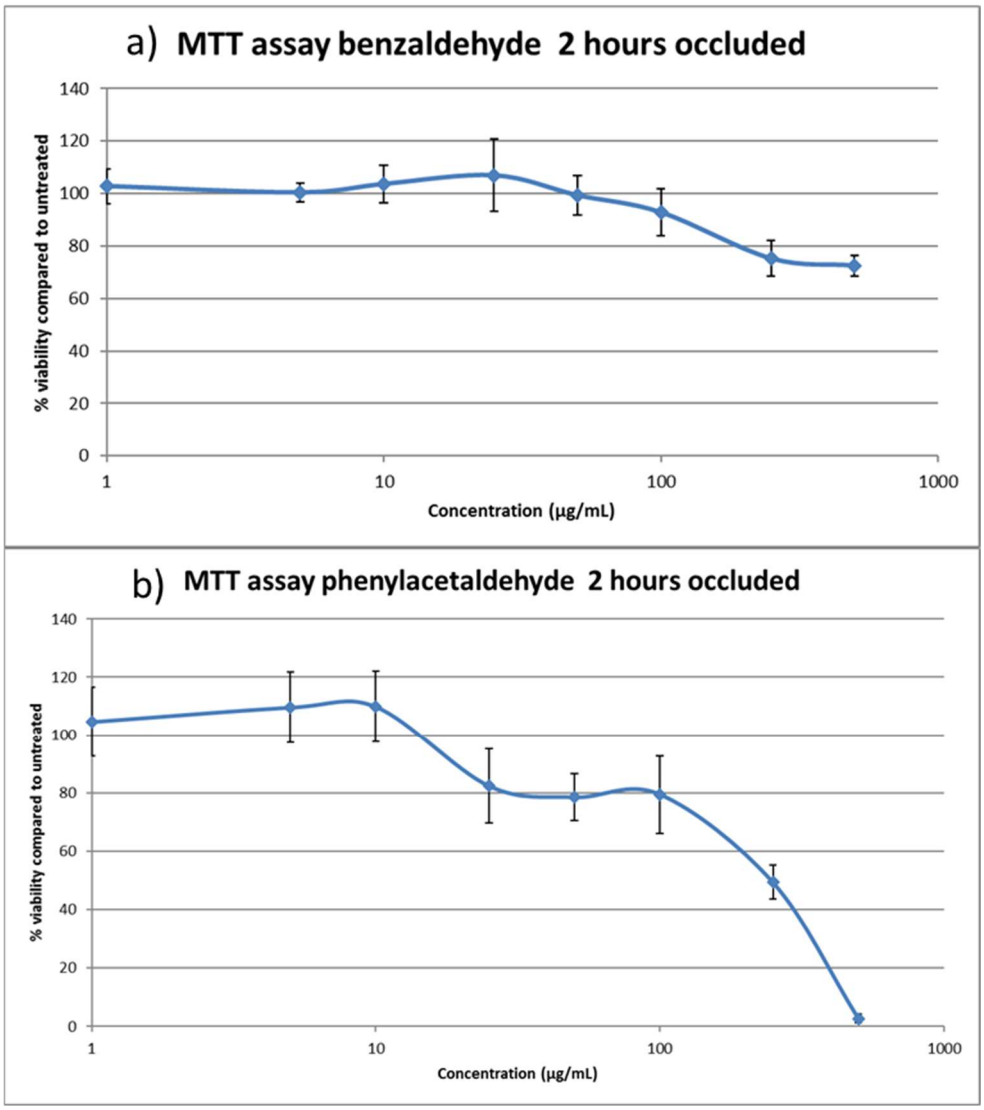

Figure 3.10: Cytotoxicity of aldehydes for a 2-hour exposure in occluded conditions. MTT assay results for (a) benzaldehyde, (b) phenylacetaldehyde covering the range 0-500 µg/mL. Each well (20 000 cells per well) was treated with the required amount of aldehyde, covered with a plastic adhesive cover and incubated for 2 hours. Cells were then rinsed and incubated with a solution of MTT (0.3 mg/mL) for 3 hours, rinsed twice with PBS and the formazan crystals diluted with isopropanol (n=8). The figure shows that cytotoxicity is observed over 100 µg/mL for benzaldehyde and over 25 µg/mL for phenylacetaldehyde. Results are presented as Mean viability ± Standard deviation.

The results of MTT assay demonstrate that the volatility of both compounds tested is not a critical parameter when occluded conditions are considered (plates were sealed immediately after exposure to the aldehydes). For both compounds a high level of toxicity influencing mitochondrial activity could be observed (i.e at 500 µg/mL

concentration) and therefore the penetration of the aldehydes into the cells was significant.

3.3.4.2. BA and PA reactivity with GSH *in chemico*

The oxidation of GSH into GSSG was investigated *in chemico*, in occluded conditions at 37 °C, using BA and PA at a concentration 10 times higher than GSH. BA incubations analysed by LC-MS only contained the two peaks related to GSSG with the retention times 1.67 and 2.74 minutes respectively (data not shown). PA incubations contained GSSG as well as minor peaks apparently unrelated to GSH (Fig 3.11).

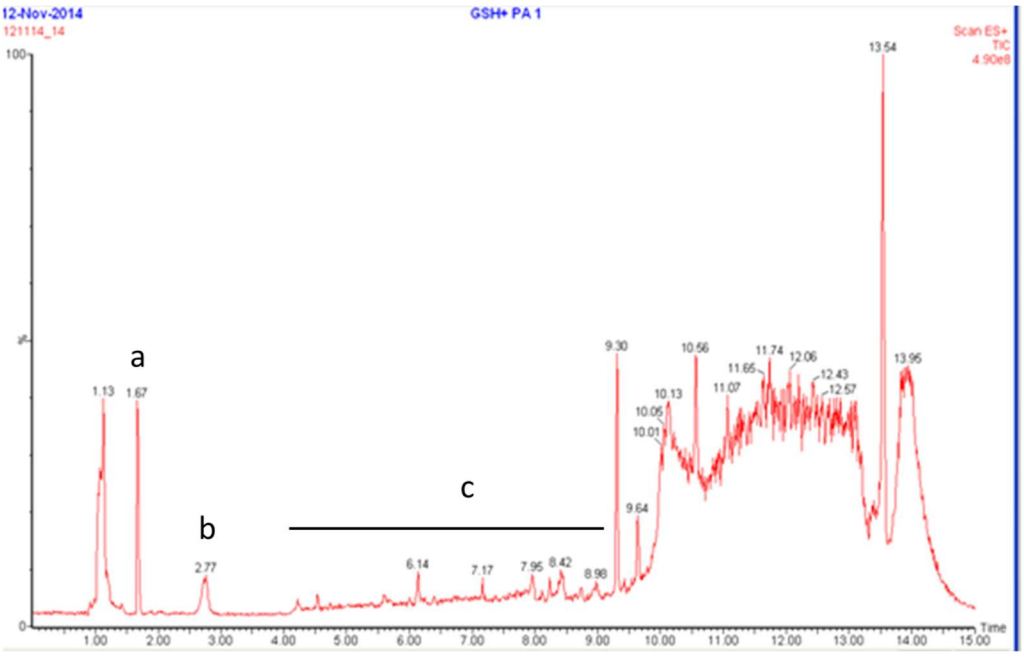

Figure 3.11: Typical chromatogram of incubation containing GSH and PA at ratio 1:10. Incubations were carried out at in 50mM potassium phosphate buffer at pH 7.4 for 24 hours. The resulting mixture was analysed by LC-MS operating in scan mode for 15 minutes (n=3). The figure shows a) GSSG (retention time 1.67 min), b) GSSG (retention time 2.77 minutes) but no reduced GSH. Phenylacetaldehyde is not visible on the chromatogram and c) is a series of unrelated minor peaks.

3.3.4.3. HaCaT cells treatments with BA and PA

Based on the previous *in chemico* experiment, the assumption was that the aldehydes are able to oxidise GSH into GSSG. However, it was unknown whether a depletion of GSH and an increase of GSSG level would be visible experimentally by mass spectrometry.

The profile of GSH concentration in cells that were treated with 0.1 mg/mL BA or 0.025 mg/mL PA is presented in Fig 3.12. The level of GSSG was below the limit of quantification (less than 0.1 µM) for all samples analysed. The level of GSH decreased slightly during the first 10 min of exposure for both BA (Fig 3.12a) and PA (Fig 3.12b). It is also noticeable that the effect of aldehydes on GSH appears to be short lived. GSH was quickly replenished, with a maximum concentration observed at 30 min for BA and 60 min for PA.

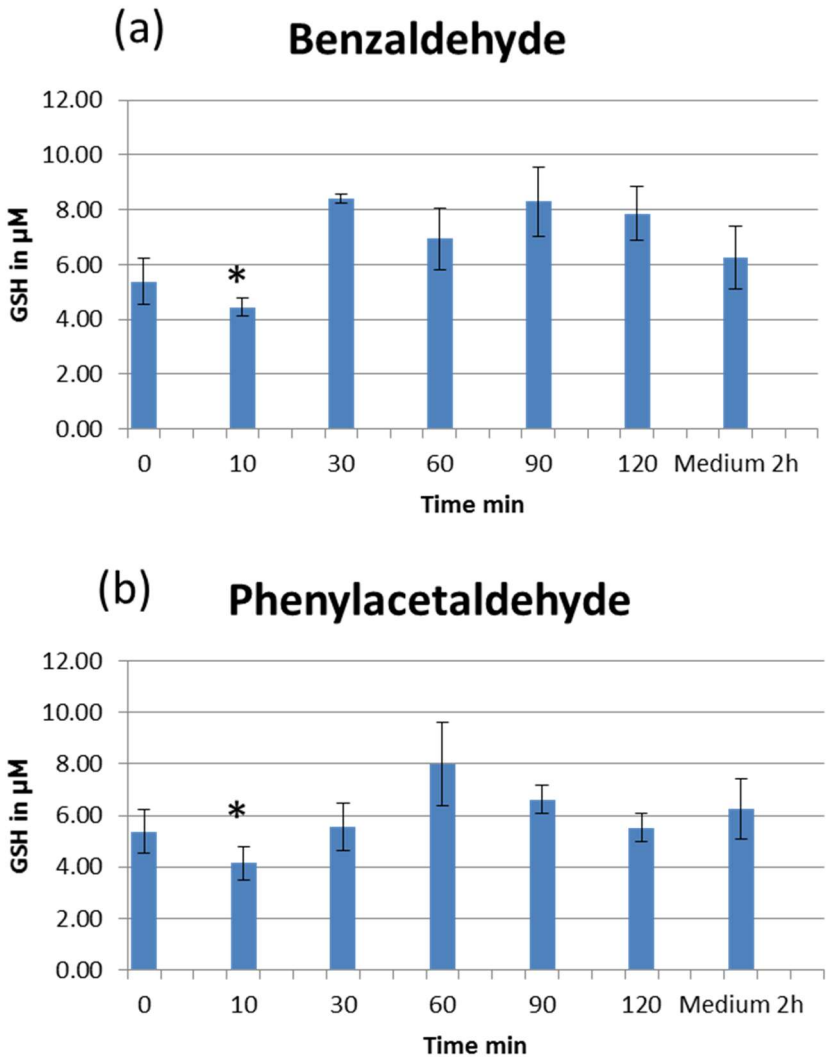

Figure 3.12: GSH level in HaCaT cells treated with (a) BA and (b) PA for a maximum of two hours. Treatment was carried out in each well (400 000 cells) for up to 2 h (100 µg/mL for BA and 25 µg/mL for PA). The time points "t=0" and "Medium 2 h" were prepared with cells that were not exposed to aldehydes. At the required time, the cells were rinsed with PBS twice, 200 µL sterile water was added and the cells lysed by storage at -80 °C. Half the lysate (equivalent to 200 000 cells) was derivatised with iodoacetamide and the GSH content measured and reported in µM (n=3). The Figure shows that GSH concentration is stable throughout the length of the assay, except for the 10 min time point. Result for each time point is reported as mean ± standard deviation. (*) Statistical difference between GSH level in samples treated for 10 min and controls (0 min) Student's t-test, p value <0.1.

3.3.5 GSH oxidation by aldehydes, influence of Glutathione Reductase inhibitor pre-treatment.

3.3.5.1. GR inhibition with carmustine before BA and PA treatment

3.3.5.1.1 Carmustine cytotoxicity

The toxicity of BCNU was investigated specifically for the HaCaT cell line, using the MTT assay. HaCaT cells were treated with a range of BCNU concentrations (1-200 µM) for 30 min or 1 h respectively.

The viability of cells was not significantly affected (more than 20 % cell death compared to control untreated cells) for the concentrations and time points investigated even though variability within the plates was higher than expected (±25 %) (Fig 3.13).

BCNU was not considered toxic to HaCaT cells at the maximum concentration of 200 µM for an exposure time of 1 h.

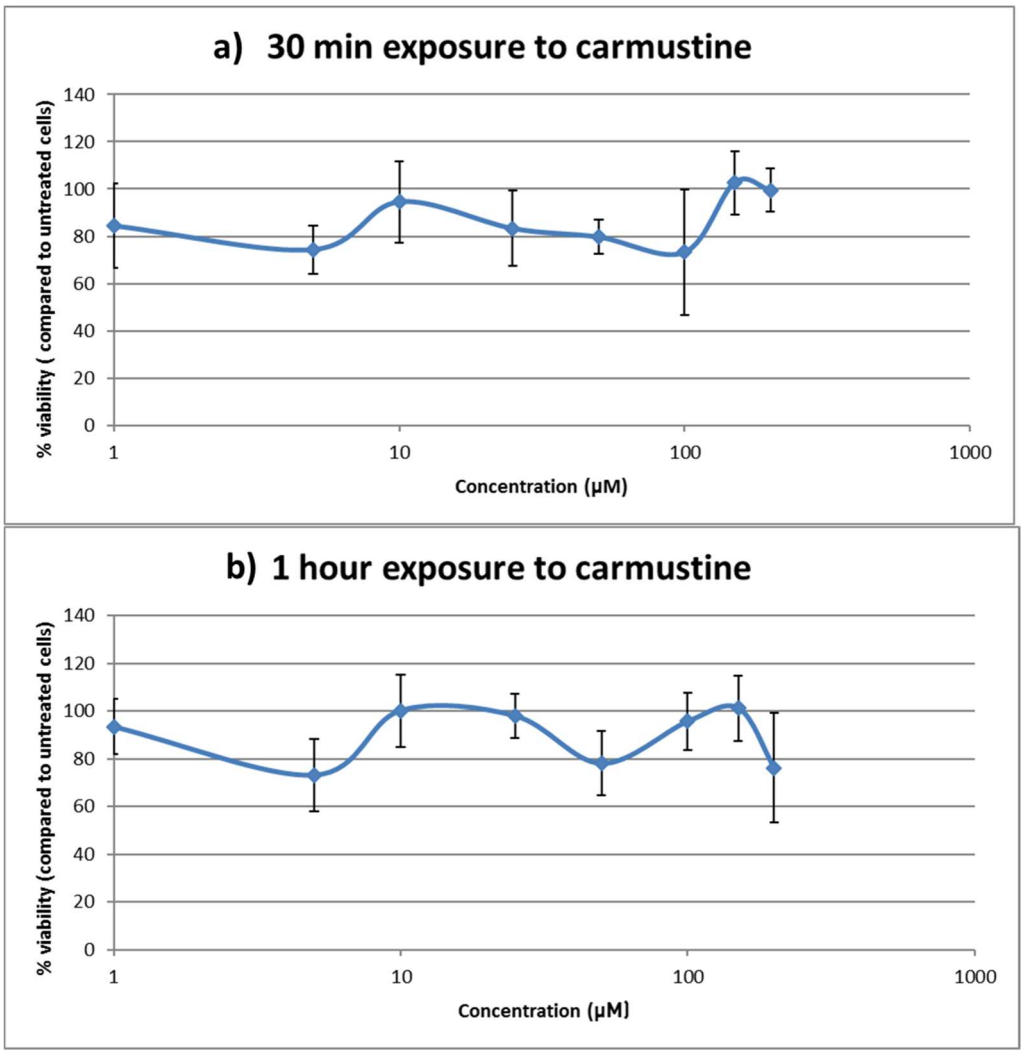

Figure 3.13: Cytotoxicity of carmustine after 30 min and 1-hour exposure. Results of MTT assay after a) 30 min exposure and b) 1 h exposure. Each well (20 000 cells per well) was treated with the required amount of carmustine covering the range 0-200 µM and incubated for up to 1 hour. Cells were then rinsed twice with PBS and incubated with a solution of MTT (0.3 mg/mL) for 3 hours. The cells were rinsed twice with PBS and the formazan crystals diluted with isopropanol (n=8). In both graphs, the toxicity of carmustine does not follow a decreasing trend as the concentration applied increases. Maximum concentration (200 µM) can therefore be applied to HaCaT cells. Results are presented as Mean viability ± Standard deviation.

3.3.5.1.2 Effect of carmustine treatment on GSH level in HaCaT cells

The influence of BCNU, in the absence of any other treatment, on GSH levels was also investigated. Each concentration was investigated in triplicate analysis and GSH level

expressed as a percentage of GSH left compared to untreated cells (concentration carmustine 0 µM). Results are summarised in Table 3.2.

Concentration carmustine (µM)	Average GSH (µM)	Standard Deviation (µM)	GSH remaining (% of 0µM)
0	1.926	0.163	100
10	1.881	0.238	97.7
50	1.543	0.144	80.1
100	1.999	0.463	104
200	1.988	0.643	103
0	1.847	0.391	100
10	1.61	0.29	87.2
50	2.316	0.859	125
100	1.664	0.504	90.1
200	2.139	0.221	116
Statistical analysis: Equivalence test, TOST (two-one-sided-test): Aim, show that results at 30 min and 1 hour are equivalent there is no trend.			
Mean 30 min data	1.867	Test	P- value
Defined boundary	20% Mean	Upper	0.0276
Lower/upper boundary	± 0.373	Lower	0.0075
Test result	Equivalent	Overall	0.0276

Table 3.2: Effect of carmustine on GSH level in HaCaT cells. Each well (400 000 cells per well) was treated with the required amount of carmustine covering the range 0-200 µM and incubated for *orange*) 30 min and *pink*) 1 hour. Cells were then rinsed twice with PBS, 200 µL of sterile water added and the cells frozen to -80 °C. Half the generated lysate (200 000 cells) was derivatised with iodoacetamide and the GSH content measured. Results were expressed in µM (n=3). In both cases, carmustine does not influence significantly on GSH levels (TOST test, P value <0.05). Maximum concentration (200 µM) can therefore be applied to HaCaT cells for 1 hour. Results are presented as Mean ± Standard deviation.

As with the MTT assay, the GSH level was similar in all samples and was comparable to untreated cells. It was estimated that 200 µM of BCNU applied on HaCaT cells for 1 hour would not induce a depletion (or overproduction) of GSH.

3.3.5.1.3 BA and PA treatment after pre-treatment with 200 µM carmustine

Cells were treated with 200 µM of BCNU for 1 hour, after which the cells were washed with PBS and treated with the two aldehydes in occluded conditions (BA 0.1 mg/mL and PA 0.025 mg/mL). The variation of GSH level was plotted versus the time of application. Results are summarised in Fig 3.14.

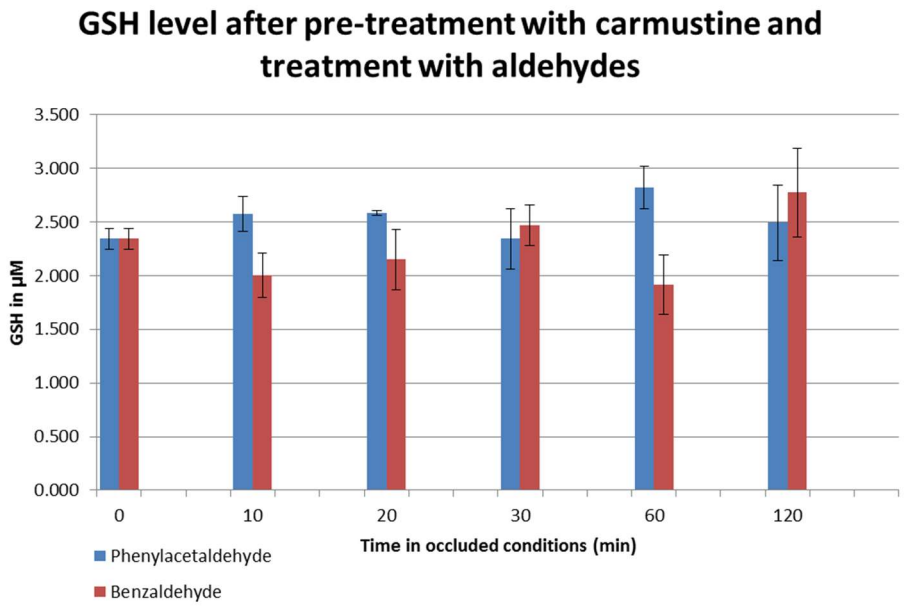

Figure 3.14: Effect of aldehydes on GSH level in HaCaT cells incubated in occluded conditions. Each well (400 000 cells per well) was treated with 200 µM of carmustine and incubated for 1 hour. Cells were then rinsed twice with PBS, treated with *red:* 0.1 mg/mL of benzaldehyde or *blue:* 0.025 mg/mL of phenylacetaldehyde, covered with a plastic adhesive cover and incubated at 37 °C for the required amount of time. Cells were rinsed, lysed and derivatised with iodoacetamide as described in previous figures. Results were expressed in µM (n=3) and presented as Mean ± Standard deviation. The figure shows that for both aldehydes, variability within the plates was high (±20 %) but GSH concentration did not follow a trend. A Student t-test was carried out to measure difference between the mean at each time point and the mean at t = 0 and showed no statistical difference (with a P value<0.05).

It appeared that the concentration of GSH did not significantly decrease as a function of time. Moreover, there was no increase in GSSG level in the samples during LC-MS analysis (no values were significantly over the limit of quantification of 0.1 µM). As it

was unclear why the increase of GSSG seen *in chemico* could not be reproduced *in vitro* another GR inhibitor, 2-AAPA was selected to repeat the experiment.

3.2.5.2. GR inhibition with 2-AAPA before BA and PA treatment

Cells were treated for 2 hours with a 50 µM solution of 2-AAPA before exposure to the aldehydes under experimental procedure identical to the one previously described. The results are available in Fig 3.15.

For BA, no significant depletion of GSH level was observed (Fig 3.15a). The last two time points suggest an overproduction of GSH. For PA, a depletion of approximately 20 % was observable up to 1 hour (Fig 3.15b) but the same phenomenon of GSH repletion was observed for the later time points (90 and 120 min).

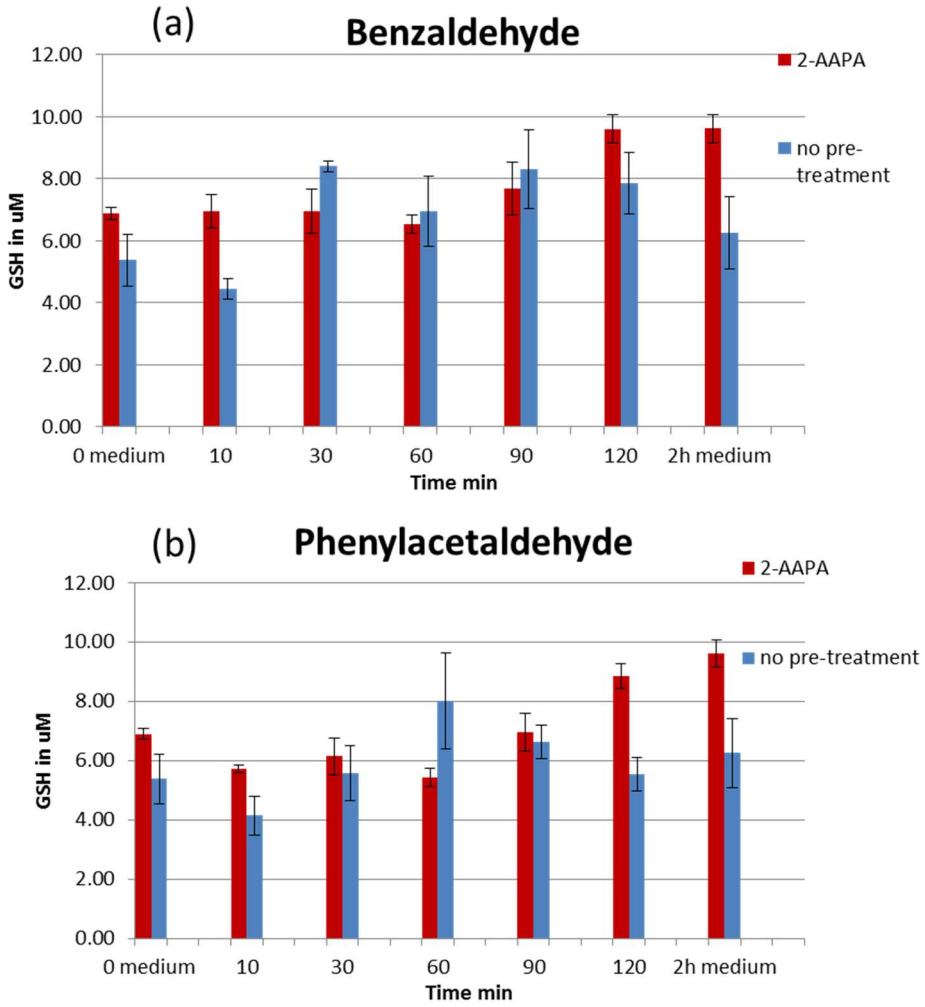

Figure 3.15: GSH levels in HaCaT cells treated with BA or PA with or without pre-treatment with 2-AAPA. *Red:* Half the wells (400 000 cells per well) was treated with 50 µM of 2-AAPA and incubated for 2 hours. *Blue:* Cells were incubated without treatment for 2 hours. Cells were then rinsed twice with PBS, treated with a) 0.1 mg/mL of benzaldehyde or b) 0.025 mg/mL of phenylacetaldehyde, covered with a plastic adhesive cover and incubated at 37 °C for the required amount of time. Cells were rinsed, lysed and derivatised with iodoacetamide as described in previous figures. Results were expressed in µM (n=3) and presented as Mean ± Standard deviation. The figure shows that for both aldehydes, variability within the plates was high (±20 %) but GSH concentration did not follow a trend. A Student t-test was carried out to measure difference between the mean at each time point and the mean at t = 0 and showed no statistical difference (with a P value<0.05).

3.3.5.2.1 Influence of 2-AAPA on GSH overproduction

The influence of 2-AAPA in the GSH cycle is suspected to be an inhibition of the GR enzyme in an "oxido-reduction" context. However, it was unknown whether this

particular compound could influence the synthesis of de novo GSH in cells. To verify whether 2-AAPA was at the origin of the GSH overproduction, HaCaT cells were cultured without any treatment for 2 hours. One set of cells were treated with 2-AAPA for 2 hours.

Untreated time matched controls had a limited GSH production compared to t=0; at 2 hours an increase from 5.4±0.8 µM to 6.3±1.2 µM (16 % increase) was observed (Fig 3.16). In contrast, 2-AAPA treated cells showed an overproduction of GSH of almost 40 % in the same timeframe. This might explain why the level of GSH did not seem to reduce as much as expected in the experiments involving exposure to aldehydes, especially PA, which seemed to induce the highest level of toxicity to cells in the MTT assay.

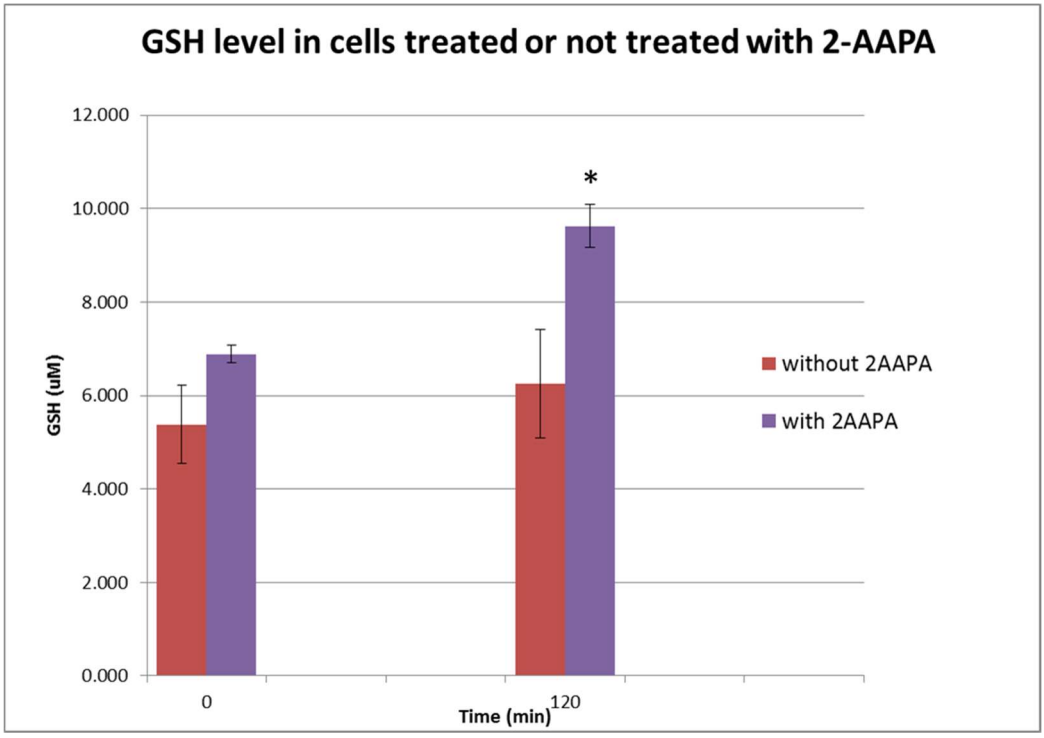

Figure 3.16: GSH levels in HaCaT cells treated/not treated with 2-AAPA for 2 hours. *Purple:* Half the wells (400 000 cells per well) was treated with 50 µM of 2-AAPA and incubated for 2 hours. *Red:* Cells were incubated without treatment for 2 hours. Cells were rinsed, lysed and derivatised with iodoacetamide as described in previous figures. Results were expressed in µM (n=3) and presented as Mean ± Standard deviation. The figure shows that 2-AAPA induces the production of GSH in HaCaT cells. (*) Statistical difference between cells treated with 2-AAPA for 2 hours and initials controls (t=0 min), Student's t-test, p value <0.05.

3.3.5.2.2 10 min treatment with BA and PA

For all samples analysed up to this point the level of GSSG was below the limit of quantification (less than 0.1 µM). It was expected that the earliest time point (10 min) where GSH seemed to have been depleted (Fig 3.15) would show an increase in GSSG level above the limit of quantification.

The BA and PA treatments were limited to 10 minutes and the concentration in aldehydes was increased to see whether the depletion in GSH was dose dependent (this increase in concentration was carried out without taking into account the increased toxicity probably involved) and whether high concentrations could help the potential formation of GSSG above limit of quantification.

The results obtained are illustrated in Fig 3.17. The concentration of benzaldehyde applied on the cells was increased up to 5 times (Fig 3.17a), which appeared to favour the detoxification of the aldehydes by increasing the level of GSH produced. Indeed, after 10 min exposure to 0.1 mg/mL of BA the level of GSH measured was on average 30 % lower than in control cells, while for a 0.5 mg/mL solution it was only 9 % lower. The same phenomenon was observed for PA (Fig 3.17b) where a 0.025 mg/ml solution applied for 10 min resulted in a GSH level approximately 40 % lower than in control cells but a 0.2 mg/mL solution led to a decrease of only 19 % in GSH. In this particular experiment, the pre-treatment with 2-AAPA did not seem to influence significantly the level of GSH measured at various concentrations of aldehydes applied. Both experimental dose-response curves followed the same trend.

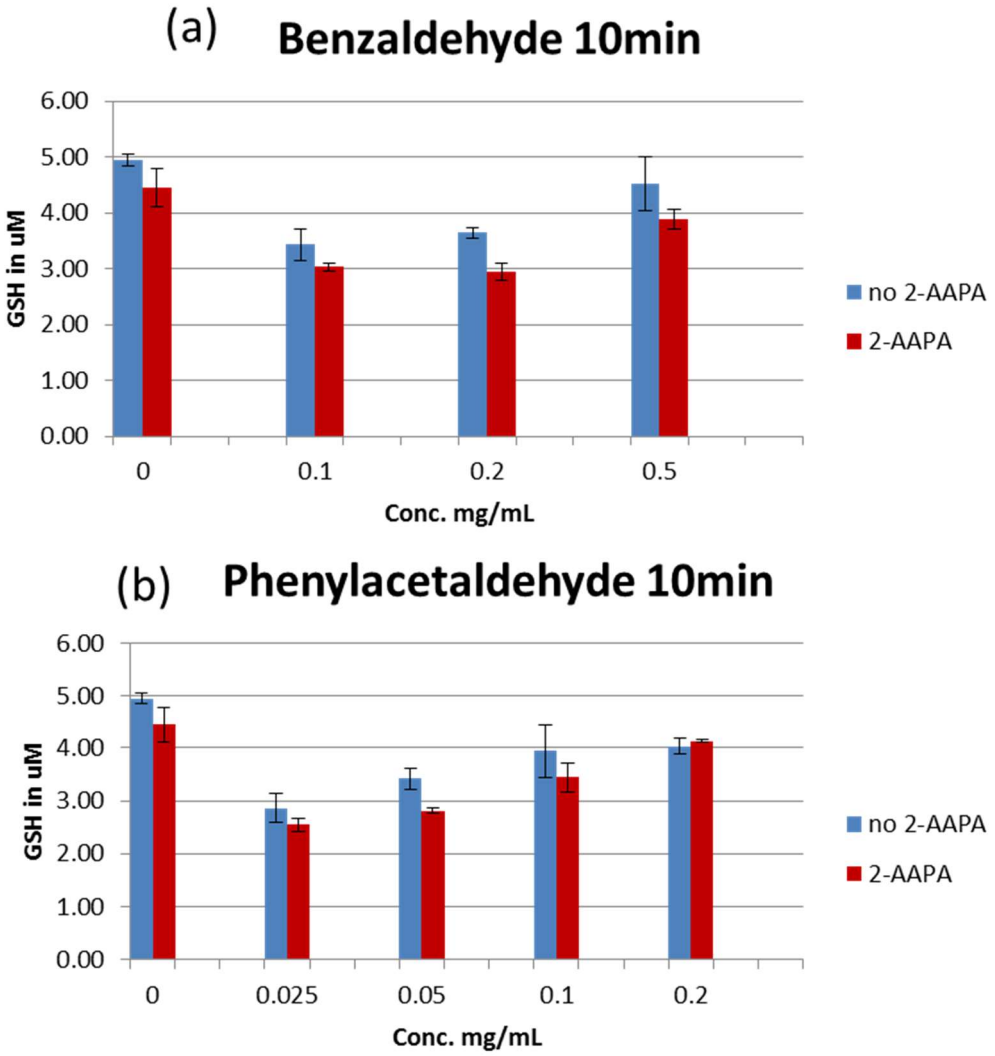

Figure 3.17: Effect of pre-incubation with 2-AAPA on HaCaT cells treated for 10 minutes with aldehydes. Each well (400 000 cells per well) was treated with 50 µM of 2-AAPA and incubated for 2 hours. Cells were then rinsed twice with PBS, treated with a) benzaldehyde or b) phenylacetaldehyde, covered with a plastic adhesive cover and incubated at 37 °C for 10 minutes. Cells were rinsed, lysed and derivatised with iodoacetamide as described in previous figures. Results were expressed in µM (n=3) and presented as Mean ± Standard deviation. The figure shows that for both aldehydes, GSH does not deplete as a function of the dose applied. A Student t-test was carried out to measure difference between the mean at each time point and the mean at t = 0 and showed no statistical difference (with a P value<0.05).

GSH level in HaCaT cells treated with (a) BA and (b) PA for 10 min. Blue columns are the results for cells treated with aldehydes only. Red columns show the influence of a pre-treatment of HaCaT cells with 50 µM of 2-AAPA for 2 hours, previous to the exposure to aldehydes.

3.4 Discussion.

The characterisation of the GSH pathway in the HaCaT cell line focussed specifically on the following points: 1) the synthesis of *de novo* GSH, with or without the inhibition of GCL by BSO was quantified, 2) the formation of GSSG due to oxidative stress was investigated using HP, BA and PA, 3) the inhibition of GR activity was carried out using two different probes, carmustine and 2-AAPA, 4) an estimation of PA and BA detoxification by the GSH pathway in the HaCaT cell line was given.

The level of GSH in HaCaTs, as measured in our assay, was in the low µM range for a 100 000-cell lysate. The level of GSH depletion observed in the HaCaT cell line due to the inhibition of GCL by BSO was in accordance with results reported in the literature for a similar experiment using Hepa-1c1c7 cells [155]. In our assay, after 24 hours of incubation a dose as low as 50 µM BSO reduced the GSH pool to less than 10 %. GSH turnover in skin cells has not been published for comparison, but the half-life of GSH in liver is approximated at 3-4 hours [156]. It is generally accepted that GSH production in the liver covers for most of the GSH needs throughout the body [123]. Therefore, a turnover of GSH stock taking 6-8 hours is likely to be one of the fastest times observed under normal, non-stressed conditions in human organs. Here, HaCaT cells consumed the vast majority of the GSH pool under normal conditions in 24 hours. Even though human skin is not solely constituted of keratinocytes (the *stratum corneum* being constituted of cells non-enzymatically active and the dermis being constituted of fibroblasts, which were not studied here) it is possible to estimate GSH turnover after 24 hours, without disagreeing with the fact that skin requirements in GSH are realistically lower than liver.

The ratio GSH:GSSG is an indicator of cellular health. At homeostasis and in healthy conditions, this ratio is estimated to be at least 100:1 [157], and as a result GSSG is rarely

measured in biological samples using standard assays. In the HaCaT cell line, GSH, in its reduced form, could be measured in the 5-10 µM range while GSSG was systematically below the limit of quantification (0.1 µM), which looked in accordance with the healthy GSH:GSSG ratio expected.

Generating oxidative stress leads to an imbalance of the GSH:GSSG ratio in cells. This is usually achieved by treatment with HP. HP is a potent oxidant that induced complete oxidation of GSH *in chemico* at pH 7.4 and pH 9.5 in our experiments. This was in accordance with previous observations made by Finley *et al* [158], who studied the kinetics of oxidation of GSH *in chemico* at different pHs. However, 0.5-2.5 mM HP treated HaCaT cells demonstrated a dose response trend in GSH depletion for concentrations above 1mM but not the formation of GSSG in the cells. This could be due to two main factors: 1) the GSH is not used for the formation of oxidised GSH (GSSG) but used to quench other ROS and form separate entities or 2) GSSG potentially formed by oxidation is rapidly reduced back to GSH (reaction catalised by Glutathione reductase).

HP toxicity, as measured by MTT assay, was significantly increased at concentrations above 1 mM (data not shown), which corroborates with findings in other studies in which HP induced significant toxicity for a concentration range 50-500 µM after 2 hours exposure [159] and a 1 mM dose decreased cell viability by 60 % within 4 hours [160]. This tends to justify the GSH depletion observed experimentally by cell death rather than oxidation of GSH into GSSG, in this particular set of experiments.

To investigate the detoxification of compounds with skin sensitisation relevance, model aldehydes (BA and PA) were incubated *in chemico* with GSH. Both compounds demonstrated oxidising properties that enabled the complete oxidation of GSH into GSSG, while no secondary products (i.e GSH-conjugates) could be identified. This was in accordance with previous observations made with Cys containing peptides [20, 24].

Cytoxicity of BA in the HaCaT cell line (occluded conditions) was considered satisfactory (<20 % cell death) for a concentration up to 0.1 mg/mL, while for PA, which was more toxic, the maximum concentration applied before significant cell death occurred was 0.025 mg/mL. It was expected that these concentrations would be high enough compared to the intracellular GSH concentration to induce GSH depletion by dimerisation. However, in our set of experiments the formation of GSSG could not be measured. Increasing these concentrations to toxic levels (Figure 3.14) and reducing the experimental period to 10 minutes (time at which the GSH levels seemed the lowest in Figure 3.9) did not increase the formation of GSSG. It was therefore considered that, if the detoxification mechanism of aldehydes was the same *in chemico* and *in vitro*, the speed at which GR reduced GSSG back to GSH was higher than the time required to prepare the samples (i.e < 10 min + sample freezing time). These experiments were therefore repeated with the introduction of an inhibition step using BCNU.

The oxidation of GSH into GSSG after exposure to aldehydes was investigated. While BCNU was not significantly toxic nor induced a depletion or overproduction of GSH when applied at 200 µM for an hour, the experiment set up did not demonstrate an increase in GSSG level due to oxidation by aldehydes. The level of GSH was also constant during the two hours of exposure to each of the aldehydes and were not significantly different from control cells at t=0 h.

Changing BCNU for 2-AAPA, a more specific inhibitor of GR, did not increase the formation of GSSG in HaCaTs. 2-AAPA was applied at a concentration of 50 µM for 2 hours prior to any aldehyde treatment. However, the level of GSSG did not increase above the limit of quantification. More surprisingly 2-AAPA appeared to induce the production of fresh GSH (up to 40 % compared to untreated controls). A 10 min dose response to aldehydes showed that GSH was not depleting but increasing slightly with the dose, whether or not the cells were pre-treated with 2-AAPA.The only rationale to

explain why the level of GSH increased proportionally to the concentration of aldehydes applied is to consider that the synthesis of GSH in HaCaT cells can be quicker than 10 minutes.

The lack of GSSG might be due to 1) BCNU and 2-AAPA not being able to inhibit GR in the HaCaT cell line to a suitable level, using this particular protocol (medium, temperature, time) or 2) aldehydes did not oxidise GSH in HaCaT cells but were mainly consumed elsewhere.

Considering the relative volatility of BA and PA, an important amount might be present in the headspace above the cell medium in the occluded wells. This would explain the availability of aldehydes to react with GSH in solution (*in chemico* experiment, where samples are sealed in Eppendorf tubes and maintained under low agitation) is significantly different than the one observed in a biological sample (HaCaT cells covered with a plastic or aluminium seal but left resting in an incubator without agitation).

The proportion of aldehydes that penetrated the cells might have reacted using a combination of mechanisms: A few cases of skin allergy involving contact with PA have been reported, therefore the aldehyde must be involved in covalent binding with skin proteins. The main mechanism involved is a Schiff base formation with residues containing a primary amine, such as lysine residues. The mechanism reported with thiols *in chemico* is an oxidation yielding a sulfur dimer. This reaction appears relatively minor in proportion compared to the Schiff base reaction, as dimerisation of GSH was not observed in our experiments even though detoxification by oxido-reduction mechanism is usually fast. This type of chemistry with thiols is not favoured by the local environment in skin compared to Schiff reaction with amines. Oxidation of thiols, once it had occurred, even to a relatively small extent might have triggered cellular defence systems such as the production of GSH, as was observed in the 10 minutes experiment, in which GSH levels increased for a short period.

3.5. Conclusion

After initial investigations on the basal level of GSH present in these cells (in the 5-10 µM range using our assay) it was demonstrated that, under homeostatic conditions, the natural consumption of the GSH pool took 24 hours, between two and six times slower than estimated in the liver by Reed *et al* [161], who reported a half-life value of cellular GSH in the range 2-6 h based on previous work published by Ookhtens *et al* [162] and Lauterburg *et al* [163]. HaCaT cells are equipped with the required level of working enzymes to synthesise *de novo* GSH, i.e GCL and GS, and when the cells were left in culture medium for 24 hours, the level of GSH usually doubled in the culturing well.

This cell line appeared relatively resilient to oxidative stress as exposure to oxidants such as HP, and to a lesser extent BA and PA, usually did not deplete the pool of GSH or increased significantly the level of GSSG before high level of cytotoxicity was observed. This suggested that the recycling enzyme Glutathione Reductase was very efficient in this cell line.

In terms of detoxification of xenobiotics, oxido-reduction mechanisms are fast and reliable in the HaCaT cell line. In our experiments, the defence mechanism involving GSH was in direct competition with reactivity with proteins in terms of kinetics. In the case of the two aldehydes studied, reaction with GSH did not seem to be a major reaction, even though mechanistically, the reaction was possible and easily observed *in chemico*. Covalent binding with proteins via a Schiff base mechanism with primary amines seemed to be preferred in the conditions of the assay. The protein content of HaCaT cell lysates has not been fully characterised yet but the ratio of cysteine/lysine is suspected to be in favour of lysine residues. This is based on findings relating to proteome analysis of human skin for which over 600 proteins were characterised, where lysine represented 5.7 % and cysteine 0.9 % of all residues, nucleophilic or not [154].

To conclude, in the study of the detoxification of skin sensitisers by GSH, the use of the HaCaT cell line is justified as the main enzymes involved in the GSH pathway are present. However, focus should be placed on detoxification by a conjugation mechanism, in which the main enzymes used are Glutathione-S-Transferases (GSTs). This mechanism will be at the centre of the investigations carried out within the next chapter of this thesis.

Chapter 4: GSH conjugation as clearance mechanism of dinitrohalobenzenes in the HaCaT cell line.

Contents

4.1 Overview.

4.1.1 GSTs in the HaCaT cell line and other skin models.

The previous chapter highlighted the presence of detoxification enzymes included in the GSH pathway that are linked to countering oxidative stress such as Glutathione Reductase [164]. Evidence of detoxifying enzymes operating by formation of glutathione conjugates (GSTs) has also been found in the HaCaT cell line by identifying a few peptides characteristic of each enzymes using high resolution mass spectrometry [165]. Van Eijl *et al* demonstrated that HacaT cells contained GSTs from the pi and omega isoforms and compared the results to whole human skin samples, which were found to cover a wider range of isoforms as they also contained the alpha and mu isoforms. Primary keratinocytes, which would be less complex than fresh *ex vivo* skin but more specific than an immortalised cell line, might or might not contain GSTs mu and alpha at a protein level, as gene expression for GST A4, GST M2 and GST pi have been reported but activity measurements have only been highlighting the activity due to GST pi [166]. Such differences at the protein expression level might not be detrimental to the use of the HaCaT cell line in our studies of detoxification of sensitisers by conjugation mechanisms.

4.1.2 GSH reactivity with DNCB.

GST activity in cells is usually measured by consumption of the substrate DNCB. DNCB is considered a broad-spectrum substrate as it is not confined to a specific isoform of GST and the conjugate dinitrophenyl-glutathione (DNP-SG) can be formed in all cases. To measure the GSH conjugate formed, DNP-SG, several methods have been developed, including spectrophotometric ones. It is now very common to measure the increased in

absorbance at 340 nm using kits commercially available. The conjugation reaction between GSH and DNCB is illustrated in Fig 4.1.

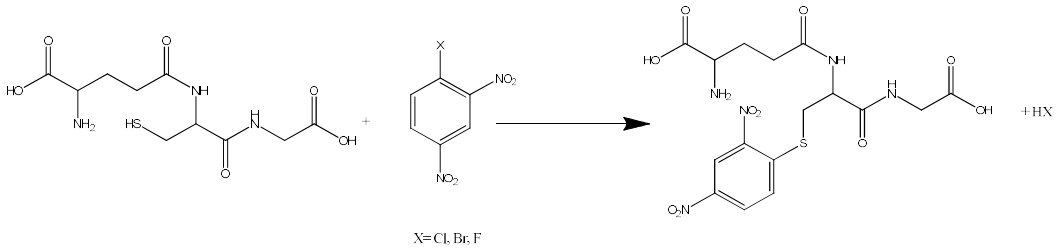

Figure 4.1: Formation of dinitrophenyl-glutathione (DNP-SG)

The mechanism by which the thiol contained in GSH reacts with the electrophilic DNCB is an aromatic nucleophilic substitution (S_NAr), which results with the substitution of Cl for the GSH moiety and the release of hydrochloric acid (HCl). The GSH conjugation of DNCB can happen spontaneously *in chemico* at pH 8 and has been used extensively to prepare this conjugate using a general method such as the one described in Vince *et al* [127]. The ability of GSH to conjugate an extensive range of electrophiles, not limited to the ones reacting by S_NAr, without the necessity for enzymes has been used to develop *in chemico* assays in the past [167]. Therefore, it cannot be ruled out that a mixture of enzymatic and non-enzymatic reactions between DNCB and GSH might happen in cells to some extent. However, experimentally, the second order rate constant for the spontaneous reaction between GSH and DNCB has been reported at $4.2\pm0.2 \times 10^2\ \mu M^{-1}.min^{-1}$ but the introduction of GST enzymes (purified and in isolation) made the conjugation reaction much faster, with a kinetics rate k_{cat}/K_m reported ranging from 93 ± 19 to $716\pm234 \times 10^2\ \mu M^{-1}.min^{-1}$ [168, 169]. It is expected that overall, spontaneous reaction should not be the main driver for GSH depletion in the HaCaT cell line or any other cell line demonstrating the presence of GSTs.

As a result, DNCB was used as a non specific probe for the overall determination of GST activity, regardless of isoform, in skin related cell lines. GST activity in the HaCaT cell line was measured at approximately 150 nmol/min/mg soluble protein and was found to be 38 % lower than the activity measured in normal keratinocytes (NHEK)[79]. More recently, a similar study measured GST activity in the 50 nmol/min/mg soluble protein range, these results being comparable to activity measured in the other immortalised keratinocyte cell line used in the study (NCTC) and primary keratinocytes (NHEK)[53]. The general consensus for this is that GST activity in human skin and related cultured models should be in the low nmol/min/mg soluble protein range [53]. Jewell *et al* also measured the formation of DNP-SG in human *ex vivo* skin during skin penetration measurements of DNCB [170], demonstrating that GST activity in skin could be maintained for a number of hours after the skin was excised and GSTs should therefore, be fully operational in living keratinocyte based cells such as the HaCaT cell line.

4.1.3 2,4-dinitrohalobenzenes as model skin sensitisers.

DNCB and DNFB have both been used as model sensitisers to reveal hypersensitivity in patients by patch testing since the early 70s as patients are unlikely to be in contact with these chemicals outside the clinic. Reports of healthy volunteers tested with DNFB [171] or DNCB [111] are available. However, rare cases of Occupational Contact Dermatitis, linked to the use of DNFB [172] or DNBB [173] [174] by chemistry students can still occur. It has been noted that induction of a certain level of sensitisation to DNCB can also have a beneficial effect in the treatment of recalcitrant warts. Historical treatment with DNCB 0.05 % to 1 % in acetone, applied daily to twice daily, removed warts within 2-42 weeks (average of 15.2 weeks) [175]. Side effects were also described and moderate signs of sensitisation such as localised erythema and oedema were expected

but sometimes observed at an unacceptable level, which required extra treatment and removal from the panel. This highlighted the fact that this treatment should be reserved only for extreme medical cases, for which other treatments have failed. A more recent review of the use of DNCB for medical treatment is available [112] but the general consensus is that its use should be extremely well controlled.

All of these observed immunological responses are a direct consequence of the dinitrohalobenzenes ability to haptenate proteins, phenomenon that is now clearly defined based on all the evidence accumulated throughout the years. DNCB, DNFB and DNBB are all very potent skin sensitisers that have been classified as “extreme” in terms of potency (% EC3 values less than 0.1, this value being the estimated concentration of a chemical required to produce a 3-fold stimulation of draining lymph node cell proliferation compared with concurrent controls, expressed as a %) in the Local Lymph Node Assay (LLNA) [176] and are now commonly referred to as “extreme sensitisers”. As a result, most new *in vitro* methods which aim to detect potential skin sensitisers use dinitrohalobenzenes (first DNCB then extending to DNFB when the number of chemicals tested is increased, whereas DNBB is not often used) as part of their chemical evaluation set (Direct Peptide Reactivity Assay [19], Myeloid U937 Skin Sensitisation Test, now U-Sens [177], Human Cell Line Activation Test, h-CLAT [178], KeratinoSens [179]). Our choice to investigate these three dinitrohalobenzenes in GSH investigations is linked to both the skin sensitisation evidence (suitable for investigations in the HaCaT cell line) and the fact that the reactivity with GSH is similar to the reactivity with skin proteins containing a cysteine residue.

4.1.4 Inducing GSTs activity and enzymes linked to the production of GSH: the Nrf2 pathway.

Nrf2 (Nuclear factor erythroid 2-related factor 2) is a stress signalling protein. While cells are maintained in homeostatic conditions, Nrf2 is sequestered by Kelch-like ECH-associated protein 1 (Keap1) in the cytosol and therefore tagged for regular degradation by ubiquitination. Modification of Keap1 however, enables the release of Nrf2 in the cytosol and its migration to the nucleus where it is recruiting ARE (Antioxidant Response Element) sequences of genes coding for protective enzymes, including Phase II metabolism enzymes [180].

Some, if not most skin sensitisers are electrophilic compounds capable of direct Nrf2 activation by covalent modification of the cysteine residues present. The protein sequencing of Keap1 has demonstrated that Keap1 contains a total of 4.3 % cysteine residues (27 cysteine residues present) but not all of them are targets for these electrophiles and it has been suggested that Cys151, 273 and 288 might play a more important role [180]. This particular feature of sensitisers (i.e their ability to covalently bind to protein) usually helps to differentiate them from skin irritants. The HaCaT cell line, treated with eight sensitisers and six irritants, was used to demonstrate that in a gene expression study looking at upregulation of Nrf2 dependent genes such as HMOX1, upregulation only happens with sensitisers [181].

The Nrf2-keap1 sensor is now well characterised and has been used for the development of a luciferase assay for assessment of skin sensitisation potential. Initially, a modified female breast cancer cell line transfected with eight copies of the ARE sequence coding for a luciferase reporter gene (AREc32 cells) was used and results were compared to the activation of Nrf2 in an unmodified hepatic cell line (Hepa1C_1C_7) [182]. This was then exploited further in the development of the KeratinoSens assay®, in which a custom made cell line of keratinocytes transfected with the ARE sequence of the human gene AKR1C2 (aldoketoreductase) linked to a luciferase gene (Luc2) is used

[183]. The OECD carried out a review of this test [184], which is now included in their Test Guideline 442d.

These luciferase based assays have proven useful for the detection of skin sensitisers (as opposed to non-sensitisers) but they are not usually used for assessing the effect of these sensitisers on skin cells. Nrf2 activation has been shown to induce detoxification enzymes, including Phase II metabolism enzymes such as GSTs [174]. GSTs requiring GSH as co-factor to form conjugates with the sensitisers (after which GSH cannot be recycled and the conjugates are excreted), it is essential to the cell's health that a fresh supply of GSH is available. Hence Nrf2 activation has also been linked to the upregulation of enzymes required for the synthesis of *de novo* GSH such as GCL [185].

Using the HaCaT cell line, without further genetic modifications should enable detecting of Nrf2 activation by treatment with model sensitisers in our set of experiments and link it to the synthesis of GSH to help cellular defence.

4.2 Aims and Objectives.

The following experiments aimed to demonstrate that GST activity in the HaCaT cell line was sufficient to deplete stocks of GSH present in the cells using the dinitrohalobenzenes selected (demonstration of GST activity in HaCaTs). However, this could be achieved using a freshly prepared HaCaT cell lysate. The aim here was to select a concentration in dinitrohalobenzenes that would be as close as possible to the point at which HaCaT cells were able to clear the dose they were exposed to and induce a repletion of GSH by *de novo* synthesis of GSH stock without irreparably compromising the cells' health. The selection of such a dose of dinitrohalobenzene involved a combination of toxicity consideration (cytotoxicity measured here by MTT assay after 24 hours of treatment) and observation of a significant GSH depletion followed by an

increase by liquid chromatography-mass spectrometry (dose response measurements after 1 hour and 24 hours exposure). Activation of the Nrf2 pathway, here release of NRf2 into the cytosol, was also used as an indirect measure of the ability of HaCaT cells to synthesise *de novo* GSH after induction of GCL and ability to clear the dose after induction Phase II metabolism GSTs. Full 24 hour time course experiments at the fixed dose for the three dinitrohalobenzenes enabled us to highlight some differences in the ability of HaCaT cells to synthesize GSH after exposure to the three compounds. The experimental data were then fitted to simple mathematical model, which could be used in the future as a benchmark for estimating the influence of concentration of electrophile on the GSH synthesis pathway in skin within 24 hours, for chemicals of the same reactive domain (S_NAr reaction).

4.3 Results.

4.3.1 Cytotoxicity of 2,4-dinitrohalobenzenes in HaCaT cells.

Cytotoxicity of 2,4-dinitrohalobenzenes was measured at 24 h to coincide with the maximum time of exposure in the GSH assay. The range of concentrations applied varied between 0 and 10 µg/mL. Concentrations resulting in 80 % or over of viable cells, compared to untreated cells kept in culture medium containing 0.5 % DMSO, were considered non-toxic. For the three 2,4-dinitrohalobenzenes the non-toxic concentrations were determined to be below 2000 ng/mL (10µM) (Fig. 4.2).

The toxicity of DNCB and DNBB appeared to follow a similar trend as a function of concentrations, with a viability of 20 % or less at 5000 ng/mL, in contrast to DNFB for which percentage viability was still 40 % at the same concentration. These data suggest that HaCaT cells are less affected by exposure to DNFB compared with DNCB and DNBB, with the general order of toxicity being DNFB < DNCB = DNBB at 5000 ng/mL (Fig 4.2).

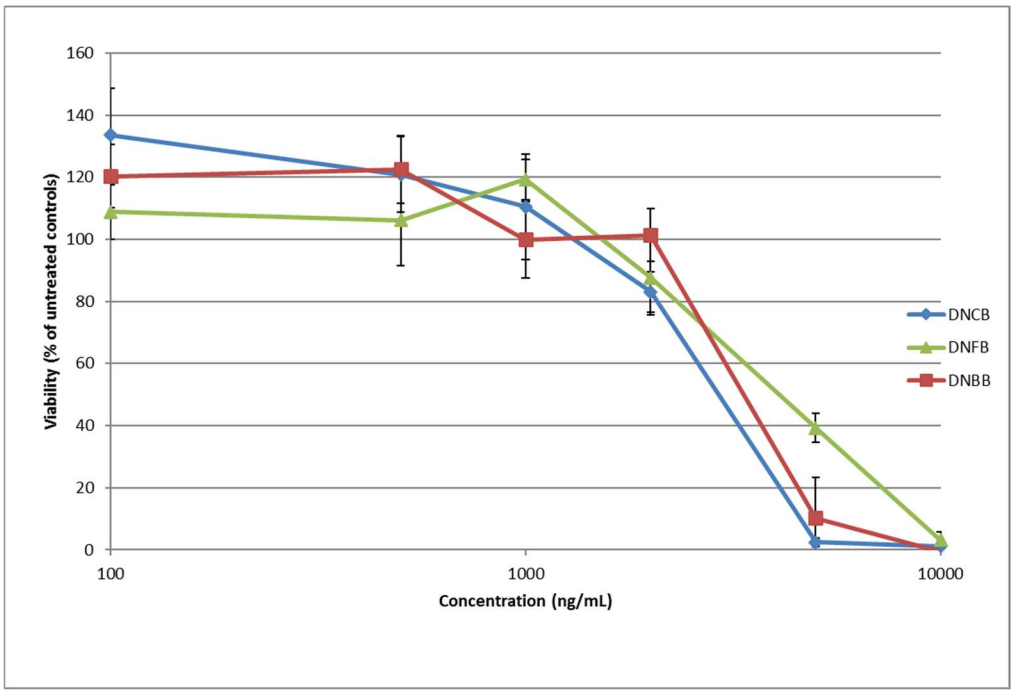

Figure 4.2: Cytotoxicity of dinitrohalobenzenes in HaCaT cells after 24 hours. The toxicity of DNCB, DNFB and DNBB was determined using the MTT assay after 24 hours of exposure. Each well (20 000 cells/well) was treated with the appropriate concentration of either DNCB, DNBB or DNFB. The concentration applied was considered non-toxic when the cell viability is at least 80 % compared to control cells kept in culture medium containing 0.5 % DMSO for a similar length of time. Each concentration was tested in 8 wells (n=8) and the result was presented as Mean viability ± Standard deviation. The figure shows that all concentrations lower or equal to 2000 ng/mL (10 µM) for DNCB, DNBB and DNFB were non-toxic.

4.3.2 GSH depletion after exposure to 2,4-dinitrohalobenzenes is dose dependent.

Significant depletion of GSH was observed with all three 2,4-dinitrohalobenzenes at concentrations over 5 µM (approximately 1 µg/mL) after a 1 hour incubation. The depletion was dose dependent and no observable differences were noted between the compounds at this time point (Fig 4.3 a). However, at 24 hours significant differences were observed between the chemicals as well as in relative GSH levels between treated and control cells (Fig 4.3 b). At a concentration of 10 µM a marked difference in GSH levels was observed between the chemicals. DNBB-treated cells had less than 50 % GSH compared to concomitantly-run control, whereas DNFB- and DNCB-treated cells were

comparable to controls. At 10 µM the relative GSH levels were significantly different to control (Fig 4.3) with less than 20 % cell death (Fig 4.2, 10 µM= approx. 2 µg/mL) so this concentration was chosen for all three compounds for the time-course study.

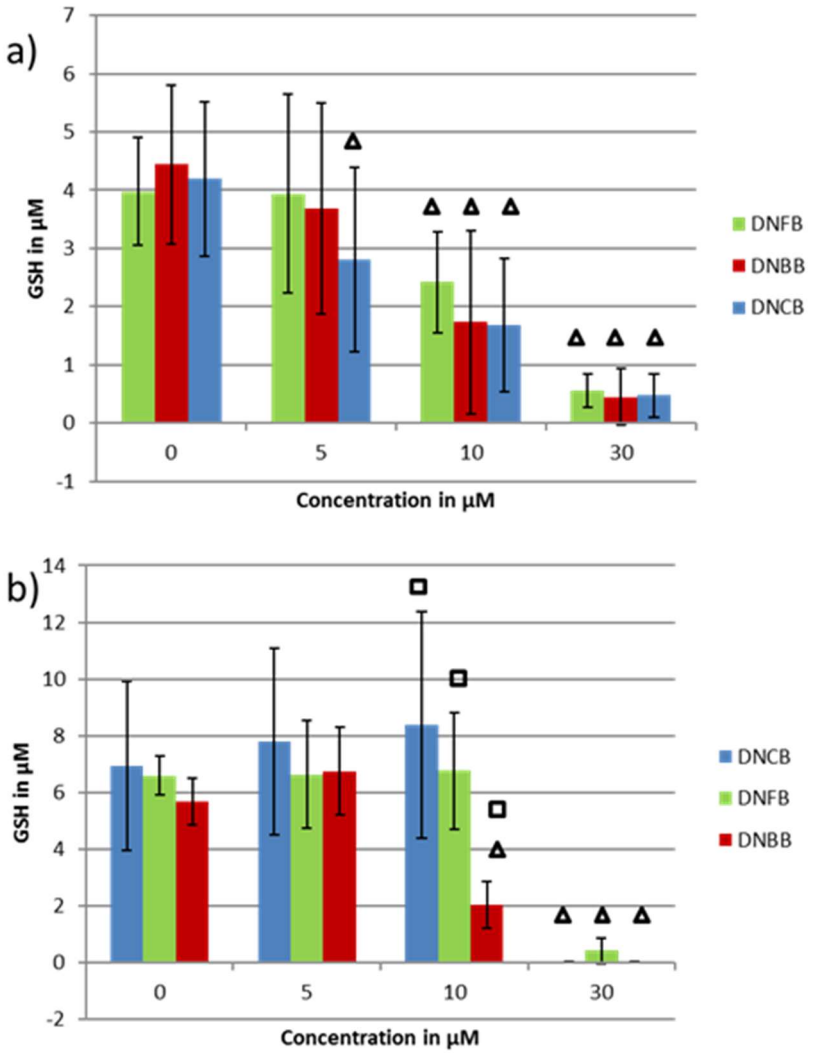

Figure 4.3: GSH levels in HaCaT cells treated with dinitrohalobenzenes. HaCaT cells (400 000 cells/well) were treated with 0-30 µM dinitrohalobenzenes for a) 1 hour and b) 24 hours. The cells were then rinsed twice with PBS and 200 µL water were added to the well. The cells were lysed at -80 °C and half the lysate (equivalent to 200 000 cells) was derivatised with iodoacetamide for GSH quantification. GSH levels were expressed in µM and reported as Mean ± Standard deviation (n= 4). (Δ) Statistical difference between GSH level in treated samples and concomitantly run controls (0 µM) Student's t-test, p value <0.05. (□) Statistical difference between GSH level in samples treated with 10 µM DNCB, 10 µM DNFB or 10 µM DNBB, ANOVA, p value <0.05.

4.3.3 GSH depletion and repletion after exposure to a single 10 µM dose of 2,4-dinitrohalobenzenes.

Depletion of GSH in HaCaT cells was observed for the first two hours of monitoring following treatment with 10 µM of DNCB, DNFB or DNBB. The GSH level was approximately halved at the two hour time point and this depletion trend was similar for all compounds (Fig 4.4).

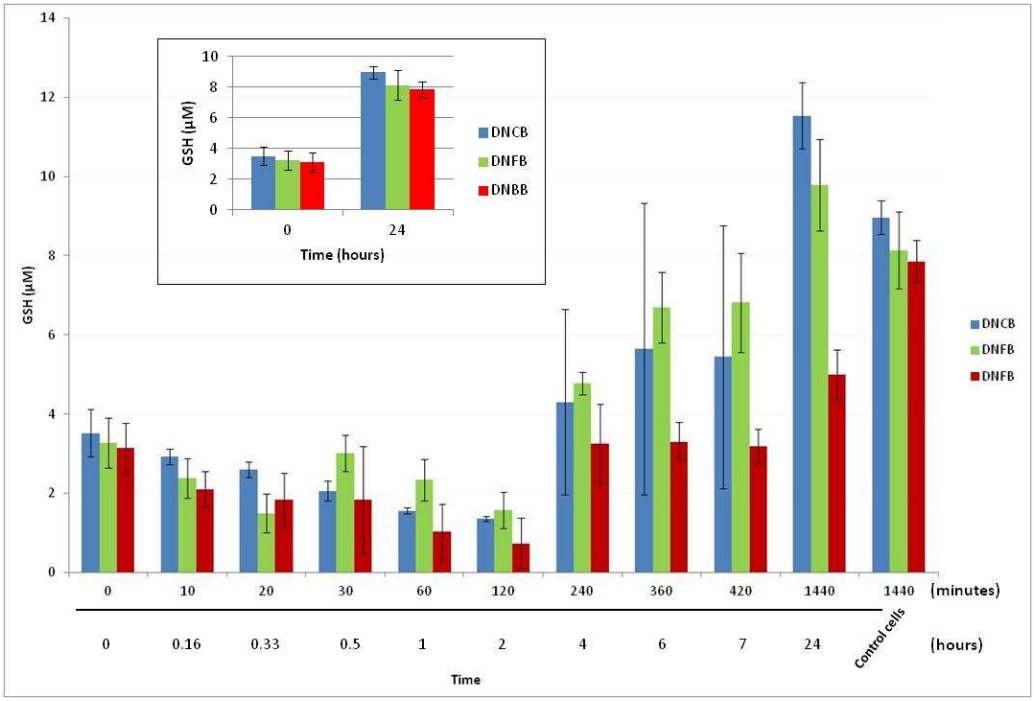

Figure 4.4: GSH level in HaCaT cells treated with 10 µM of 2,4-dinitrohalobenzenes over a 24-hour time course period. Each well (400 000 cells/well) was treated with the 10 µM of either DNCB, DNBB or DNFB and incubated for the required amount of time. The cells were then rinsed with PBS, lysed and derivatised with iodoacetamide as described in previous figures. GSH levels were measured in half the lysate (equivalent to 200 000 cells, and the concentration expressed in µM and presented as Mean viability ± Standard deviation (n=4). The figure shows that the rate of repletion of GSH is chemical dependent, with DNCB and DNFB allowing for the quickest recovery while the DNBB only allows partial GSH replenishment. *Insert:* Comparison between t=0 h and 24 h in control cells. Statistical analysis of the results is covered in Section 4.4 Modelling approaches.

At 4 hours of exposure, it is evident that the HaCaT cells have reached a maximum depletion of GSH. In response, the cellular defence system has triggered a production of GSH to replace the missing antioxidant, regardless of which dinitrohalobenzene was used. The later time points (6, 7 and 24 hours) highlighted considerable differences between the three structurally similar 2,4-dinitrohalobenzenes. While both DNCB- and DNFB-treatment allowed for a replenishment of GSH to a level equivalent to untreated cells (Fig 4.4 insert), with DNBB-treatment the measured GSH level was 5.0±0.6 µmol/L, approximately half the level observed at 24 hours for untreated cells.

4.3.4 Exposure to 2,4-dinitrohalobenzenes activates the Nrf2 pathway in HaCaT cells.

HaCaT cells were exposed to identical concentrations of DNCB, DNFB and DNBB (0-10 µM) for 2 hours. Western blots of the cell lysates showed that all three compounds activated the Nrf2 pathway (Table 4.1, Fig 4.5).

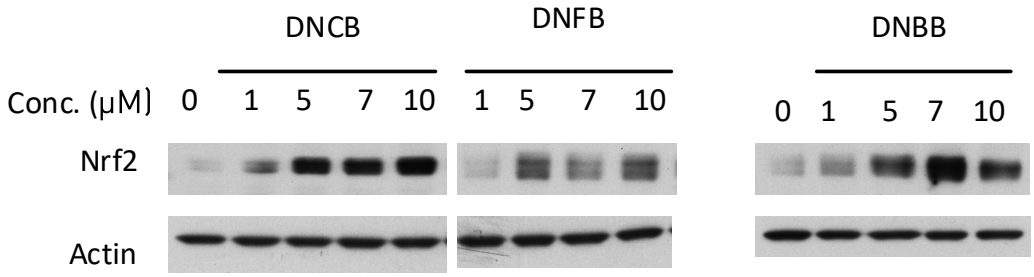

Figure 4.5: Representative example of Western Blot analysis. HaCaT cells (100 000 cells/well) were treated with 0-10 µM dinitrohalobenzenes for two hours, rinsed twice with culture medium and lysed with 80 µL of RIPA buffer enriched with 0.2 % protease inhibitor per well. Control experiments were carried out with 0.5 % DMSO in culture medium. 10 µg protein for DNCB and DNFB samples, 8 µg for DNBB (adjusted for protein concentration) were denatured at 85 °C for 10 minutes, loaded on gels and separated by electrophoresis at 90 V for 10 minutes followed by 170 V for 1 hour. The content of each gel was then transferred to a nitrocellulose blotting membrane (230 mA for 65 minutes), which was stained with Ponceau S and blocked with non-fat dry milk solution (10 % in Tris-Buffered Saline) overnight. Membranes were treated with rabbit anti-Nrf2 primary antibody for 3 hours (or mouse anti-actin primary antibody for 30 minutes) and

Nrf2 secondary antibody for 1 hour. Membranes were treated with a Western Lightning plus enhanced chemiluminescence (ECL) reagent kit (Perkin Elmer, Coventry, UK) for film development. Quantification of free Nrf2 was carried out using a GS-800 calibrated densitometer and the Quantity One software version 4.6.1. Data were normalised to actin (n=3). Results are presented in Table 4.1.

	Ratio: Nrf2 in sample/ Nrf2 in solvent control (0µM)		
Concentration of dinitrohalobenzene (µM)	DNCB	DNFB	DNBB
0	1	1	1
1	1.6 ± 0.7	1.2 ± 0.2	1.3 ± 0.4
5	2.4 ± 0.9	1.7 ± 1.1	1.9 ± 0.5
7	2.0 ± 0.7	1.6 ± 0.8	2.0 ± 1.0
10	2.1 ± 1.0	1.4 ± 1.5	1.5 ± 0.7

Table 4.1: Representative Activation of the Nrf2 pathway after exposure to 2,4-dinitrohalobenzenes relative to solvent control. The results are presented as Mean ± Standard Deviation (n= 3).

All compounds showed activation of Nrf2 at a range of concentrations (5-10 µM), which is consistent with the results observed in the GSH assay, in which the application of 5-10 µM of DNCB and DNFB (Fig 4.3) induced a significant repletion of GSH (up to control levels) in 24 h. However, at 10 µM the Nrf2 activation is evident with DNBB (Fig 4.5) but the repletion of GSH is significantly lower than for DNCB and DNFB (Fig 4.3 b).

4.4 Modelling approaches.

4.4.1 Overview of techniques available to model GSH in a skin sensitisation context.

Reed *et al* have developed a very complex mathematical model, which included the whole of the GSH pathway in liver, i.e synthesis, breakdown, oxidative stress defence mechanism (GPx and GR) and export to the blood stream, as part of their attempt to represent metabolism in liver. With this model they tried to show how oxidative stress influenced this metabolic pathway in Down syndrome patients [161]. The same research group then improved their model by including GST as a detoxifying pathway as well as the metabolism of 5-oxoproline and ophthalmic acid [186] two biomarkers previously linked to the GSH pathway, the former being a precursor of L-glutamate [59] and the latter a biomarker of hepatic GSH consumption due to oxidative stress [187].

So far, a fully operational mathematical model does not exist for GSH metabolism in skin and it is unrealistic to try and reproduce a model with such a level of details as the one developed by Reed *et al* [161]. If a GSH based model for detoxification is to be useful in terms of skin sensitisation predictions, it should be incorporated into a broader model covering all of the sensitiser's bioavailability in the skin after topical application. Predictive chemistry software packages (alerting the user of skin sensitisation potential by highlighting the electrophilic and pro-electrophilic moieties of a molecule) are already available but are so far incomplete and under constant improvements. The TIssue METabolism Simulator platform used for predicting Skin Sensitisation (TIMES-SS) is a software developed to give alerts for the potential for skin sensitisation and the potential for metabolism, which is based on chemical structure [188, 189]. Lhasa Limited also offers such a software, with the Derek Nexus skin sensitisation model giving a predicted EC3 value for the compound entered and the Meteor Nexus software making Phase I and Phase II metabolites prediction of the compound of interest, based on rules

derived from available literature data and experimental data given by collaborative partners [190, 191].

Using the HaCaT cell line, our experiments put the dinitrohalobenzenes in direct contact with viable cells, which gives a good overall overview of their bioavailability in skin as several mechanisms are in competition: the chemicals can simultaneously react with membranes, intracellular proteins, free amino-acids or small-sized peptides such as GSH (in this case covering the potential for metabolism). In our set of experiments, we observed both a depletion and a repletion of GSH levels over a 24 h time course. We decided to focus our simplified model around these two phenomena.

4.4.2 Model.

Whilst it is most likely that depletion of GSH and the synthesis of *de novo* GSH occur concomitantly, the method used to interpret our dataset separates depletion of GSH due to dinitrohalobenzene exposure and the replenishment subsequently observed, while fitting a linear equation through each event (Figure 4.6). This was achieved using the non-linear mixed (NLMIXED) procedure in the SAS software version 9.3 (SAS Institute, Marlow, UK). The depletion was modelled by the equation

$$GSH = a + b * Time^{1/3}$$

where *a* is the GSH value at the start of the experiment (in µM) and *b* is the rate of depletion (in µM/min$^{1/3}$). The tipping point at which depletion changes to replenishment was denoted *tp* (in min$^{1/3}$). The replenishment of GSH was thus modelled by the equation

$$GSH = a + b * tp + c\,(Time^{1/3} - tp)$$

where *a and b* are unchanged compared to the depletion equation and c is the rate of repletion (in µM/ $min^{1/3}$).

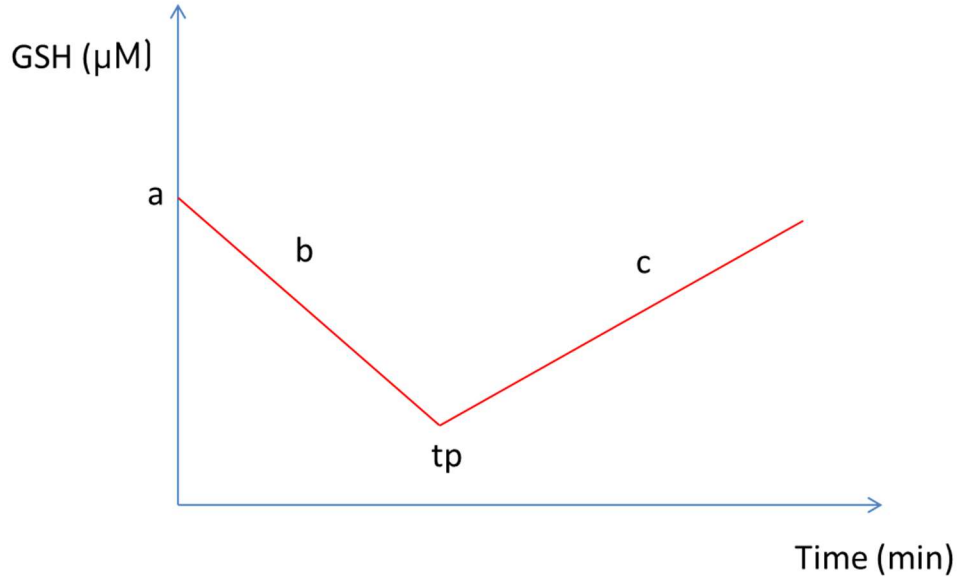

Figure 4.6: Schematic of the variation of GSH in HaCaT cells after a single treatment. HaCaT cells were treated with 10 µM of dinitrohalobenzene. Time course results were represented as two events following a linear curve (depletion from a to tp and replenishment starting from tp). Model was fitted using the SAS institute NLMIXED procedure.

4.4.3 Model results.

Initially, all data points were taken into account (regardless of which dinitrohalobenzene experiment they related to) and the model was run to estimate an average value for *a*, *b*, *c* and *tp* (Figure 4.7, Table 4.2) across the three compounds. The fitting of the models for each dinitrohalobenzene could then be investigated following two hypotheses.

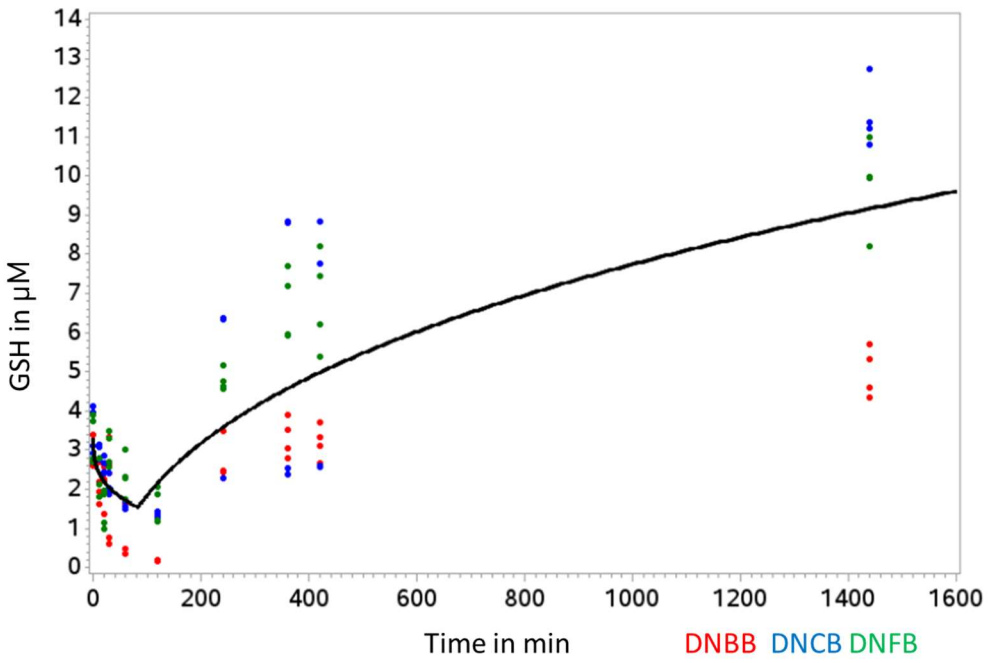

Figure 4.7: Model fitting a value for tp and c when averaging all data points available. Exepriments were carried out in triplicate measurements for each compound and each time point (n=9), irrespective of dinitrohalobenzene.

Parameter estimates			Fit statistics
Parameter	Estimate	Standard error	AIC
tp	4.351	0.345	464.2
a	3.313	0.427	
b	-0.409	0.157	
c	1.099	0.097	

Table 4.2: Estimated parameters and fit statistics values for a model fitting one value for tp and one value for c, where all data points were considered. This gives an average value which is used as starting point for comparison to cases where dinitrohalobenzenes are taken individually and the rate-limiting steps considered.

In the first hypothesis, the depletion of GSH was the significant factor and the fitting therefore consisted of individual *tp* values for each chemical, while the repletion rate *c*

was fixed regardless of chemical applied (Figure 4.8). The *tp* values estimated in this manner for DNCB (3.78) and DNFB (3.55) were similar but considerably different from that for DNBB (5.41) (Table 4.3).

Parameter estimates			Fit statistics
Parameter	Estimate	Standard error	AIC
tp_DNBB	5.418	0.356	421.6
tp_DNCB	3.776	0.270	
tp_DNFB	3.555	0.269	
a	3.423	0.342	
b	-0.488	0.125	
c	1.113	0.074	

Table 4.3: **Estimated parameters and fit statistics values for a model fitting one value for c and individual values for tp**. This is used for modelling the depletion of GSH due to treatment with dinitrohalobenzenes.

The Akaike information criterion (AIC) is used to assess candidate models for a specific set of data. AIC rewards goodness of fit (as assessed by the likelihood function) and penalises the number of estimated parameters in each model, hence discouraging an overfit of the data. The preferred model is the one with the minimum AIC value [192]. The AIC value obtained for fitting this model was lower than in the model in which all chemicals were averaged, demonstrating an improvement in the fitting and thus the difference between DNBB and the other two dinitrohalobenzenes.

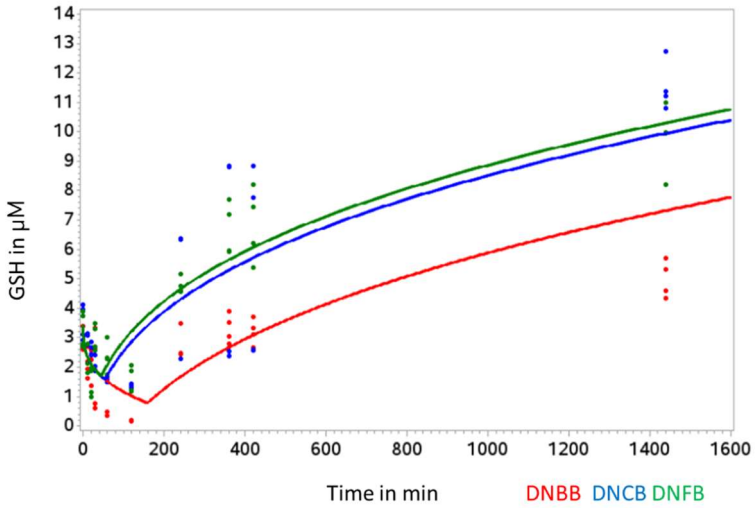

Figure 4.8: Model fitting a value for tp for each dinitrohalobenzene, while the value of c is fixed and the same for the three compounds. This is used for modelling the depletion of GSH due to treatment with dinitrohalobenzenes.

In the second hypothesis, the repletion rate was the significant factor, therefore the depletion of GSH was fixed (the tipping point was set as the same value regardless of compound) and the fitting consisted of three individual c values, representing the replenishment rates observed for each dinitrohalobenzene (Figure 4.9).

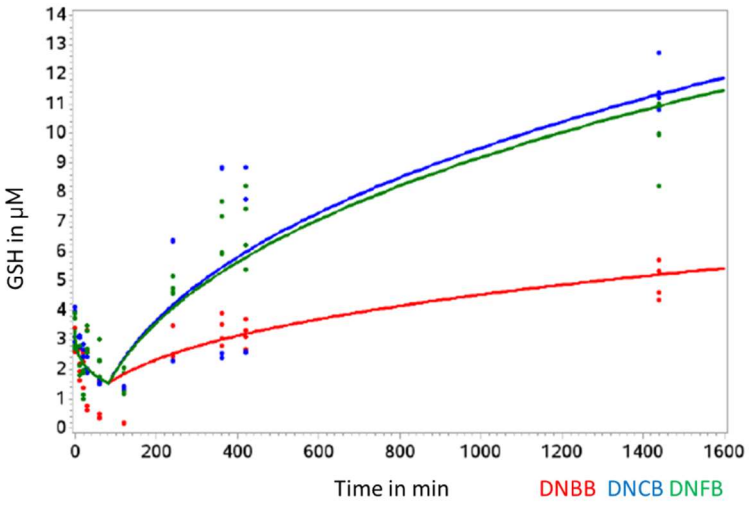

Figure 4.9: Model fitting a value for c for each dinitrohalobenzene, while the value of tp is fixed and the same for the three compounds. This is used for modelling the repletion of GSH, after HaCaT cells have cleared the dose of dinitrohalobenzenes.

Again the two c values estimated for DNCB (1.40) and DNFB (1.35) were similar while the value obtained for DNBB (0.53) was considerably different. The fitting for this hypothesis (AIC value 399.2, Table 4.4) was improved when compared to the first hypothesis (AIC value 421.6, Table 4.3) suggesting that the significant difference between the dinitrohalobenzenes (Figure 4.9) stemmed from GSH repletion rate.

Parameter estimates			Fit statistics
Parameter	Estimate	Standard error	AIC
tp	4.32	0.24	399.2
a	3.325	0.318	
b	-0.417	0.115	
c_DNBB	0.529	0.084	
c_DNCB	1.405	0.103	
c_DNFB	1.349	0.097	

Table 4.4: Estimated parameters and fit statistics values for a model fitting one value for tp and individual values for c. This is used for modelling the replenishment of GSH after the cells have cleared the dinitrohalobenzenes applied.

4.5 Discussion.

Here we considered both GSH conjugation from the level of reduced GSH remaining in cells after exposure to dinitrohalobenzenes and modifications of Keap1 by the increased amount of free Nrf2 protein in cell lysates.

Of the chemicals studied, DNCB appeared to be the most potent Nrf2 activator and DNFB the weakest, but the three dinitrohalobenzenes examined all induced Nrf2 at

lower concentrations than those required to induce detectable GSH depletion (1-5 µM). Modification of Keap1 cysteine residues has been detailed for DNCB in [193] but the same level of information is not available for the DNFB and DNBB. However, since these dinitrohalobenzenes are close structural relatives and the translocation of Nrf2 was observed for all three, it is likely that modification of cysteine residues has happened with DNFB and DNBB as has been reported for DNCB. The induction of antioxidant response element (ARE)-dependent genes regulates the synthesis of enzymes such as glutamyl-cysteine ligase (GCL), which is necessary for the generation of *de novo* GSH in cells, but also GSTs that will help the conjugation of this newly synthesised GSH to electrophiles. Our results suggest both the activation of Nrf2 and depletion of GSH in the cytosol are observed simultaneously. The translocation of Nrf2 was observed at 2 h time point, concomitant with the most pronounced GSH depletion (2-4 h based on time course experiment). The differentiation between our three dinitrohalobenzenes during the repletion of the GSH pool is most likely linked to the toxicity of the halogens themselves once released into the cells [194-196].

The order of cytotoxicity of the compounds (as measured by MTT assay) was difficult to determine for concentrations less than 2 µg/mL= 10 µM, although DNFB seemed the least toxic at a concentration of 5 µg/mL. The MTT assay is based on measurements of mitochondrial activity which can be influenced by the availability of antioxidants. However, most of the widely used assays present differences of their own and the cytotoxicty level at 24 h can vary from assay to assay [197]. Therefore observation of biological effects linked to exposure at the organ level (viable skin) or *in vivo* when possible, provides more valuable information than cytotoxicyty in one cell type alone.

All three compounds are extremely potent sensitisers in the local lymph node assay (LLNA), with very similar LLNA EC3 expressed as a % (DNFB 0.0323 < DNCB 0.0765 < DNBB 0.0849)[176]. Similar LLNA EC3 values were reported by in Natsch *et al* [198] with

slightly different halogen order. Human data is rather scarce as occupational exposure to either dinitrohalobenzene is very occasional but data on sensitisation was obtained in controlled conditions by patch testing healthy volunteers with DNFB [171] or DNCB [111]. In the DNFB study 15 out of 16 people tested demonstrated some level of sensitisation after initial exposure to a 2 % solution of DNFB in acetone (2000 µg dose) followed 7 days later by a re-exposure to a quarter of the original dose. The DNCB study showed that for an initial exposure to 500 µg of DNCB all patients were sensitised (re-exposure 4 weeks later with DNCB doses to up to 12.5 µg). Data for patch testing using DNBB was not available but it would also be expected to generate high level of sensitisation in volunteers. Based on this, it would be difficult to differentiate between the three compounds as they have almost identical biological effects.

The order of reactivity for dinitrohalobenzenes with a peptide containing a cysteine residue (Ac-RFAACAA) is DNFB>>DNCB comparable to DNBB [198] and follows the electronegativity order of the halogens in Pauling's electronegativity table (F 3.98 > Cl 3.16 > Br 2.96). The expectation is therefore that DNFB>DNCB>DNBB in terms of pure reactivity towards nucleophiles. This is observed when glutathione is used as the model thiol nucleophile in an *in chemico* assay at physiological pH, where the RC_{50} values (concentration in mM for which half of GSH used in the assay is consumed) reported follow this rule (DNFB (0.07) << DNBB (1.00) comparable to DNCB (1.60)) [115]. Megherbi *et al.* have shown that dinitrohalobenzenes appear to haptenate cell proteins to different extents irrespective of their order of reactivity [199]. However it is difficult to draw direct conclusions about the relative order of reactivity of the dinitrohalobenzenes using a complex protein mixture and an antibody detection system, as compared to a simpler *in chemico* reactivity assay.

The GSH depletion data described here do not challenge the expected order of reactivity, as all three dinitrohalobenzenes were found to deplete available GSH over a

short period of time (2-4 hours) to a similar extent. However, the fact that DNBB and DNCB appeared more toxic than DNFB at 24 h at a concentration of 5 µg/mL highlights the need to investigate the potential of the biological system to recover from exposure to external chemicals to obtain a better understanding of the effect of topical application on humans.

4.6 Conclusion.

The data showed that the HaCaT cell line was a suitable model to represent the clearance of dinitrohalobenzenes by the GSH pathway in human skin. HaCaT cells possessed the required enzymes to form dinitrophenyl-glutathione conjugates (GSTs) and synthesise *de novo* GSH (GCL, GS). The Nrf2 signalling pathway was activated after exposure for each compound, enhancing the Phase II enzymes linked to the GSH pathway involved in this defence mechanism. The critical piece of information obtained from this piece of work is that for a non-toxic level of exposure, cell recovery (here GSH repletion) might be a differentiating factor for compounds which all react with GSH by the same mechanism. This might be important to assess new chemicals. Overall, when studying the MIE of skin sensitisation, i.e protein haptenation, it might be possible, in theory, to cumulate the kinetics rates at which a molecule conjugates to small peptides *in chemico* [20, 24] (even though this is not systematically measured, to assess the potential for protein binding) and GSH conjugation rate *in chemico* [167] (to assess the skin protective mechanism) to get an estimation of this molecule haptenation potential in an *in silico* model. However, the data is not really representative of skin *in vivo* and would only be used for risk measurements. We have shown in our simplistic mathematical model that all three dinitrohalobenzenes react with GSH at approximately

the same rate in HaCaT cells (Figure 4.9) but the repletion step, which is rarely studied was a differentiating factor. Efforts should be made in the future to integrate the potential for skin “recovery from exposure” in *in silico* predictions.

Chapter 5: GSH conjugation of model sensitisers of various potencies: Case study for DNCB, DPCP and DEM.

Contents

5.1 Overview.

5.1.1 Using the HaCaT cell line GSH assay for comparing chemicals.

As previously discussed in Chapter 4, 24 hour experiments enabled a comparison of the effect of model skin sensitisers of similar structure, i.e dinitrohalobenzenes, on the GSH pathway in the HaCaT cell line. Repletion rate, rather than the kinetics of reactivity during the depletion process, proved to be a differentiating factor. It was also demonstrated that some of the differences could be due to variations in toxicity in the chemicals themselves (for example, Br (DNBB) was slightly more toxic than F (DNFB)). To exploit this theory further, this chapter aimed to reproduce 24 hour experiments using two different model sensitisers, which react with thiols via a different mechanism to that explored so far with DNCB (SNAr). The two chemicals were also selected with a difference in potency in the LLNA, one being an extreme sensitiser (diphenylcyclopropenone, DPCP), comparable to DNCB, and the other being less potent (diethyl maleate, DEM) and classified as a moderate sensitiser.

5.1.2 Diphenylcyclopropenone (DPCP) and diethyl maleate (DEM) as model skin sensitisers.

Based on a recommendation made by the Scientific Committee on Cosmetics Products and Non-food Products Intended for Consumers (SCCNFP) which was presented in 2000, DEM should not be used in any fragrance mixture used in cosmetics [200]. As a result, the general population should not be exposed to DEM on a normal basis. However, some leathers and textiles are treated with dimethyl fumarate (DMF), which is structurally quite similar to DEM (Fig 5.1) as these are *cis*/*trans* isomers and DMF related skin allergy has been reported recently [121]. Patch testing studies for people who had

suffered contact allergy to sofas and furniture that had been treated with dimethyl fumarate (DMF), included control chemicals such as diethyl fumarate (DEF, 1 carbon longer in the chain) and diethyl maleate (DEM, *cis* isomer of DEF) [121]. Results showed that people sensitised to DEF could also have an allergic reaction to DEM. The rationale for explaining this cross sensitisation between fumarates and maleates is that the antigens formed by reaction with proteins would have the same structure and chiral centres for both compounds [201]. The structure itself is discussed further below, in Section 5.1.3.

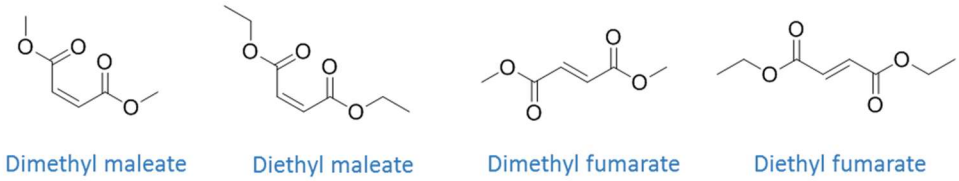

Figure 5.1: Diethyl maleate (DEM) is structurally related to dimethyl maleate (DMM), dimethyl fumarate (DMF) and diethyl fumarate (DEF).

DPCP is not used in personal care products or other commercial products available to the public and is solely considered as a drug. It is a very potent skin sensitiser, classed as extreme in the LLNA [202], which when topically applied enables the induction of an immune response [203]. The immunotherapy technique with DPCP is used in the treatment of alopecia areata and occasionally as an alternative to DNCB in the treatment of persistent warts [112]. Therefore, as is the case for DEM, the general population, with the exception of some patients suffering from the two conditions described above, is not exposed to DPCP but occupational allergic reaction in laboratory or clinical staff is always a possibility [204].

5.1.3 Model skin sensitiser reactivity with proteins.

As DEM is classified as a moderate skin sensitiser in the LLNA [202] it is often used as a benchmark chemical in *in vitro* assays aiming at evaluating skin sensitisation potential. *In chemico* reactivity assays using small peptides have used DEM as a probe and showed that it extensively reacted with cysteine residues in these assays [19, 20]. More specifically for our study, the strong electrophilicity of DEM has made it an attractive compound to deplete GSH stock in biological tissues [123] and this methodology has been used for a long time. Recently DEM has been used in the *in vitro* test SenCeeTox® assay for skin, for a new applicability to medical devices. In this assay, DEM was found to deplete 73 % of GSH present in saline buffer and 69 % in sesame oil [205], meaning that GSH could potentially detoxify DEM in organs presenting localised variations in hydrophobicity, such as the various layers of human skin. The mechanism by which the conjugation between GSH and DEM happens is a Michael addition and is illustrated in Fig. 5.2. The formation of the DEM conjugates with GSH has been monitored by NMR and structures have been confirmed [206]. Under non-specific conditions of pH (i.e pH 7.4 in phosphate buffer and in most cases of cell culture medium or tissue extracts) diastereoisomers are formed in equal proportions. For the purpose of this work, we will only represent one isomer and call it “GSH+DEM” adduct.

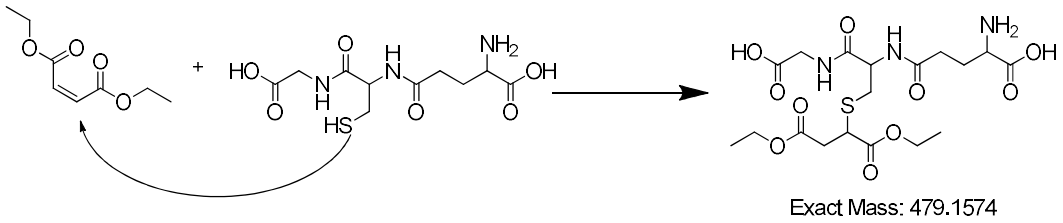

Figure 5.2: Reaction between DEM and GSH occurs via a Michael addition mechanism, yielding a “DEM+GSH” conjugate of molecular weight 479 g/mol.

The molecule DPCP itself was only synthesised for the first time in 1959. However, the mechanism by which it reacts with nucleophiles has been investigated reasonably early by Eicher and Weber in the mid-1970s, before it started to be used by dermatologists to treat skin conditions. Eicher and Weber reported that DPCP could react with hydroxide or alkoxide ions, primary and secondary amines, hydrazines, carboxylates and amides, by reaction on the carbonyl group followed by opening of the ring [207]. They did not comment on reactivity with thiols but the more recent *in chemico* peptide reactivity studies have shown that DPCP could extensively deplete cysteine-containing peptides [19, 20]. In the reactivity assay using the peptide Cor1C-420 (sequence Ac-NKKCDLF) more information is given about adduct formation as LC-MS analysis was carried out: three adducts with DPCP were observed, two being direct adducts of the same mass (peptide+ DPCP) and one being described as a di-adduct (peptide + 2DPCP) [20]. Extrapolating from all this information, reactivity with GSH could lead to the following conjugates (Fig 5.3).

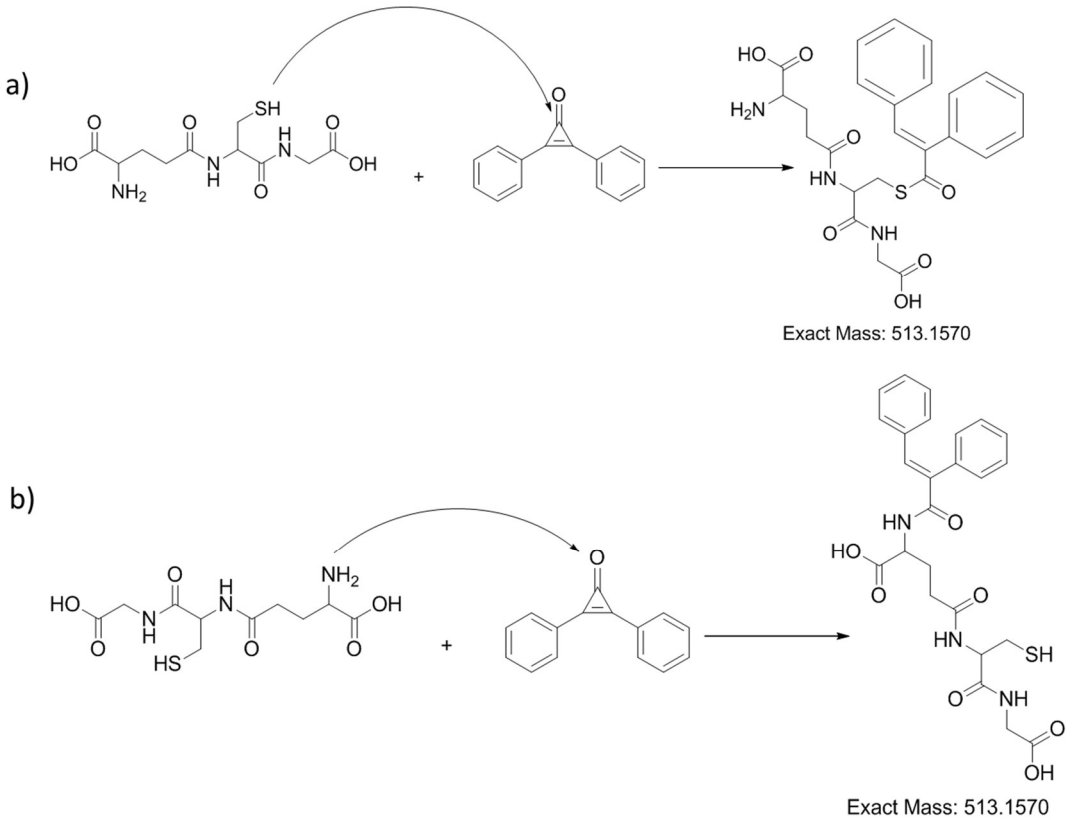

Figure 5.3: Reaction between DPCP and GSH lead to the opening of DPCP's ring. Depending on the nucleophile attacking the carbonyl group (thiol or amine) two structures (a and b) can be hypothesised for a "DPCP+GSH" conjugate of molecular weight 513 g/mol, even though option a) should be prevalent.

5.2 Aims and Objectives.

The following experiments aimed to illustrate how compounds of various skin sensitisation potency influenced the GSH clearance pathway in the HaCaT cell line. First, the comparison focussed on two extreme sensitisers, DNCB and DPCP and how their different chemistries played a role on their metabolic clearance. Secondly, results observed for an extreme sensitiser were assessed against a moderate sensitiser, here DNCB and DEM. These chemicals have all been reported to be thiol reactive, with various level of details given concerning the structure of adducts formed. In a first instance, the formation of GSH conjugates was verified *in chemico*, with a very brief mention to the formation of DNP-SG by GSH conjugation of DNCB, which was implicit

throughout the previous chapter. Cytotoxicity of each new compound was assessed by MTT assay on the HaCaT cell line. As described previously, toxicity was only considered acceptable when cell viability was at least 80% of untreated control cells, over a 24 hour period. In order to select an optimum concentration, for which a 24 h time course experiment could be carried out using our GSH assay, GSH depletion was also assessed after 1 h exposure (to highlight any significant depletion).

The objective of these comparisons was to demonstrate that chemical reactivity with GSH *in chemico* was not a sufficient factor to assess behaviour on the GSH pathway in human skin after exposure. Bioavailability and toxicity in a living *in vitro* system, here HaCaT cells, led to different outcomes, even though the detoxification pathways involved were predicted to be the same (thiol clearance), based on *in chemico* studies.

5.3 Results.

5.3.1 *In chemico* incubations of model skin sensitisers.

5.3.1.1. Incubations at pH 7.4 for 24 h at 37 °C, with ratio GSH: chemical fixed at 1:10

DNCB was incubated as a control experiment only, as the formation of dinitrophenyl-glutathione (DNP-SG) was relatively easy to carry out [127] and formed the basis of GST activity spectrometric measurements in most commercial kits sold. A typical chromatogram is presented in Fig 5.4. The major peak (RT = 5.65 min) was the expected DNP-SG adduct with m/z 474 (Fig 5.5). There were three minor peaks on the chromatogram (RT =1.54 min, 7.17 min and 8.15 min), all with low m/z, unlikely to be related to the reaction between GSH and DNCB (Fig 5.4).

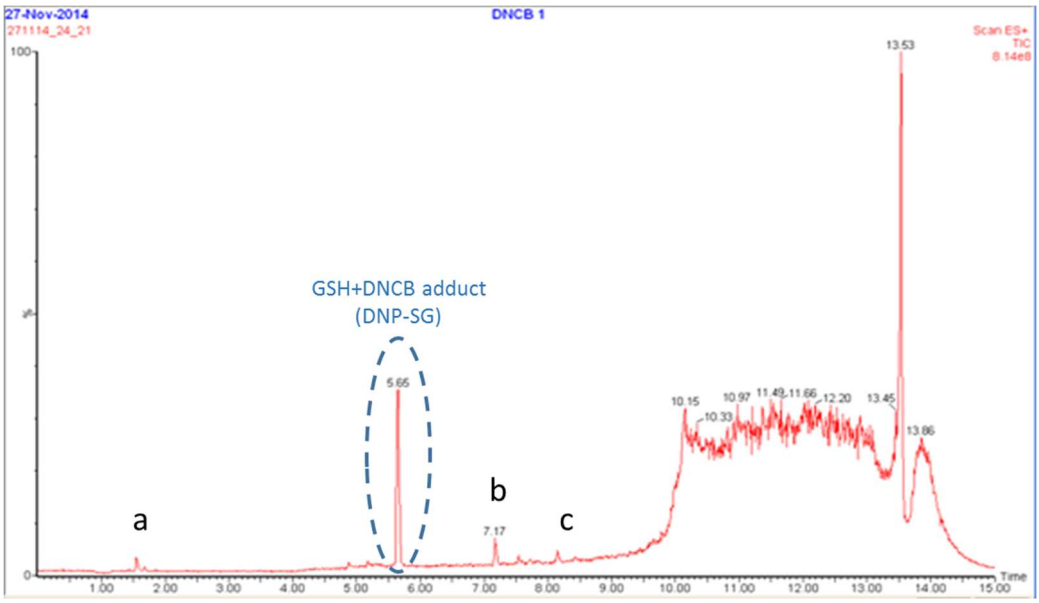

Figure 5.4: Typical chromatogram obtained for DNCB incubation with GSH at pH 7.4 for 24 h. *Blue highlight:* the DNP-SG conjugate formed during the incubation and was observed at a retention time (RT) of 5.65 minutes (details of extracted mass m/z 474 is available in Figure 5.5). Other peaks at RT = a) 1.54 min, b) 7.17 min and c) 8.15 min, all with low m/z, were unrelated to DNCB or GSH. Incubations were carried out in plastic Eppendorf tubes in triplicate (n=3).

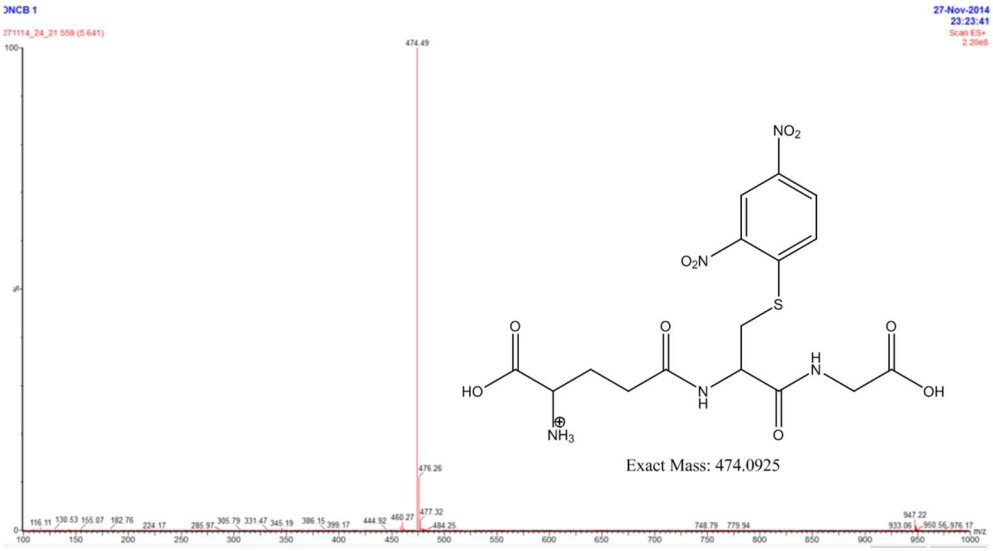

Figure 5.5: Representative extracted mass for peak observed at RT 5.65 minutes. Mass spectrum of DNP-SG conjugate $[M+H]^+$ ion at m/z 474 (extracted from chromatogram presented in Fig 5.4 in the blue highlight).

A typical chromatogram of DEM incubations is presented in Fig. 5.6. It contained signals corresponding with oxidation of unreacted GSH (retention time 1.67 and 2.74 min), unreacted DEM (retention time 7.34 min) and a "DEM+GSH" conjugate (retention time

5.43 min) with m/z 480 (Fig. 5.7). This conjugate was structurally the same as the conjugate formed by Kubal *et al* [206]. Minor peaks at retention time 5.30 min, 5.96 min, 7.86 min and 8.05 min could not easily be linked to the structure of either GSH or DEM. Peaks at retention time 1.13 min and 13.54 min were linked to the mobile phase or buffer used for the incubations.

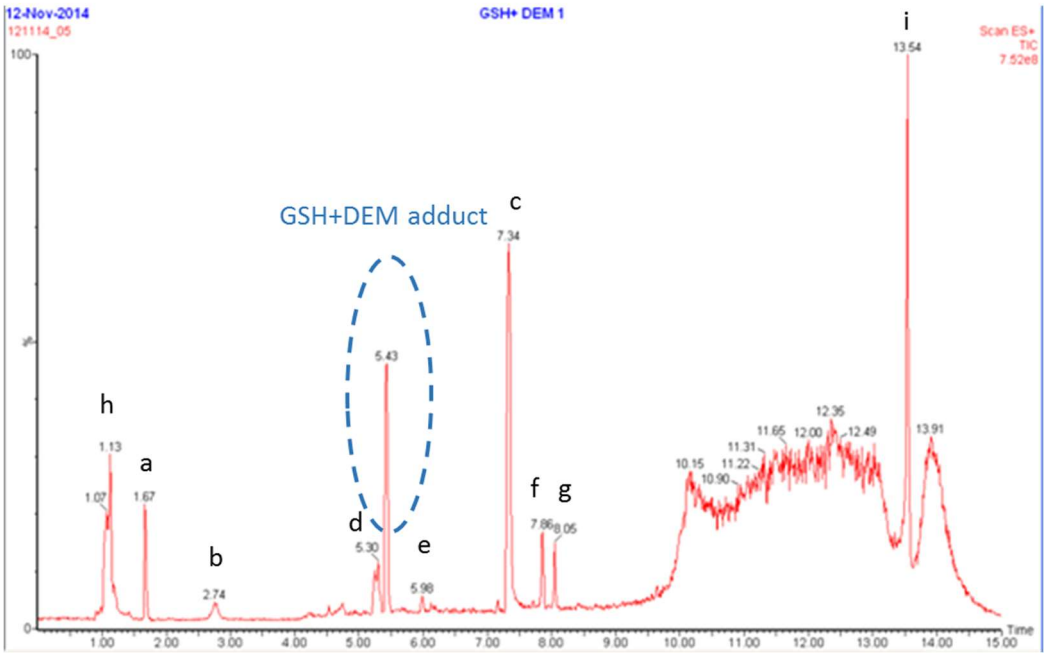

Figure 5.6: Typical chromatogram obtained for DEM incubation with GSH at pH 7.4 for 24 h. *Blue highlight:* the "GSH + DEM" conjugate formed during the incubation and was observed at a retention time (RT) of 5.43 minutes (details of extracted mass m/z 480 is available in Figure 5.7). Peaks at RT = a) 1.67 min and b) 2.74 min were due to unreacted GSH. Peak at RT = c) 7.34 min was unreacted DEM. Other peaks at RT = d) 5.30 min, e) 5.96 min, f) 7.86 min and g) 8.05 min could not easily be linked to the structure of either GSH or DEM. Peaks at retention time h) 1.13 min and i) 13.54 min were linked to the mobile phase. Incubations were carried out in plastic Eppendorf tubes in triplicate (n=3).

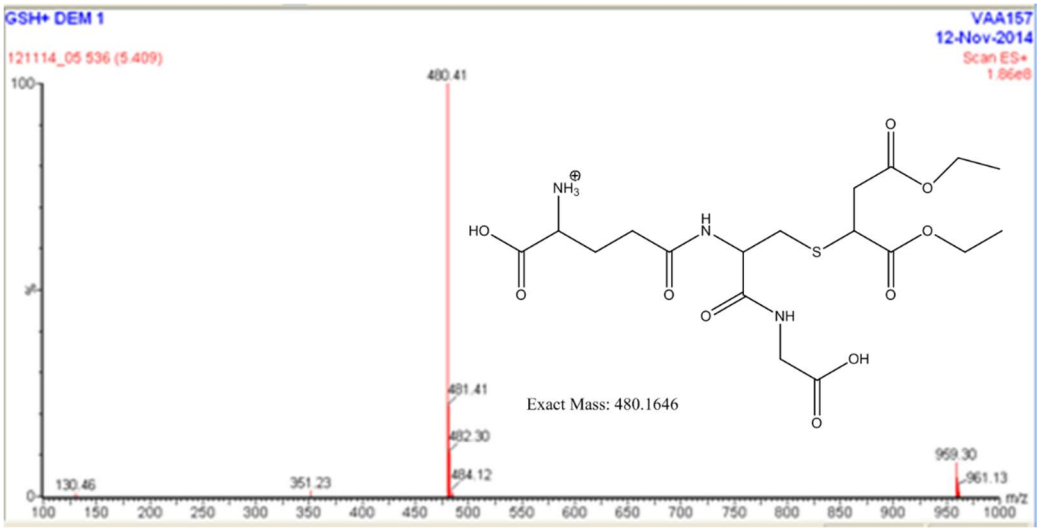

Figure 5.7: Representative extracted mass for peak observed at RT 5.43 minutes. Mass spectrum of "DEM + GSH" conjugate with $[M+H]^+$ ion at m/z 480 (extracted from chromatogram presented in Fig 5.6 at retention time 5.43 min).

The chromatograms obtained for incubations containing DPCP were more complex and some peaks were not assigned (Fig 5.8). Small peaks of GSSG (retention time 1.67 and 2.74 min) as well as unreacted DPCP (retention time 7.83 min) were observed. The peak with a retention time of 6.56 min and the peak immediately following (retention time 6.77 min) have a mass m/z 514, likely to be the conjugate "DPCP+ GSH" (Fig 5.9). The two peaks with a retention time 8.55 and 8.6 min have a mass m/z 720, which is likely to be the adduct of structure "2 DPCP + GSH" (Fig 5.10).

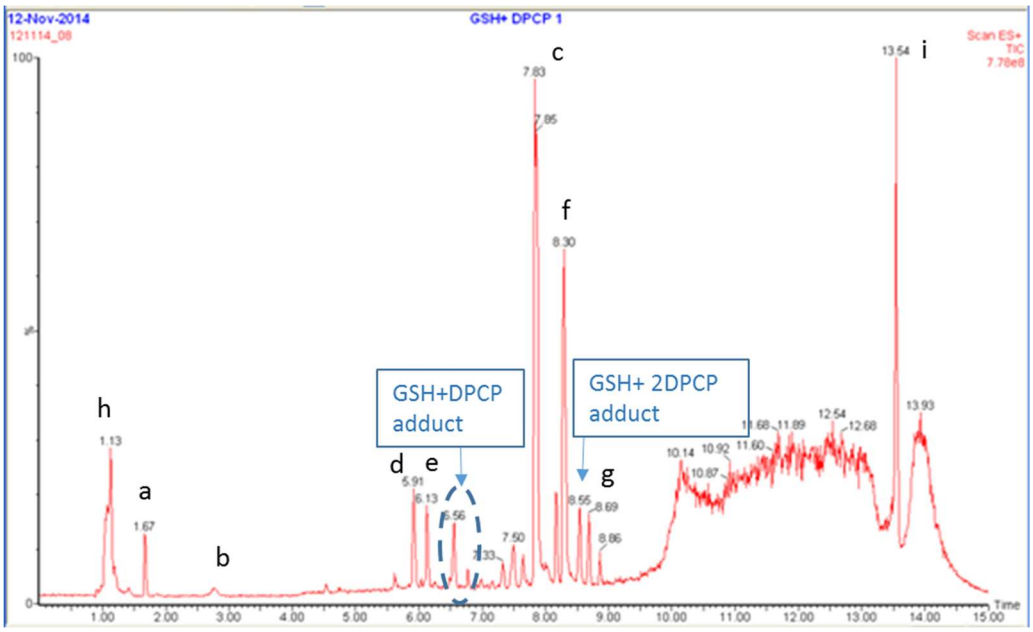

Figure 5.8: Typical chromatogram obtained for DPCP incubation with GSH at pH 7.4 for 24 h. *Blue highlight:* the "GSH + DPCP" conjugate formed during the incubation and was observed at a retention time (RT) of 6.77 minutes (details of extracted mass m/z 514 is available in Figure 5.9) and "GSH+ 2 DPCP" at retention times 8.55 and 8.69 min (details of extracted mass m/z 720 is available in Figure 5.10). Peaks at RT = a) 1.67 min and b) 2.74 min were due to unreacted GSH. Peak at RT = c) 7.83 min was unreacted DPCP. Other peaks at RT = d) 5.91 min, e) 6.13 min, f) 8.30 min and g) 8.69 min could not easily be linked to the structure of either GSH or DPCP. Peaks at retention time h) 1.13 min and i) 13.54 min were linked to the mobile phase. Incubations were carried out in plastic Eppendorf tubes in triplicate (n=3).

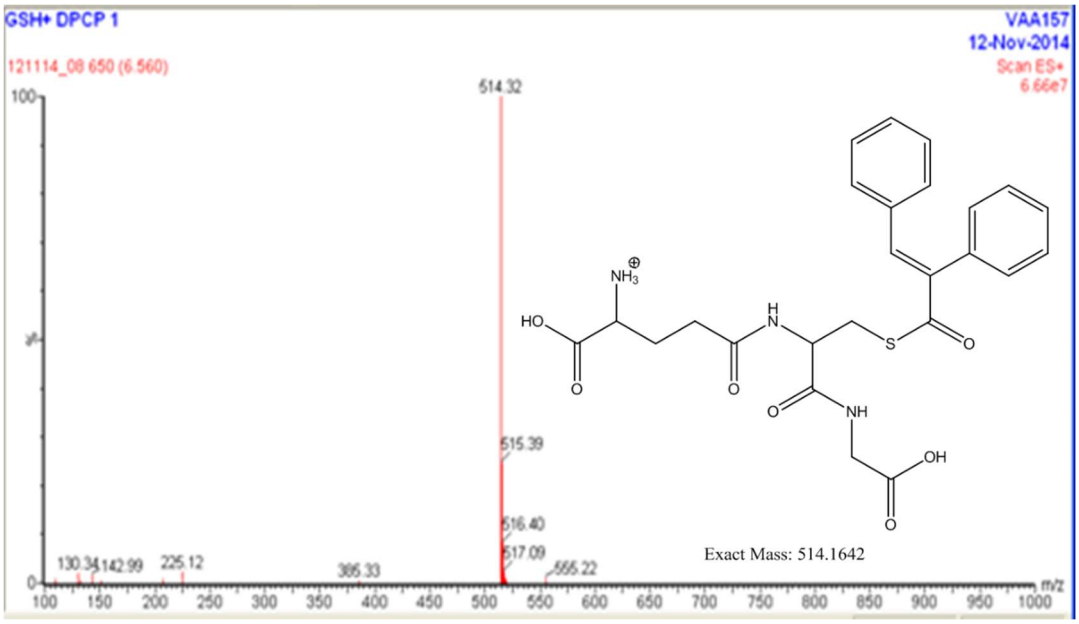

Figure 5.9: Representative extracted mass for peak observed at RT 6.56 minutes. Mass spectrum of "DPCP + GSH" conjugate with $[M+H]^+$ ion at m/z 514 (extracted from chromatogram presented in Fig 5.8 at retention time 6.56 min).

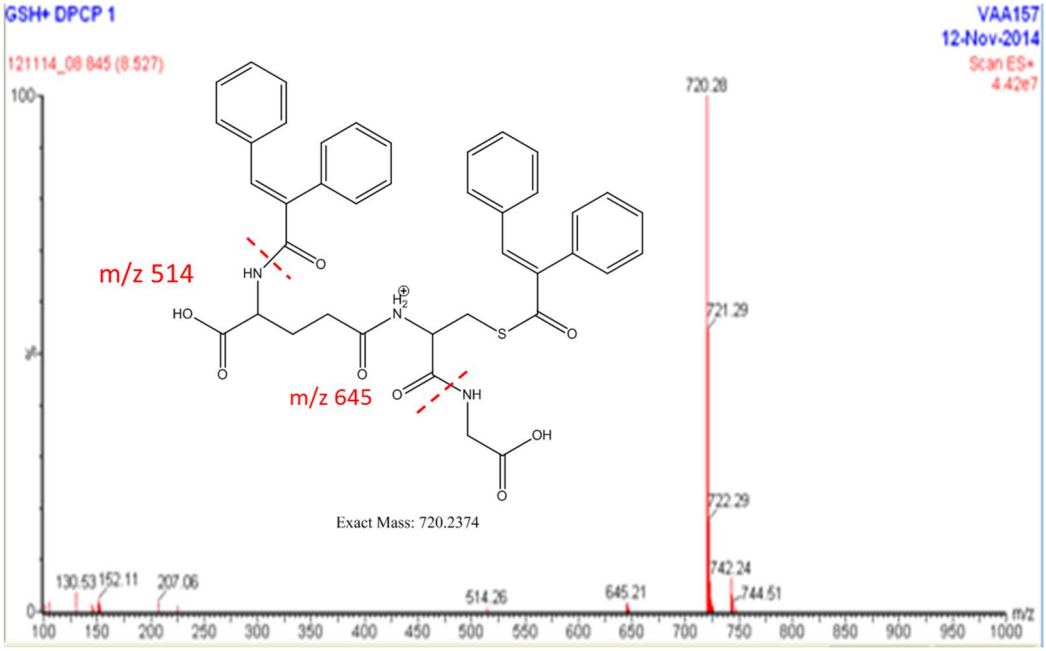

Figure 5.10: Representative extracted mass for peak observed at RT 8.55 minutes. Mass spectrum of "2 DPCP + GSH" conjugate with $[M+H]^+$ ion at m/z 720 (extracted from chromatogram presented in Fig 5.8 at retention time 8.55 min).

5.3.1.2. Incubations at pH 9.5 for 24 h at 37 °C, with ratio GSH: chemical fixed at 1:10

To attempt to increase the reactivity between the chemicals and the thiol present on GSH, the pH was increased above the pKa of GSH, reported to be between 9.2 and 9.4 [130, 131]. A typical chromatogram for Incubations with DEM is presented in Fig 5.11. As observed at pH 7.4 a "DEM+GSH" adduct was observed at retention time 5.43 min. Contrary to expectations the reaction between DEM and GSH was still not complete and some GSH was oxidized to GSSG instead (retention time 1.68 min).

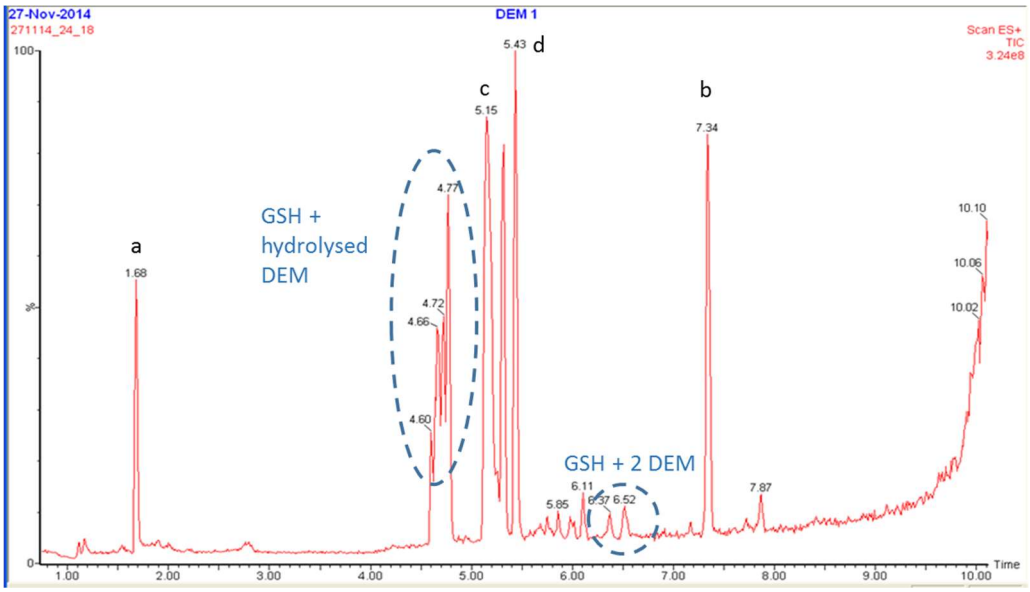

Figure 5.11: Typical chromatogram obtained for DEM incubation with GSH at pH 9.5 for 24 h. *Blue highlight:* the "GSH + hydrolysed DEM" conjugate formed during the incubation and was observed at a retention time (RT) of 4.6-4.77 minutes (split peak details of extracted mass m/z 452 is available in Figure 5.12) and "GSH+ 2 DEM" at retention times 6.37 and 6.52 min (details of extracted mass m/z 652 is available in Figure 5.13). Peak at RT = a) 1.67 min was unreacted GSH. Peak at RT = b) 7.34 min was unreacted DEM. Peaks at RT = c) 5.15-5. 32 min (split peak) could not be assigned to DEM or GSH. Peak at RT = d) 5.43 min (similar to one observed in figure 5.6) was "GSH + DEM" conjugate. Incubations were carried out in plastic Eppendorf tubes in triplicate (n=3).

New products were formed at pH 9.5 compared to pH 7.4. A major peak was broadly defined at retention time 4.6-4.7 min with a consistent m/z 452 throughout the width of the peak. The extracted spectrum is presented in Fig 5.12. It seems that increasing the pH to 9.5 enabled the hydrolysis of one of the ethyl moiety in DEM. The resulting hydrolysed compound then reacts with GSH in the same way that DEM would and both conjugates are observed. Two minor peaks at retention time 6.37 and 6.52 min have an extracted mass m/z 652, which is consistent with the addition of two DEM molecules to a molecule of GSH (Fig 5.13). Two major peaks at retention times 5.15 and 5.32 min could not be easily assigned a structure.

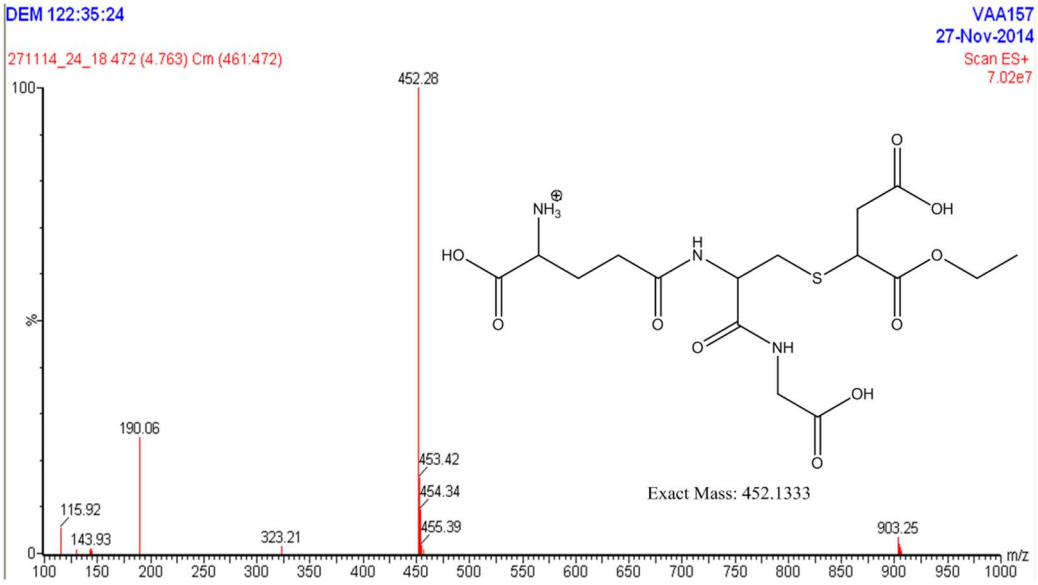

Figure 5.12: Representative extracted mass for peak observed at RT 4.7 minutes. Mass spectrum of "hydrolysed DEM + GSH" conjugate with $[M+H]^+$ ion at m/z 452 (extracted from chromatogram presented in Fig 5.11 at retention time 4.7 min).

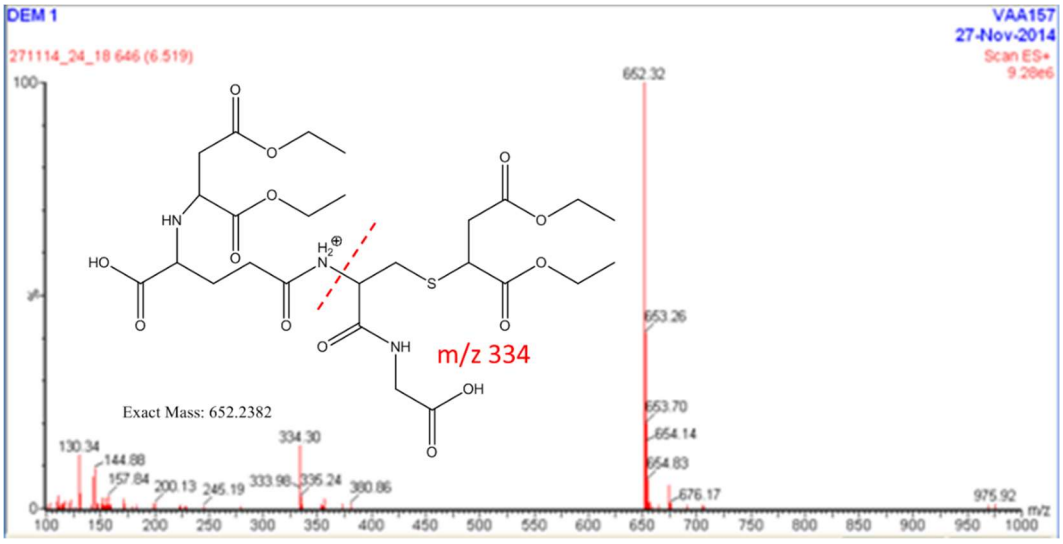

Figure 5.13: Representative extracted mass for peak observed at RT 6.52 minutes. Mass spectrum of "2 DEM + GSH" conjugate with $[M+H]^+$ ion at m/z 652 (extracted from chromatogram presented in Fig 5.11 at retention time 6.52 min).

An apparent increase in complexity was also observed in chromatograms issued from DPCP incubations (Fig.5.14). Two peaks with a retention time of 5.92 and 6.14 minutes with a m/z 819 showing an apparent fragmentation pattern of 206-203-203-206 could be related to tetramerisation of DPCP (data not shown). The peak with a retention time of 6.5 minutes with a m/z 514 is consistent with a "DPCP+GSH" conjugate and the two

minor peaks at retention time 8.55 and 8.69 minutes with m/z 720 are consistent with a "2DPCP+ GSH" conjugate. Both conjugates were previously observed in incubations carried out at pH 7.4 at the same retention times.

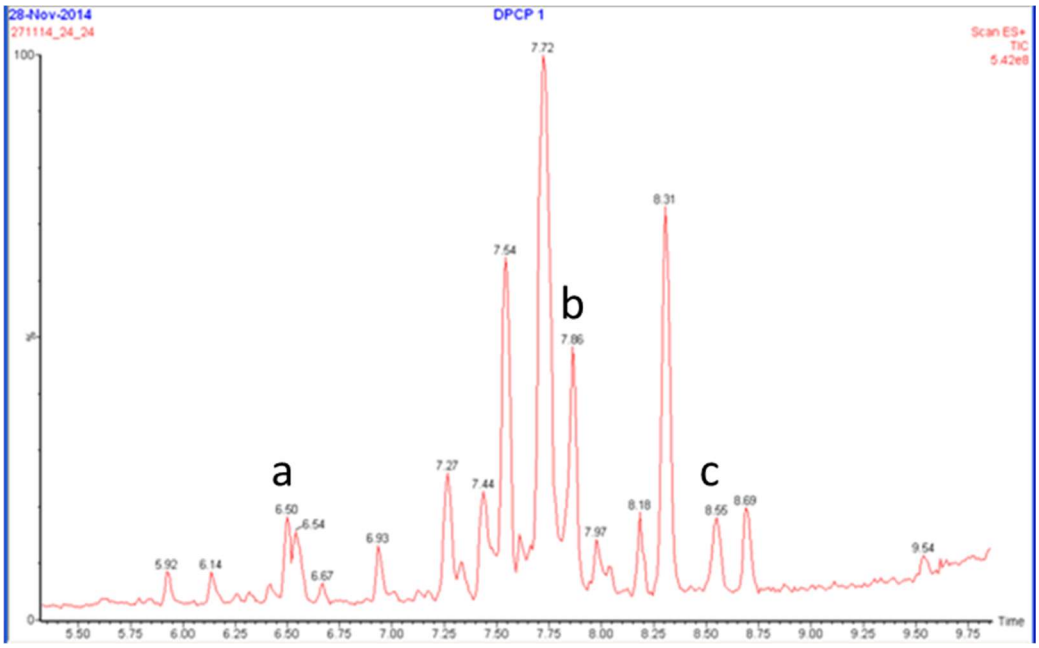

Figure 5.14: Typical chromatogram obtained for DPCP incubation with GSH at pH 9.5 for 24 h. the peak at RT = a) 6.5 min was the "GSH = DPCP" conjugate (m/z 514), the peak at RT = b) 7.86 min was unreacted DPCP and the peak at RT = c) 8.55 min was the "GSH + 2DPCP" adduct (m/z 720), all similar to ones observed in figure 5.8. Incubations were carried out in plastic Eppendorf tubes in triplicate (n=3). The level of complexity of the chromatogram increased but there wasn't any new GSH adducts detected compared to pH 7.4 incubations. The intensity of the peaks linked to GSH conjugates did not increase significantly compare to pH 7.4 incubations.

5.3.2 Cytotoxicity assay (MTT assay).

Cytotoxicity measurement for DNCB has been carried out in the HaCaT cell line as part of the previous chapter (Chapter 4, Section 4.2.1), in which the maximum concentration that did not induce more than 20 % loss of viability was 10 µM. Similarly, DPCP showed a high level of toxicity to HaCaT cells exposed for 24 h (Fig 5.15). The maximum concentration that did not induce significant toxicity was 2.4 µM, which was rounded down to 2 µM for future experiments for practical reasons.

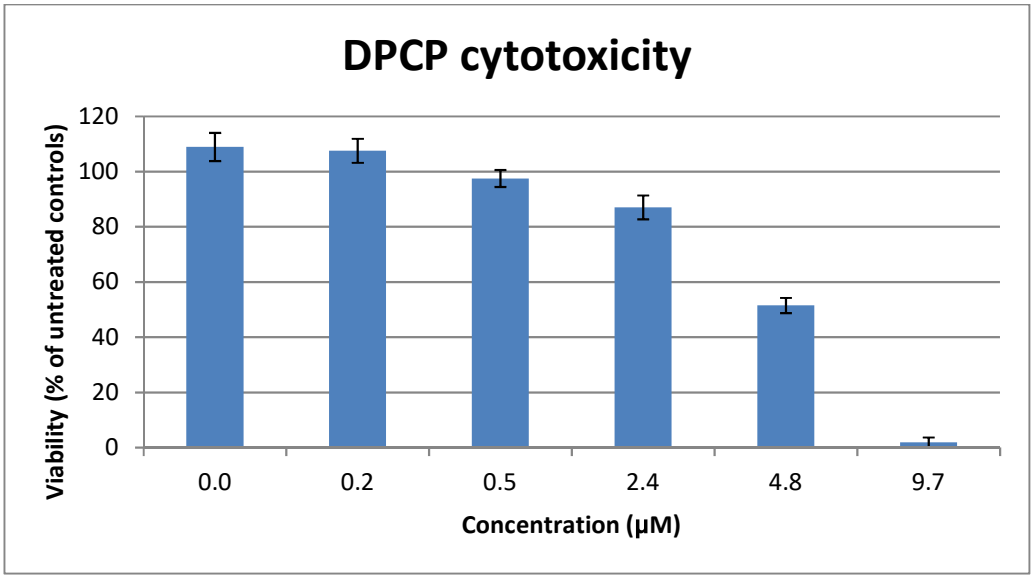

Figure 5.15: Cytotoxicity of diphenylcyclopropenone in HaCaT cells after 24 hours. The toxicity of DPCP was determined using the MTT assay after 24 hours of exposure. Each well (20 000 cells/well) was treated with the appropriate concentration of DPCP. The concentration applied was considered non-toxic when the cell viability is at least 80 % compared to control cells kept in culture medium containing 0.5 % DMSO for a similar length of time. Each concentration was tested in 8 wells (n=8) and the result was presented as Mean viability ± Standard deviation. The figure shows that all concentrations lower or equal to 2 µM were non-toxic.

DEM did not exhibit significant toxicity to HaCaT cells when applied at concentrations of up to approximately 90 µM in the MTT assay (Fig 5.16). Above this threshold, the viability of cells decreases slowly with increasing concentration with approximately 20 % of cells still viable when DEM was present at a concentration of approximately 580 µM.

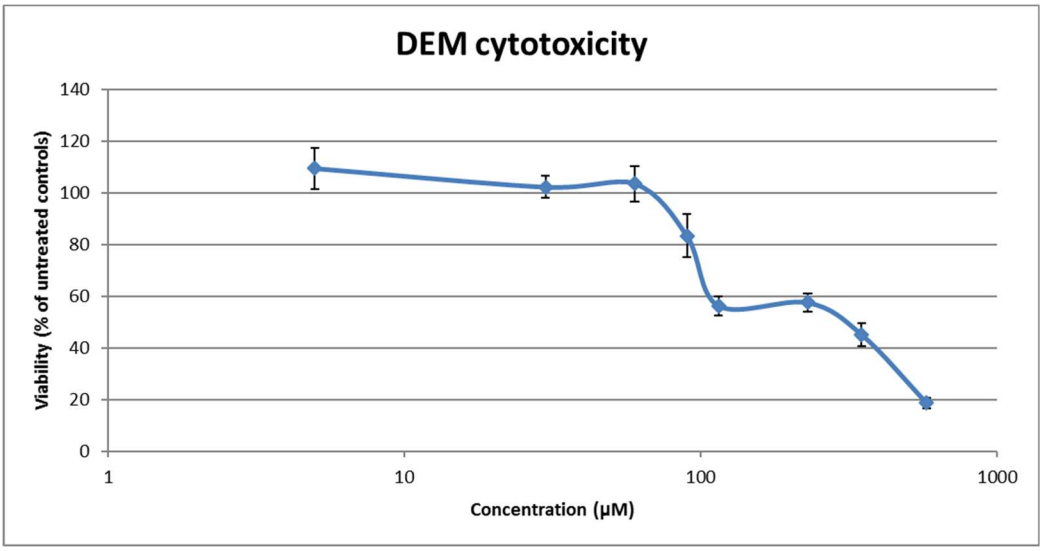

Figure 5.16: Cytotoxicity of diethylmaleate in HaCaT cells after 24 hours. The toxicity of DEM was determined using the MTT assay after 24 hours of exposure. Each well (20 000 cells/well) was treated with the appropriate concentration of DEM. The concentration applied was considered non-toxic when the cell viability is at least 80 % compared to control cells kept in culture medium containing 0.5 % DMSO for a similar length of time. Each concentration was tested in 8 wells (n=8) and the result was presented as Mean viability ± Standard deviation. The figure shows that all concentrations lower or equal to 580 µM were non-toxic.

5.3.3 GSH cycling in the HaCaT cell line.

5.3.3.1. DEM and DPCP show different GSH dose responses from DNCB after 1 hour and 24 hour exposure.

The following results are expressed as a percentage of GSH remaining in viable cells after exposure, the amount of GSH in untreated cells remaining in HaCaT cell culture medium for the length of time of the experiment being used as the reference for 100 % GSH (untreated controls, shown as 0 µM concentration in figures).

The results for DNCB were presented in Section 4.2.2, Chapter 4 (Fig 4.3) and are not repeated here. Dose responses showed that the optimum concentration for which DNCB depleted GSH at 1 hour and replenished at 24 hours was 10 µM. These results will be discussed further to compare them with DEM and DPCP.

In experiments where the exposure time was 1 h, the level of GSH was not significantly lower in treated compared to untreated cells, regardless of the concentration of DEM (approximately 75 % of GSH present for a concentration of 150 µM), even though DEM has been shown to covalently bind to GSH *in chemico.* When the exposure time was increased to 24 hour, DEM did not deplete GSH but a clear upregulation of the synthesis of GSH was observed for all concentrations applied up to 150 µM. The highest level being observed for a 50 µM concentration where the level of glutathione was double that of untreated cells. Considering the results obtained in the MTT assay for DEM, it was expected that at high concentrations (100-150 µM) the level of GSH would be approximately 60 % of basal untreated cells to match cell viability but this did not seem to be the case (Fig 5.17).

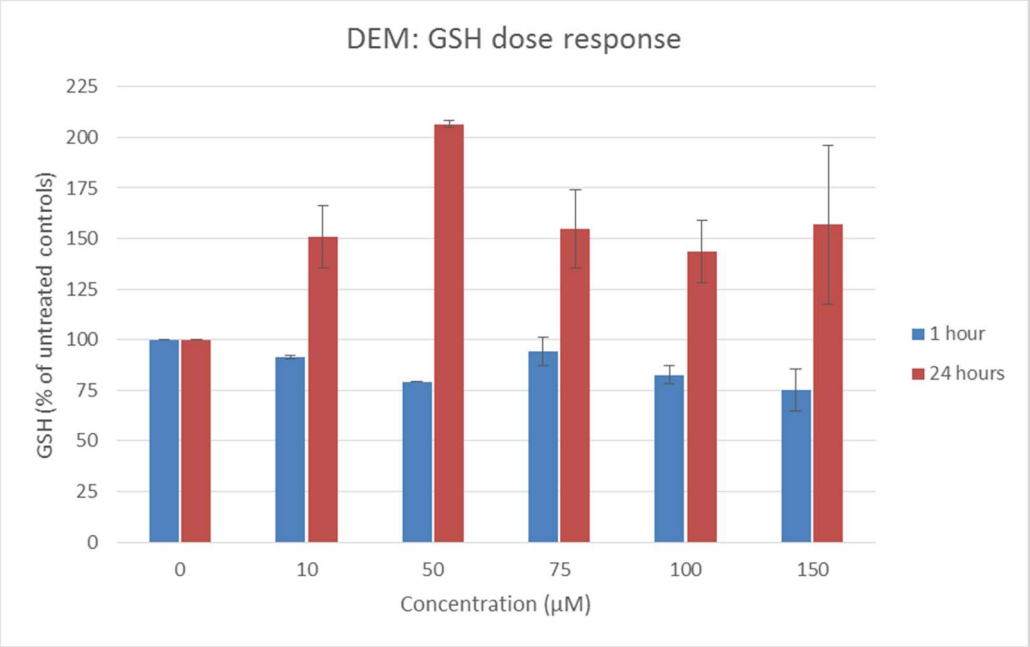

Figure 5.17: **GSH levels in HaCaT cells treated with various concentrations of DEM for 1 hour or 24 hours.** Each well (400 000 cells/well) was treated with DEM and incubated for *blue:* 1 hour and *red:* 24 hours. The cells were then rinsed with PBS, lysed and derivatised with iodoacetamide as described in previous figures. GSH levels were measured in half the lysate (equivalent to 200 000 cells, and the concentration expressed in µM. GSH levels were reported as percentage of untreated cells controls matching the exposure time and presented as Mean % of GSH in untreated cells ± Standard deviation (n=2). The figure shows that GSH level after 1 hour of exposure was

within ± 20 % of GSH level in untreated control cells but GSH levels at 24 hours were higher than in control cells.

A potential explanation for this result is that some cell death is likely occurring during the experiment but the remaining cells produce a very high GSH upregulation (probably up to 200 % of basal level as was the case for a 50 µM dose) resulting in the total amount of reduced GSH available higher than the level observed in untreated cells.

DPCP showed very different results (Fig 5.18). The concentration range investigated (0-30 µM) was closer to the one used for DNCB, as both chemicals are extreme sensitisers. A 24 hour exposure period to DPCP could not deplete GSH levels at a concentration that was not toxic for the cells. GSH upregulation was observed for a concentration of 1 µM. A complete depletion of GSH was observed at approximately 10 µM and over, however this concentration would normally result in 100 % reduction in cell viability over a 24 h period. For an incubation time of 1 hour only, the level of GSH was not significantly depleted in treated cells up to 20 µM. The most significant depletion was observed at the top concentration of 30 µM, where approximately 70 % of the GSH level of the cells remained. From this, it can be observed that DPCP is more toxic than DNCB but the speed of reaction with GSH in *in vivo* conditions is slower.

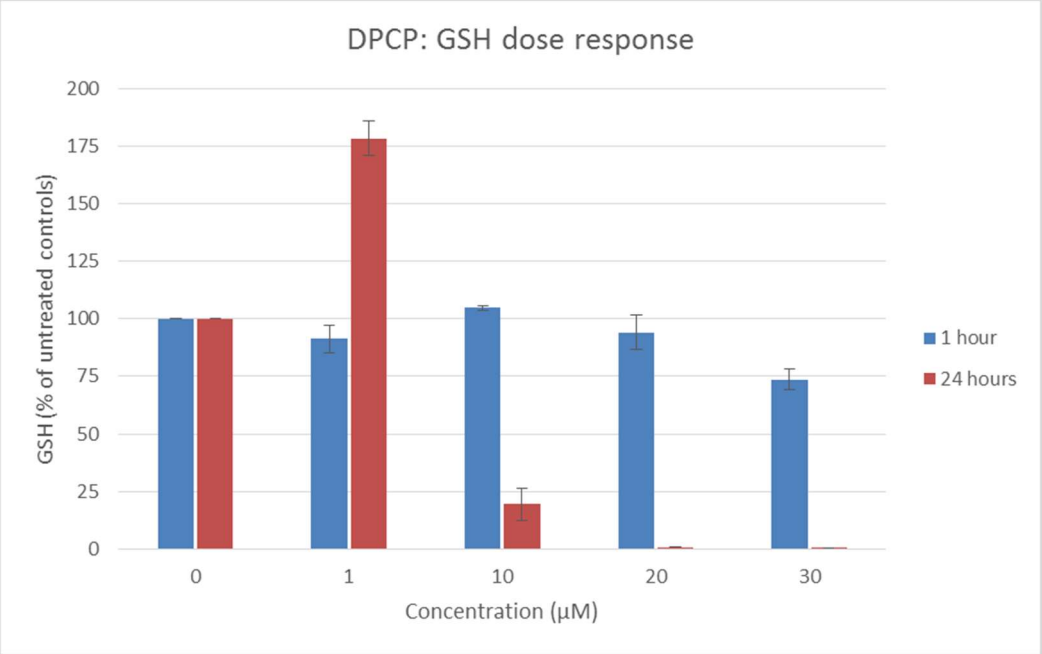

Figure 5.18: GSH levels in HaCaT cells treated with various concentrations of DPCP for 1 hour or 24 hours. Each well (400 000 cells/well) was treated with DPCP and incubated for *blue:* 1 hour and *red:* 24 hours. The cells were then rinsed with PBS, lysed and derivatised with iodoacetamide as described in previous figures. GSH levels were measured in half the lysate (equivalent to 200 000 cells, and the concentration expressed in µM. GSH levels were reported as percentage of untreated cells controls matching the exposure time and presented as Mean % of GSH in untreated cells ± Standard deviation (n=2). The figure shows that GSH level after 1 hour of exposure was within ± 20 % of GSH level in untreated control cells but GSH levels at 24 hours were higher than in control cells (1 µM dose) or depleted (10-30 µM).

5.3.3.2. GSH 24 hour time course in HaCaTs after treatment with DEM or DPCP showed a different pattern than the one seen with DNCB.

The results for DNCB were presented in Section 4.2.3, Chapter 4 and Fig 4.4. The time course experiment at a 10 µM showed a depletion of GSH up to 2 hours followed by a period of repletion of GSH stock (Fig 5.19, extracted from Fig 4.4). These results will be discussed further to compare them with DEM and DPCP.

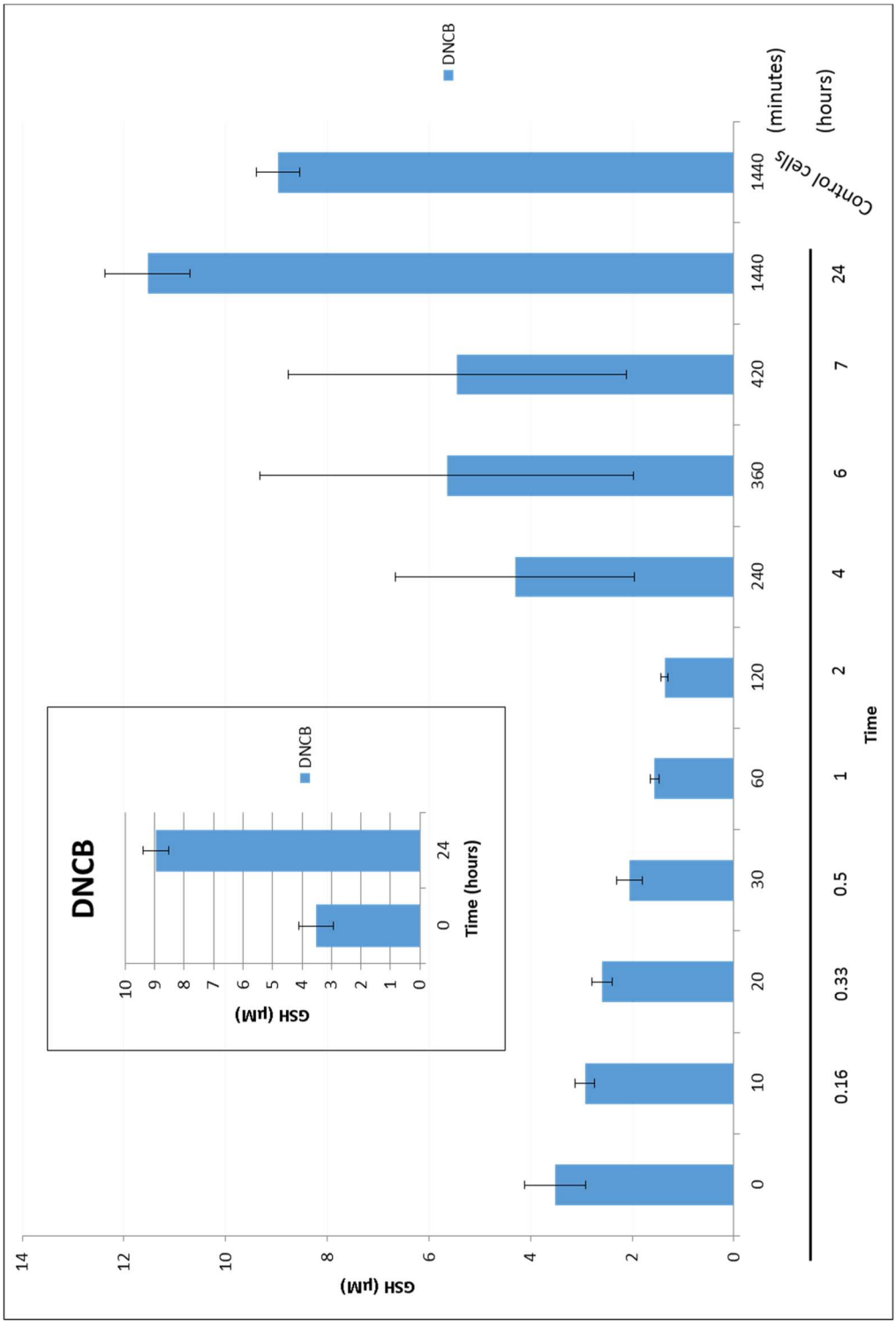

Figure 5.19: *Main*: GSH levels in HaCaT cells treated with 10 µM DNCB for 24 hours. GSH levels are expressed in µM. *Insert:* Comparison between controls cells at t= 0 hour and t= 24 hours, representing the GSH increase due to cell division in the well during the length of the experiment (n= 4). This figure is extracted from the results presented in Fig. 4.4 (Chapter 4).

HaCaT cells were treated with the DEM concentration leading to the maximum upregulation of GSH over 24 h observed in Section 5.3.3.1 (50 µM). This concentration was not toxic over the 24 hour period in the MTT assay. The aim was to observe some depletion of GSH (at early time points up to 1 hour) followed by a sharp repletion above control levels. A significant depletion of GSH levels was not observed in the early time points and GSH levels were fluctuating between 75-125 % of their basal value (t= 0 hour) for up to 4 hours (Fig 5.20). An exponential increase in GSH concentration in the cells was visible between 4-6 hours and 24 hours to reach approximately 450 % of their basal value (t= 0 hour) or double the level observed in cells that were left untreated for 24 hours (basal value t= 24 hours, Fig 5.20 *insert*) due to natural cell division in the well, which was similar to the result observed for DNCB in Fig 5.19.

HaCaT cells were treated with the DPCP concentration which was not toxic over the 24 hour period in the MTT assay, here 2 µM (Fig 5.15). This was expected to lead to a potential upregulation of GSH over 24 hours, as seen with a 1 µM dose (Fig 5.18). The GSH levels did not decrease with time at the early time points and fluctuated between 90-130 % of the basal value at t= 0 hour for the first two hours of experiment. Between 4 hours and 24 hours the levels observed were higher, 130-160 % and were generally in line with the value observed in the control cells at 24 hours (173 %). This indicated that a 2 µM dose of DPCP had no significant influence on the GSH cycling pathway in the HaCaT cell line (Fig 5.20).

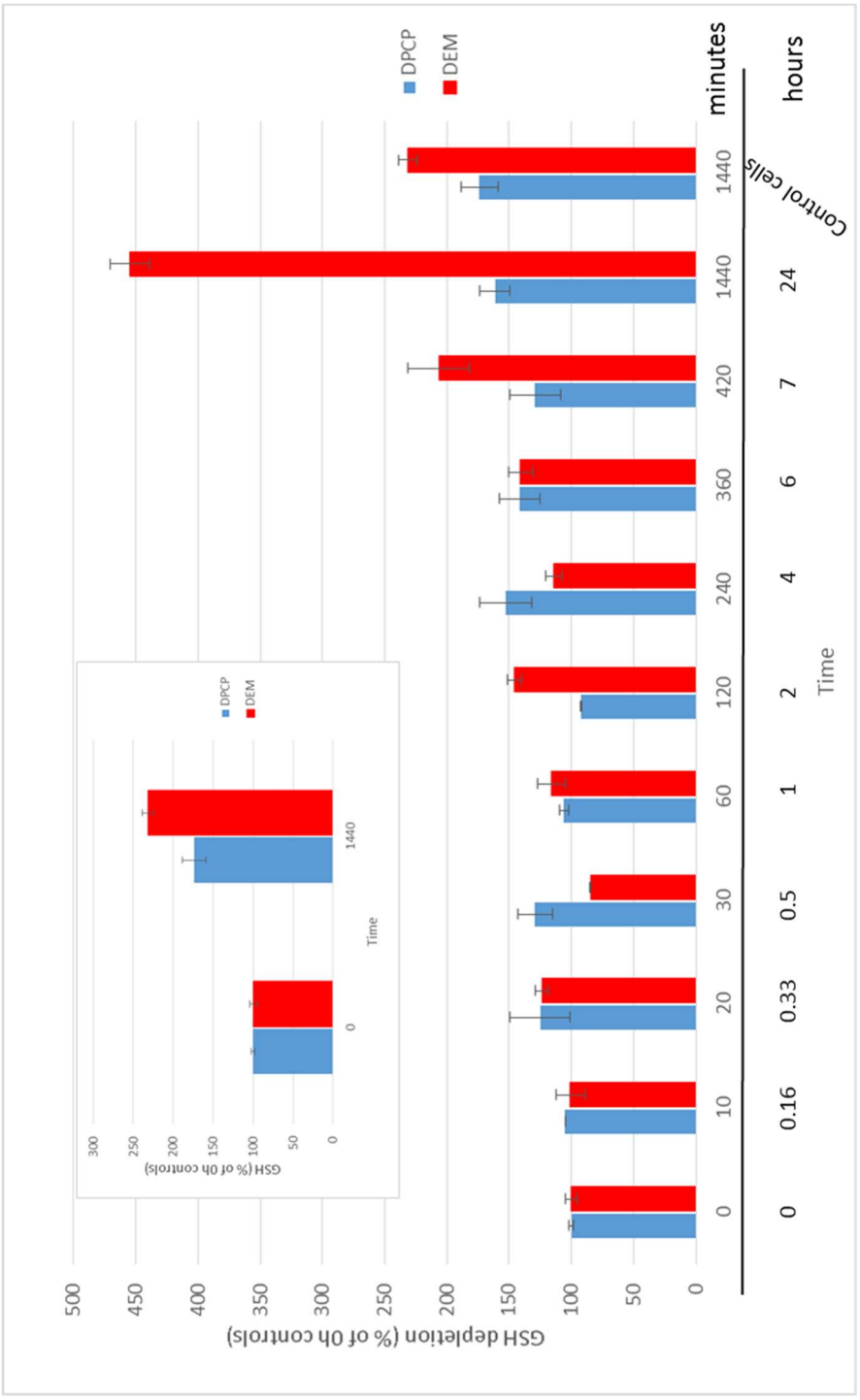

Figure 5.20: GSH levels in HaCaT cells treated with DEM or DPCP. *Main*: GSH levels in HaCaT cells treated with 50 µM DEM or 2 µM DPCP for 24 hours. *Insert:* Comparison between controls cells at t=0 hour and t=24 hours, representing the GSH increase due to cell division in the well during the length of the experiment. Each well (400 000 cells/well) was treated with DEM or DPCP for the required amount of time. The cells were then rinsed with PBS, lysed and derivatised with iodoacetamide as described in previous figures. GSH levels were measured in half the lysate (equivalent to 200 000 cells, and the concentration expressed in µM. GSH levels were reported as percentage of untreated cells controls matching the exposure time and presented as Mean % of GSH in untreated cells ± Standard deviation (n=2).

5.4 Discussion.

Cytotoxicity considerations formed the basis of the assumption that GSH would be able to detoxify any dose that would not induce more than 20 % cell death in the MTT assay. This was the case for DNCB and other dinitrohalobenzenes studied previously, where a visible depletion of GSH levels was observed as well as a repletion period after the dose was cleared (by a combination of GSH conjugation and protein haptenation). Historically, DEM has been used as a mean to deplete thiols in organs, including GSH, after treatment with high doses (low mmol/kg range) administered on animals by injection [208]. Hence, when pre-treatment of cultured cells by DEM was used as a mean to reduce GSH before evaluation of other parameters, high doses (hundreds of µM to low mM) tended to be used as well [209]. In our experiments the moderate sensitiser DEM induced significant cytotoxicity when the concentration was increased above 90 µM. Comparing this result with the extreme sensitiser DNCB, it seemed reasonably intuitive that the less potent sensitiser could be applied at a higher dose before detrimental effect was observed.

However, levels of GSH did not deplete significantly after 1 hour in a dose response manner, as was seen for DNCB, and the maximum dose investigated (150 µM) only depleted GSH stock by 25 %. West *et al* tried to rationalise the observed toxicities of DEM and related molecules (containing an α,β-unsaturated carbonyl group) and reached the conclusion that concentrations inducing toxicity correlated directly with concentrations inducing DNA damage and apoptosis. As in our GSH assay, while DEM IC_{50} in their cytotoxicity assay was approximately 130 µM, DNA fragmentation was the most visible at the high concentration range of 200-400 µM [210]. This hinted at the fact that a concentration inducing mild cytotoxicity (80 % cell viability) was artificially "masking" the effect of DEM conjugation with GSH. Potentially, the kinetics of reaction

(GSH conjugation) might have been initially relatively slow compare to the kinetics of synthesis of GSH and visible depletion could only be detected in our assay if DEM concentration was high and toxic (generating other detrimental impact on cell health, including a slowdown of GSH synthesis).

To investigate this further, we chose DPCP as an extreme sensitiser (same potency for skin sensitisation as DNCB) that also contained an α,β-unsaturated carbonyl group (same as DEM). Cytotoxicity to the HaCaT cell line at 24 hours was much closer to the results observed for DNCB and mild cytotoxicity (80 % viability) was obtained in the concentration range 2-3 μM. *In chemico* kinetics reported for nitrobenzenethiol also supported the assumption that DPCP ($k = 3x10^{-6}$ s^{-1}, first order kinetics) and DNCB ($k= 2.1x\ 10^{-5}$ s^{-1}, first order kinetics) should react with GSH at comparable speed [211]. Recently, DNCB and DPCP treatments were carried out on both HaCaT cells and freshly excised human skin to show that a specific set of genes was over expressed in the same way in both cells and skin [212]. More importantly for us, this study showed that DNCB and DPCP were broadly influencing the same genes. However, when HaCaT cells were dosed with concentrations of DPCP varying between 0-30 μM for 1 hour, there was no significant trend in GSH depletion and levels varied between 100-75 % GSH remaining at the end of the experiment (Fig 5.18), which was significantly different from the results previously obtained for DNCB. This suggests that either GSH was not the main thiol reacting with DPCP (protein haptenation was somehow favoured) and/or that DPCP might be a poor substrate of GSTs. It is also likely that DPCP had not physically reached the intracellular pool of GSH after 1 hour of exposure. This second option can be considered a serious possibility as it has been reported that DPCP (4-38 μM concentration range) reacted with the thiols present in the membranes at the surface

of THP-1 cells, while no effect on the intracellular GSH/GSSG ratio was seen for short periods of exposure (here 2 hours) [213].

Furthermore, incubations of 10 μM DPCP in skin S9 freshly prepared from frozen *ex vivo* skin carried out by Unilever SEAC collaborators at the University of Bradford (Prof P. Loadman's research group, personal communication) led to similar conclusions. After 1 hour, DPCP in skin S9 (with addition of an extra 10 μM GSH to the mixture or not), generated three new peaks in the UV trace recorded during analysis, none of which corresponding to a DPCP adduct with GSH (Fig 5.21). Control incubations carried out in PBS showed that GSH conjugation to DPCP was not visible after 1 hour of incubation, similar to the results we obtained *in chemico*, where the DPCP conjugates (single or double) were present but not visible as the main peaks in a chromatogram acquired after 24 hours incubation (Fig 5.8 and 5.14).

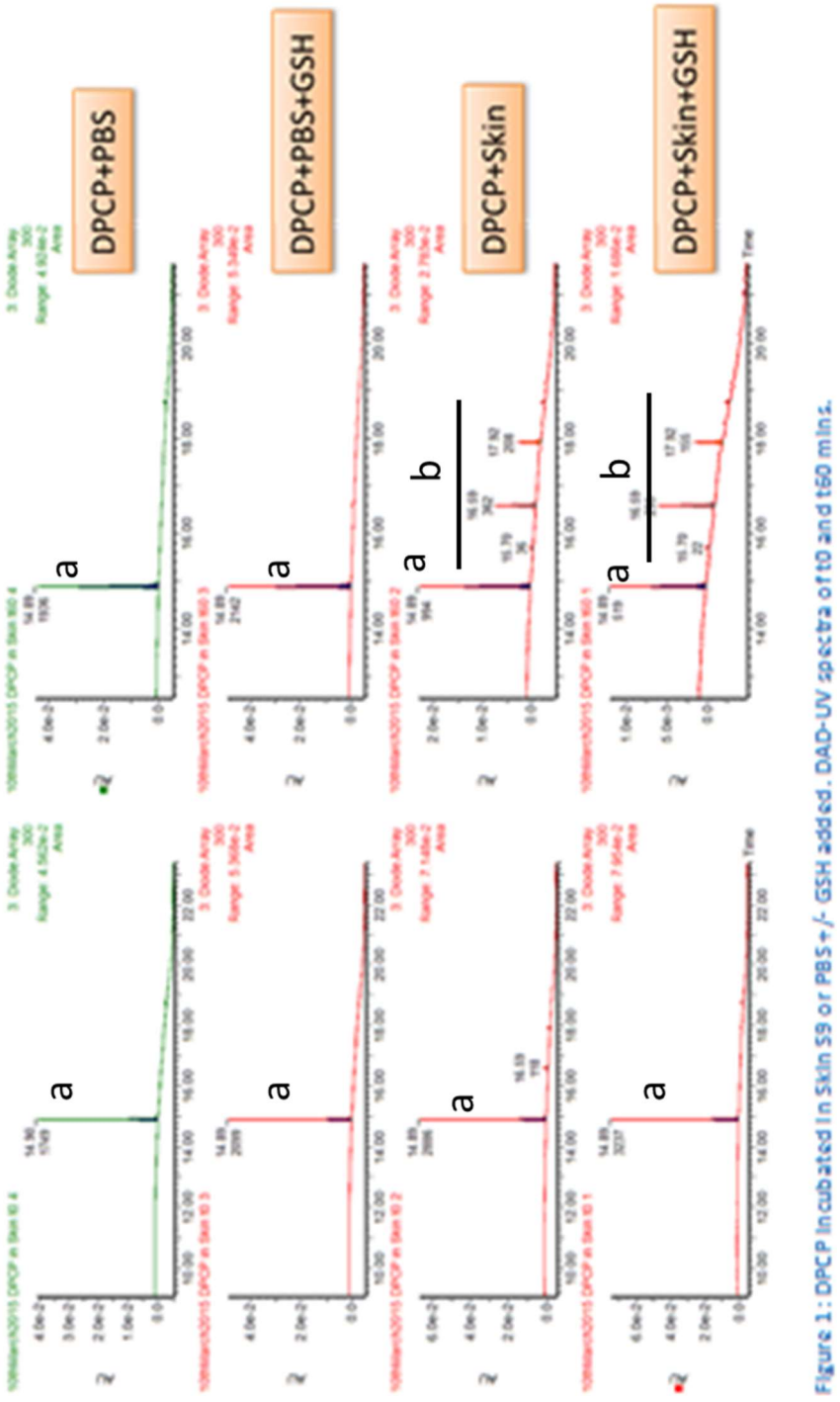

Figure 5.21: UV analysis of DPCP incubations in skin S9 or PBS, with or without the addition of extra 10 µM of GSH. *Left*: UV trace at t=0 min and *Right:* UV trace at t=60 min containing a) DPCP peak at RT = 14.8 min) and b) three new peaks generated in the UV trace issued from S9 incubations with RT included in the 15-18 min range. After 1 hour of incubation (n =1) DPCP was not fully depleted and the new peaks (b) could not be related to DPCP+GSH conjugates. Reproduced from Unilever internal report for work carried out in partnership with the University of Bradford.

The formation of "DEM + GSH" conjugate ($[M+H]^+$ ion at m/z 480) was obtained in the same experimental conditions (Fig 5.22). This conjugate was also formed in S9, with or without extra GSH added, though GSH availability in the S9 was a limiting factor. The reaction stopped after 30 min when GSH had run out in the extract but carried out linearly when GSH was available, demonstrating that GST activity was not compromised in the S9 after 30 min. Results also showed that DEM was reacting slower with GSH than DNCB, which consumed the extra 10 µM added within a few minutes (data not shown).

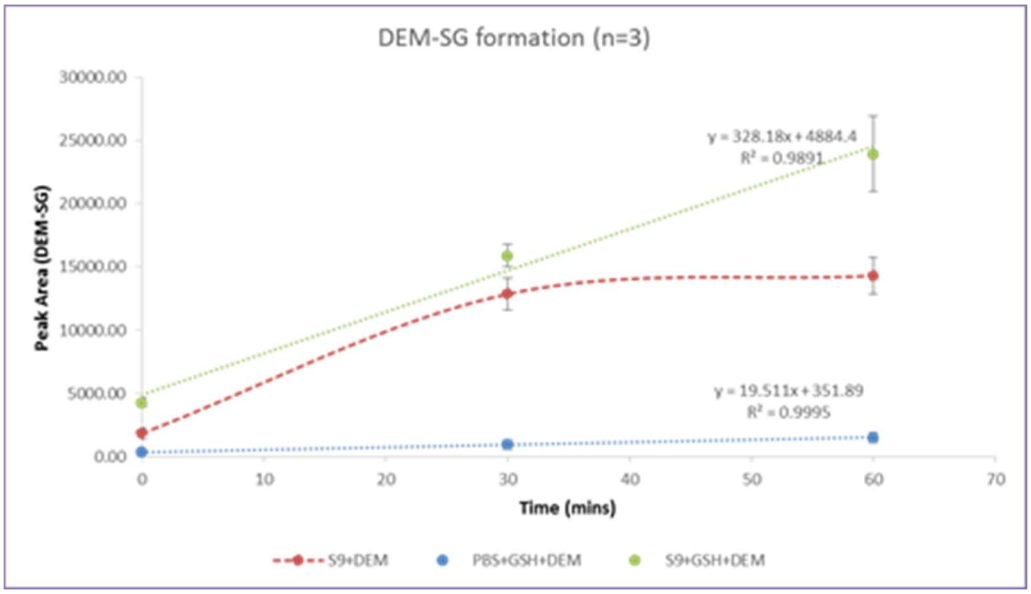

Figure 5.22: DEM incubations in skin S9 with or without the addition of extra 10 µM of GSH. Triplicate incubations of 10 µM DEM were carried out in freshly prepared skin S9 or in phosphate buffer saline (n= 3). DEM conjugate was formed in skin S9 as long as GSH was available in the mixture (green vs red curves). Control incubations in PBS show that reactivity is significantly slower when GSTs are not present. Reproduced from Unilever internal report for work carried out in partnership with the University of Bradford.

The GSH repletion in the HaCaT cell line after 24 hours provided more information to differentiate between the selected model sensitisers. While DNCB induced an upregulation of GSH production in the range of 20-40 % at the maximum non-toxic dose of 10 µM (Chapter 4, Fig 4.4) it was less visible for lower concentrations. This could be rationalised by the fact that the cells produced more GSH as the external damage caused

by DNCB was higher and seemed to correlate well with Nrf2 activation results also presented in Chapter 4. Using the same assay, DPCP treatment did not induce significant variation in GSH concentration after 24 hours compared to untreated cells, except when toxicity was high (GSH depletion was then due solely to cell death in the well). DEM however, induced an upregulation of GSH over the full range of concentrations applied (10-150 µM). At a non-toxic dose of 50 µM, GSH levels after 24 hours had doubled compared to untreated controls. We have previously linked the upregulation of GSH to an activation of the Nrf2 pathway in the HaCaT cell line after treatment with dinitrohalobenzenes, including DNCB. Natsch and collaborators have tested DNCB, DPCP and DEM in the Nrf2-induced luciferase assay KeratinoSens® and reported an EC3 value for each (concentration in µM for which an induction of Nrf2 3-fold above the value observed in untreated cells is obtained) [202]. Both DNCB and DPCP were able to induce Nrf2 at relatively low concentrations with EC3 values of 3.89 µM for DNCB and 1.84 µM for DPCP, while DEM EC3 value was significantly higher (82.85 µM). These values are consistent with the concentrations used in our GSH assay. As all chemicals induced a 3-fold increase of Nrf2 in the luciferase assay, this does provide an obvious explanation as to why 2-4 µM DPCP did not generate an upregulation of GSH in our experiments (one would suspect that Nrf2 activation would lead to an increase in the ARE-related gene coding for GCL and subsequently an increase in GSH in the cells) or why the upregulation was not of the same magnitude for all three chemicals (none for DPCP, 20-40 % for DNCB and 200 % for DEM). Thus, to estimate the ability of skin to clear a xenobiotic dose using the GSH pathway it is crucial to measure GSH at both an early time point (0-2 hours, for obvious depletion measurements) and after clearance of dose (24 hours, after which time GSH levels should have recovered) and supplement this information with results from an assay measuring Nrf2 activation if the GSH results are difficult to interpret. This is a more complete assessment of the biological impact of

skin sensitisers than the workflow developed by Naven *et al*, who combined an *in chemico* assay using GSH, BSA and human liver microsomes with a luciferase based assay to measure Nrf2 activation but only use this set of results to provide a general assessment of thiol reactivity [214].

5.5 Conclusion.

To understand the biological effect of skin sensitisers on the GSH pathway and potentially incorporate it into a mathematical model for skin sensitisation predictions, we have shown that it is important to consider:

1) The ability of the sensitiser to react with GSH specifically as well as other thiols.

   We have demonstrated that DNCB, DPCP and DEM were able to bind covalently to GSH, either by SNAr for DNCB or Michael addition for DPCP or DEM. Others have also reported reactivity with small thiol-containing peptides for all three compounds elsewhere. Activation of the Nrf2 pathway, as shown in the KeratinoSens assay, also indirectly hinted at reactivity with the cysteine residues in Keap1.

2) The bioavailability of each sensitiser in skin, i.e whether the chemical is likely to be in contact with intracellular GSH? If this is the case, would the presence of GSTs catalyse the reaction?

   Though we have demonstrated reactivity *in chemico*, demonstrating GSH conjugation in the HaCaT cell line or skin S9 proved a challenge for DPCP. For this particular compound, reactivity with external thiols (membranes) was potentially favoured. Even when the compound was in contact with GSH, as was the case for DEM, GSTs did not seem to catalyse the reaction to the extent that they did for DNCB. GSH depletion was not obvious in our assay and it was suspected that the kinetics of GSH synthesis (GCL and GS enzymatic activities) were of the same order

of magnitude as the kinetics of GSH conjugation. Hence the concentration in GSH in the cells appeared stable for the first 6 hours of exposure.

3) The magnitude of GSH repletion.

An important information gained from this piece of work was that the GSH repletion observed was different for each of the compounds. All of them were Nrf2 inducers in the KeratinoSens assay, generating a three-fold increase in the luciferase readout. The order of affinity for this assay was DPCP>DNCB>DEM (DPCP concentration required to generate the readout was smaller than DNCB concentration, which was lower than DEM). However, the GSH levels at 24 hours in our assay, expressed as percentage of untreated cells, was in reversed order to that and followed the trend DPCP<DNCB<DEM (DPCP did not generate any increase, DNCB 20-40 % and DEM 200 %). It is worth noting that some sensitisers can also act as oxidant and therefore alter the ratio GSH:GSSG in cells. As we have shown in Chapter 3 of this thesis, accurately measuring the change in GSH:GSSG ratio in HaCaT cells for the moderate skin sensitiser phenylacetaldehyde (applied at concentrations for which the cells are still able to recover) proved very challenging. However, phenylacetaldehyde is suspected to generate an imbalance in GSH:GSSG ratio and has been shown to induce Nrf2 in the KeratinoSens assay [202]. Therefore, a sensitiser's oxidative potential should be considered as well as the ability to conjugate GSH. Nrf2 activation information needs to be complemented by information on GSH repletion for all sensitisers, regardless of mechanism of action, to be meaningful in terms of skin defence capacity.

The simplistic model developed using the HaCaT cell line gives an idea of the complexity involved in understanding the effect of a chemical on human skin. Qualifying the

defence mechanisms, here the GSH pathway, alongside the sensitisation potential (of which thiol reactivity offers one possibility of haptenation to proteins) seemed to be chemical specific. Grouping chemical by skin sensitisation potency (DNCB and DPCP) or by chemical reactivity (DPCP and DEM) proved difficult. The next question is now to understand the effect of multiple exposures to the same dose of a specific sensitiser on skin and whether any differences in GSH repletion, an indirect measure of skin defence potential, would be seen.

Chapter 6: Effect of multiple dosing of DNCB on the Reconstructed Human Epidermis model.

Contents

6.1 Overview.

6.1.1 3D skin models: current uses.

One of the principal roles of skin is to protect against external factors (such as temperature variations, chemicals and moderate mechanical pressures). Consequently, it is able to process a wide variety of chemicals to which individuals are exposed as part of everyday lives. Assessing the effect of these chemicals on skin, whether associated with intended use (i.e., topically applied at recommended concentration for the recommended amount of time) or misuse from high exposure through single or repeated use, presents a challenge. Skin *in vitro* models that emulate metabolic mechanisms in skin, and which can be used to characterise the clearance of topical medicines or environmental chemicals still require refinement. Here we have used a recently developed Reconstructed Human Epidermis (RHE) skin model to study the metabolic clearance of DNCB by GSH.

Immortalised cell lines such as HaCaT or primary cells such as normal human epidermal keratinocytes (NHEK) have been used in co-culture with other cell types [34, 215] in an attempt to reproduce some of the biological responses observed in skin *in vivo*. A disadvantage of these cell systems is that they grow as monolayers, which may lead to differences in compound distribution and metabolic competence when compared with intact skin. As a result, to mimic skin in an *in vitro* environment, models have been developed over the past 20 years to reproduce a 3D structure. The least complex models simply comprise keratinocytes grown at the air interface of an inert insert while more complex ones include a collagen bedding, in which cultured fibroblasts are located [3]. These are cultured until they develop several layers of specialised keratinocytes and corneocytes and form a structure resembling a *stratum corneum*. Recent studies have demonstrated that the *stratum corneum* of *in vitro* cultured models differs from native

skin in terms of lipid composition and lipid spatial organisation [216], however they still present a clear improvement on 2D cell cultures. Examples where reconstructed skin models have been used for skin penetration studies have been reported [217, 218]. Though these models have probably been selected due to their availability, previous studies by Garcia *et al,* in which the penetration rate for caffeine was measured [219] and Schafer-Korting *et al,* in which a wider selection of chemicals were used for validation purposes [220] showed that the *stratum corneum* of these reconstructed models is not as effective as the *stratum corneum* of *ex vivo* skin. Currently, reconstructed 3D skin models are not recommended for skin penetration studies. However, the models have been validated and found suitable for assessment of skin corrosion and skin irritation potential [221-224]. Recent studies have also tried to link cell viability and cytokine secretion in these models to the sensitizing potential of chemicals [225, 226]. These skin equivalents can however be used more broadly to understand human skin biology and skin sensitization on a molecular level [227-229].

6.1.2 Measuring GST activity in 3D skin models.

The relatively few metabolism studies conducted using 3D skin models have only evaluated Phase I and Phase II enzyme expression and activity [48, 49, 53]. In the reported protocols, the test compound is usually applied as a single dose topically or by dissolving the test compound in the culture medium [49, 230] and the rate of metabolite formation is monitored. Other techniques use skin fractions freshly prepared from the models to carry out metabolism studies. For example, cytosolic fractions of 3D skin models have been prepared to measure glutathione-S-transferase (GST) activity by monitoring the formation of dinitrophenyl-glutathione (DNP-SG) conjugates following exposure to 2,4-dinitrochlorobenzene (DNCB)[231, 232].

GSH is a key molecule in the skin defense system as it has antioxidant properties and it can conjugate electrophilic xenobiotics. Understanding the extent to which GSH can detoxify compounds in healthy *in vivo* skin is vital, however existing tools do not allow non-invasive investigations in humans. Consequently, this process is poorly understood. This problem is only partially addressed by measuring GST activity in fresh *ex vivo* skin or 3D skin models fractions, since non-enzyme mediated GSH conjugation is a well characterised phenomenon.

6.1.3 Repeated dosing *in vitro*.

Assuming that either 3D skin models or cultured *ex vivo* skin can be maintained in a healthy state close to the one observed *in vivo*, current publications do not report the influence of repeated dosing on their defense mechanisms, or what is it expected to be in human skin. Most of the research in the field is focusing on chemical/drug permeability for one application *in vitro* with extrapolation being made for multiple exposures *in silico.* Mathematical modelling of the repeated application of a fixed concentration of drug on skin has been attempted by Kubota *et al* [233]. The first set of parameters that they used to test their model was representing a treatment comprising 13 daily applications of 1 h followed by a 23 h recovery period. The amount of drug in the skin (noted A_s in the published work) was plotted and showed a characteristic 'saw tooth' pattern, with a maximum and minimum value that did not vary after the first treatment (Fig 6.1).

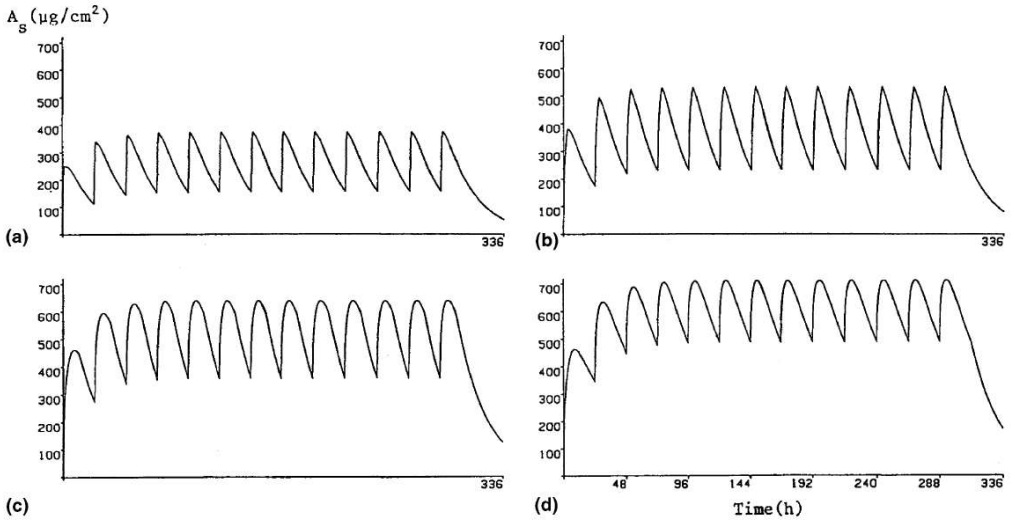

Fig. 3. Profiles of A_s versus time using $M = 8$, $N = 48$, $k = (1/84)$ h: (a) Experiment 1, (b) Experiment 3, (c) Experiment 5, (d) Experiment 6.

Figure 6.1: Profile of internal drug concentration in skin treated daily with a fixed concentration of drug for a) 1 h, b) 3 h, c) 12 h and d) 24 h. The internal concentration increased as the application time increased. Figure reproduced from [233].

To refine mathematical models such as the one described above, researchers are now developing strategies using cell systems and/or tissue models for repeated dosing and attempts at quantitative *in vitro-in vivo* (QIVIVE) extrapolation [234] but these have mostly been focussing on liver, kidney or brain so far. Another *in vitro* model trying to mimic the fate of a drug entering the body via topical application on skin is the "human on a chip" model (i.e *ex vivo* skin in one compartment, liver equivalent in the other) developed by Maschmeyer *et al* [235]. Information on the homeostatic state of these new in vitro models and most 3D skin models is missing and the disturbance of the models defence mechanisms (in our case the GSH pathway) has not been reported yet.

6.2 Aims and Objectives.

6.2.1 Aims.

GSH metabolism being a vital component of human skin defence system, we initially studied modulations of the GSH pathway in one of the most simplistic model to represent human skin, i.e the HaCaT cell line (Chapters 3-5). In this chapter, the concept of GSH pathway as a defence mechanism was investigated further, using a skin model of increased complexity, the RHE model. The main objective was to use this model, physiologically closer to human skin, to attempt a 7 day long experiment thought to mimic the daily use of a personal care product or even a topically applied drug: the model would be submitted to one daily treatment with a model skin sensitiser, rinsed with PBS and left to recover from exposure until the next treatment the following day.

First, we aimed at characterising the basal level of GSH in the RHE model for a 7 day period. This could be used as an estimation of what the basal level of GSH in healthy skin in a resting state would be (i.e without exposure to external xenobiotics and without the potential oxidative stress induced by handling a biopsy sample before being able to measure GSH). We then extended our experiments to single and multiple exposures to the model skin sensitiser DNCB, to increase our understanding of the GSH depletion/repletion cycle following repeat exposures *in vitro*. We investigated whether there was a cumulative effect of DNCB treatments, which could either decrease or increase the overall availability of reduced GSH to clear the subsequent doses applied (i.e. Is there an induction of GST activity after several exposures? Is GSH production increased in the RHE? Or, on the contrary, does the defence system get overwhelmed with time and the clearance capacity gets affected?). Finally, we questioned whether the dynamics of danger signalling which influence the GSH pathway at a cellular level,

in this case the activation of the Nrf2 pathway, were anticipating the future variations of GSH level after a series of doses were applied to this *in vitro* model.

6.2.2 Experimental design.

The RHE model is commercially available and supplied with a 48 h maintenance medium. Additional growth medium can be purchased for culturing the models for longer periods. The composition of these media was not disclosed by the supplier and little detail was provided about the conditions under which the models should be cultured, with the exception of a recommended daily change of medium. The first set of experiments carried out aimed at selecting the most appropriate medium to maintain the level of GSH in the model over a 7 day period. Moreover, the basal level of GSH in the RHE model is not reported in the literature or by the supplier, so this was also assessed as soon as the models were received from the supplier.

Once optimal culture conditions were obtained, we investigated the clearance of DNCB over a 24 hour period to match/compare them with the previous findings from our studies in the HaCaT cell line. This was followed by further investigations to increase the number of topical applications of DNCB in the RHE skin model. RHE models were topically exposed to a non-toxic dose of DNCB and clearance was measured. Moreover, we quantified GSH replenishment in the topically-treated RHE models as a measure of recovery from chemical stress and evaluated the effect of multiple non-toxic and toxic daily doses of DNCB on GSH depletion/repletion. Finally, activation of the Nrf2 pathway, which up-regulates the synthesis of glutamyl-cysteine ligase (GCL) and GST, was measured after each DNCB treatment.

6.3 Results.

6.3.1 Basal level of GSH in RHE model.

RHE samples are structurally close to skin explants as they contain differentiated layers of viable keratinocytes as well as terminally differentiated top layers, forming an *in vitro* equivalent of *stratum corneum*. Basal GSH levels were evaluated on receipt of the samples. The mean value was 4.26±0.99 µg/mg soluble protein (14±3 nmol/mg soluble protein) (protein content in RHE expressed against BSA standards in the BCA assay) for six samples delivered on four different days. The GSSG levels were below the limit of detection. These results were comparable to the results obtained in the HaCaT cell line (7 nmol/mg soluble protein GSH) measured in the previous chapters and not dissimilar to the GSH levels in skin explants reported by others, which were in the 85-480 nmol/g wet tissue range (see details in Chapter 3, Section 3.1.1).

The models were maintained in culture in different types of medium: the RHE maintenance medium (recommended by the supplier for model maintenance for up to 48 h), the HaCaT cell culture medium, for which the recipe has been optimised in house for the culture of HaCaT cells and the RHE growth medium (recommended by the supplier for model culture over several days).

To evaluate the suitability of the RHE maintenance medium, time points investigated were t= 0 h, when the models are just received from the supplier, t=3 h, which is a realistic representation of the time required to prepare solutions to treat the models, t=24 h, which is a usual time at which a read-out of experiment is carried out (i.e. end of 24 h MTT assay) and t= 48 h, which is the maximum time for which the models can be maintained in the RHE maintenance medium (recommendation from the supplier). The results are presented in Table 6.1.

Time point (hour)	*GSH level, Normalised data (in µg/mg soluble protein)*	*Standard deviation (in µg/mg soluble protein)*
0	4.71	0.57
3	5.83	1.57
24	3.41	0.69
48	4.73	Not Applicable (*)

Table 6.1: **GSH level in RHE models cultured for 0, 3, 24 and 48 h in SkinEthic RHE maintenance medium without medium change.** Two separate models were used for each time point (n= 2). Soluble protein concentration was measured by BCA assay to normalise the GSH concentration measured. (*) GSH level was below the limit of quantification of the assay for one of the two models, GSH level is reported for a single model for this particular time point.

It appeared that the level of GSH in the models decreased erratically over time and was lower at 24 h than at t=0. After 48 h of culture one of the models had a GSH level below the limit of quantification of the method, 0.05 µM, while the other had GSH maintained at the same level as t=0. Therefore, it was concluded that while the maintenance medium is provided for experiments carried out less than 48 h after reception from supplier, its use in experiments involving the maintenance or regeneration of GSH was not appropriate.

A similar experiment was carried out in HaCaT cell culture medium and in RHE growth medium for a period of 7 days (single replicate). The medium was refreshed daily in all 6-well plates containing RHE models. The results are presented in Table 6.2. Both media allowed for the culture of RHE models for several days, with the exception that the RHE model cultured in HaCaT medium for 7 days had a lower level of GSH. The stability of the GSH level was better achieved with the RHE growth medium, which was subsequently used for RHE models culture experiments.

In contrast to the HaCaT cell line, for which the level of GSH doubles over a 24 h period, in line with cell proliferation in the well [236], GSH levels are stable for several days in RHE.

Time point in hours (day)	*Sample ID*	*GSH (in µg/mg soluble protein)*
0 (1)	HaCaT medium	9.35
24 (2)	HaCaT medium	6.34
48 (3)	HaCaT medium	7.55
72 (4)	HaCaT medium	7.84
96 (5)	HaCaT medium	9.00
144 (7)	HaCaT medium	3.06
0 (1)	RHE growth medium	5.63
24 (2)	RHE growth medium	5.40
48 (3)	RHE growth medium	5.04
72 (4)	RHE growth medium	6.39
96 (5)	RHE growth medium	7.68
144 (7)	RHE growth medium	6.15

Table 6.2: **GSH level in RHE models cultured for 7 days in RHE growth medium or HaCaT cell culture medium.** RHE models were cultured in medium for the required length of time, washed with PBS and lysed in 2 mL RIPA buffer. GSH quantification was carried out after derivatisation with iodoacetamide. Protein quantification was carried out by BCA assay and the GSH concentration expressed in µg/mg soluble protein for each model (n=1). Based on these results, RHE model were subsequently cultured in RHE growth medium to maintain GSH levels at a relatively constant concentration for several days.

6.3.2 Cytotoxicity assay (MTT) after exposure to a single dose of DNCB.

Cytotoxicity of DNCB was assessed by MTT assay at 24 hours to evaluate the likelihood that the washing step of the RHE samples after 2 hours of exposure with replacement of the medium would not remove the DNCB introduced (worst case scenario). Doses ranging 0.05-0.1 mM were non-toxic but doses ranging 0.5-1 mM showed cytotoxicity, highlighting the importance of this washing step with PBS after 2 hours accompanied by a complete replacement of the medium (Fig 6.2).

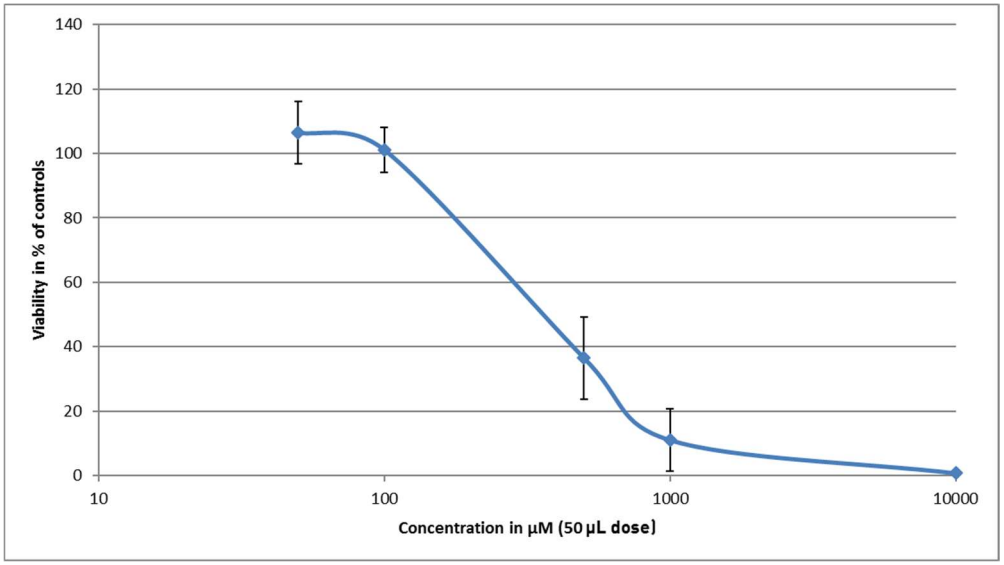

Figure 6.2: 24 hour cytotoxicity in RHE samples treated with a single dose of DNCB. The RHE samples were treated with 50 µL of DNCB solutions ranging 0-10 mM prepared in RHE growth medium containing 10 % DMSO. DNCB toxicity was determined using the MTT assay after 24 hours of exposure. The concentration applied was considered non-toxic when the model viability is at least 80 % compared to control RHE model kept in culture medium containing 10 % DMSO for a similar length of time. Each concentration was tested in duplicate (n=2) and the result was presented as Mean viability ± Standard deviation.

6.3.3. GSH depletion/repletion cycle after exposure to a single dose of DNCB.

To evaluate the effect of the DNCB treatment on GSH levels, the DNCB concentration was fixed at 1 mM (20 µg/cm^2) and 0.1 mM (2 µg/cm^2). The samples were treated, washed with PBS after 2 hours and left to recover in fresh RHE growth medium for 22 hours. At both DNCB concentrations GSH was depleted during the 2 h exposure period. Treatment of RHE models with 1 mM DNCB was associated with greater than 90 % depletion of intracellular GSH. In contrast, treatment with the lower DNCB concentration (0.1 mM) depleted GSH levels by approximately 30 % (Fig 6.3). GSH replenishment started as soon as soluble DNCB was removed through washing. Repletion of GSH levels was observed after 24 h with both treatment regimens.

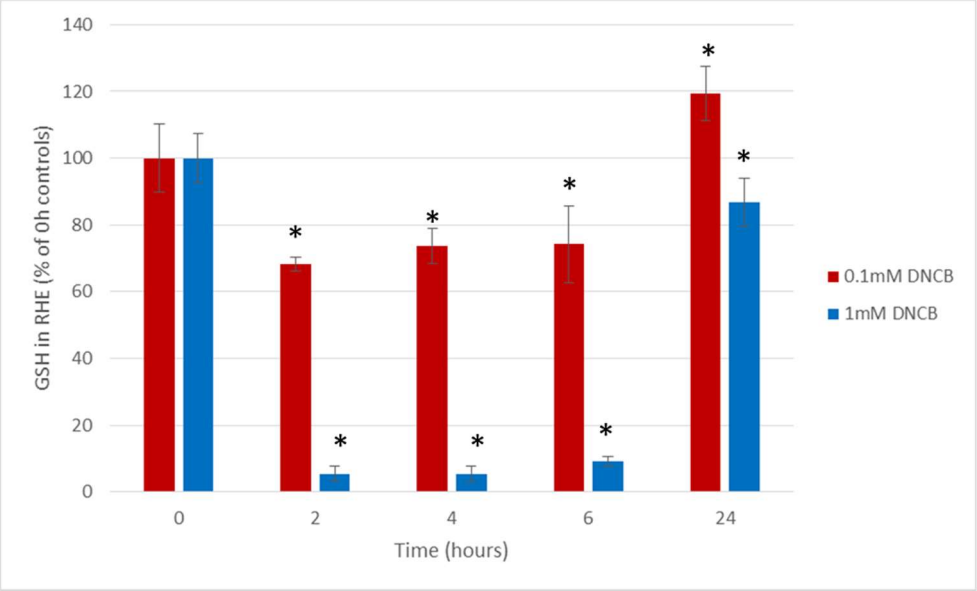

Figure 6.3: 24 hour GSH cycle in RHE samples treated with a single dose of DNCB. The RHE samples were treated with 50 µL of DNCB solutions prepared in RHE growth medium containing 1 % DMSO, washed with PBS after 2 hours and left to recover in fresh RHE growth medium for the remaining time of the experiment. RHE models were lysed in 2mL RIPA buffer. 100 µL of lysate was derivatised for GSH quantification and the results obtained expressed in % of 0 h controls(n=3). (*) Statistical difference between GSH level in treated RHE samples and RHE samples lysed before treatment (t= 0 hour) Student's t-test, p value <0.05.

However, the outcome of the repletion process was dose-dependent: 0.1 mM DNCB induced a slight up-regulation of GSH in the samples, similar to previous observations in the HaCaT cell line [236], whereas GSH levels were not completely replenished for 1 mM DNCB treatment (GSH concentrations at 24 hours statistically different from initial levels, Student's t-test, p value <0.05).

6.3.4. GSH depletion/repletion cycle after three repeated treatments with DNCB.

Based on the partial GSH repletion observed with 1 mM DNCB (Fig 6.3), multiple exposure experiments were designed using 0.1 mM (2 µg/cm^2) and an intermediate dose of 0.5 mM (10 µg/cm^2). The RHE samples were treated daily with a single concentration of DNCB (0.1 mM or 0.5 mM), washed with PBS after 2 hours and left to recover in fresh RHE growth medium for 22 hours. For each exposure to DNCB the GSH

pool was partially but significantly depleted after 2 h *(Student's t-test, p value <0.05)* (Fig 6.4). During the recovery period, GSH was replenished to levels that were similar to the initial levels at t= 0 hour (t= 24, 48 and 72 hours), without upregulation, for both doses investigated (Fig 6.4). The repletion of GSH after the third 0.5 mM DNCB treatment (t=72 hours) was not statistically different from the levels observed at t=0 hour (Student 's t-test).

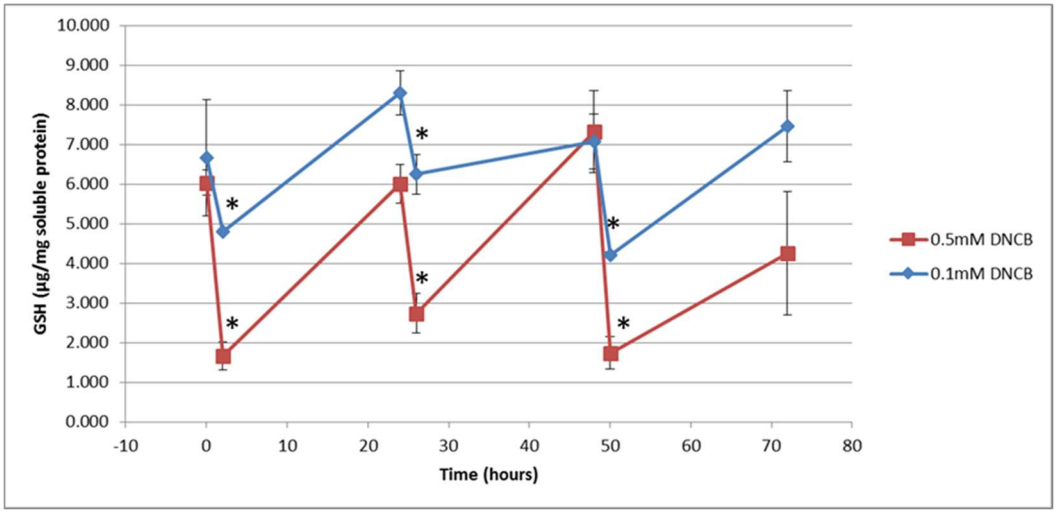

Figure 6.4: 72 hour GSH cycle in RHE samples treated daily with DNCB. The RHE models were treated with 50 µL of DNCB solutions prepared in RHE growth medium containing 1 % DMSO, washed with PBS after 2 hours and left to recover in RHE growth medium for 22 hours. The process was repeated three times over a 72 hour period. RHE models were lysed in 2mL RIPA buffer. 100 µL lysate was derivatised with iodoacetamide for GSH quantification. Protein quantification was carried out and GSH results were expressed in µg/mL soluble protein (n=3). (*) Statistical difference between GSH level in treated RHE samples and RHE samples lysed before treatment (t= 0, 24 and 48 hours) Student's t-test, p value <0.05.

6.3.5. DNP-SG clearance is enhanced after repeated treatments with DNCB.

The difference in the levels of GSH repletion observed in single and repeat dose experiments was investigated further by measuring the levels of DNCB glutathione conjugation (DNP-SG). DNP-SG was quantified in all the samples collected during the 72 hour experiments. The level of DNP-SG found in the PBS wash collected was negligible

compared to levels observed in the RHE lysates and RHE growth medium. In each experiment, the total amount of DNP-SG formed after each DNCB exposure increased. For 1 mM DNCB, the total DNP-SG at t= 2 hours was 1.7±0.3 µM and increased to 3.1±0.5 µM at t= 50 hours. The same trend was observed for the 0.5 mM dose, DNP-SG increasing from 6.7±0.5 µM at t=2 hours to 11.3±1.1 µM at t= 50 hours (Fig 6.5). The distribution of DNP-SG differed considerably between 0.1 and 0.5 mM doses. For 0.1 mM DNCB, the level of DNP-SG in the RHE lysate was very low at each exposure (t= 2, 26 and 50 hours) (Fig 6.5 a), whereas for 0.5 mM DNCB, the amount of DNP-SG in the RHE lysate increased at each exposure (Fig 6.5 b). As well as an increase in cumulated DNP-SG at the end of the exposure periods, an increase in DNP-SG in the RHE growth medium was also observed during the recovery period after each exposure for the higher dose (0.5 mM) (Fig 6.5 b).

To determine whether there is a time-dependent increase in DNP-SG synthesis, a mean comparison test was performed using Tukey's Honest Significance Test. This method made an adjustment in rejection criteria to account for multiple tests being carried out on the same data. In this case with three tests, without any adjustment, there is a 14.3 % chance of at least one significant result under the null hypothesis. Using the Tukey method adjusts this value to 5 %, thus making it harder for a single test to yield a significant result but allowing the chance of a false positive over all the tests to remain at 5 %. Results are reported in Table 6.3.

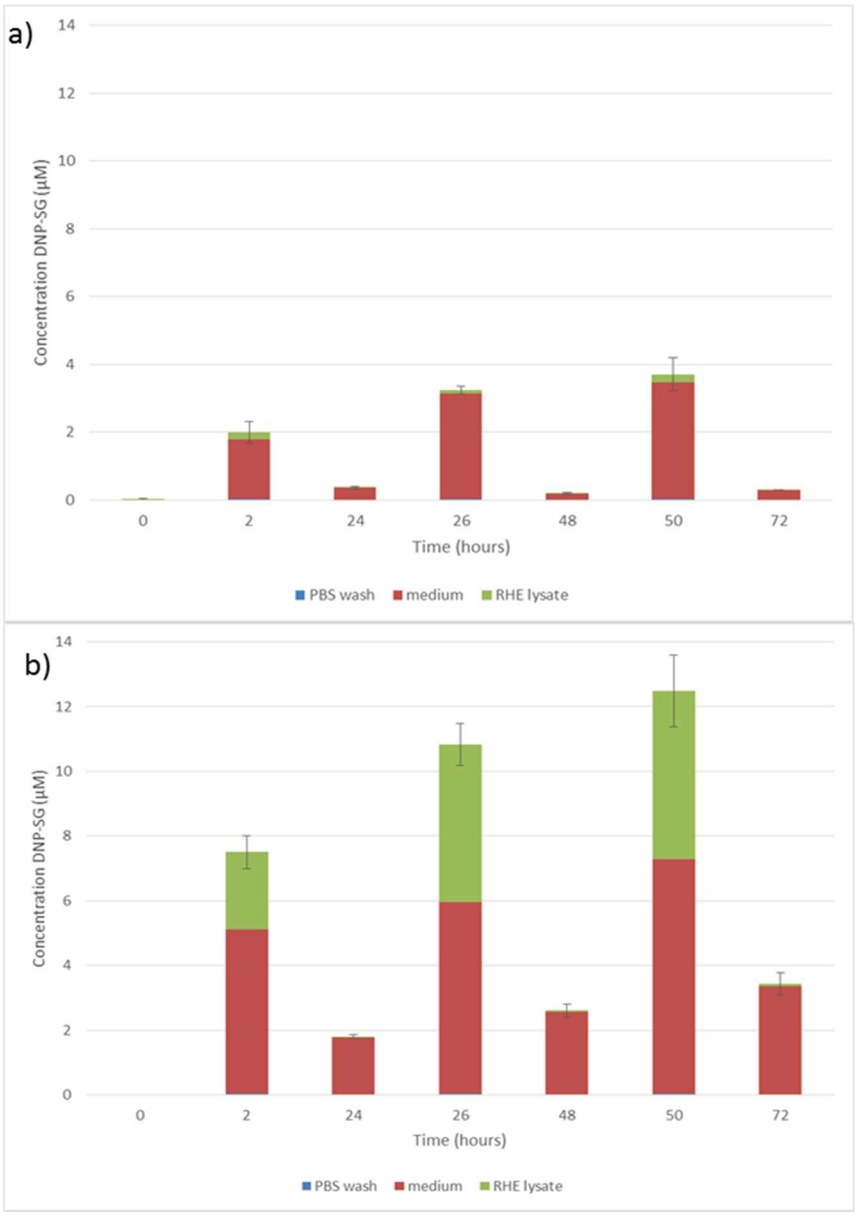

Figure 6.5: DNP-SG conjugate formation and excretion in the RHE model. The DNCB doses applied at t= 0, 24 and 48 hours were a) 0.1 mM and b) 0.5 mM. Medium and PBS wash were diluted 4:1 with acetonitrile before analysis and results expressed in µM. RHE models were lysed in 2mL of RIPA buffer and the lysate diluted 4:1 with acetonitrile for analysis. Cumulative data presented for each time point includes PBS washes, RHE growth medium and RHE lysates (n=3). After each DNCB treatment (t= 2, 26 and 50 hours), the total amount of DNP-SG in the RHE samples increases. At high dose (0.5 mM) the amount of DNP-SG in the medium at the end of the 22 hour recovery period increases at each exposure.

	DNP-SG concentration (µM) presented as Mean±Standard Deviation				
Time (hours)	**DNCB applied: 0.1 (mM)**		**DNCB applied: 0.5 (mM)**		
2	1.7117±0.3185		6.6610±0.5054		
26	2.7260±0.1265		9.8450±0.6429		
50	3.1353±0.4815		11.2807±1.1055		
DNCB Applied (mM)	**Time Comparison**	**Difference Between Means**	**Simultaneous 95 % Confidence Limits**		
0.1	**50 - 26**	0.4093	-0.4455	1.2641	
0.1	**50 - 2**	1.4237	0.5689	2.2785	***
0.1	**26 - 2**	1.0143	0.1595	1.8691	***
0.5	**50 - 26**	1.4357	-0.5532	3.4245	
0.5	**50 - 2**	4.6197	2.6308	6.6085	***
0.5	**26 - 2**	3.1840	1.1951	5.1729	***

Table 6.3: **DNP-SG conjugate formation increases after each exposure to DNCB.** The DNP-SG levels (µM) in RHE growth medium, PBS wash and RHE lysate were summed for each time point, in triplicate measurements, and the mean calculated. Means were compared using the Tukey's Honest Significance Test.******* Significant difference between the two time points investigated, confidence interval at 5 %.

For both concentrations investigated (0.1 mM and 0.5 mM), repeated exposure generated an increase in clearance that quickly reached a plateau. The second exposure to DNCB led to the generation of significantly more DNP-SG conjugate than the first exposure even though the dose was applied for the same time. However, the third exposure did not generate an increase compared to the second exposure, suggesting that the clearance capacity of the RHE model has reached its upper limit.

6.3.6. Nrf2 activation after repeated treatments with DNCB.

Since Nrf2 is known to regulate the expression of both Glutamyl Cysteine Ligase (GCL), the rate limiting enzyme in GSH synthesis, as well as GST, which mediates conjugation with GSH, a plausible explanation for the increase in DNP-SG is that Nrf2 is induced following repeated exposure to DNCB. Therefore, Nrf2 levels and NQO1 levels in cytosol following DNCB treatment was measured by Western blotting and compared with a potent Nrf2 established inducer [237], CDDO-Me, as a positive control (Fig 6.6 a). The data show a 4-7 fold increase in Nrf2 compared with the basal level (t = 0 h) during each exposure period (t = 2, 26 and 50 h, a replicate at t=2 h is a clear outlier, possibly due to sample preparation error and has been removed).

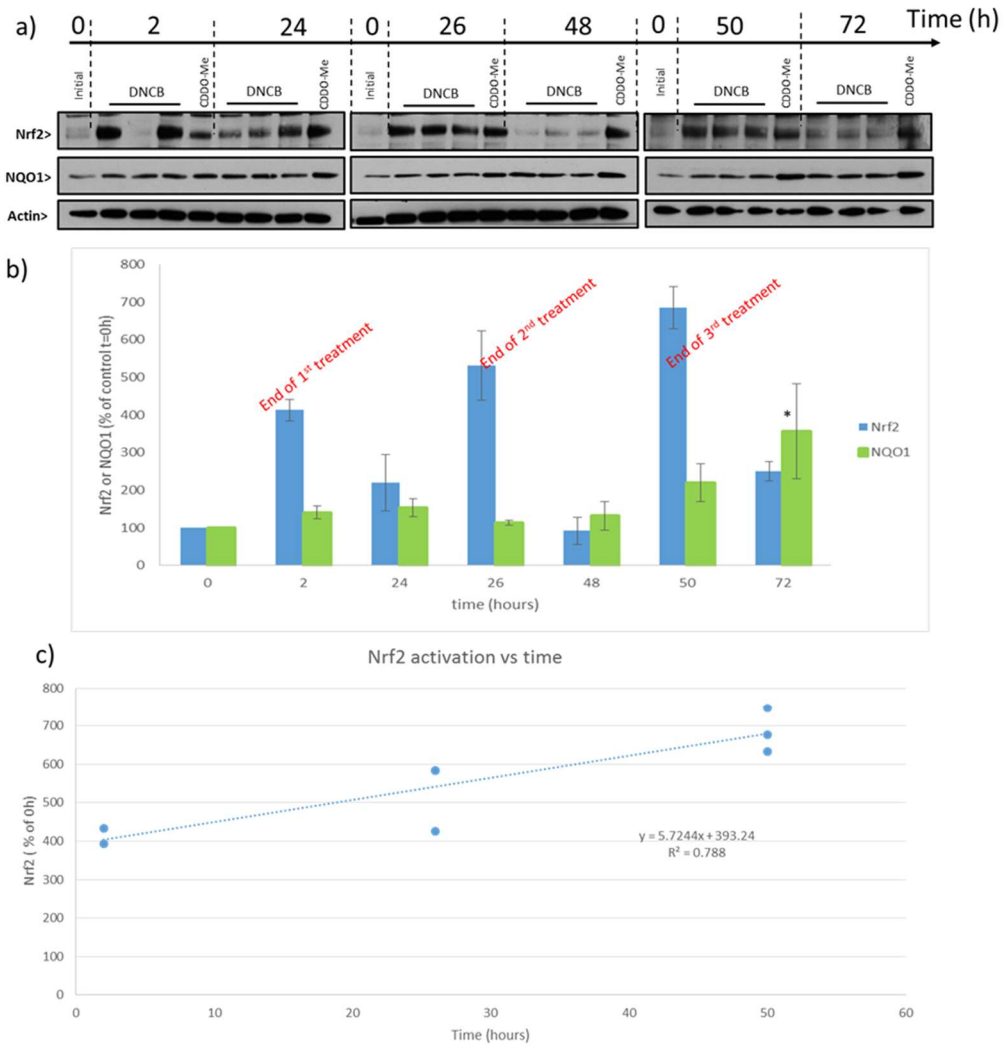

Figure 6.6: Daily DNCB dosing releases Nrf2 exclusively during exposure time. a) Typical Western Blot showing Nrf2 release during exposure to DNCB (n=3). Data normalised to actin, NQO1 enzyme measured as positive control of Nrf2 activation, positive control CDDO-Me (n=1). For t=0 h three control samples were pooled to generate a single t=0 sample, with value fixed at ratio 1 (100 % baseline value) and used to calculate the "ratio over controls" for the other samples. b) Data illustration for Nrf2 and NQO1 as a function of time. DNCB induced an increase in Nrf2 level of 4-7 fold at t= 2, 26 and 50 h during exposure and decreases back to 1-3 fold, NQO1 activation statistically significant at t=7 2h (student t-test, $p<0.1$) c) The release of Nrf2 was increased after each exposure to DNCB. The mean Nrf2 values of time points 2 h, 26 h and 50 h were statistically different (ANOVA, $p<0.05$).

During the 22h recovery period the Nrf2 decreased to within 1-3 fold of the t=0 h value. NQO1 levels were not statistically different from initial levels until the third exposure to DNCB (Student t-test, $p<0.01$) (Fig 6.6 b) possibly due to the selection of time points, which were optimised for GSH depletion measurements.

These data confirmed the observations made in the GSH experiment. Nrf2 was released the most at the time points where GSH levels were depleted the most, suggesting that the Nrf2 pathway was quickly activated to signal the need for an increased GSH production to compensate for the rapid consumption of cellular GSH by DNCB conjugation. This correlates well with findings made by Copple *et al.*, who demonstrated an increase in nucleic Nrf2 in mouse hepatocytes treated with 100 µM DNCB for 1 hour [193]. There was also a linear increase in Nrf2 release after each DNCB exposure (Fig 6.6 c), which corroborates the increase in DNP-SG being formed after each exposure (Fig 6.5).

6.3.7. Limitations of clearance capacity and dose considerations in repeated dosing experiments.

To test the limitations of the experimental design, single replicates of RHE samples were treated daily with a 1 mM dose of DNCB for one week. In the single exposure experiment, a 1 mM DNCB concentration allowed for a partial replenishment of GSH level at the end of the 22 hour recovery period (Fig 6.2). However, repeat 1 mM daily dosing with DNCB resulted in complete loss of all GSH related metabolic activity for some samples at different time points (RHE5 (lysed before the third DNCB treatment), RHE7 (lysed before the fourth DNCB treatment), RHE10 (lysed after the fifth DNCB treatment) and RHE13 (lysed before the seventh DNCB treatment) (Fig 6.7)). Overall, the metabolic capacity of all samples investigated appeared to decrease after only two

cycles of exposures. Additionally, the DNP-SG level in the RHE lysates lowered steadily after each subsequent DNCB treatment.

To pinpoint at which time point/number of DNCB exposures the RHE samples lose their metabolic activity, we measured the level of DNP-SG in PBS wash carried out before and after each treatment for all the samples (as opposed to restricting measurements to the samples that are lysed at a specific time point). With the aid of this data, it is evident that RHE7 lost its metabolic activity at 48 hours (after the third DNCB treatment), RHE10 at 74 hours (after the fourth DNCB treatment) and RHE13 at 122 hours (after the sixth treatment) (Fig 6.8).

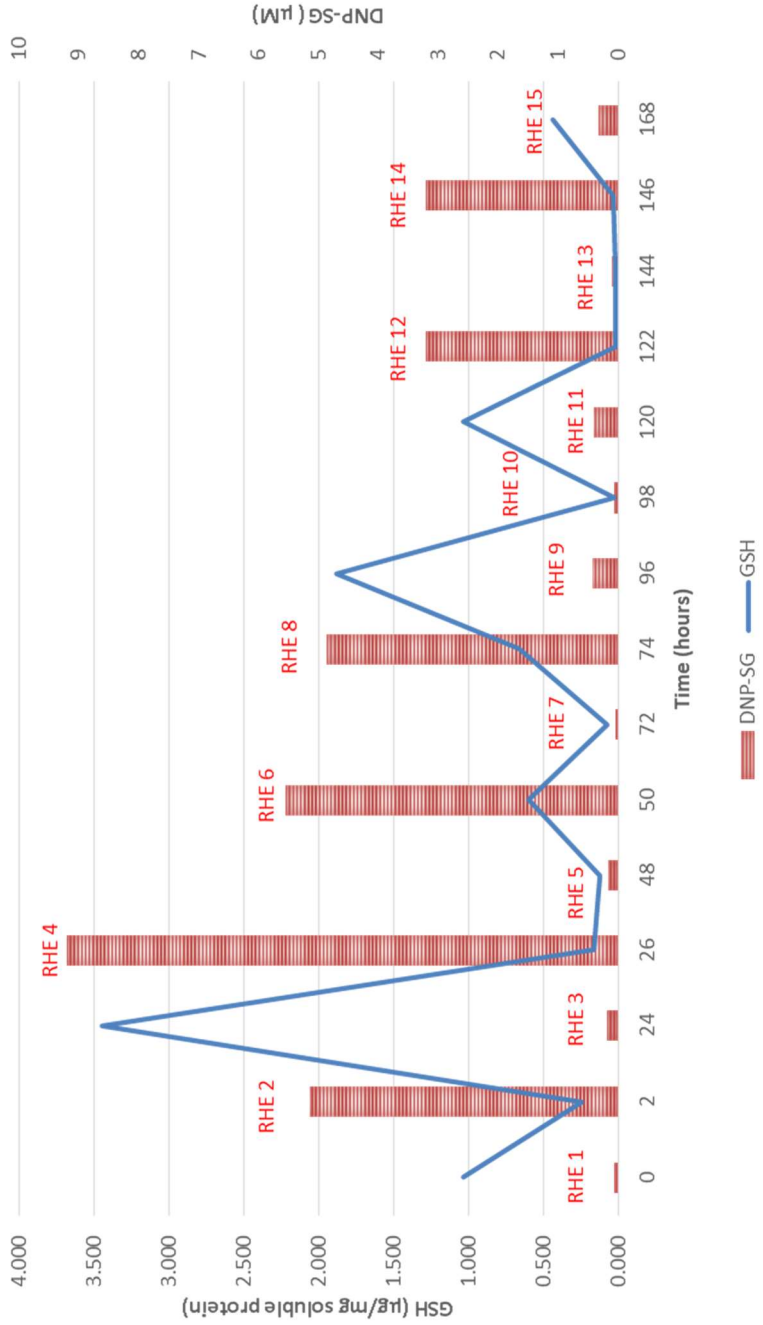

Figure 6.7: DNP-SG and GSH level in RHE samples treated daily with 1 mM DNCB for a week long period. The DNCB treatment occurred at t=0, 24, 48, 72, 96, 120 and 144 hours (n= 1). DNP-SG was quantified in lysate diluted 4:1 with acetonitrile. Protein quantification was carried out by BCA assay and results expressed in µg/mg soluble protein. The amount of DNP-SG increased in the RHE lysates between the first (RHE 2) and second treatment (RHE 4) but decreased steadily after all subsequent treatments, demonstrating a decrease in metabolic activity of the RHE models. The level of GSH was replenished after the first treatment but this was not sustained in subsequent treatments (RHE 5, RHE 7, RHE 13).

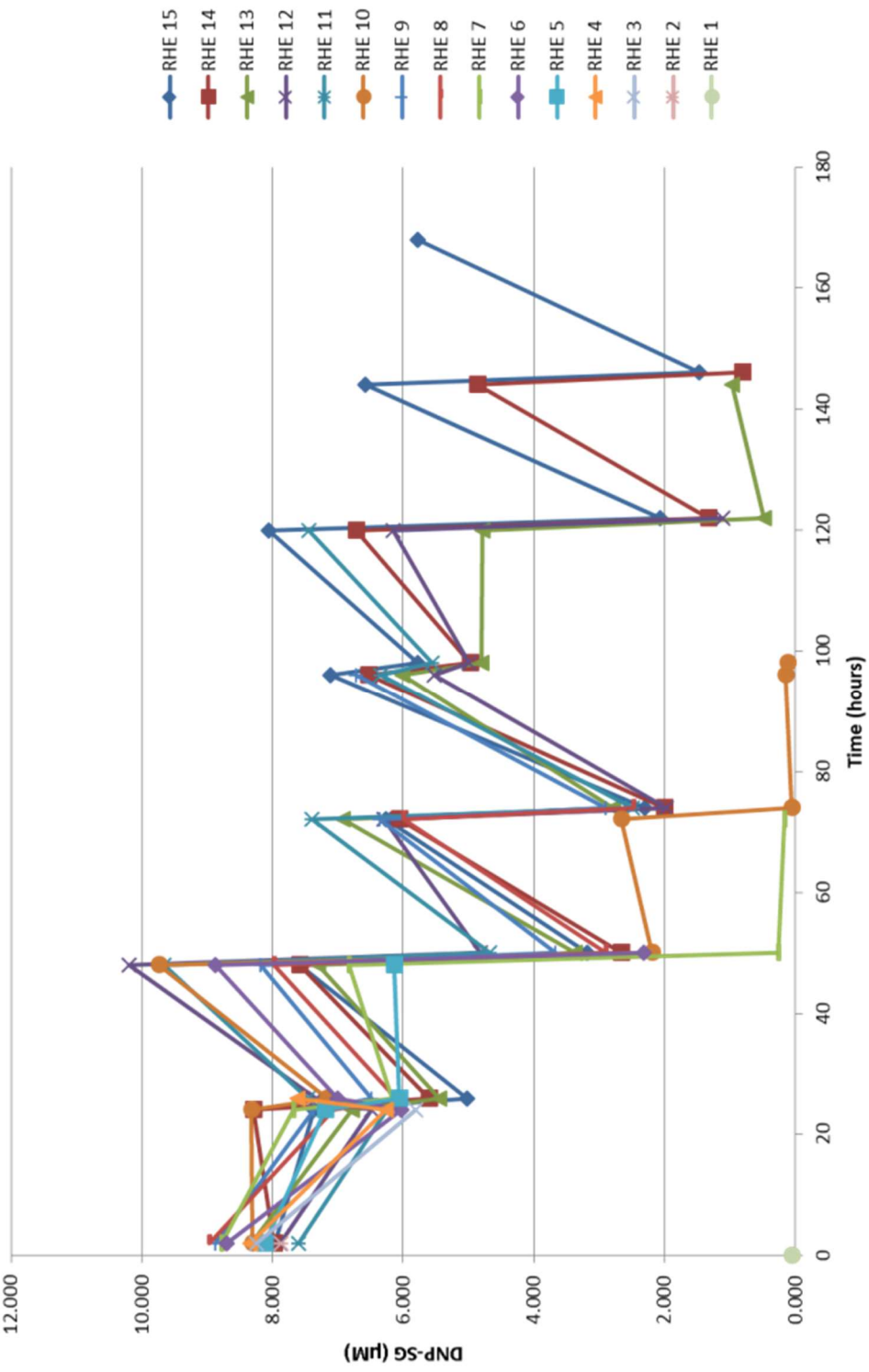

Figure 6.8: DNP-SG in PBS wash when RHE samples were treated daily with 1mM DNCB for a week long period. DNP-SG levels were measured by LC/MSMS in PBS wash (diluted 4:1 with acetonitrile) collected at each time point (n=1). The level of DNP-SG present in the washes decreased after each treatment, demonstrating an overall decrease in metabolic activity in the models as more treatments were applied. Specifically, RHE 7, RHE 10 and RHE 13 lost all metabolic activity at t= 50, 74 and 120 hours respectively.

6.4 Discussion.

Most topically applied products are designed to be used on a regular basis or at least for a few cycles of application before the desired effects are obtained. Whilst repeat product application is considered at the clinical trial stage, repeat dosing studies are not frequently performed during early *in vitro* investigations. Considering skin allergy, it is a well-known phenomenon that repeated low dosing *in vivo* may lead to the same adverse outcome as a single high dose. For example, in a clinical study comparing single and multiple exposures to a model skin sensitiser, exposing volunteers to a single dose of 60 µg/cm^2 DNCB or three times with a once weekly 10 µg/cm^2 dose led to a comparable number of sensitised volunteers after re-exposure four weeks later [238]. Therefore, appropriate precautions need to be taken to estimate a safe dose of any chemical for a specific intended use. Simulating *in silico* the fate of a chemical entering the skin while estimating the amount of modification of proteins in a dynamic model representative of skin for use in risk assessments is now being attempted [239, 240] which may present a unique opportunity to integrate the effects of repeat dosing. Similarly, considering *in vitro* skin metabolism, studies identifying metabolites and measuring enzymatic activity are mostly limited to a single exposure which do not lend themselves readily to extrapolation to *in vivo* exposure and realistic assessment of human skin metabolism.

In this study, we demonstrated that repeat topical dosing of a 3D skin model was not only feasible (at least over the 72 h period we investigated) but could deliver crucial information on the limitations of enzymatic induction in a model relatively close to skin. Based on the assumption that metabolism studies carried out at “low” doses might be more representative of the *in vivo* situation we investigated the hypothesis that the GSH

pathway could be maintained or even enhanced after multiple exposures to a model skin sensitiser. In our experiments, DNCB reproducibly depleted GSH during the two hours of exposure, three consecutive times. This correlated well with findings from Maneski *et al* [54], who demonstrated that a low dose of 10 µM DNCB was mostly cleared during the first hour of exposure in *ex vivo* skin. Additionally, our work demonstrated the limited capacity of the RHE model to synthesise *de novo* GSH.

The level of GSH in human skin has been estimated to be between low to mid hundreds of nmol/g of wet tissue [135, 136]. Although expected to be comparable to human skin, the GSH levels in 3D skin models are not extensively reported in literature. We have measured an average GSH level of 14 nmol/mg soluble protein in RHE models [236]. As far as we are aware, no literature reports of GSH levels exist for repeat exposure scenarios in RHE models. Surprisingly, the induction of GSH biosynthesis did not lead to an increase in free cytosolic GSH in our experiment. GSH levels seemed to replete to an optimum level in the range 5-9 µg/mg soluble protein, while all the overproduced GSH was immediately used to conjugate DNCB. This might have been due to a concomitant up-regulation of GST activity caused by Nrf2 activation.

These observations are in line with previously reported GSH-related metabolic events. In the experiments carried out in Chapter 4 (See Section 4.3.3 and 4.3.4), a single non-toxic exposure to DNCB induced an upregulation of GSH production in the HaCaT cell line within 24 hours and activated the Nrf2 pathway. Similarly, GSH related enzymes (i.e GCL and GST) were upregulated in keratinocytes following single dosing with non-toxic levels of inorganic arsenic and the free GSH concentration in the cells was also higher than in control cells [139]. Moreover, when multiple dosing regimens were used in a clinical trial (albeit not skin related), repeated daily dosing with 125 mg oltipraz showed a 2.6-fold increase in GST activity in volunteers compared to a weekly 500 mg dose which showed no increase in GST activity [241]. These data indicate that repeat low,

non-toxic doses have a higher impact on the GSH levels and general responsiveness of the GSH defence mechanism than single higher doses.

The complexity of the Nrf2 pathway and its role in cell protection have been recently reviewed [180]. In our experiments, the Nrf2 cytosolic accumulation observed when RHE models were lysed immediately after exposure is likely to be the result of release from the Nrf2-keap 1 complex after the cysteine residues of Keap-1 were modified covalently by DNCB [193]. Nrf2 activation, which has also been observed using other chemical probes such as resveratrol [242] and sulforaphane [243], plays a role in skin protection as demonstrated in studies with various types of isolated cell lines including keratinocytes, melanocytes and fibroblasts [244]. However, demonstration of its protective role in *in vitro* skin models such as 3D skin models is still a subject of debate. For example, a single 16 hour treatment of resveratrol, has been shown to activate the Nrf2 pathway in NHEK cells and reconstructed skin (multi-layered model grown in-house with keratinocytes on a bed of cultured fibroblasts in collagen), resulting in an up-regulation of GSH biosynthesis [245]. When considering multiple exposure regimens, daily exposure to sulforaphane for 4 hours has been shown to activate the Nrf2 pathway in human skin fibroblasts and actively contributes to cellular protection by reducing ionising radiation-induced DNA damage. The effect of Nrf2 activation on cellular protection was more pronounced after four daily exposures than after a single exposure at the same dose [246]. Our study is consistent with this finding; the level of DNCB conjugate formed was directly related to activation of the Nrf2 pathway.

6.5 Conclusion.

3D skin models such as the RHE model can be cultured for several days and offer a good *in vitro* alternative for studying repeated dosing. We focussed our study on the GSH pathway as a defence mechanism in skin and demonstrated that low non-toxic exposure

to DNCB was able to induce GSH biosynthesis to detoxify the applied chemical. Multiple exposures led to an increase in efficiency of the clearance process (more DNP-SG was produced) between the first and second exposure and for the duration of investigation this phenomenon was sustained. The increase in GSH biosynthesis was linked to the activation of Nrf2. The activation of Nrf2 occurred within the two hours of exposure and coincided with the time at which the GSH level was the lowest, demonstrating that the signalling process was rapid. Moreover, after each exposure to DNCB, the amount of Nrf2 increased, mirroring the increased formation of GSH conjugate. This confirms that repeat low dosing of electrophiles promotes up-regulation of the defence mechanisms linked to the GSH pathway in skin to protect against exogenous compounds.

Current *in silico* skin metabolism models are based on structural alerts linked to the parent compound, qualitatively estimating the structure and properties of potential metabolites. As such, they lack the combination of metabolic data with estimation of skin bioavailability [247] and do not yet provide information on the effect of the metabolites on skin biology and homeostasis or dose relationship. The data obtained from studies dealing with natural defence mechanisms and their inherent capacity to deal with exposure to chemicals should provide building blocks on how organ (in this case skin) defence systems modify the parent chemical as well as its metabolites on a qualitative as well as quantitative level. The combination of these two approaches may result in a less conservative prediction of chemical safety providing insight not only into the type and nature of generated metabolites, but also how effectively an organ system may be able to remove them. We hypothesise that integrating the dynamics of detoxification in viable skin to current *in silico* models [239, 240] designed to inform skin sensitisation potential will be vital for effective extrapolation to *in vivo* exposure scenarios for risk assessments.

Chapter 7: General Discussion.

Skin allergy / Type IV hypersensitivity is an important issue to consider when designing a product that either requires topical application (cosmetics, personal care products, certain drugs…) or can come into contact with the skin during use (paints, pesticides...). As animal-based tests such as the Guinea Pig Maximisation Test or the Local Lymph Node Assay (mouse) have now been completely phased out for personal care products aimed at being commercialised in Europe [248], skin sensitisation potential of new ingredients will be assessed using a battery of *in vitro* tests. OECD test guidelines are currently in place for the Direct Peptide Reactivity Assay (DPRA, TG 442C) and the ARE-Nrf2 Luciferase Test Method, KeratinoSens® (TG 442D), which are based on the well understood mechanistic aspects of type IV hypersensitivity. Based on further mechanistic understanding, cell-based *in vitro* tests for skin sensitisation such as the U-Sens® assay (previously known as the Myeloid U937 *skin sensitisation* test (MUSST)) [249] and the human Cell Line Activation Test (h-CLAT) using THP-1 cells [250] , have been developed partially using chemicals for which historical patch-testing data was available (for example PPD [251, 252], DNCB [111] or common fragrances [253, 254]), i.e. these specific chemicals have generated a visible rash in individuals exposed to them. Using isolated immunological cells from these patients/blood donors also helped the understanding of antigen processing, presentation and generation of an immune response which have now all been summarised into an Adverse Outcome Pathway framework [13].

Current knowledge of antigen formation (i.e haptenation of skin proteins) is mostly based on models developed *in chemico*, in which a potential sensitiser is put in contact, in solution, with either a selection of small peptides [19, 20, 24], a single model protein

such as HSA [22, 72, 255] or a mixture of proteins [256]. However, these models might not easily correlate to *in vivo* situations and are mostly used to generate chemical alerts of the potential to cause sensitisation. In the specific case of drugs, researchers form the antigens *in chemico* then use these pre-formed antigens as standards to measure actual presence in T-cells isolated from patients previously treated with the drug using mass spectrometry [257] . This approach is therefore limited to the potential diagnosis of patients who have already developed hypersensitivity to a skin sensitiser during use. A similar protocol has been followed for the model sensitiser DNCB using a combination of two model peptides, Human serum albumin and cells isolated from the blood of healthy donors [258] but this type of study remains relatively rare.

Little is known of the reactive competition between sensitisers and proteins (leading to antigen formation) and sensitisers and small nucleophilic molecules (generating non-antigenic species that can be easily removed) in skin. We chose to study GSH to represent the small nucleophilic molecules group as it is the most prominent small thiol containing peptide intracellularly as well as the biomarker of choice for oxidative stress. Surprisingly, the oxido-reduction part of the GSH pathway is well defined in liver [60, 61, 141] but relatively poorly understood in human skin. The ratio GSH:GSSG, indicative of cellular health, should be approximately 100:1 for most cell types at homeostasis [157]. Disturbance of this balance during sensitisation was a subject of several studies. High concentration of ROS has been linked to the synthesis and release of cytokines by keratinocytes and dendritic cells [85]. More recently, Corsini *et al* have reviewed the involvement of oxidative stress in the activation of skin cells by sensitisers [259]. It is therefore plausible that the level of GSH in cells could be directly linked to the initial mechanisms of skin sensitisation, GSH being a very efficient quencher of ROS. Few studies seemed to have focussed on this hypothesis so far. It has been shown that when the amount of intracellular GSH was reduced by reaction with sensitisers in monocyte-

derived dendritic cells, changing the GSH:GSSG ratio, the phosphorylation of p38 MAPK and downstream activation of the dendritic cells occurred [260].

We initially characterised the GSH:GSSG ratio in keratinocytes using the HaCaT cell line as a model. In our experiments, GSH was measured in the 5-10 µM range while GSSG was systematically below the limit of quantification (0.1 µM). The protective potential of GSH against common skin sensitisers might preferentially come from the ability of its reactive thiol to conjugate electrophiles. When particularly potent sensitisers such as dinitrohalobenzenes were used, activation of the GSH pathway occurred concomitantly to activation of the Nrf2 pathway. We showed that a 10 µM dose of either DNFB, DNCB or DNBB depleted significantly the GSH pool approximately two to four hours after exposure. The three dinitrohalobenzenes also induced Nrf2 at low concentrations (1-5 µM) within 2 hours. This information is crucial in the determination of sensitising potential for assays such as the non-enzymatic thiol depletion assay developed by Schultz *et al* [167] and the KeratinoSens assay [179] in which the ability to induce Nrf2 is directly correlated to skin sensitising potential. Currently, a combination of the two assays, GSH depletion and Nrf2 activation, is available in the SensCee tox assay [261, 262]. Naven *et al* also combined an *in chemico* assay using GSH, BSA and human liver microsomes with a luciferase based assay to measure Nrf2 activation to provide a general assessment of thiol reactivity [214]. However, our investigations went further than evaluating the potential for chemical reactivity (i.e. measuring the electrophilicity of these chemicals). After 24 hours of exposure, we noted that HaCaT cells dosed with DNCB and DNFB contained higher level of GSH than untreated control cells. The different repletion pattern of GSH in cells treated with DNBB was most likely linked to the toxicity of the halogen itself rather than the reaction mechanism [194-196]. Thus, the upregulation of GSH in cells previously exposed to skin sensitisers constitute an integral part of the cell defence mechanism system regulated by the Nrf2 pathway in

skin. We suggest that to determine the amplitude of the adverse effect of a potential sensitiser at non-toxic levels, defence mechanisms including the GSH pathway, should be investigated *in vitro* over a period of time covering both the clearance of the dose and the time for the cells to recover from the change (return to homeostasis level).

Creating an imbalance in the GSH:GSSG ratio using the oxidative potential of the model aldehydes benzaldehyde and phenylacetaldehyde proved difficult. The mechanism reported for the reaction of aldehydes with thiols *in chemico* is an oxidation yielding a sulfur dimer. We showed that both BA and PA oxidised the totality of GSH available into GSSG *in chemico* but GSH levels were not significantly changed in HaCaT cells exposed for up to 2 hours. Even a strong oxidant such as hydrogen peroxide did not increase GSSG levels in the cells before high level of cytotoxicity was observed, suggesting that Glutathione Reductase activity is high in this cell line. In skin, the reactivity of aldehydes is thought to be mainly driven by the formation of a Schiff base with the primary amine contained in the lysine residues of proteins. This has been investigated for a series of benzaldehyde derivatives [263]. The protective potential of GSH to clear these aldehydes by an oxido-reduction mechanism appears relatively minor in proportion compared to the Schiff base reaction. This questioned whether most sensitisers are detoxified by GSH via a conjugation mechanism.

For a non-toxic level of exposure, cell recovery (here GSH repletion) might be a differentiating factor for compounds which all react with GSH by the same mechanism. We attempted a comparison of chemicals by sensitising potential, using DNCB and DPCP as extreme sensitisers and DEM as a moderate sensitiser. The mechanism by which these chemicals react with GSH was very different: SNAr for DNCB or Michael addition for DPCP and DEM. GSH conjugates were observed *in chemico* for the three compounds, as was reported elsewhere using other model thiols [19, 20, 24]., The assumption that all of them could deplete GSH when applied at the highest non-toxic dose on HaCaT cells

was solely based on these initial *in chemico* results. We used relatively high doses of DEM and DPCP compared to the available 5-10 µM reduced GSH measured in untreated cells. Surprisingly, these did not induce a visible depletion of GSH in our assay and differences could only be observed after the recovery period (24 hour time point).

In chemico, DPCP and DNCB have first order kinetics rates of similar order of magnitude [211], although the reaction mechanism with thiols is different (SNAr versus Michael addition). The bioavailability of each compound in cells played a crucial role in the results obtained. To observe any kind of GSH depletion highly toxic levels of DPCP were required, hence overlapping GSH depletion linked to potential conjugation with depletion induced by loss of viability. As GSH stock was not reduced, no upregulation of GSH level was observed after 24 hours. From experimental observations, GSH conjugation was not a principal pathway for DPCP clearance and it is thought that the antigens leading to sensitisation to DPCP were probably formed extracellularly [213]. Though both DNCB and DPCP are classified as extreme sensitisers in assays such as the LLNA, their behaviour in skin seem quite different. The comparison between DNCB and DEM was based on the ability of each chemical to react with GSH intracellularly. While DNCB was depleting GSH within the first 4 hours of exposure, no depletion was visible for DEM although the concentration applied on cells was 5 times higher. This suggested that the reaction kinetics were faster for the more potent sensitiser. The formation of conjugates has been shown to be catalysed by GSTs in both cases [113, 264] but we also indirectly observed the influence of these sensitisers on other enzymes of the GSH pathway. After 24 hours, DEM had induced an over-production of GSH in the cells of approximately 200 % in our assay, far more than the upregulation of GSH observed for DNCB. Both compounds have been shown to be Nrf2 inducers in the KeratinoSens assay, generating a three-fold increase in the luciferase readout at a concentration of 3.89 µM for DNCB and 82.85 µM for DEM [202]. The activation of Nrf2 is the signalling pathway

linked to the downstream upregulation of enzyme production involved in GSH synthesis (here, GCL and GS) and in our assay, this mechanism of defence must have been triggered for both chemicals to a similar extent. The difference in GSH concentration at 24 hours might be an indirect consequence of the fact that DEM was detoxified easily and the surplus of GSH was accumulating in the cell, while all excess GSH was rapidly consumed to clear DNCB.

Nrf2 activation and GSH clearance showed that the HaCaT cell line was a suitable in vitro model to assess skin sensitisers as these immortalised keratinocytes exhibited activity for all the enzymes of the GSH pathway. However, it is suspected that the metabolic capacity of this cell line might be over-expressed compared to *in vivo* skin. GST activity towards DNCB has been reported at 50 nmol/min/mg soluble protein in HaCaT cells, while it was only 20 nmol/min/mg soluble protein in human whole skin (cytosolic fraction)[53]. Hence, a complex model more closely related to human skin than a 2D cell culture was required. In the same publication, GST activity in a reconstructed epidermis model was measured at approximately 2nmol/min/mg soluble protein, though this low value was difficult to explain [53]. When other 3D models such as the Episkin® and RHE® skin models from Episkin™ were used, GST activity was still approximately double that of normal human skin [49]. As well as being reasonably representative in terms of enzymatic activity, these models seemed more appropriate for complex experiments requiring longer time frames than what could be achieved using a cell culture. Though characterisation studies carried out on these models highlighted some structural differences with *in vivo* skin, notably in terms of presence of lipids in certain layers, these models have shown viability for several weeks, some suggesting that apoptosis would not occur before 6-7 weeks [3, 265].

The understanding of the bioavailability of skin sensitisers *in vitro* can only be useful if it is comparable to realistic consumer use scenarios or can be extrapolated as closely as

possible to these situations, i.e. multiple exposures to the same sensitiser, at the same concentration, at regular time intervals. *In vitro* models enabling repeated dosing for assessing the toxicity of pharmaceutical treatments on the liver, kidneys and brain are currently under development [234]. Equivalent applications are not this advanced for skin models yet. We have used the RHE from Episkin™ as a 3D skin model and showed that the GSH pathway could be induced after three cycles of exposure to DNCB for a limited period of time (here 2 hours). The Nrf2 pathway, a critical danger signalling pathway for cell protection [180] was also activated after each exposure and the level of Nrf2 released increased each time to meet demand [266]. This provided missing information on the limitations of metabolic clearance in a model relatively close to skin. Maneski *et al* [54] demonstrated that a low dose of 10 µM DNCB was mostly cleared during the first hour of exposure in *ex vivo* skin. We showed that this process could be replicated three times on the RHE models. This provided a first step towards a routine use of the RHE for assessment of repeated dosing with potential sensitisers. However, an extension to 1 week of treatment damaged the RHEs irreparably. This might have been due to the concentration selected for this set of experiments, which will need to be tailored on a case by case basis if repeated dosing is to be achieved without overwhelming the defence mechanisms of the models. As far as we are aware, the influence of repeated dosing with a sensitiser on the GSH levels in skin has not been studied previously. In our experiments, the level of DNP-SG formed increased after each exposure, showing that enhanced danger signalling by Nrf2 led to an increased production of GSH, which was immediately consumed to detoxify DNCB. Similarly, it has been shown that daily exposure to sulforaphane for 4 hours activated the Nrf2 pathway in human skin fibroblasts [246]. The effect on cellular protection was more pronounced after four daily exposures than after a single exposure at the same dose. Our study indirectly showed that after three exposures at non-toxic concentrations, the

level of DNCB available intracellularly to modify proteins, i.e. form potential antigenic species, decreased as the formation of non-antigenic metabolite (DNP-SG) increased. Although the amount of modified proteins required to generate an allergic reaction to a specific chemical is not known, it seems important to attempt to determine the threshold at which regular exposure to low levels of this chemical might not lead to any visible effect in the general population.

Simulating *in silico* the fate of a chemical entering the skin while estimating the amount of modification of proteins in a dynamic model representative of skin for use in risk assessments is now being attempted [239, 240, 267]. We have shown that the behaviour of GSH in cells exposed to a non-toxic dose of chemical could be easily modelled as two successive linear events: 1) clearance of the dose by GSH depletion and 2) GSH repletion (to basal level or above) for a single application. The 'tipping' point between the two events was similar for chemicals that are closely related, such as the dinitrohalobenzenes tested, while the repletion was the differentiating factor. However, for chemicals for which depletion of GSH was barely visible due to the kinetics of reaction being slower (as might be the case for DEM) this tipping point would need to be modelled at a much later (and probably only theoretical) time point. The basal level of GSH in skin appeared to be constant in between exposures to non-toxic level of sensitisers, as was seen after three cycles of treatment with DNCB. GSH was measured between 5-9 µg/mg soluble protein, which might represent the homeostatic level for the RHE model. Whether or not this value would be the same in *in vivo* skin is uncertain but it can be used as an initial estimation in a model of human skin. The aim of this research was not to submit a whole panel of chemicals to our GSH assay to inform a mathematical model but to enunciate the basics by which such information might be integrated into a more complex model, covering the whole process of skin sensitisation. Using such a model might lead to a less conservative prediction of chemical safety

providing insight not only into the type of stable metabolites formed (here GSH conjugates), but also how effectively an organ system may be able to remove them. This would help to refine the extrapolation to *in vivo* exposure scenarios for risk assessments when clinical data is scarce.

The skin models we used were exclusively keratinocyte-based (HaCaT cell line or RHE model) but the level of complexity of *in vitro* models being developed keeps increasing. Models comprising keratinocytes and fibroblasts are now fairly easily produced for commercial purposes [37, 38] and techniques used to maintain viability and presence of major biomarkers in *ex vivo* skin models are improving [268]. Some newly developed models such as the "skin-on-a chip" also include an extra layer of endothelial cells [269]. It is therefore essential to determine the level of similarity with skin *in vivo* required from these models before using biological information obtained from them, such as the efficiency of the GSH pathway. We believe that the simple models that we have chosen enable the generation of larger data sets than would be possible using more sophisticated skin equivalents. The knowledge collected as part of these investigations on the GSH system and metabolism in biologically active *in vitro* models has a wider applicability than type IV hypersensitivity alone as the methodology developed can easily be transferred to different cell types relating to other organs. The mechanistic approach used to investigate chemical clearance by the GSH pathway could also inform on the amplitude of occurrence of other biological phenomena where electrophilic chemistry is involved.

Bibliography.

1. Wickett, R.R. and M.O. Visscher, *Structure and function of the epidermal barrier.* American Journal of Infection Control, 2006. **34**(10, Supplement): p. S98-S110.
2. Madison, K.C., *Barrier function of the skin: "la raison d'etre" of the epidermis.* J. Invest Dermatol, 2003. **121**(2): p. 231-241.
3. Brohem, C.A., et al., *Artificial skin in perspective: concepts and applications.* Pigment Cell Melanoma Res, 2011. **24**(1): p. 35-50.
4. Boulais, N. and L. Misery, *The epidermis: a sensory tissue.* European Journal of Dermatology, 2008. **18**(2): p. 119-127.
5. Villablanca, E.J. and J.R. Mora, *A two-step model for Langerhans cell migration to skin-draining LN.* Eur. J. Immunol, 2008. **38**(11): p. 2975-2980.
6. Williams, A.C., *Transdermal and Topical Drug Delivery from Theory to Clinical Practice*. 2003: Pharmaceutical Press.
7. Johansen, J.D., P.J. Frosch, and J.-P. Lepoittevin, *Contact Dermatitis*. Fifth edition ed. 2011.
8. Peiser, M., et al., *Allergic contact dermatitis: epidemiology, molecular mechanisms, in vitro methods and regulatory aspects. Current knowledge assembled at an international workshop at BfR, Germany.* Cell Mol Life Sci, 2012. **69**(5): p. 763-81.
9. Thyssen, J.P., et al., *The epidemiology of contact allergy in the general population - prevalence and main findings.* Contact Dermatitis, 2007. **57**(5): p. 287-299.
10. Lindberg, M. and M. Matura, *Patch Testing*, in *Contact Dermatitis*. 2011. p. 439-464.
11. NHS. http://www.nhs.uk/Conditions/Eczema-(contact-dermatitis)/Pages/Introduction.aspx.
12. Karlberg, A.T., et al., *Allergic Contact Dermatitis- Formation, Structural Requirements, and Reactivity of Skin Sensitizers.* Chemical Research in Toxicology, 2008. **21**(1): p. 53-69.
13. OECD. *The Adverse Outcome Pathway for Skin Sensitisation Initiated by Covalent Binding to Proteins. Part 1: Scientific Evidence.Series on Testing and Assessment.No.168. ENV/JM/MONO(2012)10/PART1*. 2012 2012.
14. Landsteiner, K. and J. Jacobs, *Studies on the Sensitization of Animals with Simple Chemical Compounds.* Journal of Experimental Medecine, 1935. **61**(5): p. 643-656.
15. Divkovic, M., et al., *Hapten-protein binding: from theory to practical application in the in vitro prediction of skin sensitization.* Contact Dermatitis, 2005. **53**(4): p. 189-200.
16. Lepoittevin, J.P., et al., *Allergic Contact Dermatitis: The Molecular Basis*. 1998.
17. Jenkins, R.E., et al., *Glutathione-S-transferase pi as a model protein for the characterisation of chemically reactive metabolites.* Proteomics, 2008. **8**(2): p. 301-315.
18. Eyanagi, R., et al., *Covalent binding of nitroso-sulfonamides to glutathione S-transferase in guinea pigs with delayed type hypersensitivity.* International Immunopharmacology, 2012. **12**(4): p. 694-700.
19. Gerberick, G.F., et al., *Development of a peptide reactivity assay for screening contact allergens.* Toxicological Sciences, 2004. **81**(2): p. 332-343.
20. Natsch, A. and H. Gfeller, *LC-MS-Based Characterization of the Peptide Reactivity of Chemicals to Improve the In Vitro Prediction of the Skin Sensitization Potential.* Toxicological Sciences, 2008. **106**(2): p. 464-478.

21. Aleksic, M., et al., *Investigating protein haptenation mechanisms of skin sensitisers using human serum albumin as a model protein.* Toxicology in vitro, 2007. **21**(4): p. 723-733.
22. Parkinson, E., et al., *Stable isotope labeling method for the investigation of protein haptenation by electrophilic skin sensitizers.* Toxicol. Sci, 2014. **142**(1): p. 239-249.
23. Aleksic, M., et al., *Mass spectrometric identification of covalent adducts of the skin allergen 2,4-dinitro-1-chlorobenzene and model skin proteins.* Toxicology in vitro, 2008. **22**(5): p. 1169-1176.
24. Aleksic, M., et al., *Reactivity Profiling: Covalent Modification of Single Nucleophile Peptides for Skin Sensitization Risk Assessment.* Toxicological Sciences, 2009. **108**(2): p. 401-411.
25. Bravo, D., et al., *Effect of storage and preservation methods on viability in transplantable human skin allografts.* Burns, 2000. **26**(4): p. 367-378.
26. Castagnoli, C., et al., *Evaluation of donor skin viability: fresh and cryopreserved skin using tetrazolioum salt assay.* Burns, 2003. **29**(8): p. 759-767.
27. Oh, J.W., et al., *Organotypic skin culture.* J. Invest Dermatol, 2013. **133**(11): p. e14.
28. Bonifas, J., et al., *Evaluation of cytochrome P450 1 (CYP1) and n-acetyltransferase 1 (NAT 1) activities in HaCaT cells: Implications for the development of in vitro techniques for predictive testing of contact sensitizers.* Toxicology in vitro, 2010. **24**: p. 973-980.
29. Gross, C.L., et al., *Pretreatment of human epidermal keratinocytes with D,L-sulforaphane protects against sulfur mustard cytotoxicity.* Cutan. Ocul. Toxicol, 2006. **25**(3): p. 155-163.
30. Boukamp, P., et al., *Normal Keratinization in A Spontaneously Immortalized Aneuploid Human Keratinocyte Cell-Line.* Journal of Cell Biology, 1988. **106**(3): p. 761-771.
31. Deyrieux, A.F. and V.G. Wilson, *In vitro culture conditions to study keratinocyte differentiation using the HaCaT cell line.* Cytotechnology, 2007. **54**(2): p. 77-83.
32. Varani, J., et al., *Human skin in organ culture and human skin cells (keratinocytes and fibroblasts) in monolayer culture for assessment of chemically induced skin damage.* Toxicol. Pathol, 2007. **35**(5): p. 693-701.
33. Lei, T.C., et al., *A melanocyte-keratinocyte coculture model to assess regulators of pigmentation in vitro.* Analytical Biochemistry, 2002. **305**(2): p. 260-268.
34. Hennen, J., et al., *Cross talk between keratinocytes and dendritic cells: impact on the prediction of sensitization.* Toxicol. Sci, 2011. **123**(2): p. 501-510.
35. Boelsma, E., et al., *Characterization and comparison of reconstructed skin models: Morphological and immunohistochemical evaluation.* Acta Dermato-Venereologica, 2000. **80**(2): p. 82-88.
36. Netzlaff, F., et al., *The human epidermis models EpiSkin, SkinEthic and EpiDerm: an evaluation of morphology and their suitability for testing phototoxicity, irritancy, corrosivity, and substance transport.* Eur. J. Pharm. Biopharm, 2005. **60**(2): p. 167-178.
37. Episkin. http://www.episkin.com/. 2015 2015.
38. MatTek. http://www.mattek.com/. 2015 2015.
39. model, P.F., http://www.henkel-adhesives.de/de/content_data/247926_Flyer_Phenion_FT_Skin_Models.pdf.
40. Ackermann, K., et al., *The Phenion full-thickness skin model for percutaneous absorption testing.* Skin Pharmacol Physiol, 2010. **23**(2): p. 105-12.
41. Jackh, C., et al., *Characterization of enzyme activities of Cytochrome P450 enzymes, Flavin-dependent monooxygenases, N-acetyltransferases and UDP-*

glucuronyltransferases in human reconstructed epidermis and full-thickness skin models. Toxicol In Vitro, 2011. **25**(6): p. 1209-14.
42. Innovenn, http://www.innovenn.co.uk/. 2016.
43. Liu, H., et al., *Human in vitro skin organ culture as a model system for evaluating DNA repair.* J. Dermatol. Sci, 2014. **74**(3): p. 236-241.
44. Mitbauerova, A., et al., *A human skin culture system for a wound-healing model.* Comput. Methods Biomech. Biomed. Engin, 2012. **15 Suppl 1**: p. 102-103.
45. Yasuoka, H., et al., *Human skin culture as an ex vivo model for assessing the fibrotic effects of insulin-like growth factor binding proteins.* Open Rheumatol J, 2008. **2**: p. 17-22.
46. Genoskin. http://www.genoskin.com/. 2015 2015.
47. Svensson, C.K., *Biotransformation of Drugs in Human Skin.* Drug Metabolism and Disposition, 2009. **37**(2): p. 247-253.
48. Gotz, C., et al., *Xenobiotic metabolism capacities of human skin in comparison with a 3D epidermis model and keratinocyte-based cell culture as in vitro alternatives for chemical testing: activating enzymes (Phase I).* Exp. Dermatol, 2012. **21**(5): p. 358-363.
49. Eilstein, J., et al., *Comparison of xenobiotic metabolizing enzyme activities in ex vivo human skin and reconstructed human skin models from SkinEthic.* Arch. Toxicol, 2014. **88**(9): p. 1681-1694.
50. Jackh, C., et al., *Relevance of xenobiotic enzymes in human skin in vitro models to activate pro-sensitizers.* J. Immunotoxicol, 2012. **9**(4): p. 426-438.
51. Oesch, F., et al., *Xenobiotic-metabolizing enzymes in the skin of rat, mouse, pig, guinea pig, man, and in human skin models.* Arch. Toxicol, 2014. **88**(12): p. 2135-2190.
52. Lee, M.S. and M. Zhu, *Mass Spectrometry in Drug Metabolism and Disposition: Basic Principles and Applications*. 5 ed. 2011: John Wiley & Sons.
53. Gotz, C., et al., *Xenobiotic metabolism capacities of human skin in comparison with a 3D-epidermis model and keratinocyte-based cell culture as in vitro alternatives for chemical testing: phase II enzymes.* Exp. Dermatol, 2012. **21**(5): p. 364-369.
54. Manevski, N., et al., *Phase II metabolism in human skin: skin explants show full coverage for glucuronidation, sulfation, N-acetylation, catechol methylation, and glutathione conjugation.* Drug Metab Dispos, 2015. **43**(1): p. 126-139.
55. Goebel, C., et al., *Skin metabolism of aminophenols: human keratinocytes as a suitable in vitro model to qualitatively predict the dermal transformation of 4-amino-2-hydroxytoluene in vivo.* Toxicol. Appl. Pharmacol, 2009. **235**(1): p. 114-123.
56. Xu, C., C.Y. Li, and A.N. Kong, *Induction of phase I, II and III drug metabolism/transport by xenobiotics.* Arch. Pharm. Res, 2005. **28**(3): p. 249-268.
57. Joyet-Lavergne, P., *Glutathion et chondriome.* Protoplasma, 1929. **6**(1): p. 84-112.
58. Forman, H.J., H.Q. Zhang, and A. Rinna, *Glutathione: Overview of its protective roles, measurement, and biosynthesis.* Molecular Aspects of Medicine, 2009. **30**(1-2): p. 1-12.
59. Griffith, O.W. and A. Meister, *5-Oxo-L-prolinase (L-pyroglutamate hydrolase). Studies of the chemical mechanism.* J. Biol. Chem, 1981. **256**(19): p. 9981-9985.
60. Meister, A., *Selective modification of glutathione metabolism.* Journal of Biological Chemistry, 1988. **263**(33): p. 17205-17208.
61. Meister, A., *New developments in glutathione metabolism and their potential application in therapy.* Hepatology, 1984. **4**(4): p. 739-742.
62. Haddad, J.J. and H.L. Harb, *L-gamma-Glutamyl-L-cysteinyl-glycine (glutathione; GSH) and GSH-related enzymes in the regulation of pro- and anti-inflammatory*

cytokines: a signaling transcriptional scenario for redox(y) immunologic sensor(s)? Mol. Immunol, 2005. **42**(9): p. 987-1014.

63. Wu, G., et al., *Glutathione metabolism and its implications for health.* J. Nutr, 2004. **134**(3): p. 489-492.
64. Ellinger, J.J., I.A. Lewis, and J.L. Markley, *Role of aminotransferases in glutamate metabolism of human erythrocytes.* Journal of Biomolecular Nmr, 2011. **49**(3-4): p. 221-229.
65. Smith, T.K., *Dietary modulation of the glutathione detoxification pathway and the potential for altered xenobiotic metabolism.* Adv. Exp. Med. Biol, 1991. **289**: p. 165-169.
66. Griffith, O.W., *Biologic and pharmacologic regulation of mammalian glutathione synthesis.* Free Radical Biology and Medicine, 1999. **27**(9-10): p. 922-935.
67. Curello, S., et al., *Improved procedure for determining glutathione in plasma as an index of myocardial oxidative stress.* Clin. Chem, 1987. **33**(8): p. 1448-1449.
68. Aptula, A.O., et al., *Non-enzymatic glutathione reactivity and in vitro toxicity: A non-animal approach to skin sensitization.* Toxicology in vitro, 2006. **20**: p. 239-247.
69. Pompella, A., et al., *The changing faces of glutathione, a cellular protagonist.* Biochem. Pharmacol, 2003. **66**(8): p. 1499-1503.
70. van Bladeren, P.J., *Formation of toxic metabolites from drugs and other xenobiotics by glutathione conjugation.* Trends in Pharmacological Sciences, 1988. **9**(8): p. 295-299.
71. Dekant, W., *Biosynthesis of toxic glutathione conjugates from halogenated alkenes.* Toxicology Letters, 2003. **144**(1): p. 49-54.
72. Alvarez-Sanchez, R., et al., *Effect of glutathione on the covalent binding of the 13C-labeled skin sensitizer 5-chloro-2-methylisothiazol-3-one to human serum albumin: identification of adducts by nuclear magnetic resonance, matrix-assisted laser desorption/ionization mass spectrometry, and nanoelectrospray tandem mass spectrometry.* Chem. Res. Toxicol, 2004. **17**(9): p. 1280-1288.
73. Awasthi, Y.C. and S. Dhanani, *Glutathione S transferase isozyme composition of human tissues*, in *Toxicology of glutathione transferases*. 2007, CRC Press. p. 321-338.
74. *PDB file*. 2015 2015; Available from: http://www.rcsb.org/pdb/explore/jmol.do?structureId=1PKW&bionumber=1.
75. Armstrong, R.N., *Structure, catalytic mechanism, and evolution of the glutathione transferases.* Chem. Res. Toxicol, 1997. **10**(1): p. 2-18.
76. Prade, L., et al., *Structures of class pi glutathione S-transferase from human placenta in complex with substrate, transition-state analogue and inhibitor.* Structure, 1997. **5**(10): p. 1287-1295.
77. Singhal, S., et al., *Glutathione S-transferases of human skin: qualitative and quantitative differences in men and women.* Biochimica et Biophysica Acta, 1993. **1163**: p. 266-272.
78. Moral, A., et al., *Immunohistochemical study of alpha, mu and pi class glutathione S transferase expression in malignant melanoma. MMM Group. Multidisciplinary Malignant Melanoma Group.* Br. J. Dermatol, 1997. **136**(3): p. 345-350.
79. Zhang, Y., V. Gonzalez, and M. Jian Xu, *Expression and regulation of glutathione S-transferase P1-1 in cultured human epidermal cells.* Journal of Dermatological Science, 2002. **30**: p. 205-214.
80. Sharma, R., et al., *Transport of glutathione-conjugates in human erythrocytes.* Acta Biochim. Pol, 2000. **47**(3): p. 751-762.
81. Keppler, D., *Export pumps for glutathione S-conjugates.* Free Radic. Biol. Med, 1999. **27**(9-10): p. 985-991.

82. Belinsky, M.G., et al., *Characterization of the drug resistance and transport properties of multidrug resistance protein 6 (MRP6, ABCC6).* Cancer Res, 2002. **62**(21): p. 6172-6177.
83. Ellison, I. and J.P. Richie, Jr., *Mechanisms of glutathione disulfide efflux from erythrocytes.* Biochem. Pharmacol, 2012. **83**(1): p. 164-169.
84. Osman-Ponchet, H., et al., *Characterization of ABC transporters in human skin.* Drug Metabol. Drug Interact, 2014. **29**(2): p. 91-100.
85. Fuchs, J., et al., *Redox-modulated pathways in inflammatory skin diseases.* Free Radic. Biol. Med, 2001. **30**(4): p. 337-353.
86. Schafer, F.Q. and G.R. Buettner, *Redox environment of the cell as viewed through the redox state of the glutathione disulfide/glutathione couple.* Free Radical Biology and Medicine, 2001. **30**(11): p. 1191-1212.
87. Brigelius-Flohe, R., *Tissue-specific functions of individual glutathione peroxidases.* Free Radical Biology and Medicine, 1999. **27**(9-10): p. 951-965.
88. Maher, P., *The effects of stress and aging on glutathione metabolism.* Ageing Res. Rev, 2005. **4**(2): p. 288-314.
89. Klaus, V., et al., *1,4-Naphthoquinones as inducers of oxidative damage and stress signaling in HaCaT human keratinocytes.* Arch. Biochem. Biophys, 2010. **496**(2): p. 93-100.
90. Nzengue, Y., et al., *Oxidative stress and DNA damage induced by cadmium in the human keratinocyte HaCaT cell line: role of glutathione in the resistance to cadmium.* Toxicology, 2008. **243**(1-2): p. 193-206.
91. Steghens, J.P., et al., *Fast liquid chromatography-mass spectrometry glutathione measurement in whole blood: micromolar GSSG is a sample preparation artifact.* J. Chromatogr. B Analyt. Technol. Biomed. Life Sci, 2003. **798**(2): p. 343-349.
92. Camera, E. and M. Picardo, *Analytical methods to investigate glutathione and related compounds in biological and pathological processes.* J. Chromatogr. B Analyt. Technol. Biomed. Life Sci, 2002. **781**(1-2): p. 181-206.
93. Iwasaki, Y., et al., *Chromatographic and mass spectrometric analysis of glutathione in biological samples.* J. Chromatogr. B Analyt. Technol. Biomed. Life Sci, 2009. **877**(28): p. 3309-3317.
94. Monostori, P., et al., *Determination of glutathione and glutathione disulfide in biological samples: an in-depth review.* J. Chromatogr. B Analyt. Technol. Biomed. Life Sci, 2009. **877**(28): p. 3331-3346.
95. Pastore, A., et al., *Analysis of glutathione: implication in redox and detoxification.* Clin. Chim. Acta, 2003. **333**(1): p. 19-39.
96. Brigelius, R., et al., *Identification and quantitation of glutathione in hepatic protein mixed disulfides and its relationship to glutathione disulfide.* Biochem. Pharmacol, 1983. **32**(17): p. 2529-2534.
97. Anderson, M.E., *Determination of glutathione and glutathione disulfide in biological samples.* Methods Enzymol, 1985. **113**: p. 548-555.
98. Hissin, P.J. and R. Hilf, *A fluorometric method for determination of oxidized and reduced glutathione in tissues.* Anal. Biochem, 1976. **74**(1): p. 214-226.
99. Rousar, T., et al., *Assessment of reduced glutathione: Comparison of an optimized fluorometric assay with enzymatic recycling method.* Analytical Biochemistry, 2012. **423**(2): p. 236-240.
100. Zeng, X.D., et al., *A colorimetric and ratiometric fluorescent probe for quantitative detection of GSH at physiologically relevant levels.* Sensors and Actuators B-Chemical, 2011. **159**(1): p. 142-147.

101. Yoshida, T., *Determination of reduced and oxidized glutathione in erythrocytes by high-performance liquid chromatography with ultraviolet absorbance detection.* J. Chromatogr. B Biomed. Appl, 1996. **678**(2): p. 157-164.
102. McDermott, G.P., et al., *Determination of intracellular glutathione and glutathione disulfide using high performance liquid chromatography with acidic potassium permanganate chemiluminescence detection.* Analyst, 2011. **136**(12): p. 2578-2585.
103. Camera, E., et al., *Simultaneous determination of reduced and oxidized glutathione in peripheral blood mononuclear cells by liquid chromatography-electrospray mass spectrometry.* J. Chromatogr. B Biomed. Sci. Appl, 2001. **757**(1): p. 69-78.
104. Harwood, D.T., et al., *Simultaneous determination of reduced glutathione, glutathione disulphide and glutathione sulphonamide in cells and physiological fluids by isotope dilution liquid chromatography-tandem mass spectrometry.* Journal of Chromatography B-Analytical Technologies in the Biomedical and Life Sciences, 2009. **877**(28): p. 3393-3399.
105. Guan, X., et al., *A simultaneous liquid chromatography/mass spectrometric assay of glutathione, cysteine, homocysteine and their disulfides in biological samples.* J. Pharm. Biomed. Anal, 2003. **31**(2): p. 251-261.
106. Reed, D.J., et al., *High-Performance Liquid Chromatography Analysis of Nanomole Levels of Glutathione, Glutathione Disulfide and Related Thiols and Disulfides.* Analytical Biochemistry, 1980. **106**: p. 55-62.
107. New, L.-S. and E.C.Y. Chan, *Evaluation of BEH C_{18}, BEH HILIC and HSS T3 (C_{18}) column chemistries for the UPLC-MS-MS analysis of glutathione,glutathione disulfide and ophtalmic acid in mouse liver and human plasma.* Journal of Chromatographic Science, 2008. **46**: p. 209-213.
108. Booth, G., *Nitro Compounds, Aromatic*, in *Ullmann's Encyclopedia of Industrial Chemistry*. 2000, Wiley-VCH Verlag GmbH & Co. KGaA. p. 301-349.
109. *Pubchem*. 2015 2015; Available from: http://pubchem.ncbi.nlm.nih.gov/.
110. Friedmann, P.S., *The relationships between exposure dose and response in induction and elicitation of contact hypersensitivity in humans.* Br. J. Dermatol, 2007. **157**(6): p. 1093-1102.
111. Friedmann, P.S., et al., *Quantitative relationships between sensitizing dose of DNCB and reactivity in normal subjects.* Clin. Exp. Immunol, 1983. **53**(3): p. 709-715.
112. Buckley, D.A. and A.W. Du Vivier, *The therapeutic use of topical contact sensitizers in benign dermatoses.* Br. J. Dermatol, 2001. **145**(3): p. 385-405.
113. Habig, W.H., M.J. Pabst, and W.B. Jakoby, *Glutathione S-transferases. The first enzymatic step in mercapturic acid formation.* J. Biol. Chem, 1974. **249**(22): p. 7130-7139.
114. SANGER, F. and H. TUPPY, *The amino-acid sequence in the phenylalanyl chain of insulin. I. The identification of lower peptides from partial hydrolysates.* Biochem. J, 1951. **49**(4): p. 463-481.
115. Enoch, S.J., T.W. Schultz, and M.T. Cronin, *The definition of the applicability domain relevant to skin sensitization for the aromatic nucleophilic substitution mechanism.* SAR QSAR. Environ. Res, 2012. **23**(7-8): p. 649-663.
116. Breslow, R., R. Haynie, and J. Mirra, *The Synthesis Of Diphenylcyclopropenone.* Journal of the American Chemical Society, 1959. **81**(1): p. 247-248.
117. Kursanov, D.N., M.E. Vol'pin, and Y.D. Koreshkov, Journal of General Chemistry USSR, 1960. **30**: p. 2855-2860.
118. Sotiriadis, D., et al., *Topical immunotherapy with diphenylcyclopropenone in the treatment of chronic extensive alopecia areata.* Clin. Exp. Dermatol, 2007. **32**(1): p. 48-51.

119. Wilkerson, M.G., J. Henkin, and J.K. Wilkin, *Diphenylcyclopropenone: examination for potential contaminants, mechanisms of sensitization, and photochemical stability.* J. Am. Acad. Dermatol, 1984. **11**(5 Pt 1): p. 802-807.
120. Passaglia, E., et al., *Grafting of diethyl maleate and maleic anhydride onto styrene-b-(ethylene-co-1-butene)-b-styrene triblock copolymer (SEBS).* Polymer, 2000. **41**(12): p. 4389-4400.
121. Lammintausta, K., et al., *Sensitization to dimethyl fumarate with multiple concurrent patch test reactions.* Contact Dermatitis, 2010. **62**(2): p. 88-96.
122. Weber, C.A., et al., *Depletion of tissue glutathione with diethyl maleate enhances hyperbaric oxygen toxicity.* Am. J. Physiol, 1990. **258**(6 Pt 1): p. L308-L312.
123. Deneke, S.M. and B.L. Fanburg, *Regulation of cellular glutathione.* Am. J. Physiol, 1989. **257**(4 Pt 1): p. L163-L173.
124. Gerberick, G.F., et al., *Compilation of historical local lymph node data for evaluation of skin sensitization alternative methods.* Dermatitis, 2005. **16**(4): p. 157-202.
125. Wohrl, S., et al., *The significance of fragrance mix, balsam of Peru, colophony and propolis as screening tools in the detection of fragrance allergy.* Br. J. Dermatol, 2001. **145**(2): p. 268-273.
126. Andersen, A., *Final report on the safety assessment of benzaldehyde.* Int. J. Toxicol, 2006. **25 Suppl 1**: p. 11-27.
127. Vince, R., S. Daluge, and W.B. Wadd, *Studies on the inhibition of glyoxalase I by S-substituted glutathiones.* J Med Chem, 1971. **14**(5): p. 402-4.
128. Mosmann, T., *Rapid colorimetric assay for cellular growth and survival: application to proliferation and cytotoxicity assays.* J. Immunol. Methods, 1983. **65**(1-2): p. 55-63.
129. Zhao, Y., et al., *Increase in thiol oxidative stress via glutathione reductase inhibition as a novel approach to enhance cancer sensitivity to X-ray irradiation.* Free Radic. Biol. Med, 2009. **47**(2): p. 176-183.
130. Tajc, S.G., et al., *Direct determination of thiol pKa by isothermal titration microcalorimetry.* J. Am. Chem. Soc, 2004. **126**(34): p. 10508-10509.
131. Tang, S.S. and G.G. Chang, *Kinetic characterization of the endogenous glutathione transferase activity of octopus lens S-crystallin.* J. Biochem, 1996. **119**(6): p. 1182-1188.
132. Santori, G., et al., *Different efficacy of iodoacetic acid and N-ethylmaleimide in high-performance liquid chromatographic measurement of liver glutathione.* J Chromatogr B Biomed Sci Appl, 1997. **695**(2): p. 427-33.
133. Smith, P.K., et al., *Measurement of protein using bicinchoninic acid.* Anal. Biochem, 1985. **150**(1): p. 76-85.
134. Shindo, Y., et al., *Enzymic and non-enzymic antioxidants in epidermis and dermis of human skin.* Journal of Investigative Dermatology, 1994. **102**: p. 122-124.
135. Rhie, G., et al., *Aging and Photoaging-Dependent Changes of Enzymic and Nonenzymic Antioxidants in the Epidermis and Dermis of Human Skin in vivo.* Journal of Investigative Dermatology, 2001. **117**: p. 1212-1217.
136. Kaur, S., et al., *Patients with allergic and irritant contact dermatitis are characterized by striking change of iron and oxidized glutathione status in nonlesional area of the skin.* J. Invest Dermatol, 2001. **116**(6): p. 886-890.
137. Masaki, H., et al., *alpha-tocopherol increases the intracellular glutathione level in HaCaT keratinocytes.* Free Radic. Res, 2002. **36**(6): p. 705-709.
138. Zheng, J., et al., *Fucoxanthin enhances the level of reduced glutathione via the Nrf2-mediated pathway in human keratinocytes.* Mar. Drugs, 2014. **12**(7): p. 4214-4230.

139. Schuliga, M., S. Chouchane, and E.T. Snow, *Upregulation of glutathione-related genes and enzyme activities in cultured human cells by sublethal concentrations of inorganic arsenic.* Toxicol. Sci, 2002. **70**(2): p. 183-192.
140. Campbell, E.B., M.L. Hayward, and O.W. Griffith, *Analytical and preparative separation of the diastereomers of L-buthionine (SR)-sulfoximine, a potent inhibitor of glutathione biosynthesis.* Anal Biochem, 1991. **194**(2): p. 268-77.
141. Griffith, O.W., *Mechanism of action, metabolism, and toxicity of Buthionine Sulfoximine and its higher homologs, potent inhibitors of glutathione synthesis.* Journal of Biological Chemistry, 1982. **257**(22): p. 13704-13712.
142. Biterova, E.I. and J.J. Barycki, *Structural basis for feedback and pharmacological inhibition of Saccharomyces cerevisiae glutamate cysteine ligase.* J Biol Chem, 2010. **285**(19): p. 14459-66.
143. Frischer, H., et al., *Glutathione, cell proliferation, and 1,3-bis-(2-chloroethyl)-1-nitrosourea in K562 leukemia.* J. Clin. Invest, 1993. **92**(6): p. 2761-2767.
144. Rice, K.P., et al., *Differential inhibition of cellular glutathione reductase activity by isocyanates generated from the antitumor prodrugs Cloretazine and BCNU.* Biochem. Pharmacol, 2005. **69**(10): p. 1463-1472.
145. Lin, S.H. and L.R. Kleinberg, *Carmustine wafers: localized delivery of chemotherapeutic agents in CNS malignancies.* Expert Rev Anticancer Ther, 2008. **8**(3): p. 343-59.
146. Shinohara, K. and K.R. Tanaka, *Mechanism of inhibition of red blood cell glutathione reductase activity by BCNU (1,3-bis(2-chloroethyl)-1-nitrosourea).* Clin Chim Acta, 1979. **92**(2): p. 147-52.
147. Kehrer, J.P., *The effect of BCNU (carmustine) on tissue glutathione reductase activity.* Toxicol Lett, 1983. **17**(1-2): p. 63-8.
148. Cohen, M.B. and D.L. Duvel, *Characterization of the inhibition of glutathione reductase and the recovery of enzyme activity in exponentially growing murine leukemia (L1210) cells treated with 1,3-bis(2-chloroethyl)-1-nitrosourea.* Biochem Pharmacol, 1988. **37**(17): p. 3317-20.
149. Seefeldt, T., et al., *Characterization of a novel dithiocarbamate glutathione reductase inhibitor and its use as a tool to modulate intracellular glutathione.* J. Biol. Chem, 2009. **284**(5): p. 2729-2737.
150. Zhao, Y., et al., *Effects of glutathione reductase inhibition on cellular thiol redox state and related systems.* Arch. Biochem. Biophys, 2009. **485**(1): p. 56-62.
151. Basketter, D.A., et al., *Human potency predictions for aldehydes using the local lymph node assay.* Contact Dermatitis, 2001. **45**(2): p. 89-94.
152. Fregert, S., *Sensitization to phenylacetaldehyde.* Dermatologica, 1970. **141**(1): p. 11-14.
153. Sanchez-Politta, S., et al., *Allergic contact dermatitis to phenylacetaldehyde: a forgotten allergen?* Contact Dermatitis, 2007. **56**(3): p. 171-172.
154. Parkinson, E., et al., *Proteomic analysis of the human skin proteome after in vivo treatment with sodium dodecyl sulphate.* PLoS One, 2014. **9**(5): p. e97772.
155. Chia, A., et al., *Differential effect of covalent protein modification and glutathione depletion on the transcriptional response of Nrf2 and NF-κB.* Biochemical Pharmacology, 2010. **80**: p. 410-421.
156. van Klaveren, R.J., M. Demedts, and B. Nemery, *Cellular glutathione turnover in vitro, with emphasis on type II pneumocytes.* Eur. Respir. J, 1997. **10**(6): p. 1392-1400.
157. Sastre, J., F.V. Pallardo, and J. Vina, *Glutathione*, in *The Handbook of Environmental Chemistry*. 2005, Springer-Verlag. p. 91-108.

158. Finley, J.W., E.L. Wheeler, and S.C. Witt, *Oxidation of glutathione by hydrogen peroxide and other oxidizing agents.* Journal of Agricultural and Food Chemistry, 1981. **29**(2): p. 404-407.
159. Wang, X.Y., et al., *Quercetin in combating H2O2 induced early cell apoptosis and mitochondrial damage to normal human keratinocytes.* Chin Med. J. (Engl.), 2010. **123**(5): p. 532-536.
160. Nguyen, C.N., H.E. Kim, and S.G. Lee, *Caffeoylserotonin protects human keratinocyte HaCaT cells against H2 O2 -induced oxidative stress and apoptosis through upregulation of HO-1 expression via activation of the PI3K/Akt/Nrf2 pathway.* Phytother. Res, 2013. **27**(12): p. 1810-1818.
161. Reed, M.C., et al., *A mathematical model of glutathione metabolism.* Theor Biol Med Model, 2008. **5**: p. 8.
162. Ookhtens, M., et al., *Sinusoidal efflux of glutathione in the perfused rat liver. Evidence for a carrier-mediated process.* J Clin Invest, 1985. **75**(1): p. 258-65.
163. Lauterburg, B.H., J.D. Adams, and J.R. Mitchell, *Hepatic glutathione homeostasis in the rat: efflux accounts for glutathione turnover.* Hepatology, 1984. **4**(4): p. 586-90.
164. Espinosa-Diez, C., et al., *Antioxidant responses and cellular adjustments to oxidative stress.* Redox Biol, 2015. **6**: p. 183-97.
165. van Eijl, S., et al., *Elucidation of xenobiotic metabolism pathways in human skin and human skin models by proteomic profiling.* PLoS. One, 2012. **7**(7): p. e41721.
166. Rasmussen, C., et al., *Expression and induction of xenobiotic metabolism genes in the Strata Test human skin model. SOT 2011.* Toxicologist, 2011. **120**(Suppl 2): p. 139.
167. Schultz, T.W., et al., *Structure-activity relationships for abiotic thiol reactivity and aquatic toxicity of halo-substituted carbonyl compounds.* SAR QSAR Environ Res, 2007. **18**(1-2): p. 21-9.
168. van der Aar, E.M., et al., *Enzyme kinetics and substrate selectivities of rat glutathione S-transferase isoenzymes towards a series of new 2-substituted 1-chloro-4-nitrobenzenes.* Xenobiotica, 1996. **26**(2): p. 143-55.
169. Van der Aar, E.M., et al., *Structure-activity relationships for chemical and glutathione S-transferase-catalysed glutathione conjugation reactions of a series of 2-substituted 1-chloro-4-nitrobenzenes.* Biochem J, 1996. **320 (Pt 2)**: p. 531-40.
170. Jewell, C., et al., *Percutaneous absorption and metabolism of dinitrochlorobenzene in vitro.* Arch Toxicol, 2000. **74**(7): p. 356-65.
171. Milner, J.E., *In vitro lymphocyte responses in contact hypersensitivity IV.* J. Invest Dermatol, 1974. **62**(6): p. 591-594.
172. Garcia-Perez, A., *Occupational dermatitis from DNFB with cross sensitivity to DNCB.* Contact Dermatitis, 1978. **4**(3): p. 125-127.
173. Ridley, C.M., *Accidental Sensitization to 1-bromo-2,4-dinitrobenzene.* Proceedings of the Royal Society of Medecine, 1975. **68**: p. 27-28.
174. Kensler, T.W., N. Wakabayashi, and S. Biswal, *Cell survival responses to environmental stresses via the Keap1-Nrf2-ARE pathway.* Annu Rev Pharmacol Toxicol, 2007. **47**: p. 89-116.
175. Buckner, D. and N.M. Price, *Immunotherapy of verrucae vulgares with dinitrochlorobenzene.* Br J Dermatol, 1978. **98**(4): p. 451-5.
176. Basketter, D., et al., *Dinitrohalobenzenes:evaluation of relative skin sensitization potential using the local lymph node assay.* Contact Dermatitis, 1997. **36**: p. 97-100.
177. Ade, N., et al., *Activation of U937 cells by contact sensitizers: CD86 expression is independent of apoptosis.* J Immunotoxicol, 2006. **3**(4): p. 189-97.

178. Ashikaga, T., et al., *Development of an in vitro skin sensitization test using human cell lines: the human Cell Line Activation Test (h-CLAT). I. Optimization of the h-CLAT protocol.* Toxicol In Vitro, 2006. **20**(5): p. 767-73.
179. Natsch, N., et al., *The intra- and inter-laboratory reproducibility and predictivity of the KeratinoSens assay to predict skin sensitizers in vitro: Results of a ring-study in five laboratories.* Toxicology in Vitro, 2011. **25**(3): p. 733-744.
180. Bryan, H.K., et al., *The Nrf2 cell defence pathway: Keap1-dependent and -independent mechanisms of regulation.* Biochem. Pharmacol, 2013. **85**(6): p. 705-717.
181. Vandebriel, R.J., et al., *Keratinocyte gene expression profiles discriminate sensitizing and irritating compounds.* Toxicol Sci, 2010. **117**(1): p. 81-9.
182. Natsch, A. and R. Emter, *Skin sensitizers induce antioxidant response element dependent genes: Application to the in vitro testing of the sensitization potential of chemicals.* Toxicological Sciences, 2008. **102**(1): p. 110-119.
183. Emter, R., et al., *Gene expression changes induced by skin sensitizers in the KeratinoSens cell line: Discriminating Nrf2-dependent and Nrf2-independent events.* Toxicol In Vitro, 2013. **27**(8): p. 2225-32.
184. OECD, *OECD Guideline For TheTesting Of Chemicals, Draft Proposal For A New Test Guideline, In Vitro Skin Sensitisation: ARE-Nrf2 Luciferase Test Method*
185. Natarajan, V.T., et al., *Transcriptional upregulation of Nrf2-dependent phase II detoxification genes in the involved epidermis of vitiligo vulgaris.* J Invest Dermatol, 2010. **130**(12): p. 2781-9.
186. Geenen, S., et al., *A mathematical modelling approach to assessing the reliability of biomarkers of glutathione metabolism.* Eur J Pharm Sci, 2012. **46**(4): p. 233-43.
187. Soga, T., et al., *Differential metabolomics reveals ophthalmic acid as an oxidative stress biomarker indicating hepatic glutathione consumption.* J Biol Chem, 2006. **281**(24): p. 16768-76.
188. Patlewicz, G., et al., *TIMES-SS--a promising tool for the assessment of skin sensitization hazard. A characterization with respect to the OECD validation principles for (Q)SARs and an external evaluation for predictivity.* Regul Toxicol Pharmacol, 2007. **48**(2): p. 225-39.
189. Patlewicz, G., et al., *TIMES-SS--recent refinements resulting from an industrial skin sensitisation consortium.* SAR QSAR Environ Res, 2014. **25**(5): p. 367-91.
190. Greene, N., et al., *Knowledge-based expert systems for toxicity and metabolism prediction: DEREK, StAR and METEOR.* SAR QSAR Environ Res, 1999. **10**(2-3): p. 299-314.
191. Langton, K., et al., *Structure-activity relationships for skin sensitization: recent improvements to Derek for Windows.* Contact Dermatitis, 2006. **55**(6): p. 342-7.
192. Akaike, H., *A new look at the statistical model identification.* IEEE Transactions on Automatic Control, 1974. **19**(6): p. 716-723.
193. Copple, I.M., et al., *The hepatotoxic metabolite of acetaminophen directly activates the Keap1-Nrf2 cell defense system.* Hepatology, 2008. **48**(4): p. 1292-1301.
194. *SCOEL/SUM/56 final, Recommendation from Scientific Committee on Occupational Exposure Limits for Fluorine, Hydrogen Fluoride and Inorganic Fluorides (not uranium hexafluoride)*. 1998 1998.
195. https://www.gov.uk/government/uploads/system/uploads/attachment_data/file/316642/Bromine_guidance.pdf. 2015 2015.
196. White, C.W. and J.G. Martin, *Chlorine gas inhalation: human clinical evidence of toxicity and experience in animal models.* Proc. Am. Thorac. Soc, 2010. **7**(4): p. 257-263.

197. Fotakis, G. and J.A. Timbrell, *In vitro cytotoxicity assays: comparison of LDH, neutral red, MTT and protein assay in hepatoma cell lines following exposure to cadmium chloride.* Toxicology Letters, 2005. **160**: p. 171-177.
198. Natsch, A., T. Haupt, and H. Laue, *Relating skin sensitizing potency to chemical reactivity: reactive Michael acceptors inhibit NF-kappaB signaling and are less sensitizing than S(N)Ar- and S(N)2- reactive chemicals.* Chem. Res. Toxicol, 2011. **24**(11): p. 2018-2027.
199. Megherbi, R., et al., *Role of protein haptenation in triggering maturation events in the dendritic cell surrogate cell line THP-1.* Toxicol. Appl. Pharmacol, 2009. **238**(2): p. 120-132.
200. SCCNFP, *An Initial List of Perfumery Materials Which Must Not Form Part of Fragrances Compounds Used in Cosmetic Products.* ec.europa.eu/health/ph_risk/committees/sccp/documents/out116_en.pdf, 2000.
201. Hansson, C. and K. Thorneby-Andersson, *Stereochemical considerations on concomitant allergic contact dermatitis to ester of the cis-trans isomeric compounds maleic acid and fumaric acid.* Skin Pharmacol Appl Skin Physiol, 2003. **16**(2): p. 117-22.
202. Natsch, A., et al., *A dataset on 145 chemicals tested in alternative assays for skin sensitization undergoing prevalidation.* J Appl Toxicol, 2013. **33**(11): p. 1337-52.
203. Gulati, N., et al., *Molecular characterization of human skin response to diphencyprone at peak and resolution phases: therapeutic insights.* The Journal of investigative dermatology, 2014. **134**(10): p. 2531-2540.
204. Basu, S. and A. Adisesh, *Management of occupational hazards in healthcare: exposure to diphencyprone.* BMJ Case Rep, 2013. **2013**.
205. Coleman, K.M., L. ; Grailer, T. ; Willoughby, Sr, J. ; Keller, D. ; Patel, P. ; Thomas, S. ; Dilworth, C.; , *Evaluation of an In Vitro Human Dermal Sensitization Test for Use with Medical Device Extracts.* Applied in Vitro Toxicology, 2015. **1**(2): p. 118-130.
206. Kubal, G., et al., *Investigations of glutathione conjugation in vitro by 1H NMR spectroscopy. Uncatalyzed and glutathione transferase-catalyzed reactions.* Chem Res Toxicol, 1995. **8**(5): p. 780-91.
207. Eicher, T. and J.L. Weber, *Structure and reactivity of cyclopropenones and triafulvenes.* Top Curr Chem, 1975. **57**: p. 1-109.
208. Galinsky, R.E., *Role of glutathione turnover in drug sulfation: differential effects of diethylmaleate and buthionine sulfoximine on the pharmacokinetics of acetaminophen in the rat.* J Pharmacol Exp Ther, 1986. **236**(1): p. 133-9.
209. Mitchell, J.B., et al., *Cellular glutathione depletion by diethyl maleate or buthionine sulfoximine: no effect of glutathione depletion on the oxygen enhancement ratio.* Radiat Res, 1983. **96**(2): p. 422-8.
210. West, J.D., C.E. Stamm, and P.J. Kingsley, *Structure-activity comparison of the cytotoxic properties of diethyl maleate and related molecules: identification of diethyl acetylenedicarboxylate as a thiol cross-linking agent.* Chem Res Toxicol, 2011. **24**(1): p. 81-8.
211. Chipinda, I., et al., *Rapid and simple kinetics screening assay for electrophilic dermal sensitizers using nitrobenzenethiol.* Chem Res Toxicol, 2010. **23**(5): p. 918-25.
212. van der Veen, J.W., et al., *Human relevance of an in vitro gene signature in HaCaT for skin sensitization.* Toxicol In Vitro, 2015. **29**(1): p. 81-4.
213. Hirota, M., et al., *Changes of cell-surface thiols and intracellular signaling in human monocytic cell line THP-1 treated with diphenylcyclopropenone.* The Journal of Toxicological Sciences, 2010. **35**(6): p. 871-879.

214. Naven, R.T., et al., *High throughput glutathione and Nrf2 assays to assess chemical and biological reactivity of cysteine-reactive compounds.* Toxicology Research, 2013. **2**(4): p. 235-244.
215. Regnier, M., et al., *Keratinocyte-melanocyte co-cultures and pigmented reconstructed human epidermis: models to study modulation of melanogenesis.* Cell Mol. Biol. (Noisy. -le-grand), 1999. **45**(7): p. 969-980.
216. Thakoersing, V.S., et al., *Nature versus nurture: does human skin maintain its stratum corneum lipid properties in vitro?* Exp. Dermatol, 2012. **21**(11): p. 865-870.
217. Lombardi, B.S., et al., *In vitro skin absorption and drug release - a comparison of six commercial prednicarbate preparations for topical use.* Eur. J. Pharm. Biopharm, 2008. **68**(2): p. 380-389.
218. Rozman, B., et al., *Simultaneous absorption of vitamins C and E from topical microemulsions using reconstructed human epidermis as a skin model.* Eur. J. Pharm. Biopharm, 2009. **72**(1): p. 69-75.
219. Garcia, N., et al., *Characterization of the barrier function in a reconstituted human epidermis cultivated in chemically defined medium.* Int J Cosmet Sci, 2002. **24**(1): p. 25-34.
220. Schafer-Korting, M., et al., *The use of reconstructed human epidermis for skin absorption testing: Results of the validation study.* Altern Lab Anim, 2008. **36**(2): p. 161-87.
221. El Ghalbzouri, A., et al., *Leiden reconstructed human epidermal model as a tool for the evaluation of the skin corrosion and irritation potential according to the ECVAM guidelines.* Toxicol. In Vitro, 2008. **22**(5): p. 1311-1320.
222. Kandarova, H., et al., *The EpiDerm test protocol for the upcoming ECVAM validation study on in vitro skin irritation tests--an assessment of the performance of the optimised test.* Altern. Lab Anim, 2005. **33**(4): p. 351-367.
223. Kandarova, H., et al., *Assessment of the human epidermis model SkinEthic RHE for in vitro skin corrosion testing of chemicals according to new OECD TG 431.* Toxicol. In Vitro, 2006. **20**(5): p. 547-559.
224. Katoh, M., et al., *Assessment of the human epidermal model LabCyte EPI-MODEL for In vitro skin corrosion testing according to the OECD test guideline 431.* J. Toxicol. Sci, 2010. **35**(3): p. 411-417.
225. dos Santos, G.G., et al., *A potential in vitro epidermal equivalent assay to determine sensitizer potency.* Toxicol. In Vitro, 2011. **25**(1): p. 347-357.
226. Gibbs, S., et al., *An epidermal equivalent assay for identification and ranking potency of contact sensitizers.* Toxicol. Appl. Pharmacol, 2013. **272**(2): p. 529-541.
227. Elbayed, K., et al., *HR-MAS NMR spectroscopy of reconstructed human epidermis: potential for the in situ investigation of the chemical interactions between skin allergens and nucleophilic amino acids.* Chem. Res. Toxicol, 2013. **26**(1): p. 136-145.
228. Frankart, A., et al., *Studies of cell signaling in a reconstructed human epidermis exposed to sensitizers: IL-8 synthesis and release depend on EGFR activation.* Arch. Dermatol. Res, 2012. **304**(4): p. 289-303.
229. OECD, *The Adverse Outcome Pathway for Skin Sensitisation Initiated by Covalent Binding to Proteins. Part 2: Use of the AOP to Develop Chemical Categories and Integrated Assessment and Testing Approaches. Series on Testing and Assessmentp.No. 168. ENV/JM/MONO(2012)/PART2.* 2012.
230. Hu, T., et al., *Dermal penetration and metabolism of p-aminophenol and p-phenylenediamine: application of the EpiDerm human reconstructed epidermis model.* Toxicol. Lett, 2009. **188**(2): p. 119-129.

231. Harris, I.R., et al., *Comparison of activities dependent on glutathione S-transferase and cytochrome P-450 IA1 in cultured keratinocytes and reconstructed epidermal models.* Skin Pharmacol. Appl. Skin Physiol, 2002. **15 Suppl 1**: p. 59-67.
232. Wiegand, C., et al., *Dermal xenobiotic metabolism: a comparison between native human skin, four in vitro skin test systems and a liver system.* Skin Pharmacol. Physiol, 2014. **27**(5): p. 263-275.
233. Kubota, K., et al., *A repeated-dose model of percutaneous drug absorption.* Applied Mathematical Modelling, 2002. **26**(4): p. 529-544.
234. Kramer, N.I., et al., *Biokinetics in repeated-dosing in vitro drug toxicity studies.* Toxicol In Vitro, 2015. **30**(1 Pt A): p. 217-24.
235. Maschmeyer, I., et al., *Chip-based human liver–intestine and liver–skin co-cultures – A first step toward systemic repeated dose substance testing in vitro.* European Journal of Pharmaceutics and Biopharmaceutics, 2015. **95, Part A**: p. 77-87.
236. Jacquoilleot, S., et al., *Glutathione metabolism in the HaCaT cell line as a model for the detoxification of the model sensitisers 2,4-dinitrohalobenzenes in human skin.* Toxicol Lett, 2015. **237**(1): p. 11-20.
237. Thimmulappa, R.K., et al., *Preclinical evaluation of targeting the Nrf2 pathway by triterpenoids (CDDO-Im and CDDO-Me) for protection from LPS-induced inflammatory response and reactive oxygen species in human peripheral blood mononuclear cells and neutrophils.* Antioxid. Redox. Signal, 2007. **9**(11): p. 1963-1970.
238. Paramasivan, P., et al., *Repeated low-dose skin exposure is an effective sensitizing stimulus, a factor to be taken into account in predicting sensitization risk.* Br. J. Dermatol, 2010. **162**(3): p. 594-597.
239. MacKay, C., et al., *From pathways to people: applying the adverse outcome pathway (AOP) for skin sensitization to risk assessment.* ALTEX, 2013. **30**(4): p. 473-486.
240. Maxwell, G., et al., *Applying the skin sensitisation adverse outcome pathway (AOP) to quantitative risk assessment.* Toxicol. In Vitro, 2014. **28**(1): p. 8-12.
241. Kwak, M.K., et al., *Role of phase 2 enzyme induction in chemoprotection by dithiolethiones.* Mutat. Res, 2001. **480-481**: p. 305-315.
242. Krajka-Kuzniak, V., et al., *The effect of resveratrol and its methylthio-derivatives on the Nrf2-ARE pathway in mouse epidermis and HaCaT keratinocytes.* Cell Mol. Biol. Lett, 2014. **19**(3): p. 500-516.
243. Hu, C., et al., *Modification of keap1 cysteine residues by sulforaphane.* Chem. Res. Toxicol, 2011. **24**(4): p. 515-521.
244. Gegotek, A. and E. Skrzydlewska, *The role of transcription factor Nrf2 in skin cells metabolism.* Arch. Dermatol. Res, 2015. **307**(5): p. 385-396.
245. Soeur, J., et al., *Skin resistance to oxidative stress induced by resveratrol: from Nrf2 activation to GSH biosynthesis.* Free Radic. Biol. Med, 2015. **78**: p. 213-223.
246. Mathew, S.T., P. Bergstrom, and O. Hammarsten, *Repeated Nrf2 stimulation using sulforaphane protects fibroblasts from ionizing radiation.* Toxicol. Appl. Pharmacol, 2014. **276**(3): p. 188-194.
247. Dumont, C., et al., *Review of the availability of in vitro and in silico methods for assessing dermal bioavailability.* Applied In Vitro Toxicology, 2015. **1**(2): p. 147-164.
248. Union, O.J.o.T.E., *REGULATION (EC) No 1223/2009 Of The European Parliament And Of The Council of 30 November 2009 on cosmetic products.* 2009.
249. Piroird, C., et al., *The Myeloid U937 Skin Sensitization Test (U-SENS) addresses the activation of dendritic cell event in the adverse outcome pathway for skin sensitization.* Toxicology in Vitro, 2015. **29**(5): p. 901-916.

250. Nukada, Y., et al., *Prediction of skin sensitization potency of chemicals by human Cell Line Activation Test (h-CLAT) and an attempt at classifying skin sensitization potency.* Toxicology in Vitro, 2012. **26**(7): p. 1150-1160.
251. Hillen, U., et al., *Late reactions to the patch-test preparations para-phenylenediamine and epoxy resin: a prospective multicentre investigation of the German Contact Dermatitis Research Group.* British Journal of Dermatology, 2006. **154**(4): p. 665-670.
252. Mukkanna, K.S., N.M. Stone, and J.R. Ingram, *Para-phenylenediamine allergy: current perspectives on diagnosis and management.* Journal of Asthma and Allergy, 2017. **10**: p. 9-15.
253. Buckley, D.A., et al., *Contact allergy to individual fragrance mix constituents in relation to primary site of dermatitis.* Contact Dermatitis, 2000. **43**(5): p. 304-5.
254. Frosch, P.J., et al., *Patch testing with fragrances: results of a multicenter study of the European Environmental and Contact Dermatitis Research Group with 48 frequently used constituents of perfumes.* Contact Dermatitis, 1995. **33**(5): p. 333-42.
255. Meng, X., et al., *Auto-oxidation of Isoniazid Leads to Isonicotinic-Lysine Adducts on Human Serum Albumin.* Chem Res Toxicol, 2015. **28**(1): p. 51-8.
256. Parkinson, E.A., M. ; Cubberley R.; Skipp,P., *Quantifying the effect of exposure to the model sensitiser DNCB on the human skin proteome.* http://www.tt21c.org/wp-content/uploads/2016/09/IMSC2016_final.pdf, 2016. **poster presentation at 21st INTERNATIONAL MASS SPECTROMETRY CONFERENCE August 2016**.
257. Meng, X., et al., *Antigen exposure required for T cell activation.* Clinical and Translational Allergy, 2014. **4**(Suppl 3): p. P115-P115.
258. Dietz, L., et al., *Tracking Human Contact Allergens: From Mass Spectrometric Identification of Peptide-Bound Reactive Small Chemicals to Chemical-Specific Naive Human T-Cell Priming.* Toxicological Sciences, 2010. **117**(2): p. 336-347.
259. Corsini, E., et al., *Role of oxidative stress in chemical allergens induced skin cells activation.* Food Chem Toxicol, 2013. **61**: p. 74-81.
260. Mizuashi, M., et al., *Redox imbalance induced by contact sensitizers triggers the maturation of dendritic cells.* J Invest Dermatol, 2005. **124**(3): p. 579-86.
261. McKim, J.M., D.J. Keller, and J.R. Gorski, *An in vitro method for detecting chemical sensitization using human reconstructed skin models and its applicability to cosmetic, pharmaceutical, and medical device safety testing.* Cutaneous and Ocular Toxicology, 2012. **31**(4): p. 292-305.
262. McKim, J.M., D.J. Keller, and J.R. Gorski, *A new in vitro method for identifying chemical sensitizers combining peptide binding with ARE/EpRE-mediated gene expression in human skin cells.* Cutaneous and Ocular Toxicology, 2010. **29**(3): p. 171-192.
263. Natsch, A., et al., *Chemical reactivity and skin sensitization potential for benzaldehydes: can Schiff base formation explain everything?* Chem Res Toxicol, 2012. **25**(10): p. 2203-15.
264. Boyland, E. and L.F. Chasseaud, *Enzyme-catalysed conjugations of glutathione with unsaturated compounds.* Biochem J, 1967. **104**(1): p. 95-102.
265. Ponec, M., et al., *Characterization of reconstructed skin models.* Skin Pharmacol. Appl. Skin Physiol, 2002. **15 Suppl 1**: p. 4-17.
266. Spriggs, S., et al., *Effect of Repeated Daily Dosing with 2,4-Dinitrochlorobenzene on Glutathione Biosynthesis and Nrf2 Activation in Reconstructed Human Epidermis.* Toxicol Sci, 2016. **154**(1): p. 5-15.

267. Wittwehr, C., et al., *How Adverse Outcome Pathways Can Aid the Development and Use of Computational Prediction Models for Regulatory Toxicology.* Toxicological Sciences, 2017. **155**(2): p. 326-336.
268. de Wever, B., Kurdykowski, S. and Descargues, P., *Human Skin Models for Research Applications in Pharmacology and Toxicology: Introducing NativeSkin®, the "Missing Link" Bridging Cell Culture and/or Reconstructed Skin Models and Human Clinical Testing.* Applied In Vitro Toxicology, 2015. **1**(1): p. 26-32.
269. Wufuer, M., et al., *Skin-on-a-chip model simulating inflammation, edema and drug-based treatment.* Scientific Reports, 2016. **6**: p. 37471.